HYPERCROSSLINKED POLYMER MICROSPHERES:

Synthesis, Functionalisation and Application

A thesis submitted to the Department of Pure and Applied Chemistry, in partial fulfilment of the regulations for the Degree of Doctor of Philosophy in Chemistry.

Arlene Davies

July 2012

Signed:

Date:

ACKNOWLEDGEMENTS

First and foremost I would like to thank all the people who have made the work presented here possible. It has been a pleasure working with you all and I am extremely grateful for all of the help and advice that I have received.

I wish to express my deep gratitude to my supervisor Prof Peter Cormack for believing in me and for all of his encouragement, guidance and support through the good times, the bad times and the explosive times. It has been an honour to work in the group.

Thank you also to Prof David Sherrington for sharing his wealth of experience and knowledge and for all of his support.

Thank you to Dra. Núria Fontanals for all of her support and guidance in matters of SPE.

Without the support of the technical staff in the Department, many of the analyses would not have been possible; thank you very much to Denise Gilmour, Pat Keating and Jim Morrow. Also, thank you very much to Gavin Bain – the lab could not run without his untiring support and commitment!

A huge thank you to all members of the Polymer Group, past and present, for all of their support and for making my time in the Group such an enjoyable and memorable experience. Thank you also to the Grup de Cromatografia for their warm welcome and support during my time in Tarragona.

Last, but definitely not least, I would like to express my thanks to all of my friends and family for their unwavering support and encouragment throughout my time at University.

ABSTRACT

Hypercrosslinked polymers are an exciting class of polymeric materials with unique properties which have found success in several fields of application. In order to further develop the potential of these materials, but also open them up to new applications, the introduction of functional groups would be extremely beneficial. New methods for the chemical functionalisation of such materials are thus the primary focus of the work presented in this thesis.

Introduction of ion-exchange functionality into hypercrosslinked polymers has been demonstrated. Post-polymerisation sulfonation reactions provided access into hypercrosslinked polymers with strong cation-exchange (SCX) functionality. Different sulfonation reagents were investigated and the sulfonation conditions optimised. Using these optimised conditions, hypercrosslinked polymers with specific surface areas in excess of 1,000 m^2/g and controllable sulfonic acid loading levels were synthesised. Strong anion-exchange (SAX) functionality was also introduced into hypercrosslinked polymers as a complementary functionality to that present in the SCX materials. The synthetic protocol was optimised to allow the synthesis of polymers with ultra-high specific surface areas and variable quaternary ammonium salt loading levels. The novel SCX and SAX polymers were then applied as solid-phase extraction (SPE) sorbents in the selective extraction of pharmaceuticals from complex real water samples, and were shown to compare favourably with commercially available SCX and SAX SPE sorbents.

The copper(I) catalysed azide-alkyne cycloaddition reaction, the most popular reaction of the Sharpless 'click chemistry' family, was investigated as a potential route for functionalising hypercrosslinked materials. Azide- and alkyne-containing monomers were prepared and incorporated into the polymers, however the synthesis conditions employed during the hypercrosslinking reactions resulted in loss of these functionalities, thus the cycloaddition was

carried out prior to hypercrosslinking. A method of post-hypercrosslinking click functionalisation was also developed. Using both functional monomer and post-hypercrosslinking reaction strategies, functionalised polymers with ultra-high specific surface areas, in excess of 1,000 m^2/g, were prepared.

CONTENTS

ACKNOWLEDGEMENTS **i**

ABSTRACT **ii**

ABBREVIATIONS **x**

CHAPTER 1 – INTRODUCTION **1**

1.1. Polymers 2
1.2. Polymer Microspheres 6
1.3. Precipitation Polymerisation 7
1.3.1. Solvent Requirements for Precipitation Polymerisation 12
1.4. Hypercrosslinking 17
1.5. Uses of Polymer Microspheres 23
1.5.1. Uses of Hypercrosslinked Polymers 25
1.6. Polymer Modifications 29
1.6.1. Chemical Modification of Polymer Microspheres 31
1.7. PhD Hypothesis and Aims 36
1.8. References 36

CHAPTER 2 – SYNTHESIS, CHARACTERISATION AND APPLICATION OF HYPERCROSSLINKED POLYMER MICROSPHERES WITH SCX PROPERTIES **43**

2.1. Introduction 44
2.1.1. Cation-Exchange Resins 44
2.1.2. Uses of Sulfonated Polymers 45
2.1.3. Sulfonation of Polystyrene 48

2.1.4. Solid-Phase Extraction 51
2.1.4.1. Strong Cation-Exchange Solid-Phase Extraction 57
2.2. Experimental 59
2.2.1. Materials 59
2.2.2. Equipment 60
2.2.3. Typical Preparation of Poly(DVB-*co*-VBC) Precursors by Precipitation Polymerisation 62
2.2.4. Typical Hypercrosslinking Reaction 63
2.2.5. Typical Sulfonation of HXL Particles Using Acetyl Sulfate 65
2.2.6. Typical Sulfonation of HXL Particles Using Lauroyl Sulfate 66
2.3. Results and Discussion 68
2.3.1.Synthesis of HXL Particles 68
2.3.1.1. Precipitation Polymerisation 68
2.3.1.2. Hypercrosslinking 71
2.3.2. Sulfonation of HXL Material Using Acetyl Sulfate 76
2.3.3. Sulfonation of HXL Material Using Lauroyl Sulfate 78
2.3.4. Ion-Exchange Capacity 80
2.3.5. Optimisation of Conditions 82
2.3.6. Synthesis of SCX Material for SPE 84
2.3.7. Application of HXL-PP-SCX Material in Ion-Exchange SPE 88
2.3.7.1. SPE Method Development 90
2.3.7.2. Comparison of HXL-PP-SCX with Commercial Sorbents 93
2.3.7.3. Application to Real Samples 95
2.4. Chapter Conclusion 103
2.5. References 104

CHAPTER 3 – SYNTHESIS, CHARACTERISATION AND APPLICATION OF HYPERCROSSLINKED POLYMER MICROSPHERES WITH SAX PROPERTIES 108

3.1. Introduction 109
3.1.1. Anion-Exchange Resins 109

3.1.2. Uses of Aminated Polymers 110
3.1.3. Amination Reactions 110
3.1.4. Strong Anion-Exchange Solid-Phase Extraction 111
3.2. Experimental 112
3.2.1. Materials 112
3.2.2. Equipment 114
3.2.3. Typical Preparation of Poly(DVB-*co*-VBC) Precursors by PP 115
3.2.4. Typical Hypercrosslinking Reaction 117
3.2.5. Typical Amination of HXL Particles Using Triethylamine 118
3.2.6. Typical Amination of HXL Particles Using Dimethylbutylamine 119
3.2.7. Amination of Precursor Particles Prior to HXL 120
3.2.7.1. Amination of Precursor Particles 120
3.2.7.2. HXL of Aminated Precursor Particles 122
3.2.8. Aminated Particle Solvent Uptake Tests 123
3.3. Results and Discussion 124
3.3.1. Amination of HXL Material Using Triethylamine 124
3.3.2. Amination of HXL Material Using Dimethylbutylamine 126
3.3.3. Investigation of Pendent Chloromethyl Groups from Hypercrosslinking Reaction 128
3.3.4. Amination of the Polymer Produced Using Short Hypercrosslinking Reaction Times 133
3.3.5. Amination Prior to Hypercrosslinking 135
3.3.5.1. Amination of Precursor Particles 135
3.3.5.2. Hypercrosslinking of Aminated Precursor Particles 137
3.3.6. Synthesis of SAX Material for SPE 141
3.3.7. Application of HXL-PP-SAX Material in Ion-Exchange SPE 144
3.3.7.1. SPE Method Development 146
3.3.7.2. Comparison of HXL-PP-SAX with Commercial Sorbents 148
3.3.7.3. Application to Real Samples 150
3.4. Chapter Conclusion 153
3.5. References 153

CHAPTER 4 – FUNCTIONALISATION OF HYPERCROSSLINKED POLYMER MICROSPHERES USING CLICK CHEMISTRY **156**

4.1. Introduction 157
4.1.1. Click Chemistry Definition and Criteria 157
4.1.2. Click Chemistry Reactions 158
4.1.3. Azide-Alkyne Cycloaddition 159
4.1.3.1. Azide-Alkyne Cycloaddition Reaction Mechanism 160
4.1.3.2. Addition of Ligands to the Copper Catalyst 163
4.1.3.3. Azide-Alkyne Cycloaddition with Internal Alkynes 164
4.1.3.4. Alternative Azide-Alkyne Cycloaddition Conditions 166
4.1.4. Use of Click Chemistry in Polymer Synthesis 170
4.1.5. Use of Click Chemistry for Polymer Modification 174
4.1.5.1. Soluble Polymers 174
4.1.5.2. Polymer Microspheres 176
4.1.6. Previous Work Within Our Group 177
4.1.6.1. Jonathan Chua – Nuffield Summer Student 177
4.1.6.2. Rachel Mark – Final Year MSci Undergraduate Student 179
4.2. Experimental 183
4.2.1. Materials 183
4.2.2. Equipment 184
4.2.3. Synthesis of Fmoc-Glycine Propargyl Ester 185
4.2.4. Synthesis of Azide-Protected *L*-Phenylalanine 187
4.2.5. Typical Vinylbenzyl Azide (VBAz) Synthesis 188
4.2.6. Propargyl Methacrylate (PMA) Synthesis 189
4.2.7. Typical Synthesis of Poly(DVB-*co*-VBC-*co*-VBAz) by PP 190
4.2.8. Click Chemistry Modification of Poly(DVB-*co*-VBC-*co*-VBAz) 191
4.2.9. Hypercrosslinking Reaction of Poly(DVB-*co*-VBC-*co*-VBAz) 194
4.2.10. Typical Synthesis of Poly(DVB-*co*-VBC-*co*-PMA) by PP 195

4.2.11. Click Click Chemistry Modification of Poly(DVB-*co*-VBC-*co*-PMA) 196
4.2.12. Hypercrosslinking Reaction of Poly(DVB-*co*-VBC-*co*-PMA) 198
4.2.13. Typical Synthesis of Poly(DVB-*co*-VBC) by PP 199
4.2.14. Hypercrosslinking Reaction of Poly(DVB-*co*-VBC) 200
4.2.15. Azidation of HXL Poly(DVB-*co*-VBC) 201
4.2.16. Click Chemistry Modification of Azide-Containing HXL Microspheres 202
4.2.17. Synthesis by Precipitation Polymerisation of Poly(DVB-*co*-VBAz) 206
4.2.18. Click Chemistry Hypercrosslinking of Poly(DVB-*co*-VBAz) 207
4.2.19. Poly(DVB-*co*-VBAz) Solvent Uptake Tests 208
4.3. Results and Discussion 209
4.3.1. Synthesis of Azide-Containing 'Clickable' Polymer Microspheres 209
4.3.2. Hypercrosslinking of Poly(DVB-*co*-VBC-*co*-VBAz) 213
4.3.3. Click Chemistry Modification of Azide-Containing Polymer Microspheres 215
4.3.4. Hypercrosslinking of Click Chemistry Modified Polymer Microspheres 224
4.3.5. Synthesis of Alkyne-Containing 'Clickable' Polymer Microspheres 227
4.3.6. Hypercrosslinking of Poly(DVB-*co*-VBC-*co*-PMA) 230
4.3.7. Click Chemistry Modification of Alkyne-Containing Polymer Microspheres 232
4.3.8. Hypercrosslinking of Click Chemistry Modified Polymer Microspheres 238
4.3.9. Post-Hypercrosslinking Azidation and Subsequent Click Chemistry Functionalisation 240
4.3.10. Hypercrosslinking Using Click Chemsitry 248
4.3.10.1. Synthesis of Poly(DVB-*co*-VBAz) Precursor Polymers 248

4.3.10.2. Hypercrosslinking of Poly(DVB-*co*-VBAz) Using Dialkyne and Click Chemistry 251
4.4. Chapter Conclusion 256
4.5. References 257

Chapter 5 – General Conclusions and Future Work 261

5.1. General Conclusions 262
5.2. Future Work 266

ABBREVIATIONS

AIBN	2,2'-Azo*bis*(isobutyronitrile)
ATRP	Atom transfer radical polymerisation
DCC	Dicyclohexylcarbodiimide
DCE	1,2-Dichloroethane
DCM	Dichloromethane
DCU	Dicyclohexylurea
DFT	Density functional theory
DMAP	*4*-Dimethylaminopyridine
DMF	*N,N*-Dimethylformamide
DVB	Divinylbenzene
EGDMA	Ethylene glycol dimethacrylate
FT-IR	Fourier Transform-infrared
HEMA	Hydroxyethyl methacrylate
HDA	Hetero Diels-Alder
HPLC	High performance liquid chromatography
HXL	Hypercrosslinked
IEC	Ion-exchange capacity
NAD	Non-aqueous dispersion
NHC	*N*-Heterocyclic carbene
NIPAM	*N*-Isopropylacrylamide
NP	Normal phase
NSAID	Non-steroidal anti-inflammatory drug
PBrCL	Poly(2-bromo-ε-caprolactone)
PCL	Poly(ε-caprolactone)
PMA	Propargyl methacrylate
PP	Precipitation polymerisation
RAFT	Reversible addition-fragmentation chain-transfer
ROP	Ring-opening polymerisation
RP	Reversed phase

SAX	Strong anion-exchange
SCX	Strong cation-exchange
SEM	Scanning electron microscopy
SPE	Solid-phase extraction
TBTA	*Tris*-(benzyltriazolylmethyl)amine
VBAz	Vinylbenzyl azide
VBC	Vinylbenzyl chloride
WAX	Weak anion-exchange
WCX	Weak cation-exchange

CHAPTER 1

INTRODUCTION

1.1. POLYMERS

A polymer is a high molecular weight species constructed from many lower molecular weight structural units known as monomers. The process of joining these monomers together is known as polymerisation.[1] The two most important types of polymerisation are step-growth and chain-growth polymerisation. Step-growth polymerisation is used for -OH, -COOH, -COCl, *etc.*, containing monomers, and the resulting polymers are formed frequently, but not always, through the loss of water in a succession of condensation reactions. Chain-growth polymerisations can be used for many types of polymerisation, including the conversion of vinyl monomers into polymers, which proceed *via* chain reactions that begin with an initiator-derived reactive species attacking/opening a double bond in the monomer to create one covalent link and a new reactive centre, which leads to the opening of a second double bond in a similar manner.[2]

With regards to vinyl monomers, chain-growth polymerisation exploits the reactivity of the π-bond of the vinyl group. The π-bond is activated through the use of a free-radical or ionic initiator. This creates the active centre, which then propagates to form a single polymer chain until the active centre is either lost to a termination reaction, or the monomer is consumed completely.[2]

Chain-growth polymerisation begins with the initiation process. In the specific case of chain-growth polymerisation using radicals (free radical polymerisation), in order for an initiator to be effective it should be able to break down when subjected to heat, electromagnetic radiation or a chemical (redox) reaction, to give radical species. These radicals should be sufficiently stabilised so that they can be formed readily and also be able to react with a monomer to generate an active centre. Azo compounds such as 2,2'-azo*bis*(isobutyronitrile) (AIBN) (**1**), and peroxides, such as benzoyl

peroxide, are good initiators for many vinyl polymerisations as they readily break down to give radical species[2] (Figure 1.1.1).

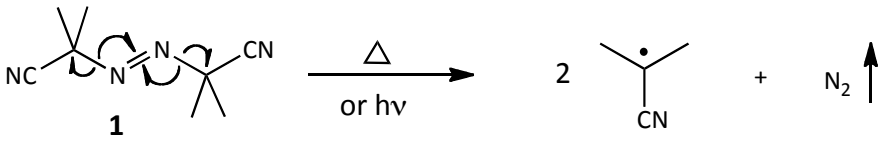

Figure 1.1.1. – Thermal and photochemical breakdown of AIBN.

Once formed, these initiator-derived radicals (I•) can then react with the π-bond of a monomer unit, transferring the radical to the monomer to generate a new free radical species. This radical then acts as a new active centre (Figure 1.1.2).

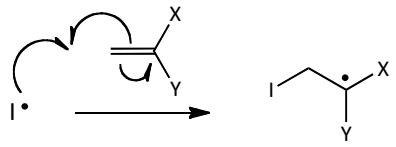

Figure 1.1.2. – Radical initiation process.

The radical of the active centre can then react with the π-bond of another monomer present to create a σ-bond, subsequently creating a new active centre, thus allowing it to react with another monomer. Chain-growth occurs through a series of these monomer addition reactions in a process known as propagation (Figure 1.1.3). Propagation is normally an exothermic process that occurs rapidly.[1]

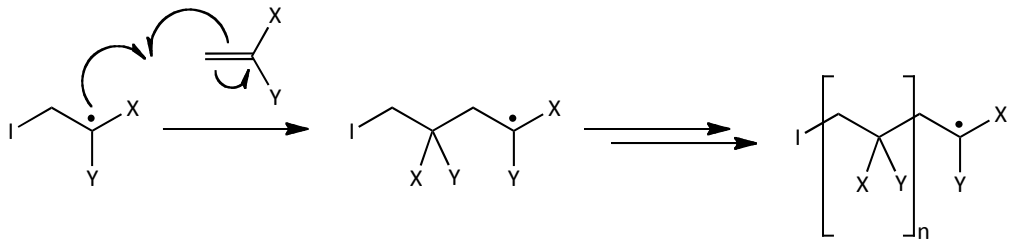

Figure 1.1.3. – Propagation of the polymer chain.

Polymerisation then ends with a termination step, which involves loss of the radical by either combination or disproportionation. Termination reactions arise due to the relatively high reactivity of the radical species, which can react readily in a number of undesirable ways to give non-radical products, which are unable to propagate. Sometimes the active radical species reacts with another propagating chain instead of a monomer unit, thus terminating two propagating species. This can occur as the combination of two radical species, resulting in a single 'dead' polymer chain (Figure 1.1.4).

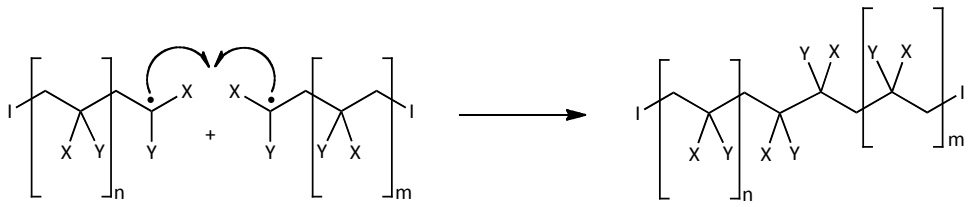

Figure 1.1.4. – Termination by combination.

A second mechanism by which termination can occur is disproportionation, where one propagating radical abstracts a hydrogen atom from another chain, leaving behind an unsaturated group and generating a new saturated end group. This results in the conversion of two active chains into two 'dead' polymer chains (Figure 1.1.5).

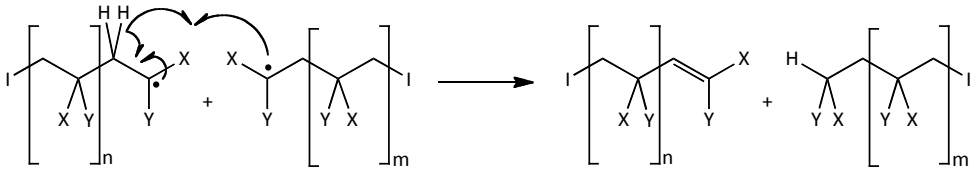

Figure 1.1.5. – Termination by disproportionation.

The dominant method of termination observed is dictated by the monomer used and the polymerisation conditions employed. Termination can occur by one of these methods alone, or by both processes simultaneously. Experimental evidence suggests that polystyrene is terminated predominantly by combination reactions. Poly(methyl methacrylate), on the other hand, is more likely to terminate by disproportionation during polymerisations above 60 °C, but can be terminated by both processes when polymerised below 60 °C.[2]

These processes result in linear polymers, however, backbiting reactions or the addition of crosslinking monomers can allow non-linear polymers to form.

Backbiting is a process where the radical at the active end of a polymer chain abstracts a hydrogen atom from somewhere within its own chain, resulting in a mid-chain radical. This radical can then continue to propagate as normal, leading to a branched polymer (Figure 1.1.6). The more backbiting reactions that occur, the more highly branched the polymer product will be.

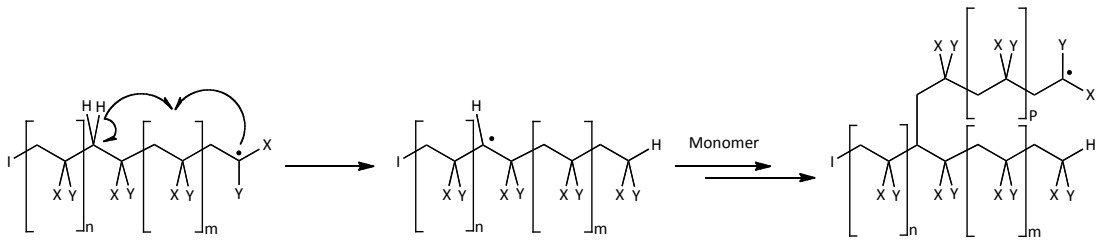

Figure 1.1.6. – Branched polymer formation.

A crosslinker is a monomer with two or more vinyl groups present that can react during the polymerisation, resulting in the joining of two or more polymer chains. When the products that arise from the use of a crosslinker are insoluble and intractable they are known as crosslinked polymers. Divinylbenzene (DVB) (**2**) is an example of a crosslinking monomer that is structurally similar to styrene, but which has two polymerisable vinyl groups present (Figure 1.1.7).

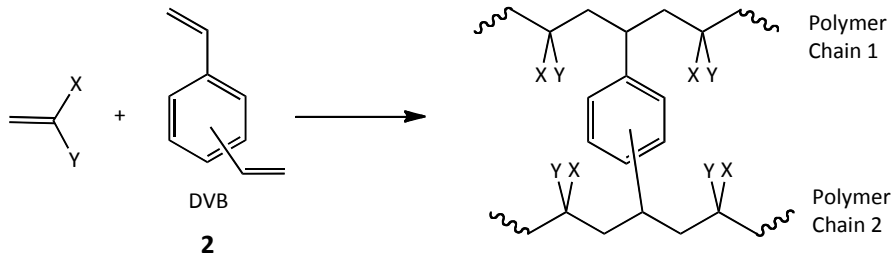

Figure 1.1.7. – Formation of crosslinked polymers.

These non-linear polymers can take the form of branched polymers, macroscopic networks or microgels (Figure 1.1.8).

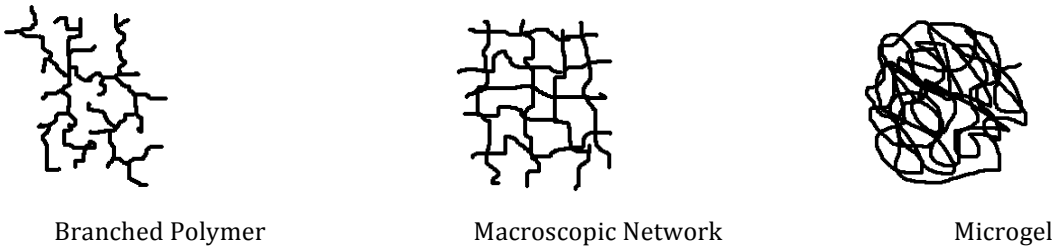

Figure 1.1.8. – Schematic representation of different forms of non-linear polymers.

1.2. POLYMER MICROSPHERES

Often, the use of a crosslinker will result in the formation of microgel particles with a discrete volume; these particles will eventually become crosslinked together into one infinite polymer network during polymerisation. On reaching the 'gel-point' the crosslinked polymer will become a monolithic material, which

is a soft gel that will conform to the shape of the polymerisation vessel. This monolith can be crushed to give small particles, however the size and shape of these particles will be very irregular.[3] In many applications, mechanically robust, spherical particles are much more useful; such spherical particles can be produced by trapping the microgel particles before they are fused together to form a monolith. These spherical particles are commonly known as beads or microspheres.

Polymer microspheres of defined size can be prepared using different polymerisation techniques. For example, emulsion polymerisation can be used to synthesise microspheres in the sub-micron range, while dispersion polymerisation typically gives microspheres with mean diameters of the order of 0.1-15 μm. Much larger diameter particles can be accessed using suspension polymerisation or emulsion polymerisation seed particles in step-wise swelling processes.[4]

The microgel particles are trapped into spheres in emulsion polymerisations by using ionic surfactants that form spherical micelles for the monomer to polymerise in. The ionic head group of the stabiliser stops the micelles from colliding by means of electrostatic repulsion and thus keeps the microgel structures apart and intact. Similarly, in suspension polymerisations stabilizers are used to stop the monomer droplets from aggregating. These work by coating the surfaces of the droplets, where they are ideally placed to prevent any collisions from resulting in coalescence/aggregation.

1.3. PRECIPITATION POLYMERISATION

Precipitation polymerisation is a method for preparing highly crosslinked monodisperse polymer microspheres in the 0.1-10 μm range. Although first reported in 1993 by Stöver *et al.*,[5] this method is a similar, but improved, approach to that used previously by Bamford *et al.*[6] Precipitation

polymerisation is advantageous over other methods of particle production as it does not require the use of a steric stabiliser or electrostatic surfactant, thus resulting in clean products which do not carry any surfactant-derived ionic charges. The absence of any stabilisers has resulted in speculation as to how stable particles can be formed. Choe *et al*.[7] proposed that particles produced by precipitation polymerisations are highly dependent on the degree of crosslinking as "increased crosslinking provides the individual particles with an enhanced hardness and resilience, which serves to prevent fusion of the particles". Downey *et al*.,[8] on the other hand, have suggested that the particle surface must consist of a partially crosslinked, solvent swollen gel layer that sterically stabilises the particle. The transient gel layer "continuously desolvates and collapses by a spinodal decomposition that is both driven and frozen by crosslinking". Most research seems to agree that the monomer concentrations must be kept low (2-5 vol. %) in order to suppress particle aggregation.[9]

Precipitation polymerisation begins with a homogeneous mixture of monomer, solvent and initiator (*i.e.*, both the monomer and initiator must be soluble in the solvent). Polymerisation then proceeds, followed by phase separation of the polymer product by either enthalpic or entropic precipitation. Enthalpic precipitation occurs where the solvent and polymer are not compatible, meaning that while the monomer is soluble in the solvent, the propagating polymer chain will eventually surpass its limit of solubility and precipitate from solution (*i.e.*, the polymer itself must be insoluble in the solvent). The nuclei resulting from this type of precipitation are thought to aggregate together to form larger polydisperse particles, which grow by capturing other polymer chains that have precipitated out of solution, and depositing them onto their surfaces. Entropic precipitation, on the other hand, is dominant where crosslinking prohibits the polymer and solvent from mixing freely. In this case, residual vinyl groups on the surfaces of the particles capture soluble oligomers from solution. Entropic precipitation into a good solvent will often result in a

sedimentary macro- or microscopic gel. Use of a poor solvent, however, normally leads to micrometer-sized particles.[8]

Downey *et al*.[8] hypothesise that divinylbenzene (DVB) (**2**) microspheres are formed in acetonitrile by a two-step process. Nucleation proceeds *via* aggregation of soluble oligomers to form swollen microgel particles that will internally desolvate resulting in particle nuclei with colloidal stability. This is followed by growth of the particles involving a reactive entropic capture mechanism, whereby soluble oligomeric radicals are captured from solution by vinyl groups on the surfaces of the particles (Figure 1.3.1). These newly captured oligomers will subsequently desolvate to form the new surfaces of the particles which will also contain residual vinyl groups, therefore allowing further capture and growth.

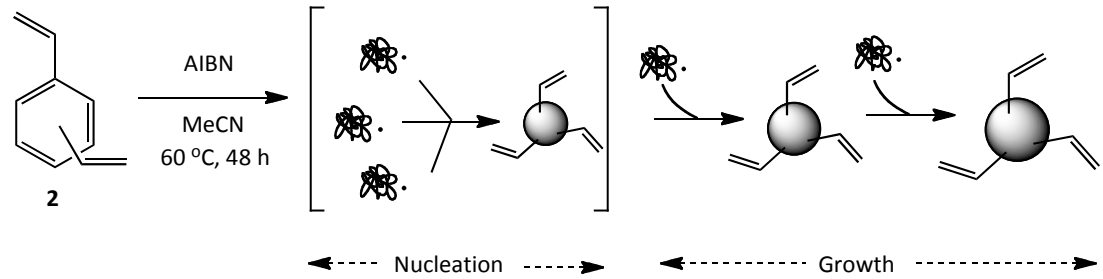

Figure 1.3.1. – Mechanism of particle formation proposed by Downey *et al*.[8]

This hypothesis was tested using seed particles which had been modified to eliminate the surface vinyl groups (Figure 1.3.2) and comparing of the results to the data arising from use of unmodified seed particles with their vinyl groups intact. The surface modification reactions involved either alkylation using an excess of *n*-BuLi to give inert hexyl groups, or hydrogenation carried out under an H_2 atmosphere in the presence of Wilkinson's catalyst to give ethyl groups.[8]

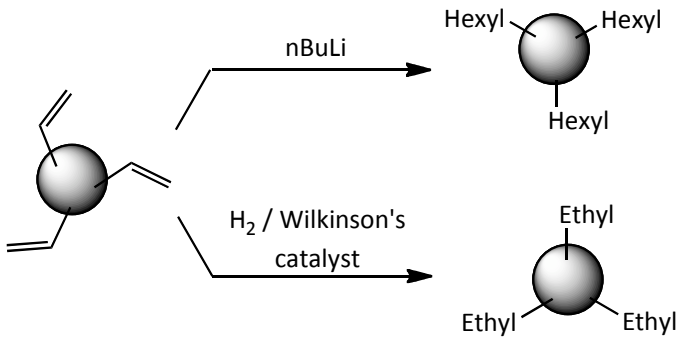

Figure 1.3.2. – Chemical modification of surface vinyl groups.[8]

The observation was that in the ensuing seeded growth reactions involving DVB and AIBN, the unmodified particles grew uniformly by capturing oligomers. However, under the same conditions, the modified, inert seed particles did not grow. As the oligomers formed were not captured by the seed particles, they instead aggregated to form secondary particles (Figure 1.3.3), resulting in a polydisperse product.[8]

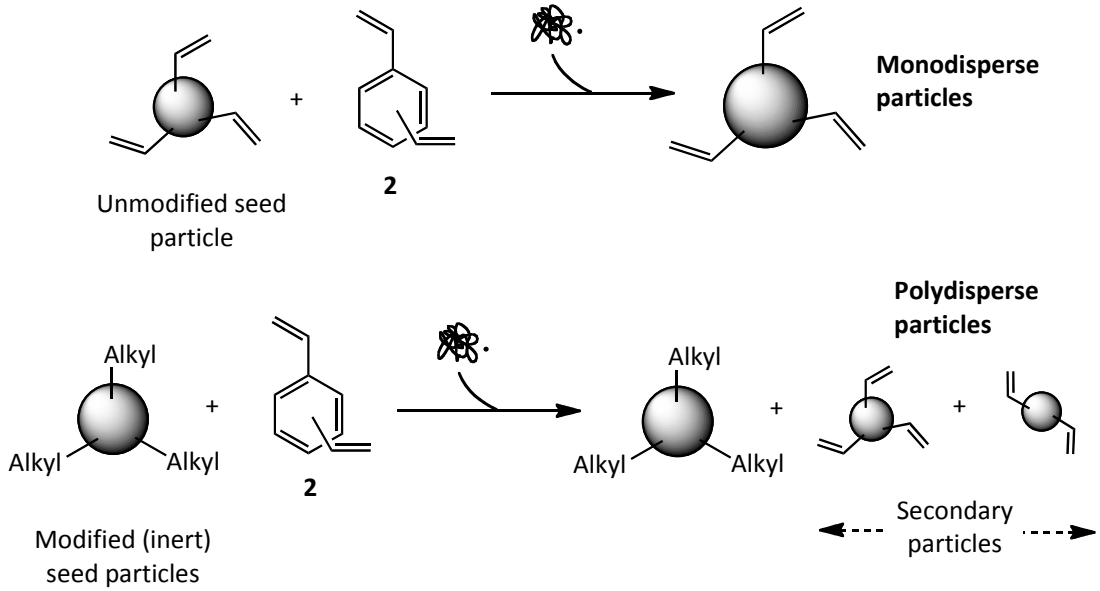

Figure 1.3.3. – Particle growth mechanisms.[8]

This supports the hypothesis that the surface vinyl groups are a key feature of the mechanism in ensuring uniform growth.

While the earlier work on precipitation polymerisation focused solely on polymerisations of styrene and DVB, it has since been applied to a much larger range of vinyl monomers. Spherical particles have been prepared using chloromethyl styrene,[10] acrylamide,[11] alkyl methacrylates,[12] methyl methacrylate[13] and maleic anhydride,[14] all with DVB as the crosslinking co-monomer. The solvent systems used in these particular precipitation polymerisations were tailored to the specific polarities of the monomers and polymers involved. Particles have also been prepared using methacrylic acid and poly(ethylene glycol) methyl ether methacrylate monomers, with ethylene glycol dimethacrylate (EGDMA) as the chosen crosslinker.[15] From our own group there are also several publications describing molecularly imprinted variants.[16,17,18,19]

The effects of varying the level of crosslinker was studied in detail by Choe *et al*.[7] It was found that the temperature at which the onset of thermal degradation occurred in thermal gravimetric analysis was higher for materials prepared with higher levels of crosslinker: 339.8 ^{o}C *vs*. 376.0 ^{o}C for 5 and 75 mol% DVB, respectively. Additionally, it was shown that materials prepared by precipitation polymerisation at all levels of DVB had higher degradation onset temperatures than those prepared by emulsion polymerisation (340.0 ^{o}C, 10 mol% DVB) and commercial materials prepared by suspension polymerisation (321.0 ^{o}C, 4 mol % DVB).[7]

Higher levels of crosslinker were also found to lead to smoother particles, as a consequence of the improved stability of the particles, which brings with it a harder surface. This improved stability was also used for justification of the lower levels of particle coagulation with higher crosslinker. Typically, it was found that doublet and triplet particles were observed at crosslinker levels below 20 %, as the particles were soft and coagulated on collision. When the level of crosslinker was increased to 40 %, no multiplet particles were formed, as the harder particles did not fuse on collision (Figure 1.3.4).[7]

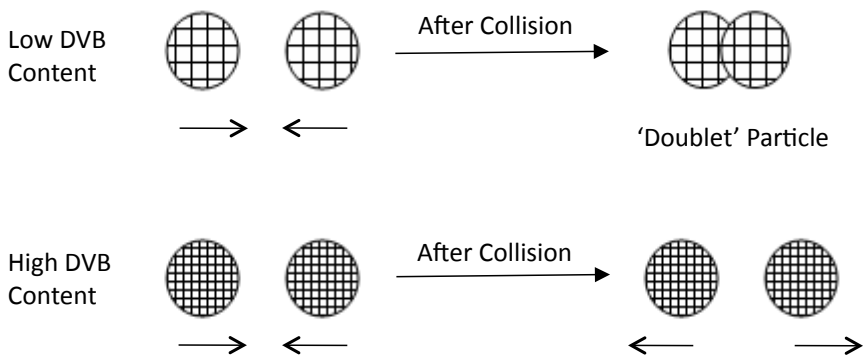

Figure 1.3.4. – Collision induced formation of multiplet particles.[7]

1.3.1. Solvent Requirements for Precipitation Polymerisation

The choice of solvent used in precipitation polymerisation is critical to the success of the polymerisation, as the monomer must be soluble in the solvent for initiation and nucleation to occur, but the polymer must be insoluble in the solvent in order to achieve precipitation. For the formation of distinct microspheres, a solvent known as a near-θ solvent is required, *e.g.*, acetonitrile for DVB-based polymerisations.[8] In order to define a near-θ solvent it is important to first consider the solvency characteristics of solvents and also the effects of a polymer in solution.

Solvents can be characterised by values known as solubility parameters. The solubility parameter can take two forms: a one-dimensional Hildebrand solubility parameter (δ),[21] which considers the overall solvent properties, and the three-dimensional Hansen solubility parameters,[20] which take the Hildebrand parameter and break it down into the interactions which are polar (δ_p), dispersive (δ_d) and those due to hydrogen bonding (δ_h). The two types of solubility parameter are related *via* the equation:

$$\delta^2 = \delta_p^2 + \delta_d^2 + \delta_h^2 \qquad \text{(Equation 1)}^{15}$$

The Hildebrand solubility parameter of a given solvent is a measure of its solvency behaviour, *i.e.*, its affinity for solutes. δ is derived from the cohesive energy density term of the solvent, which has itself been derived from the heat of vapourisation (ΔH_{vap}). ΔH_{vap} is a measure of the amount of energy that needs to be added, from the onset of boiling, to give total separation of the liquid molecules (*i.e.*, to convert all the molecules to gas). This is equivalent to the number of Van der Waals forces holding the liquid together. Since the same intermolecular forces need to be overcome to vapourise a liquid as to dissolve something in it, ΔH_{vap} can be related to solubility. The cohesive energy density is calculated using the following expression:

$$c = \frac{\Delta H \; - \; RT}{V_m} \qquad \text{(Equation 2)}$$

Where, c = cohesive energy density

ΔH = heat of vapourisation

R = universal gas constant

T = temperature

V_m = molar volume

In 1936, Hildebrand proposed that taking the square root of the cohesive energy density gave a numerical value that was a good measure of the solvency behaviour of a specific solvent.[21] This became known as the Hildebrand solubility parameter, δ.

$$\delta = \sqrt{c} \qquad \text{(Equation 3)}$$

Originally, c was measured in calories/cc, but when converted to Standard International units it was measured using cohesive pressures and is therefore quoted in mega Pascals (MPa).

Determination of the solubility parameter for a polymer is more complicated, as a polymer will decompose before the heat of vapourisation can be determined. To circumvent this problem, swelling behaviour in various solvents is used to assign Hildebrand values to polymers. For non-liquid materials, the value is often referred to as the cohesion parameter rather than the solubility parameter.[22]

When deriving the Hansen solubility parameters, the dispersion force for the solvent is calculated first, using what is called the homomorph method. The homomorph of a polar molecule is its non-polar equivalent in terms of size and structure (*e.g.*, *n*-butane is the homomorph of *n*-butyl alcohol). The Hildebrand value for the non-polar homomorph is entirely due to dispersion forces, and so is assigned to the polar molecule as δ_d. This value is then squared, δ_d^2, and subtracted from δ^2, with the remainder being designated as the overall polar interaction of the molecule δ_a (not to be confused with the polar component δ_p). Through trial and error experimentation on numerous solvents and polymers, Hansen separated δ_a into δ_p and δ_h values that best reflected empirical evidence.[23]

The mean square dimensions of a polymer in dilute solution are dependent on these interactions between the solvent and the polymer. The chain will expand in a good solvent in order to increase its favourable interactions with the solvent but, conversely, will contract in a poor solvent in order to reduce unfavourable interactions. As a result, polymers tend to aggregate or precipitate in poor solvents.[24]

The excluded volume in a polymer solution is defined by Hermans[25] as "the effective volume that is unavailable to the polymer due to steric hindrance by another polymer molecule, *i.e.*, the volume taken up by another polymer molecule. For the simple case of exclusion of spheres, the excluded volume is the volume of solution where the centre of one sphere may not be placed in the

presence of the other, and is equal to the volume of a sphere with radius equal to the sum of the radii of both spheres" (Figure 1.4.1).

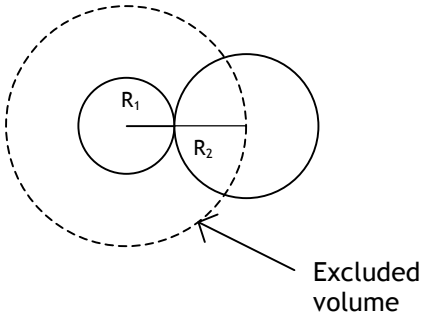

Figure 1.3.1.1. – Excluded volume effect.

Flory's θ solvent marks the boundary between good and bad solvents, with the θ solvent providing an exact compensation for the excluded volume effect. The mean square dimensions are therefore controlled solely by short-range intramolecular interactions, *i.e.*, the solvent has no effect. A carefully selected solvent and a specific temperature are required to eliminate the excluded volume effect and thus reach the θ state.[26,24]

Having considered these solvent classifications, it is clear that a near-θ solvent is one close to the boundary between a good and bad solvent, in which the excluded volume is insignificant. In terms of solubility parameters, Yoshimatsu *et al*.[27] define a near-θ solvent as one with a solubility parameter of 3-5 $(MPa)^{1/2}$ (*approx*. 1.5 – 2.5 $[cal/cm^3]^{1/2}$) away from that of the polymer being formed.

With these definitions in mind, many groups have studied the solvent system used for the formation of DVB microspheres by precipitation polymerisation, with all groups finding that acetonitrile is the only solvent capable, when used on its own, of producing monodisperse microspheres. Stöver *et al*.[5] found that microspheres were also accessible when acetonitrile was mixed in a 7:3 (v/v) ratio with *n*-butanol or *n*-propanol, however, when used alone, neither *n*-butanol nor *n*-propanol allowed access to monodisperse microspheres, despite

the very similar Hildebrand solubility parameters – both solvents resulted in irregular particles. Shim *et al.*[28] studied a range of co-solvents, including 2-propanol and 2-methoxyethanol in combination with acetonitrile, and found that spherical particles could be accessed. Again, despite these solvents having similar δ values to that of acetonitrile, when used as the sole solvent in the solvent system, these led only to coagulum. On closer inspection, it can be seen that despite the similarities in the δ value, the more defined Hansen solubility parameters for these solvents are quite different. This is also the case for a wide range of solvents in which the Hildebrand solubility parameter is quite similar to that of acetonitrile, but the different Hansen parameters result in the formation of coagulum or irregular particles instead of monodisperse spheres (Table 1.4.1).[15,28]

	Hildebrand parameter	***Hansen parameters [(cal/cm³)$^{1/2}$]***		
Solvent	***(δ) [(cal/cm³)$^{1/2}$]***	δ_d	δ_p	δ_h
t-butanol	10.6	7.4	2.8	7.1
2-propanol	11.5	7.7	3.0	8.0
acetonitrile	11.9	7.5	8.8	7.5
2-methoxyethanol	12.1	8.0	4.5	7.0
ethanol	12.7	7.7	4.3	9.5
methanol	14.5	7.4	6.0	10.9
styrene	9.3	8.2	4.4	0.0

Table 1.3.1.1. – Hildebrand and Hansen solubility parameters for a range of solvents.

From the values presented in Table 1.3.1.1, it is clear that the Hildebrand solubility parameters of these solvents are quite close to that of acetonitrile. By considering only the Hildebrand value, it is easy to see that *t*-butanol, 2-propanol, 2-methoxyethanol or even ethanol should be ideal choices as alternatives to acetonitrile, as their δ values are very similar to that of acetonitrile. However, all lead to coagulum, meaning that the δ value is not the sole parameter that controls particle formation. Inspection of the Hansen parameters shows that for these four solvents, the dispersive and hydrogen

bonding interaction terms are not too far removed from those of acetonitrile, however the polar interaction terms are much lower than that for acetonitrile. This would suggest that the solvent polarity is a very important factor in particle formation.

1.4. HYPERCROSSLINKING

Hypercrosslinking, developed by Davankov *et al*.[29,30] in the 1970s, is a means by which microporosity can be introduced into polymers, thus increasing their specific surface area (expressed in m^2/g). This increase in specific surface area is accompanied by enhanced and somewhat unusual solvent sorption characteristics. Davankov's novel methodology involved the extensive post-polymerisation crosslinking of linear polystyrene, or of poly(styrene-*co*-divinylbenzene) in its highly swollen gel state. These crosslinking reactions required a thermodynamically good solvent, such as 1,2-dichloroethane (DCE), a Lewis acid catalyst and a crosslinking agent in order to produce the hypercrosslinked styrenic derivatives.

The crosslinking agent forms rigid bridges joining neighbouring aromatic rings in the swollen gel, and can take the form of either an 'internal' or 'external' electrophile. The most common internal electrophile method uses vinylbenzyl chloride (VBC) residues, which can be introduced into the polymer by means of a comonomer in the precursor synthesis. VBC contains a CH_2-Cl (chloromethyl) substituent that reacts readily with the Lewis acid catalyst to give the electrophilic species that can then go on to form the crosslinks through Friedel-Crafts type chemistry. External crosslinking agents, on the other hand, are introduced to the polymer during the crosslinking reaction and contain at least two separate reactive groups that can react with two aromatic rings present in the polymer to form a bridge between them (Figure 1.4.1). A good example of an external electrophile is 1,4-*bis*-chloromethyldiphenyl (**3**).[31]

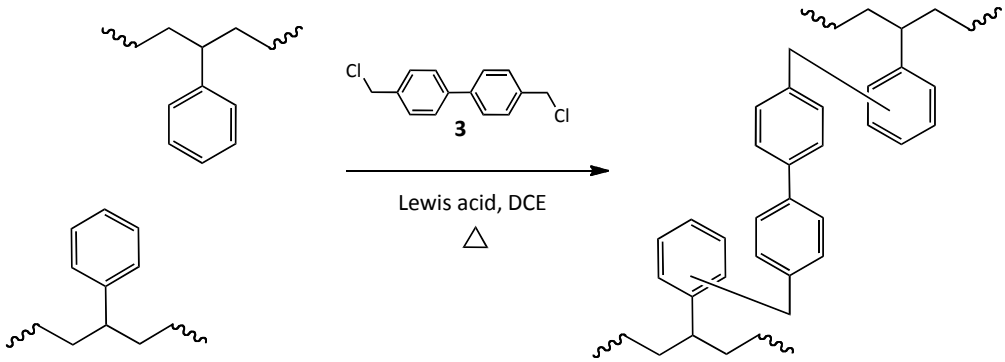

Figure 1.4.1. – Use of external crosslinking agent 1,4-*bis*-chloromethyldiphenyl (3).

The catalyst used in the hypercrosslinking reaction can be either a Lewis acid or a protonic acid such as HF. Theoretically, all Lewis acids can potentially catalyse the reaction, *i.e.*, $FeCl_3$, $AlCl_3$, $SnCl_4$, BF_3, *etc*. However, in practice, Ahn *et al*.[32] found that $FeCl_3$ is consistently more active than both $AlCl_3$ and $SnCl_4$, giving higher specific surface areas in all cases. The reason for the differences seen between the catalysts is not fully understood, but Ahn proposed that poor solubility ($AlCl_3$) and steric bulk ($SnCl_4$) may limit the hypercrosslinking reaction, therefore $FeCl_3$ may offer the best compromise in terms of solubility and size. Figure 1.4.2 shows how steric bulk may affect the reaction as the first crosslink formed can potentially prevent larger Lewis acids from accessing the second chloromethyl moiety, thus preventing formation of a second crosslink.

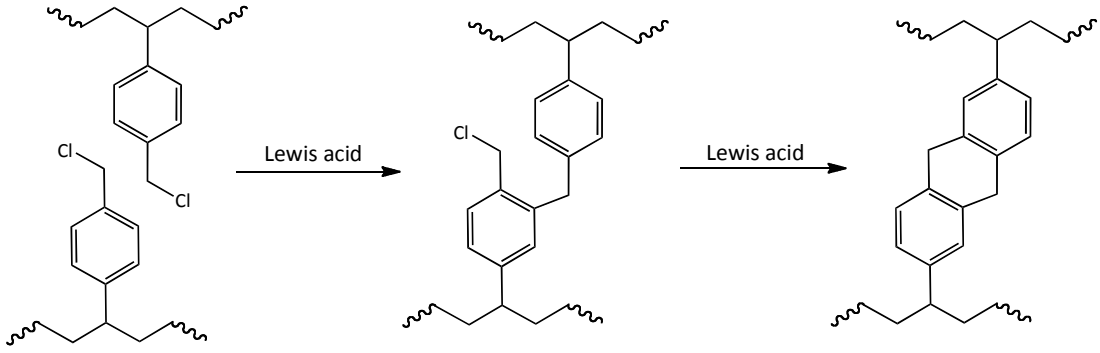

Figure 1.4.2. – Hypercroslinking reaction of poly(DVB-*co*-VBC) *via* an internal electrophile.[32]

Formation of this second crosslink is thought to be extremely favourable as the aromatic group to be substituted is already doubly alkylated and thus electron rich. Formation of the second crosslink is further enhanced for two reasons: the formation of the first crosslink brings the second chloromethyl group into close proximity of the aromatic ring; the ensuing cyclisation reaction results in a highly stable six-membered ring. It is possible that this step was limiting in the case of the relatively large $SnCl_4$ catalyst. $FeCl_3$ is smaller and presumably not limited in terms of this reaction; this, coupled with the enhanced reactivity towards the second bridge formation, could well be the reason for the high efficiency of the hypercrosslinking reaction when using $FeCl_3$.

While Davankov's methodology was developed using linear polystyrene, other groups have used various methods to produce styrenic precursor materials, such as suspension,[32,33] emulsion,[34] non-aqueous dispersion[35] and precipitation[35] polymerisations, and all of the precursor materials produced were then hypercrosslinked using the Davankov methodology. This would suggest that the Davankov methodology is generic and can be used for the production of ultra-high specific surface area particles with a range of diameters.

As the crosslinking process is intramolecular in nature, the reaction has been shown to be very efficient. A study by Ahn *et al*.[32] showed that a gel-type resin prepared by suspension polymerisation can be almost fully hypercrosslinked within only 15 minutes. This was manifest as a considerable decrease in Cl content from ~19 wt% to ~2 wt%, accompanied by a simultaneous increase in the specific surface area from ~0 m^2/g to ~1,200 m^2/g. This study also addressed the relative amount of Lewis acid required to allow the hypercrosslinking reaction to afford such high specific surface area materials. If this reaction is catalytic then the $FeCl_3$ concentration should be irrelevant and all Cl groups will be removed (Figure 1.4.3). In this case the $FeCl_4^-$ generated will be transferred back to $FeCl_3$ by the H^+ that is removed from the aromatic ring when the hypercrosslink forms, resulting in the production of HCl.

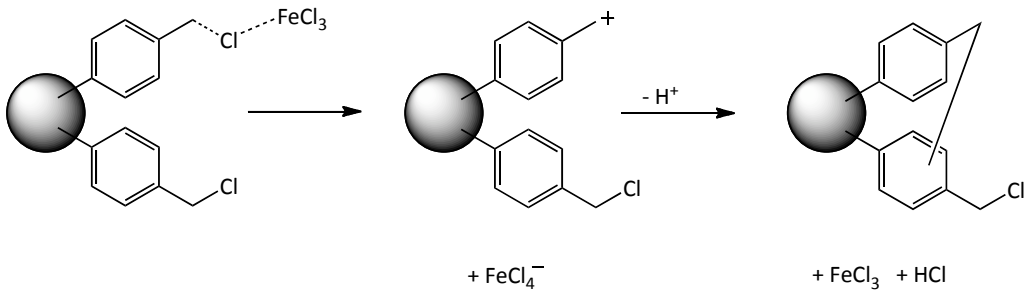

Figure 1.4.3. – Catalytic action of $FeCl_3$.

If the $FeCl_3$ removes Cl to give $FeCl_4^-$ that can form an ionic bond with the H^+ generated upon bridge formation, then lower levels of $FeCl_3$ would ultimately yield products with lower specific surface areas (Figure 1.4.4).

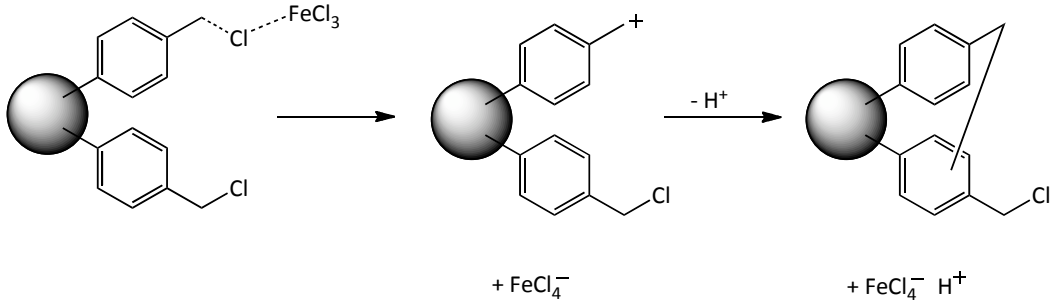

Figure 1.4.4. – $FeCl_4^-$ forming ionic bond with H^+.

In order to carry out the reaction using a 1:1 ratio of $FeCl_3$ relative to Cl in the precursor, the Ahn group needed to use 3.15 g of $FeCl_3$ per 5 g of polymeric precursor, however ultra-high specific surface area products (*i.e.*, specific surface areas in excess of 1,000 m^2/g) were easily obtained with $FeCl_3$ quantities of only 0.25 g. The catalyst quantity had to be reduced to as low as 0.1 g before a fall in the specific surface area of the product was observed, and even at that level of $FeCl_3$ the specific surface area obtained was 880 m^2/g, which is still perfectly acceptable for use of the materials in sorption/chromatographic applications. These results would suggest,

therefore, that the action of the Lewis acid within the reaction is at least partially catalytic.

Fontanals *et al*.[33] found that in the case of a poly(DVB-*co*-VBC) internal electrophile system, the composition of VBC isomers used in a precursor polymerisation can have a direct effect on the specific surface area and also the hydrophilicity of the resulting product. In a comparison of materials made with 100 % *para* isomers (*p*VBC) or a 70:30 mix of *para* and *meta* isomers (mixVBC), an unexpectedly low Cl content was found in the *p*VBC product - 8.4 wt% rather than the expected 20.9 wt% - while the levels of C and H were close to their theoretical values. The Cl content was much higher (18.7 wt%) in the analogous mixVBC product. This microanalytical data indicates the presence of another element, which was subsequently confirmed as oxygen. It was surmised that this was due to hydrolysis of the chloromethyl group, a process which occurs preferentially in the position *para* to the vinyl group in the VBC. This is feasible in high temperature suspension polymerisations which are carried out in water, due to the S_N1 nature of benzyl chloride hydrolysis, which relies on the creation of stabilised carbocation intermediates, followed by nucleophilic attack of water. As the *para* isomer of the monomer is stabilised by five canonical forms *versus* four for the *meta* isomer (four *versus* three, respectively, when present within the polymer), it is expected that carbocations would form much more readily for the *para* isomer, resulting in a more rapid hydrolysis. This is more of a concern in suspension polymerisation, however, since for precipitation polymerisation the lack of an aqueous phase prevents this hydrolysis from taking place.

It would seem that the reduced Cl content in the *p*VBC product would be highly unfavourable on the basis that a higher Cl content would lead to a higher crosslinking degree and hence a higher specific surface area. However, the presence of hydroxyl moieties will increase the hydrophilicity of the hypercrosslinked product, which may then lead to applications in other areas where a degree of hydrophilicity is required. When particles prepared using

both the *p*VBC and mixVBC were hypercrosslinked it was seen that a higher Cl content does indeed lead to a higher specific surface area. However the lower Cl containing *p*VBC resin still afforded a hypercrosslinked material with a specific surface area of 908 m^2/g, which is relatively high. A decrease in the oxygen content of the *p*VBC material upon hypercrosslinking suggested that the hydroxyl groups could also have been participating in the methylene bridge forming reaction, a not unreasonable proposition. It is possible that either the $FeCl_3$ can chlorinate the hydroxymethyl groups, therefore increasing the Cl content or, alternatively, the oxygen of the hydroxyl group might itself be able to coordinate to the powerful $FeCl_3$, hence activating it as a leaving group and allowing bridge formation.[33]

As well as the isomeric composition of VBC, the amount of VBC used in the precursor synthesis also has an effect on the specific surface area obtained upon hypercrosslinking. Fontanals *et al*.[35] found that for precursors from both non-aqueous dispersion (NAD) and precipitation polymerisations the VBC content had to be 50 % (w/w) or higher in order to generate hypercrosslinked materials with ultra-high specific surface areas of above 1,000 m^2/g. Where the VBC content is above 50 % (w/w), 100 % of the pendent aromatic rings present in the polymer should, in theory, be methylene bridged at least once, but preferably more than once.

An intriguing property of hypercrosslinked materials is their ability to sorb not only thermodynamically compatible solvents but also thermodynamically unfavourable or 'poor' solvents,[32,33,35] meaning that they can act in effect as "amphipathic polymer sponges".[35] It is thought that this phenomenon is a result of the initial swollen state in which the hypercrosslinked materials are generated. As the polymers are swollen during the reaction, post-reaction drying of the products, *i.e.*, removal of the solvent, leads to frustrated collapse of the polymer network, leaving behind a material which contains a considerable amount of stress. When this material comes into contact with a solvent, be it hydrophobic or polar, the material is able to regenerate its swollen state and

relieve the stress. Thus, uptake of even an incompatible solvent is favoured over strained existence in the dry state.

1.5. USES OF POLYMER MICROSPHERES

Polymer microspheres found their first use in size-exclusion chromatography, as reported by Moore in 1964.[36] Since then they have found many other applications including, but not limited to, stationary phases in chromatography,[37,38,39,40] as a component of photonic papers and inks[41] and in biomedical applications[42,43] (Figure 1.5.1).

This wide range of applications is a consequence of the superior mechanical strength, chemical, physical and thermal qualities, the solvent resistance characteristics, anti-slip properties and the wide variety of diameters and pore sizes that can be accessed.[11,13,14]

Silica-based stationary phases are the most utilised stationary phase material in chromatography, most likely as a result of the facile synthesis routes, however, they do suffer from a range of drawbacks. Their high cost, poor chemical resistance in acidic and basic conditions and the apparent lack of selectivity due to the residual silanol groups present in modified silica materials, all limit their suitability as chromatography supports. The superior properties of monodisperse polymer materials and the simple synthesis protocols developed in the past 10-15 years could potentially lead to cheaper, more efficient and more stable chromatographic supports.

Chromatographic stationary phases based on uniformly-sized particles out-perform chromatography supports composed of particles with a broad size distribution. Often with larger particles, the broad size distribution can limit the resolution while the presence of fine particles can reduce column permeability resulting in high back-pressures.

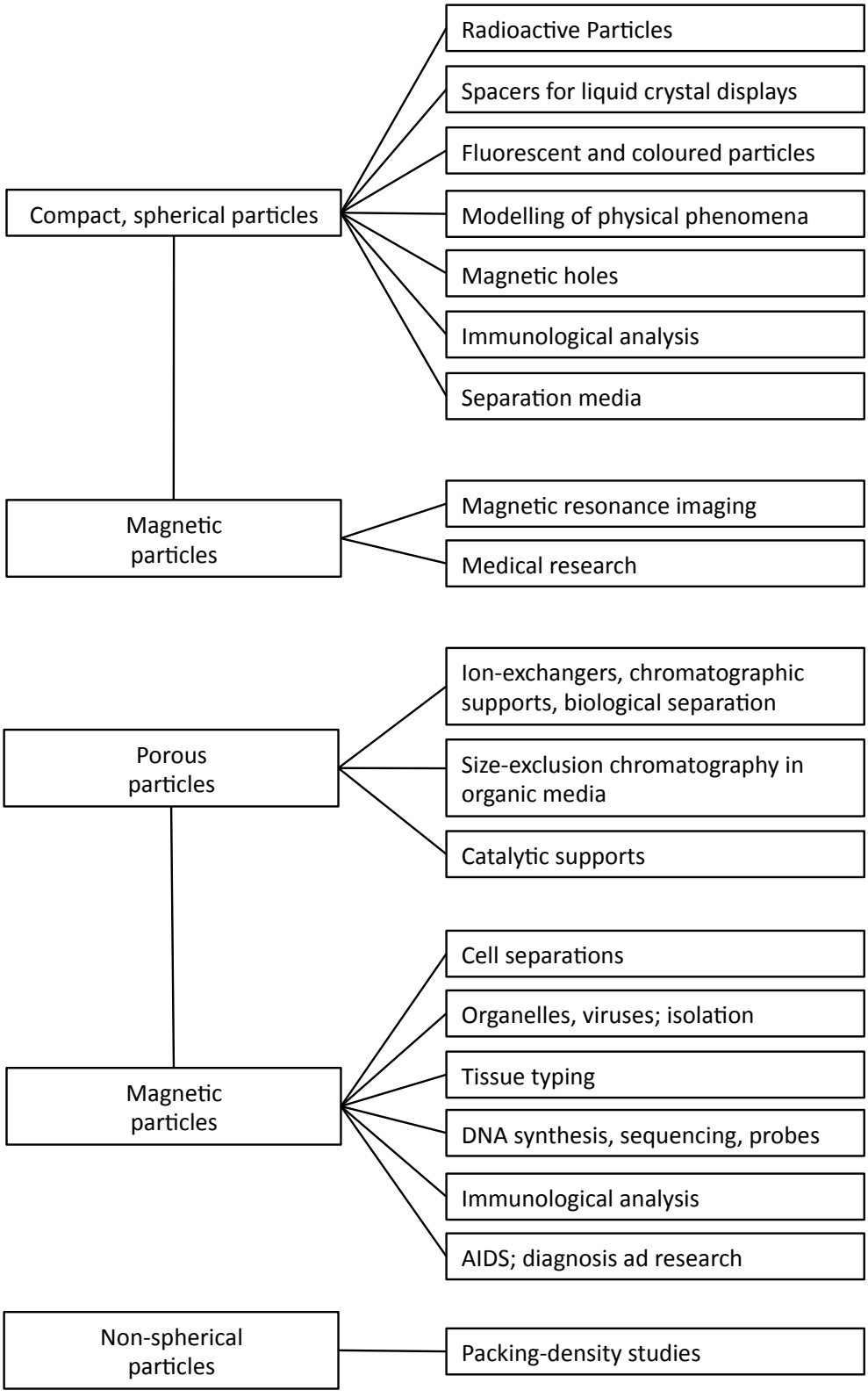

Figure 1.5.1. – Schematic diagram illustrating the wide variety of uses of polymer particles.[37]

Some advantages of monodisperse column packings include: uniform column packing and flow velocity profile; low back-pressure; high resolution; high separation speed. The optimum size distribution when considering back-pressure and resolution is therefore monodisperse.[9,37]

Dawkins *et al*.[44] demonstrated the superiority of a narrow particle size distribution in size exclusion chromatography using mechanically sieved fractions of a material obtained through suspension polymerisation.

1.5.1. Use of Hypercrosslinked Polymers

Hypercrosslinking of polymers introduces micropores into the structure of the polymer and can thus lead to new and exciting uses. The most common use of hypercrosslinked polymers is for the extraction of compounds from aqueous solution. The high specific surface areas and high micropore contents of hypercrosslinked materials have been demonstrated by Davankov[45] and by our group[46] to have improved retention capabilities compared with other polymeric sorbent materials. Chemical functionality, however, further enhances the capability of these materials by enhancing the selectivity. Hypercrosslinked polymer microspheres are available commercially, all with very large particle diameters of several hundred microns.

One series of commercially available hypercrosslinked polymer microspheres is the Hypersol-Macronet resin series from Purolite.[47] These resins are highly crosslinked polystyrene microspheres with diameters in the region of 0.3-1.2 mm and specific surface areas of 800-1,000 m^2/g (as calculated using the BET isotherm). These resins exist as unmodified styrene-based materials as well as styrene materials modified with weak base anion-exchangers. These resins have been widely used throughout the literature for the removal of polar compounds from aqueous solutions. Compounds removed successfully from water using Macronet resins include phenol, aniline,[48] methomyl,[49] acid red

dye,[50] and the endocrine disrupting compounds 17β-estradiol and 17α-ethynyl estradiol.[51] Sulman *et al.*[52] further utilised these hypercrosslinked polymers by introducing ruthenium nanoparticles into the polymer, which allowed for the solid-supported catalysis of the oxidation of D-glucose to D-gluconic acid.

Other commercially available hypercrosslinked sorbents are also available. Li and co-workers[53] aminated a styrene-*co*-DVB based hypercrosslinked polymer, obtained from Jiangsu N&G Environmental Technology Co. Ltd., using dimethylamine and trimethylamine to prepare resins functionalised with weak and strong anion-exchange character respectively. These functionalised resins had specific surface areas in excess of 700 m^2/g and proved successful for the removal of the phenolic compounds phenol, resorcinol and phloroglucin from aqueous solutions. Vergili and Barlas[54] showed that the Lewatit VP OC 1163 HXL resin could be used for the removal of the pesticides and herbicides metalaxyl, 2,4-dichlorophenoxyacetic acid and 2-methyl-4-chlorophenoxyacetic acid from aqueous solution.

Although hypercrosslinked resins can be accessed commercially, many groups choose to prepare hypercrosslinked resins within their own laboratories. Huang and co-workers have prepared a series of hypercrosslinked polymers, using a chloromethylated polystyrene resin, with additional carbonyl functionality, obtained from the Langfang Chemical Co. This chloromethylated resin was then hypercrosslinked using zinc chloride. These hypercrosslinked polymers were used for the removal of phenolic compounds from aqueous solution. The resins were compared to the commercially available Amberlite XAD-4 from Rohm and Haas.[55] This Rohm and Haas resin is a poly(styrene-*co*-divinylbenzene) material, with a particle size of ~0.6 mm and a specific surface area of ~750 m^2/g. The additional carbonyl functionality of the Huang resins proved to be more effective for the removal of phenolic compounds from aqueous solution due to the extra hydrogen bonds occurring between the carbonyl groups of the resin and the hydroxyl group of the phenolic compounds. These resins have been shown to be successful for the removal of phenol,

p-cresol,[56] *p*-nitro phenol,[57] catechol and resorcinol.[58] These resins were also modified with hydroquinone to provide further sites for hydrogen bonding with acidic compounds present in aqueous solution. These hydroquinone-modified polymers displayed lower specific surface areas, of around 450 m^2/g, yet still showed high absorption affinities for the compounds of interest, salicylic acid[59] and *p*-aminobenzoic acid.[60] Reaction of the hypercrosslinked resin with methylamine gave rise to a hypercrosslinked polymer with additional amine functionality which showed a higher adsorption capacity for phenol than the unmodified commercially available resin Amberlite XAD-4, thought to be a result of the better match of polarity of the amine-modified resin and the phenol.[61]

Long and co-workers prepared a styrene-*co*-DVB-*co*-*t*-butyl polymer, which was chloromethylated in a post-polymerisation reaction with monochloromethyl ether and subsequently hypercrosslinked using zinc chloride. These hypercrosslinked polymer beads were then applied successfully for the removal of the volatile organic compounds 1,2-dichloroethane, trichloromethane[62] and trichloroethylene[62,63] from a humid nitrogen gas stream.

Within our own group, hypercrosslinked polymer microspheres prepared by the precipitation polymerisation of DVB and VBC monomers, followed by a Friedel-Crafts catalysed crosslinking reaction, have been functionalised and used successfully as selective solid-phase extraction sorbents for the analysis of pharmaceuticals from water samples. Addition of a third, polar monomer in the initial polymerisation carried out by Bratkowska *et al*.[64] led to microspheres with a more pronounced hydrophilic character for the extraction of polar contaminants from water. Introduction of weak anion-[65,66] and weak cation-exchange[67] functionality also allowed for the selective extraction of acidic and basic pharmaceutical compounds from complex environmental water samples.

Li *et al*.[68] showed that microporous, hypercrosslinked, suspension polymerisation-derived DVB/VBC microspheres were much better suited for

the removal of toxic metal ions (Pb^{2+}, Cu^{2+}, Ni^{2+} and Cr^{3+}) from water than similar materials with only macro- and mesopores in their structure. It was surmised that the enhanced absorption of the metal ions upon introduction of the micropores through hypercrosslinking was due to a better compatibility between the size of the metal ions and the pores. In addition to the microporous structure, the adsorption was also improved by the introduction of sulfonic acid groups (and hence greater hydrophilicity) into the polymer; the sulfonic acid groups were introduced through reaction of the polymer with acetyl sulfate.

Hypercrosslinked polymers have also been shown to work well when applied as materials for gas storage and capture. Svec *et al.*[69] investigated hypercrosslinked poly(DVB-*co*-VBC), prepared *via* suspension polymerisation, as hydrogen storage materials. The hypercrosslinking reaction afforded polymers with specific surface areas of up to 1,930 m^2/g that could reversibly store 1.5 wt% hydrogen at 0.15 MPa and 77.3 K. These storage levels were shown to be comparable with the commercially available hypercrosslinked polymer Hypersol-Macronet MN200 (1.3 wt% hydrogen at 0.12 MPa). While the results were promising, the materials failed to meet the level of 6 wt% being chased by Svec and co-workers, which was, at the time, the target set by the U.S. Department of Energy for hydrogen storage materials. Cooper and co-workers[70] prepared hypercrosslinked polymers through self-condensation of bischloromethyl monomers and found that a network based upon 4,4'-*bis*(chloromethyl)-1,1'-biphenyl displayed a specific surface area of 1,900 m^2/g and was able to store 3.68 wt% of hydrogen at 1.5 MPa and 77.3 K. Similar materials prepared by the Cooper group showed CO_2 uptakes of up to 59 wt% at room temperature and 3 MPa.[71]

1.6. POLYMER MODIFICATION

Polymers bearing the required functionalities to allow them to be used for a specific application can be synthesised using two distinct strategies; post-polymerisation chemical modification reactions and the incorporation of a functional comonomer in the initial polymerisation. Post-polymerisation modification is based on the direct polymerisation of monomers possessing a substituent that is inert in terms of the polymerisation conditions but which can undergo facile conversion in a subsequent, or series of subsequent, chemical reaction(s) to give one or more functional groups.[72] Where possible, a functional monomer can be introduced into the polymerisation to remove the need for a modification step, however some of these groups may not be suitable, in precipitation polymerisation for example, in terms of solvent compatibility.

With polymeric materials based on DVB, a wide variety of post-polymerisation modifications can be carried out due to the reactivity and availability of aromatic rings. The electron-rich aromatic π-system on DVB rings will readily react in electrophilic aromatic substitution reactions. A wide variety of components can be introduced in this way, such as halogens, nitro groups and sulfonate groups, as well as alkyl and acyl side chains by means of Friedel-Crafts reactions. Any substituents that are introduced into the aromatic ring can then also be further reacted in order to access products that cannot be directly accessed in this manner, such as carboxylic acids. Carboxylic acids can instead be accessed *via* Friedel-Crafts alkylation of the aromatic ring followed by subsequent oxidative cleavage of the alkyl group by aqueous $KMnO_4$ to yield the carboxylic acid. Unreacted, pendent vinyl groups derived from DVB can also be exploited in post polymerisation modification reactions.

Any reactive handles that can be introduced through incorporation of an appropriate comonomer should, in theory, be able to react in a facile manner to introduce new functionalities. Many monomers have been polymerised under different conditions, giving polymers that can be further functionalised in a

facile manner. A wide range of functional monomers can be polymerised by free radical polymerisation and then be reacted further in post-polymerisation chemical modification reactions (Table 1.6.1).

Monomer	*Final Functionality*	*Reference*
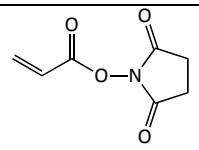	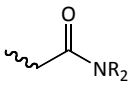	73,74,75, 76,77,78
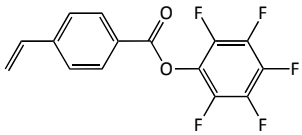	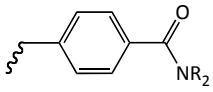	79
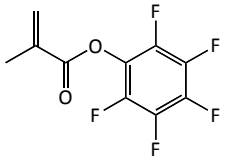	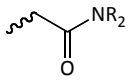	80
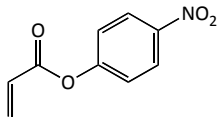	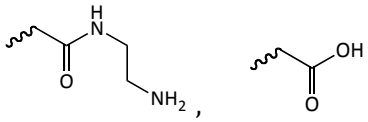	81
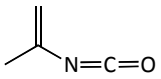	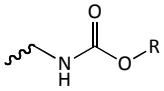	82,83
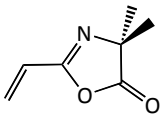	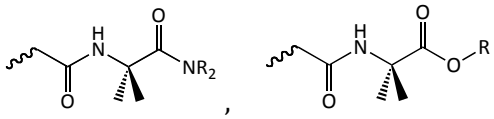	84,85,86
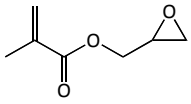	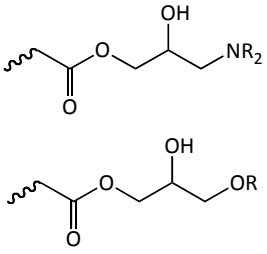	87,88
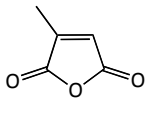	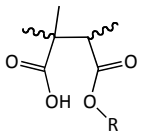	89

Table 1.6.1. – Functional monomers and their subsequent modification.

In many cases, the functionalities introduced through these post-polymerisation modifications allow the polymers to be used for a variety of new applications in which the unmodified polymer alone would not be suitable, for example, biological applications.

Mammen *et al*.[73] prepared polymers containing a sialic acid component by first synthesising an activated polymer, poly(*N*-acryloyloxysuccinimide), then reacting this with an amine-terminated sialic acid derivative. It was found that polymers prepared using this post-polymerisation functionalisation route were more than two orders of magnitude better at inhibiting hemagglutination in the influenza virus than similar polymers prepared by direct copolymerisation of a sialic acid-containing monomer. Smith *et al*.[74] increased the efficiency of thermoreversible poly(*N*-isopropylacrylamide), polyNIPAM, for use in tissue engineering by copolymerising the *N*-isopropylacrylamide with *N*-acryloyloxysuccinimide, which then allowed post-polymerisation addition of an arginine-glycine-aspartic acid peptide to improve the interaction between the polymer and mammalian cells.

Other interesting materials can also be accessed *via* this route, with Beyer *et al*.,[83] showing that polymers containing hemicyanine dyes were best prepared through reaction of isocyanate-containing polymers with a hydroxyl-containing dye molecule, as the double bond of the chromophore could potentially allow for network formation during a radical polymerisation of a monomeric compound of the dye.

1.6.1. Chemical Modification of Polymer Microspheres

Modification of polymer microspheres has also been the subject of several studies. As crosslinkers with two or more vinyl groups are used in the preparation of polymer microspheres, they can often contain unreacted vinyl moieties. Where present, these can be further reacted to provide a variety of

new functionalities. Strainx *et al.*[90] prepared polydivinylbenzene (polyDVB) microspheres and utilised the unreacted vinyl groups present in a series of addition reactions (Figure 1.6.1.1).

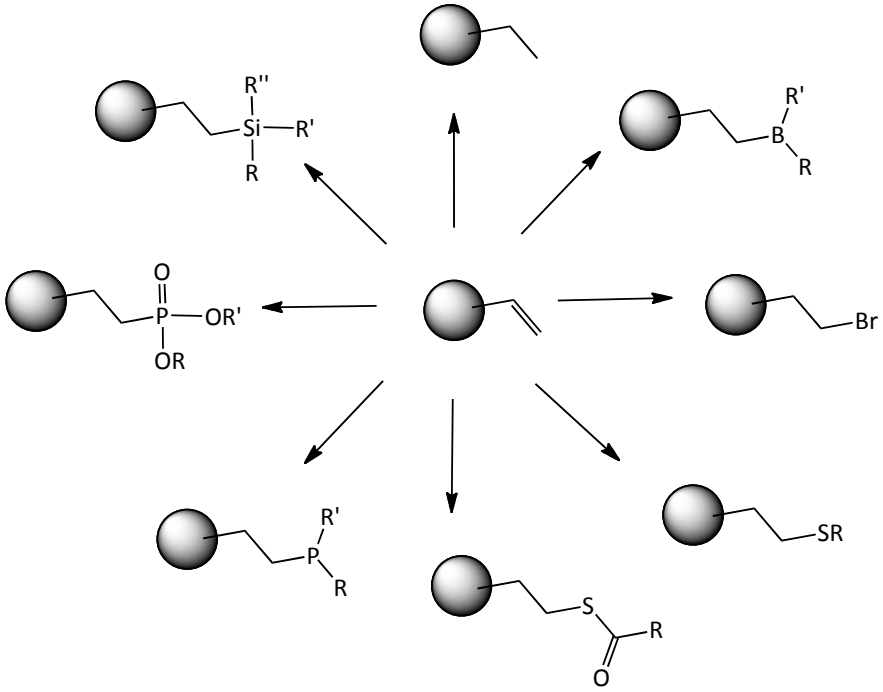

Figure 1.6.1.1. – Functionalisation of polydivinylbenzene microspheres.[90]

Kawaguchi *et al.*[91] prepared a styrene/acrylamide polymer latex by emulsifier-free aqueous polymerisation, and utilised the amide functionality in a variety of reactions to provide new functionalities. The amide functionality was converted to: carboxylic acid groups by hydrolysis; to hydroxyl groups by reaction with formaldehyde; to primary amines by the Hoffman reaction; and to tertiary amines by the Mannich reaction. By using one single batch of polymer particles, a series of polymers with different functionalities could be prepared with consistent particle sizes.

Nebhani *et al.*[92] functionalised polyDVB microspheres using two different 'grafting-to' approaches. In the first approach, a cyclopentadiene functionality was inserted into the microspheres, which could then be further reacted in a

rapid hetero-Diels-Alder (HDA) reaction with the thiocarbonyl-thio end groups of a styrene polymer prepared by reversible addition-fragmentation chain-transfer (RAFT) polymerisation. In the second approach, the residual vinyl groups already present on the microspheres were utilised as the diene, thus a highly reactive dienophile was required in order to react with the styrenic moieties; the second-generation RAFT-HDA agent, benzyl phenylsulfonyldithioformate was therefore employed. These reactions were carried out under relatively mild, catalyst-free conditions, which is very attractive.

Both the azide-alkyne cycloaddition and thiol-ene reactions from the Sharpless[93] 'click chemistry' family have been utilised widely for functionalisation of microspheres. In order to incorporate azide and alkyne functionality into the microspheres, various post-polymerisation reactions have been carried out. Breed *et al*.[94] prepared polymer microspheres with vinylbenzyl chloride included as a comonomer and subsequently utilised the pendent chloromethyl groups in reacton with sodium azide to install azide moieties in the polymer. The groups of Fréchet[95] and Du Prez[96] prepared glycidyl methacrylate containing-microspheres, which contained epoxide groups that could be easily opened by reaction with sodium azide to provide azide functionality in the polymer. As a complementary material to their azide-functionalised microspheres, the Fréchet group also prepared alkyne-containing microspheres through the use of propargyl acrylate as a comonomer.[95] Karagoz[97] and co-workers introduced an azide functionality into polyDVB microspheres by first brominating pendent, unreacted vinyl groups and then converting the bromine moieties to azide by reaction with sodium azide. Oyelere[98] 'unmasked' azide groups on an amine-functionalised resin by reacting the amine moities in a diazo-transfer reaction with triflyl azide. Welser *et al*.[99] used a slightly different approach and polymerised azide and alkyne containing comonomers in order to provide the handles required for click chemistry functionalisation. Propargyl acrylamide was used to install alkyne handles, while *N*-(11-azido-3,6,9-trioxaundecanyl)acrylamide gave the desired azide

functionality. In all cases, the azide- and alkyne–containing microspheres were further functionalised under click chemistry conditions.

Stenzel and co-workers[100] prepared microspheres with activated double bonds, *i.e.*, α,β-unsaturated carbonyl compounds, using two different methods. In the first, ethylene glycol dimethacrylate (EGDMA) microspheres were prepared by suspension polymerisation, and in the second a Wang resin was modified using acryloyl chloride. Once formed, these microspheres were then functionalised further by thiol-ene click chemistry using glucothiose. Only after functionalisation with the glucose moiety were these microspheres able to specifically bind the protein Concanavalin A.

Müller and co-workers[101] combined the thiol-ene and azide-alkyne click chemistry strategies for microsphere functionalisation. The residual vinyl groups present in polyDVB microspheres were reacted in a thiol-ene reaction with an azide end-capped thiol, 1-azidoundecanethiol. The terminal azide was then further reacted in an azide-alkyne cycloaddition reaction with alkyne end-functionalised poly(hydroxyethyl methacrylate), polyHEMA.

Gokmen *et al.*[102] studied the post-polymerisation functionalisation of thiol-containing microspheres, not only in thiol-ene click chemistry reactions, but in other reactions too. A variety of compounds were added to the thiol (Figure 1.6.1.2). The order in which the reactions occurred, in terms of reaction time, was isocyanate > norbornene > acrylate ≈ isothiocyanate > maleimide ≈ isolated ene > α-bromo ester > epoxides ≈ aziridine.

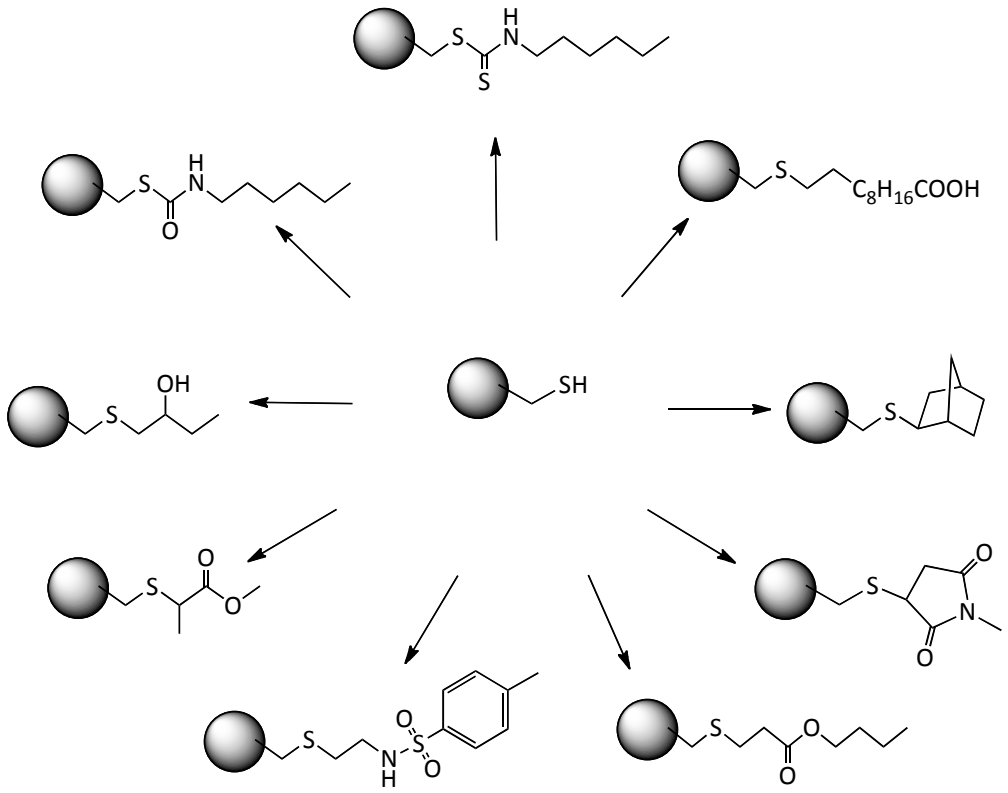

Figure 1.6.1.2. – Overview of thiol-X reactions performed on thiol-containing beads.

Immunomicrospheres, *i.e.*, microspheres functionalised with antibodies and proteins, have also been the subject of several studies. Rembaum *et al.*[103] reacted amine-containing microspheres with glutaraldehyde, followed by reaction of the second glutaraldehyde carbonyl group with the amine of a protein. Betton *et al.*[104] first activated methacrylic acid containing microspheres by forming an active ester with *N*-hydroxysulfosuccinimde, followed by reaction with a protein-bound amine. Marumoto *et al.*[105] prepared methacrylic acid containing polymers by emulsion polymerisation. The carboxylic acid groups present were reacted with both a diamine and an amino acid compound to provide amine and carboxylate functionalised particles that could be coupled to protein molecules. Arıca *et al.*[106] activated the hydroxyl groups of polyHEMA microspheres *via* reaction with epichlorohydrin. These activated microspheres were then reacted with protein molecules.

1.7. PHD HYPOTHESIS AND AIMS

Hypercrosslinked polymer microspheres have been shown to be useful in several fields of application due to their high chemical and thermal stability, their ease of production and low production cost. Addition of extra functionality could greatly enhance their application in these fields, whilst also opening them up to new areas of application. Facile routes for functionalisation are therefore required in order to further explore the potential of hypercrosslinked polymers.

The main aims of this PhD study were as follows:

1. To prepare hypercrosslinked polymer microspheres with strong cation-exchange (SCX) functionality and to apply these as SCX solid-phase extraction (SPE) sorbents for the selective extraction of basic pharmaceuticals from complex real water samples.
2. To prepare hypercrosslinked polymer microspheres with strong anion-exchange (SAX) functionality and to apply these in SAX SPE for the extraction of acidic pharmaceuticals from complex real water samples.
3. To prepare ultra-high specific surface area hypercrosslinked polymer microspheres that can be functionalised using azide-alkyne cycloaddition 'click chemistry' reactions.

1.8. REFERENCES

1. D. D. Ebbing and S. D. Gammon, *General Chemistry*, *Seventh Edition*, Houghton Mifflin, Boston, 2002, Chpt. 25.
2. J. M. G. Cowie and V. Arrighi, *Polymers: Chemistry and Physics of Modern Materials*, *Third Edition*, CRC Press, USA, 2008, Chpts. 1 and 3.
3. D. C. Sherrington, *Chem. Commun.*, (1998), 2275-2286.
4. R. Arshady, *Colloid Polym. Sci.*, (1992), **270**, 717-732.
5. K. Li and H. D. H. Stöver, *J. Polym. Sci. Part A: Polym. Chem.*, (1993), **31**, 3257-3263.

6. C. H. Bamford, A. Ledwith and P. K. Sen Gupta, *J. Appl. Polym. Sci.*, (1980), **25**, 2559-2566.
7. S. E. Shim, S. Yang, H. H. Choi and S. Choe, *J. Polym. Sci. Part A: Polym. Chem.*, (2004), **42**, 835-845.
8. J. S. Downey, R. S. Frank, W.-H. Li and H. D. H. Stöver, *Macromolecules*, (1999), **32**, 2838-2844.
9. W.-H. Li and H. D. H. Stöver, *J. Polym. Sci. Part A: Polym. Chem.*, (1998), **36**, 1543-1551.
10. W.-H. Li, K. Li and H. D. H. Stöver, *J. Polym. Sci. Part A: Polym. Chem.*, (1999), **37**, 2295-2303.
11. J. M. Jin, S. Yang, S. E. Shim and S. Choe, *J. Polym. Sci. Part A: Polym. Chem.*, (2005), **43**, 5343-5346.
12. W.-H. Li and H. D. H. Stöver, *J. Polym. Sci. Part A: Polym. Chem.*, (1999), **37**, 2899-2907.
13. S. Yang, S. E. Shim and S. Choe, *J. Polym. Sci. Part A: Polym. Chem.*, (2005), **43**, 1309-1311.
14. R. S. Frank, J. S. Downey and H. D. H. Stöver, *J. Polym. Sci. Part A: Polym. Chem.*, (1998), **36**, 2223-2227.
15. E. C. C. Goh and H. D. H. Stöver, *Macromolecules*, (2002), **35**, 9983-9989.
16. L. Ye, P. A. G. Cormack and K. Mosbach, *Anal. Commun.*, (1999), **36**, 35-38.
17. J. Wang, P. A. G. Cormack, D. C. Sherrington and E. Khoshdel, *Pure Appl. Chem.*, (2007), **79**, 1503-1517.
18. E. Turiel, J. L. Tadeo, P. A. G. Cormack and A. Martin-Esteban, *Analyst*, (2005), **130**, 1601-1607.
19. A. Beltran, R. M. Marcé, P. A. G. Cormack and F. Borrull, *J. Chromatogr. A*, (2009), **1216**, 2248-2253.
20. C. M. Hansen, *Hansen Solubility Parameters: A User's Handbook*, *2nd Edition*, C. R. C. Press, Florida, 2007.
21. J. H. Hildebrand, *The Solubility of Non-Electrolytes*, Reinhold , New York, 1936.
22. http://cool-palimpsest.stanford.edu/byauth/burke/solpar/solpar2.html (accessed on 13 Feb 2009)
23. http://cool-palimpsest.stanford.edu/byauth/burke/solpar/solpar6.html (accessed on 13 Feb 2009)
24. http://gozips.uakron.edu/~mattice/ps674/excl.htm (accessed on 13 Feb 2009)

25. J. Hermans, *J. Chem. Phys.*, (1982), **77**, 2193-2203.
26. P. J. Flory, *Principles of Polymer Chemistry*, Cornell University Press, New York, 1953, Chpt. 12.
27. K. Yoshimatsu, K. Reimhult, A. Krozer, K. Mosbach, K. Sode and L. Ye, *Anal. Chim. Acta*, (2007), **584**, 112-121.
28. S. E. Shim, S. Yang, M.-J. Jin, Y. H. Chang and S. Choe, *Colloid Polym. Sci.*, (2004), **283**, 41-48.
29. V. A. Davankov, S. V. Rogoshin and M. P. Tsyurupa, *J. Polym. Sci.*, (1974), **47**, 95-101.
30. M. P. Tsyurupa, V. A. Davankov and S. V. Rogozhin, *J. Polym. Sci.*, (1974), **47**, 189-195.
31. X. Zhang, S.Shen and L. Fan, *J. Mater. Sci.*, (2007), **42**, 7621-7629.
32. J.-H. Ahn, J.-E. Jang, C.-G. Oh, S.-K. Ihm, J. Cortez and D. C. Sherrington, *Macromolecules*, (2006), **39**, 627-632.
33. N. Fontanals, J. Cortés, M. Galià, R. M. Marcé, P. A. G. Cormack, F. Borrull and D. C. Sherrington, *J. Polym. Sci. Part A: Polym. Chem.*, (2005), **43**, 1718-1728.
34. F. S. MacIntyre, D. C. Sherrington and L. Tetley, *Macromolecules*, (2006), **39**, 5381-5384.
35. N. Fontanals, P. Manesiotis, D. C. Sherrington and P. A. G. Cormack, *Adv. Mater.*, (2008), **20**, 1298-1303.
36. J. C. Moore, *J. Polym. Sci. Part A*, (1964), **2**, 835-843.
37. T. Ellingsen, O. Aune, J. Ugelstad and S. Hagen, *J. Chromatogr.*, (1990), **535**, 147-161.
38. B. E. Christensen, M. H. Myhr, O. Aune, S. Hagen, A. Berge and J. Ugelstad, *Carbohydrate Polym.*, (1996), **29**, 217-223.
39. M. Galia, F. Svec and J. M. J. Fréchet, *J. Polym. Sci. Part A: Polym. Chem.*, (1994), **32**, 2169-2175.
40. W.-H. Li, A. E. Hamielec and H. D. H. Stöver, *J. Polym. Sci. Part A: Polym. Chem.*, (1994), **32**, 2029-2038.
41. H. Fudouzi and Y. Xia, *Adv. Mater.*, (2003), **15**, 892-896.
42. V. L. Covolan, L. H. Mei and C. L. Rossi, *Polym. Adv. Technol.*, (1997), **8**, 44-50.
43. J. Ugelstad, P. C. Mørk, R. Schmid, T. Ellingsen and A. Berge, *Polym. Int.*, (1993), **30**, 157-168.
44. J. V. Dawkins, T. Stone and G. Yeadon, *Polymer*, (1977), **18**, 1179-1184.

45. V. Davankov, L. Pavlova, M. Tsyurupa, J. Brady, M. Balsamo and E. Yousha, *J. Chromatogr. B: Biomed. Sci. and Application*, (2000), **739**, 73-80.
46. N. Fontanals, M. Galia, P. A. G. Cormack, R. M. Marcé, D. C. Sherrington and F. Borrull, *J. Chromatogr. A*, (2005), **1075**, 51-56.
47. http://www.purolite.com/Customized/Uploads/MACRONET_Brochure_062503.pdf (accessed on 19 Jul 2012).
48. C. Valderrama, J. I. Barios, A. Farran and J. L. Cortina, *Water Air Soil Pollut.*, (2010), **210**, 421-434.
49. C.-F. Chang, C.-Y. Chang, K.-E. Hsu, S.-C. Lee and W. Höll, *J. Hazardous Mater.*, (2008), **155**, 295-304.
50. C. Valderrama, J. L. Cortina, A. Farran, X. Gamisans and F. X. de las Heras, *React. Funct. Polym.*, (2008), **68**, 679-691.
51. B. Saha, E. Karounou and M. Streat, *React. Funct. Polym.*, (2010), **70**, 531-544.
52. E. Sulman, V. Doluda, S. Dzwigaj, E. Marceau, L. Kustov, O. Tkachenko, A. Bykov, V. Mateeva, M. Sulman and N. Lakina, *J. Mol. Catal. A: Chem.*, (2007), **278**, 112-119.
53. Z.-M. Jiang, A.-M. Li, J.-G. Cai, C. Wang and Q.-X. Zhang, *J. Environ. Sci.*, (2007), **19**, 135-140.
54. I. Vergili and H. Barlas, *Desalination*, (2009), **249**, 1107-1114.
55. http://www.rohmhaas.com/ionexchange/pharmaceuticals/xad.htm (accessed on 19 Jul 2012).
56. J. Huang, *J. Hazardous Mater.*, (2009), **168**, 1028-1034.
57. J. Huang, C. Yan and K. Huang, *J. Colloid and Interface Sci.*, (2009), **332**, 60-64.
58. J. Huang, K. Huang and C. Yan, *J. Hazardous Mater.*, (2009), **167**, 69-74.
59. J. Huang, *J. Appl. Polym. Sci.*, (2011), **121**, 3717-3723.
60. X. Wang, J. Huang and K. Huang, *Chem. Eng. J.*, (2010), **162**, 158-163.
61. C. He, J. Huang, J. Liu, L. Deng and K. Huang, *J. Appl. Polym. Sci.*, (2011), **119**, 1435-1442.
62. C. Long, P. Liu, Y. Li, A. Li and Q. Zhang, *Environ. Sci. Technol.*, (2011), **45**, 4506-4512.
63. P. Liu, C. Long, H. M. Qian, Y. Li, A. M. Li and Q. X. Zhang, *Chinese Chem. Lett.*, (2009), **20**, 492-495.
64. D. Bratkowska, N. Fontanals, F. Borrull, P. A. G. Cormack, D. C. Sherrington and R. M. Marcé, *J. Chromatogr. A*, (2010), **1217**, 3238-3243.

65. N. Fontanals, P. A. G. Cormack and D. C. Sherrington, *J. Chromatogr. A*, (2008), **1215**, 21-29.
66. N. Fontanals, P. A. G. Cormack and D. C. Sherrington, R. M. Marcé and F. Borrull, *J. Chromatogr. A*, (2010), **1217**, 2855-2861.
67. D. Bratkowska, R. M. Marcé, P. A. G. Cormack, D. C. Sherrington, F. Borrull and N. Fontanals, *J. Chromatogr. A*, (2010), **1217**, 1575-1582.
68. B. Li, F. Su, H.-K. Luo, L. Liang and B. Tan, *Microporous and Mesoporous Mater.*, (2011), **138**, 207-214.
69. J. Germain, J. Hradil, J. M. J. Fréchet and F. Svec, *Chem. Mater.*, (2006), **18**, 4430-4435.
70. C. D. Wood, B. Tan, A. Trewin, H. Niu, D. Bradshaw, M. J. Rosseinsky, Y. Z. Khimyak, N. L. Campbell, R. Kirk, E. Stöckel and A. I. Cooper, *Chem. Mater.*, (2007), **19**, 2034-2048.
71. C. F. Martin, E. Stöckel, R. Clowes, D. J. Adams, A. I. Cooper, J. J. Pis, F. Rubiera and C. Pevida, *J. Mater. Chem.*, (2011), **21**, 5475-5483.
72. M. A. Gauthier, M. I. Gibson and H.-A. Klok, *Angew. Chem. Int. Ed.*, (2009), **48**, 48-58.
73. M. Mammen, G. Dahmann and G. M. Whitesides, *J. Med. Chem.*, (1995), **38**, 4179-4190.
74. E. Smith, J. Bai, C. Oxenford, J. Yang, R. Somayaji and H. Uludag, *J. Polym. Sci. Part A: Polym. Chem.*, (2003), **41**, 3989-4000.
75. S. R. A. Devenish, J. B. Hill, J. W. Blunt, J. C. Morris and M. H. G. Munro, *Tetrahedron Lett.*, (2006), **47**, 2875-2878.
76. E. Pedone, X. Li, N. Koseva, O. Alpar and S. Brocchini, *J. Mater. Chem.*, (2003), **13**, 2825-2837.
77. H.-G. Batz, G. Franzmann and H. Ringsdorf, *Angew. Chem. Int. Ed.*, (1972), **11**, 1103-1104.
78. P. Ferruti, A. Bettelli and A. Feré, *Polymer*, (1972), **13**, 462-464.
79. K. Nilles and P. Theato, *Eur. Polym. J.*, (2007), **43**, 2901-2912.
80. M. Eberhardt, R. Mruk, R. Zentel and P. Theato, *Eur. Polym. J.*, (2005), **41**, 1569-1575.
81. L. Ye, P. A. G. Cormack and K. Mosbach, *Anal. Chim. Acta*, (2001), **435**, 187-196.
82. M. Dörr, R. Zentel, R. Dietrich, K. Meerholz, C. Bräuchle, J. Wichern, S. Zippel and P. Boldt, *Macromolecules*, (1998), **31**, 1454-1465.

83. D. Beyer, W. Paulus, M. Seitz, G. Maxein, H. Ringsdorf and M. Eich, *Thin Solid Films*, (1995), **271**, 73-83.
84. B. Guichard, C. Noël, D. Reyx, M. Thomas, S. Chevalier and J.-P. Senet, *Macromol. Chem. Phys.*, (1998), **199**, 1657-1674.
85. J. K. Rasmussen, S. M. Heilmann, L. R. Krepski, K. M. Jensen, J. Mickelson, K. Z. Johnson, P. L. Coleman, D. S. Milbrath and M. M. Walker, *React. Polym.*, (1992), **16**, 199-212.
86. D. C. Tully, M. J. Roberts and B. H. Geierstanger, *Macromolecules*, (2003), **36**, 4302-4308.
87. S. Edmondson and W. T. S. Huck, *J. Mater. Chem.*, (2004), **14**, 730-734.
88. V. Tsyalkovsky, V. Klep, K. Ramaratnam, R. Lupitskyy, S. Minko and I. Luzinov, *Chem. Mater.*, (2008), **20**, 317-325.
89. G. Kahraman, O, Beşkardeş, Z. M. O. Rzaev and E. Pişkin, *Polymer*, (2004), **45**, 5813-5828.
90. B. R. Strainx, J. P. Gao, R. Barghi, J. Salha, and G. D. Darling, *J. Org. Chem.*, (1997), **62**, 8987-8993.
91. H. Kawaguchi, H. Hoshino, H. Amagasa and Y. Ohtsuka, *J. Colloid Interface Sci.*, (1984), **97**, 465-475.
92. L. Nebhani, D. Schmiedl, L. Barner and C. Barner-Kowollik, *Adv. Funct. Mater.*, (2010), **20**, 2010-2020.
93. H. C. Kolb, M. G. Finn and K. B. Sharpless, *Angew. Chem. Int. Ed.*, (2001), **40**, 2004-2021.
94. D. R. Breed, R. Tibault, F. Xie, Q. Wang, C. J. Hawker and D. J. Pine, *Langmuir*, (2009), **25**, 4370-4376.
95. M. Slater, M. Snauko, F. Svec and J. M. J. Fréchet, *Anal. Chem.*, (2006), **78**, 4969-4975.
96. M. T. Gokmen, W. Van Camp, P. J. Colver, S. A. F. Bon and F. E. Du Prez, *Macromolecules*, (2009), **42**, 9289-9294.
97. B. Karagoz, Y. Y. Durmaz, B. N. Gacal, N. Bicak and Y. Yagci, *Designed Monomers Polymers*, (2009), **12**, 511-522.
98. A. K. Oyelere, P. C. Chen, L. P. Yao and N. Boguslavsky, *J. Org. Chem.*, (2006), **71**, 9791-9796.
99. K. Welser, M. D. A. Perera, J. W. Aylott and W. C. Chan, *Chem. Commun.*, (2009), 6601-6603.

100. W. Gu, G. Chen and M. H. Stenzel, *J. Polym. Sci. Part A: Polym. Chem.*, (2009), **47**, 5550-5556.
101. A. S. Goldmann, A. Walther, L. Nebhani, R. Joso, D. Ernst, K. Loos, C. Barner-Kowollik, L. Berner and A. H. E. Müller, *Macromolecules*, (2009), **42**, 3707-3714.
102. M. T. Gokmen, J. Brassinne, R. A. Prasath and F. E. Du Prez, *Chem. Commun.*, (2011), **47**, 4652-4654.
103. A. Rembaum, S. P. S. Yen and R. S. Molday, *J. Macromol. Sci. Chem.*, (1979), **A13**, 603-632.
104. F. Betton, A. Theretz and E. C. Pichot, *Colloids Surfaces B: Biointerfaces*, (1993), **1**, 97-106.
105. K. Marumoto, T. Suzuta, H. Noguchi and Y. Uchida, *Polymer*, (1978), **19**, 867-871.
106. M. Y. Arıca, V. Hasırcı and N. G. Alaeddinoğlu, *Biomaterials*, (1995), **16**, 761-768.

CHAPTER 2

SYNTHESIS, CHARACTERISATION AND APPLICATION OF HYPERCROSSLINKED POLYMER MICROSPHERES WITH STRONG CATION-EXCHANGE PROPERTIES

2.1. INTRODUCTION

While polymers and copolymers themselves can have many interesting properties and therefore a wide variety of uses, the introduction of new functional groups through copolymerisation or post-polymerisation chemical modification reactions can change the properties in a beneficial way and thus provide further potential for application.

2.1.1. Cation-Exchange Resins

In ion-exchange resins, such as those utilised in ion-exchange chromatography, the ion-exchange character is imparted on the resin by means of weak acids and bases. Sulfonic acid groups are used to provide resins with strong cation-exchange (SCX) character, while weaker carboxylic acid functionality gives rise to a weak cation-exchange (WCX) resin. Complementary to this, quaternary ammonium ions can be introduced to provide strong anion-exchange (SAX) character, while amine moieties set in place weak anion-exchange (WAX) capability.[1]

In cation-exchange resins, the acidic protons from a sulfonic acid or carboxylic acid group are able to exchange with other cations present in a sample (Figure 2.1.1.1). The equilibrium can be shifted to the left by increasing $[H^+]$ or to the right by increasing $[M^{n+}]$. Alternatively, reducing the concentration of either one of these components with respect to the amount of resin will also change the position of the equilibrium.[1]

$$nRzSO_3^- \ ^+H + M^{n+} \rightleftharpoons (RzSO_3)_nM + nH^+$$

$$nRzCO_2^- \ ^+H + M^{n+} \rightleftharpoons (RzCO_2)_nM + nH^+$$

Figure 2.1.1.1. – Exchange of protons on cation-exchange resins (Rz = resin).

Although the mode by which strong and weak cation-exchangers work is similar, their applications can be quite different. SCX resins can be used across the whole pH range from 1-14, while WCX resins are more restricted and can be used only between pH 5 and 14. This is due to the fact that at low pH values the WCX resins will interact so strongly with their protons that exchange cannot occur. WCX resins are also less efficient at removing the cations of very weak bases compared to SCX resins, which will remove them completely. SCX resins are particularly favoured for complex mixtures. WCX resins are, however, favoured for the separation of strongly basic or multifunctional ionic substances, such as proteins or peptides. SCX resins are less useful in these circumstances as they will strongly retain such analytes and therefore hinder the separation process.[1]

The ion-exchange capacity (IEC) of a cation-exchange resin is the total number of equivalents of hydrogen ions per unit weight of resin that can be replaced by another cation. The IEC is an important factor that affects the retention of cations. When separating complex mixtures it is often favourable to use an ion-exchange resin that has a high capacity as the increased retention will improve the resolution achieved.[1] The higher the IEC of the material, the larger is the sample volume that can be supported in the column without adversely affecting the separation efficiency. Where all other parameters are kept constant, the level of analyte retained and detected is linearly correlated to the IEC.

2.1.2. Use of Sulfonated Polymers

Sulfonated polymers have found use in a variety of applications, including proton-exchange membranes,[2,3,4,5] fuel cells,[6] ion-exchange chromatography supports,[7,8] solid-phase extraction sorbents[9] and conducting materials.[10]

Rubringer *et al*.[11] tested sulfonated polystyrene for use in humidity sensing applications. Films of polystyrene and sulfonated polystyrene were dip-coated onto ceramic disks and compared to assess the effect of the addition of sulfonic acid groups into the material. Saturated solutions of various salts were used to create different levels of relative humidity for impedance measurements to be taken. Overall, the results forthcoming from the study showed that an easily prepared, inexpensive, sulfonated polystyrene material was a very promising contender for use as a resistive-type humidity sensor.

Polymer-bound sulfonic acid groups can also be utilised as sorbents for protein separations. Nordborg *et al*.[12] used a series of reactions to modify divinylbenzene (DVB)-based particles, to give a combination of hydrophilicity and surface sulfonic acid groups. These were then applied as sorbents in ion-exchange chromatography for the separation of a mixture of four proteins, myoglobin, ribonuclease A, cytochrome C and lysozyme. Experiments carried out using control particles showed that the separation was in fact due to the presence of sulfonic acid moieties and not due to hydrophobic interactions with the DVB backbone of the particle. Dieterle *et al*.[13] investigated the mode of adsorption of monoclonal antibodies on sulfonated methacrylate matrices, to assess the potential of the sulfonated polymers as supports in ion-exchange chromatography, to allow purification of the antibodies during production.

Itsuno *et al*. utilised sulfonated polymers as a means to incorporate chiral quaternary ammonium catalysts onto a solid support *via* an ionic (*i.e.*, non-covalent) link.[14] The chiral catalyst was incorporated both as a side chain functional group, and as a repeating unit in the main chain of the polymer. Incorporation of the catalyst into a side chain could be done in two ways (Figure 2.1.2.1).

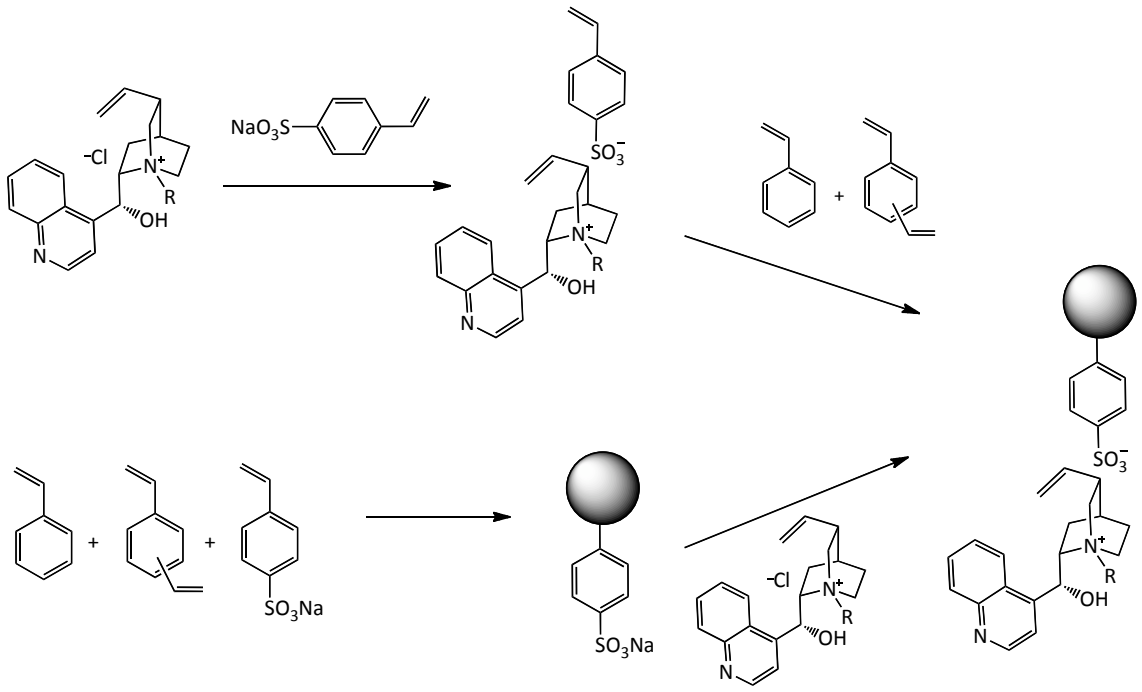

Figure 2.1.2.1. – Synthesis of polymer-supported chiral catalyst (side chain).[14]

First, an ionic interaction between the monomer and chiral catalyst was established to give a new chiral monomer, followed by subsequent copolymerisation. In an alternative synthetic strategy, styrene sulfonate was copolymerised with DVB and styrene, and the chiral catalyst later added in a post-polymerisation modification.[14] This is the preferred route since the structure of the catalyst-containing monomer allows for the formation of a stable radical, which then inhibits the radial polymerisation. Catalysts immobilised in this way include the quaternary ammonium salt of cinchonidine[14] and MacMillan's catalyst.[15]

Chiral catalysts can also be included in the main chain of a polymer.[16,17] For example, the Itsuno group showed that this can be achieved by first synthesising a chiral dimer, through reaction of two equivalents of an enantiopure tertiary amine, in this case cinchonidine (**4**), with a dihalide (**5**) followed by subsequent reaction of the dimer with 2,6-napthalene sulfonate (**6**) (Figure 2.1.2.2).[17]

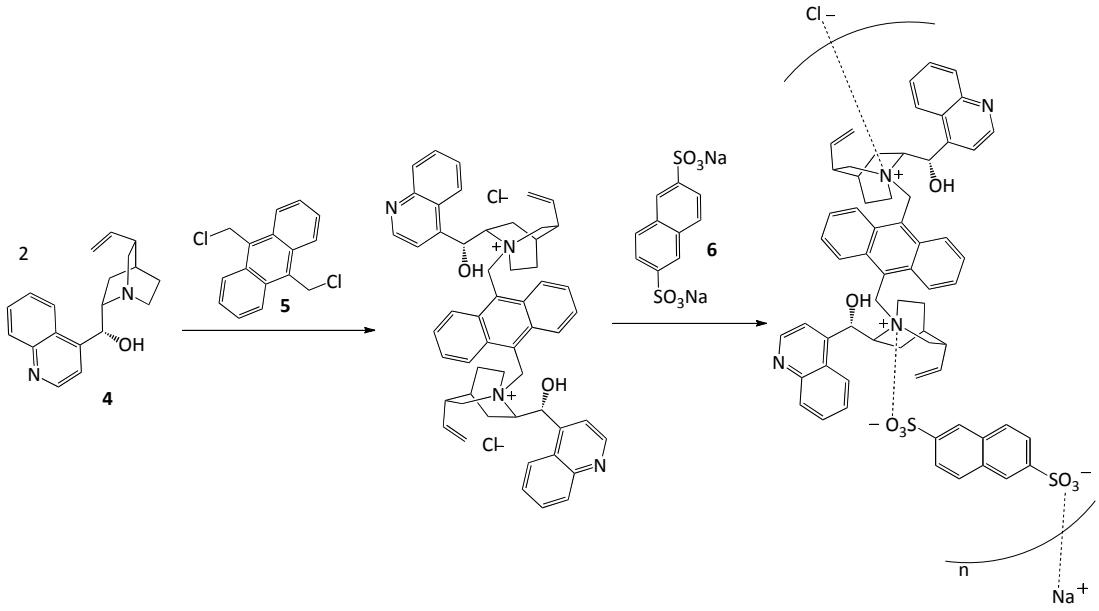

Figure 2.1.2.2. – Synthesis of main-chain polymer chiral catalyst.[17]

2.1.3. Sulfonation of Polystyrene

While the monomers styrene sulfonate[14,15,18] and 2-acrylamido-2-methyl-1-propanesulfonic acid[19] (AMPSA) can be incorporated into a polymer through copolymerisation, in some polymerisation methods, where salts of the monomer are used, the presence of salts can result in poor solubility of the growing polymer network in certain solvents. This can be particularly problematic during the initial nucleation stages of a polymerisation.[20] Additionally, in the case of hypercrosslinked polymers, addition of further comonomers will reduce the level of vinylbenzyl chloride that can be incorporated in the polymer and will thus reduce the level of hypercrosslinking possible, with a detrimental effect on the overall specific surface area of the product materials. This also means that only a small amount of comonomer can be included and thus the level of functionality will also be restricted. With this in mind, sulfonic acid groups are often added in a post-polymerisation chemical reaction, a reaction that can be carried out in many ways.

Sulfonation can be achieved in a very facile manner with the use of an acid. Chakravorty *et al*.[3] compared the use of sulfuric acid, oleum, chlorosulfonic acid and a mixture of chlorosulfonic acid and carbon tetrachloride for sulfonation of polymer films. It was found that chlorosulfonic acid mixed with carbon tetrachloride allowed the product to swell best and thus gave access to the highest ion-exchange capacities (IEC), while sulfuric acid gave rise to the lowest IEC. The order of preference of the reagents for sulfonation was listed as chlorosulfonic acid in carbon tetrachloride > oleum > chlorosulfonic acid > sulfuric acid.

These same sulfonation reagents have been used by many different groups under different reaction conditions. Chlorosulfonic acid has been used at 0 ^{o}C,[5] room temperature[6] and 50 ^{o}C,[21] giving good sulfonation levels in all cases. Chlorosulfonic acid, in 1,1,2,2-tetrachloroethane, has also been shown to be successful.[22]

Concentrated sulfuric acid has also been shown to be successful under various conditions, with reaction times at room temperature varying from 1 day[2] to up to 45 days.[20] Increases in reaction temperature can allow reaction times to be decreased to as low as 15 minutes.[9] Baharvand and Rabiee also found that addition of a phosphorus pentoxide catalyst to the sulfuric acid led to good levels of sulfonation within 24 hours. It was also noted that a second round of sulfonation led to a higher still IEC.[7]

While these sulfonation methods have been shown to be successful, they have been associated with the formation of sulfone links. These are formed through coupling of two sulfonic acid groups, expelling sulfuric acid and resulting in the loss of sulfonic acid functionality (Figure 2.1.3.1). In order to prevent this, inhibitors such as acetic anhydride[23] and silver sulfate[24,25,26] can be used.

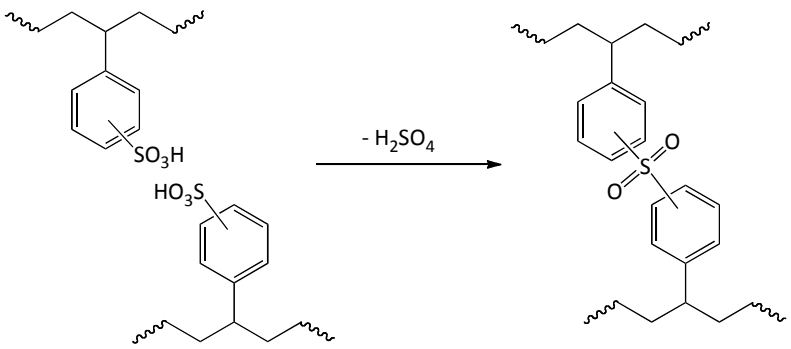

Figure 2.1.3.1. – Formation of sulfone bridges.

Addition of acetic anhydride to sulfuric acid gives acetyl sulfate, which is a much milder reagent than sulfuric acid itself, and leads to good levels of sulfonation. This reagent was first patented by Makowski *et al*.[27] in 1975 and has since become an extremely popular method for sulfonation.[4,10,11,28,29]

Cameron *et al*.[30] found that acetyl sulfate was able to sulfonate polystyrene polyHIPE® materials, however the 'yield of sulfonation' was relatively low at 35 % of styrene residues. In this case it was thought that a more hydrophobic sulfonating reagent, such as lauroyl sulfate reported by Thaler,[31] would be more compatible with the polymer matrix and thus provide a much higher level of sulfonation. This was in fact the case, with the yield of sulfonation doubling to 70 % of aromatic residues when lauroyl sulfate was used.

Other methods used for sulfonation of styrene-based polymers include sulfur trioxide vapour,[32] a sulfur trioxide-triethylphosphate complex,[33] a sulfur dioxide-oxygen-hydrogen peroxide mixture[34] and Friedel-Crafts acylation using ω-halogenoacyl chlorides, followed by a two-step reaction where the chloride atom is substituted for a dimethyl sulfide group followed by conversion to a sulfonic acid ion-exchanger using aqueous sodium sulfite.[8] Polymers containing sulfonic acid character can also be attached to the polymers using both 'grafting from'[35] and 'grafting to'[12] approaches.

2.1.4. Solid-Phase Extraction

For many samples requiring chemical analysis, the matrix in which the analytes are present is often incompatible with the method used for the analysis, or the analytes are present in very low concentrations. To overcome these problems, the analytes are often extracted into a (usually organic) solvent and preconcentrated prior to analysis. Liquid-liquid extractions are very useful in this respect, however they are limited in terms of the solvents that can be used and they demand large solvent volumes, which then require subsequent disposal.

A good way to overcome these limitations is to use solid-phase extraction (SPE). SPE involves the use of a hydrophobic organic sorbent material that can interact with organic molecules present in a sample matrix, whilst not interacting with the matrix itself, thus extracting the organic material. The sorbent is generally packed into a small tube similar to a syringe barrel (Figure 2.1.4.1) to give an SPE 'cartridge'. The sample is introduced onto the cartridge and then forced through the sorbent material by means of either positive pressure (plunger) or negative pressure (vacuum). The sample matrix passes through the sorbent, however any organic material binds reversibly. A more compatible solvent (for the analyte) can then be used to elute the organic material. This is a particularly useful technology as it allows the sample to be transferred from an incompatible solvent to one that is more suitable for any further analysis that is to be carried out. A further advantage is that the sample volume is reduced upon going from sample loading to sample elution, since a large sample volume can be passed through initially, while a much smaller volume of elution solvent can be used, thereby preconcentrating the sample in preparation for further analysis steps.[36]

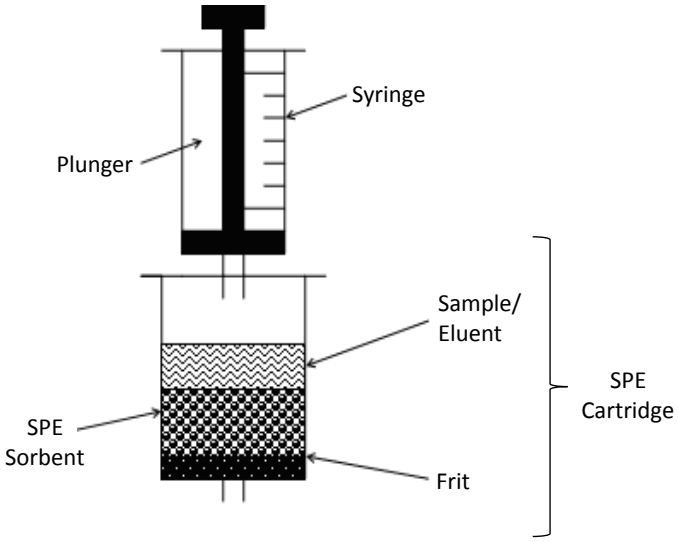

Figure 2.1.4.1. – SPE process using positive pressure.[36]

The nature of the sorbent can be varied to allow extraction of different classes of compounds, as extraction of different compounds is based on their differing interactions with the sorbent. Interaction can be by van der Waals forces, hydrogen bonding (dipolar interactions) or by electrostatic attraction (Figure 2.1.4.2).

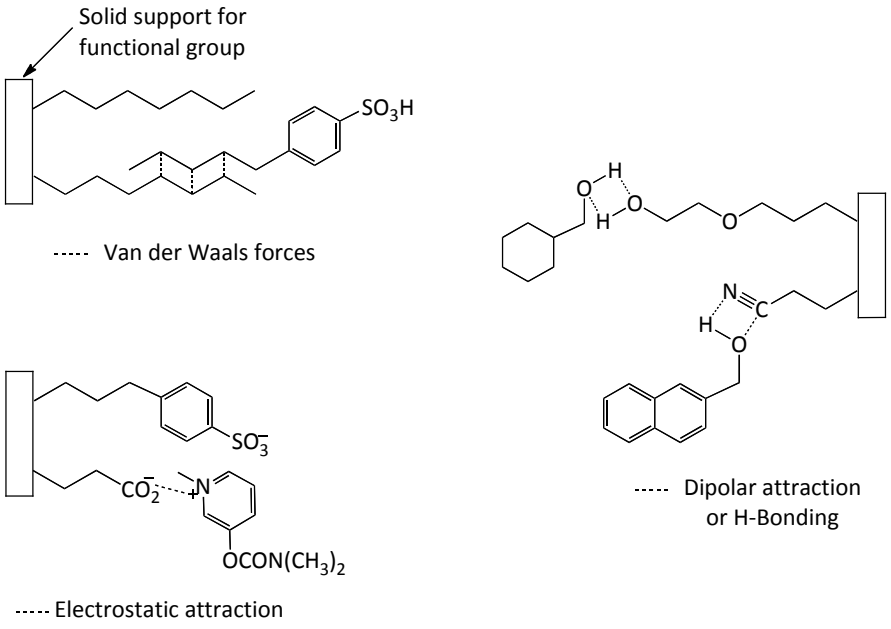

Figure 2.1.4.2. – Modes of bonding in SPE.[36]

Many sorbent materials must be conditioned prior to use with aqueous samples as they are hydrophobic in nature and will thus not allow aqueous samples to pass through. This is achieved by passing a compatible solvent, such as methanol, through the column to penetrate the hydrophobic layer and then allow the water through. The conditioning step ensures a reproducible retention of the compound of interest.

Directly after conditioning, the analyte of interest and other sample components are adsorbed onto the sorbent extraction bed. This is then rinsed to ensure that all of the water and most of the undesirable components have been removed, leaving behind only the analytes of interest and some strongly bound, unwanted constituents. The analytes of interest can then be eluted from the column using a small amount of an appropriate solvent (Figure 2.1.4.3).

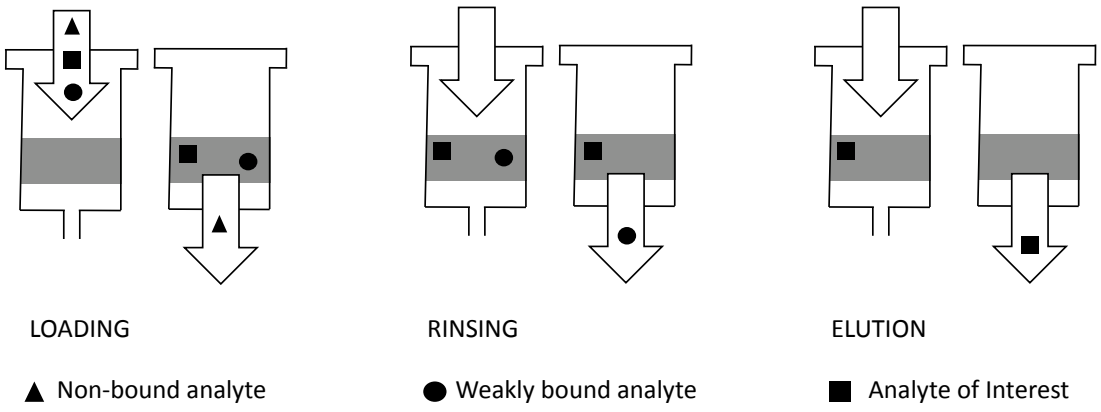

Figure 2.1.4.3. – Loading, rinsing and elution steps of SPE.[36]

The sorbents used in SPE cartridges are traditionally silica-based, composed of a silica core with functional groups chemically bonded to the surface. In order to deal with the vast differences in analyte polarity, a wide range of silica materials have been developed and commercialised, with their functional groups providing a complementary polarity range. These silica materials are classified as either reversed-phase (RP) or normal-phase (NP) sorbents, with the RP materials having hydrophobic attachments, including octadecyl (C_{18}),

octyl (C_8), ethyl (C_2), phenyl or cyclohexyl functional groups, and the NP materials containing more polar cyanopropyl, aminopropyl or diol functionalities.[37,38] Although the sorbent of choice for many years, these silica-based materials are not without problems, including low recoveries in the extraction of polar compounds, the presence of residual silanol groups and an instability at the pH extremes which are all too often faced in SPE procedures.[37]

A different class of materials that can be used to try to combat some of these issues are carbon-based products, such as graphitised carbon blacks or porous graphitic carbon. These materials are characterised by high thermal and chemical resistance properties in addition to a superior adsorption capacity and a low specific surface area (~100 m^2/g). Despite the better stability of these materials, they do suffer from the enhanced adsorption capacity often being too good, leading to excessive or irreversible binding of analytes.[37]

Porous polymeric sorbents offer a good alternative as they possess properties that overcome some of the problems associated with both silica- and carbon-based materials. Polymeric sorbents are extremely stable across the whole of the pH scale and provide good sorption characteristics coupled with facile elution capabilities.[37] Porous polymeric sorbents have been in use since the 1970s, with Fritz *et al*.[39] highlighting the potential use of the Rohm and Hass macroreticular resins XAD2 and XAD4 to separate a wide range of organic impurities from water. These resins required grinding, sizing and purification prior to use and had a wide size distribution, which perhaps hindered the practicality of these materials for everyday use. Since then, however, the use of polymeric resins as SPE materials has increased markedly with new and improved methods of polymer bead synthesis allowing access to particles of appropriate size that do not require sizing before use.[40]

The most common polymeric sorbent is a copolymer resin of styrene and DVB. This combines an essentially hydrophobic structure with a specific surface area in the region of 500-800 m^2/g. Analyte interaction is by van der Waals forces

and π-π interactions with the aromatic rings. It follows, therefore, that increasing the accessibility to the aromatic rings present will increase the interaction with analytes and thus improve the efficiency of these materials as sorbents. Better accessibility to the aromatic rings can be induced through an increase in the specific surface area of the polymer resin, most easily achieved by carrying out Davankov-type hypercrosslinking reactions to yield materials with specific surface areas in excess of 1,000 m^2/g.[37,38,41,42,43] These higher specific surface area materials have been shown by Fontanals *et al*.[41] and Davankov *et al*.[44] to give much better retention than the analogous hydrophobic materials with lower specific surface area. Both of these groups also found that in addition to high specific surface area, it is in fact the high micropore content of these hypercrosslinked materials that leads to the superior adsorption properties.

Despite the enhancement of retention induced by hypercrosslinking reactions, the resins are still highly hydrophobic when they are wetted (not to be confused with the amphipathic nature evident when hypercrosslinked polymers are present in a dried state), meaning that retention of polar compounds is often low and not reproducible. This is particularly important for analytes held in aqueous samples, as the sample can better penetrate hydrophilic materials. This means that the analytes will also have better contact with the material and hence can be better retained. Since many samples submitted for analysis that require preconcentration using SPE are in the aqueous phase, much research has focussed on the preparation of sorbents that incorporate some hydrophilic character. Hydrophilicity can be introduced to the sorbents as either a hydrophilic monomer in the initial polymerisation or through a post-polymerisation chemical modification.

While a wide range of polar monomers are available, not all can be copolymerised using the methods used typically for the preparation of such materials, *e.g.*, precipitation polymerisation, where the solvent used has to be matched specifically with all of the monomers in terms of polarity. Some polar

monomers that have been successfully copolymerised with divinylbenzene are *N*-vinylimidazole[43], 4,4'-*bis*-(maleimido)diphenylmethane, di(methacryloyloxymethyl)naphthalene, 4,4'-dihydroxyphenylmethane diglycidyl methacrylic ester and 4,4'-dihydroxydiphenylpropane diglycidyl methacrylic ester.[42]

With many aromatic groups present in the poly(styrene-*co*-DVB) materials, post-polymerisation chemical reactions can be extremely facile to effect. Fontanals *et al*.[50] unintentionally modified a poly(DVB-*co*-*p*VBC) material to give hydroxymethyl groups in place of the original chloromethyl groups. Masqué *et al*.[51-54] prepared many polar sorbents by chemically modifying the commercially available Amberchrom GC161 poly(styrene-*co*-DVB) material with acetyl, benzoyl, *o*-carboxybenzoyl, 2,4-dicarboxybenzoyl and 2-carboxy-3/4-nitrobenzoyl groups (Table 2.1.4.1).

Both unmodified and modified polymeric sorbents have been used to extract a wide variety of organic molecules from complex samples. These include alcohols, aldehydes and ketones, esters, polynuclear aromatics, alkyl benzenes, acids, ethers, nitrogen compounds,[39] halogen compounds,[39,45] phenols,[39,41-54] amines,[46] pesticides and herbicides[39,51-54].

An array of sample matrices can also be tolerated, such as water,[39,41,45] plant material,[45] cosmetics,[47] blood,[48] human plasma,[49] fish tissue and beers.[46]

Modifier group	*Structure*	*Target analyte*	*Ref.*
Hydroxymethyl	-CH_2-OH	No data	50
Acetyl	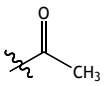	Phenols	51
Benzoyl	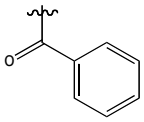	Phenols and pesticides	52
O-carboxybenzoyl	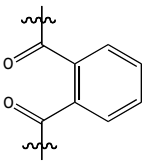	Phenols and pesticides	53
2,4-dicarboxybenzoyl	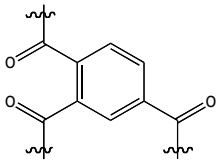	Phenols and pesticides	54
2-carboxy-3/4-nitrobenzoyl	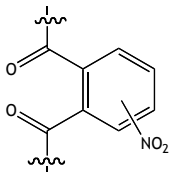	Phenols and pesticides	54

Table 2.1.4.1. – Functional groups introduced to impart polarity onto poly(styrene-*co*-DVB).

2.1.4.1. Strong Cation-Exchange Solid-Phase Extraction

Cation-exchange character can also be introduced into SPE sorbents by incorporation of sulfonate or carboxylate groups. These materials have a higher degree of polarity than their hydrophobic precursor materials and this can combine with the cation-exchange character to provide materials of high interest. Several studies have been carried out using commercially available cation-exchange SPE materials (Table 2.1.4.1.1).

Sorbent	*Supplier*	*Sorbent Properties*				*Ref.*
		Polymer base	*Ionic group*	*Ionic mode*	*Meq g^{-1}*	
Oasis MCX	Waters	Oasis HLB [poly(DVB-*co*-*N*-vinyl pyrrolidone)]	-SO_3H	Strong cation	1.00	55
Oasis WCX			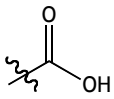	Weak cation	0.75	
Strata-X-C	Phenomenex	Strata X [poly(styrene-*co*-DVB)]	-SO_3H	Strong cation	1.00	56
Strata-X-CW			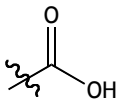	Weak cation	0.74	
SampliQ SCX	Agilent	SampliQ OPT [polyDVB]	-SO_3H	Strong cation	1.00	57
SampliQ WCX			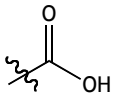	Weak cation	0.75	
Bond Elut PCX	Varian	Bond Elut Plexa [poly(styrene-*co*-DVB)]	-SO_3H	Strong cation	0.90	58

Table 2.1.4.1.1. – Properties of commercially available cation-exchange SPE sorbents.

These mixed-mode polymeric sorbents with cation-exchange character have been used successfully to remove a wide range of compounds from a variety of chemically complex matrices. Compounds extracted include pharmaceuticals,[59,60,61,62,63] illicit drugs,[59,64] sunscreen agents,[59] fluoroquinolone[65] and sulfonamide-based antibiotics,[66] acrylamides,[67] nicotinic acid,[68] herbicides[69] and wood preservatives,[70,71] while matrices tolerated are wastewater,[59,60,62,65,66] surface waters[59], raw and treated sewage,[61] human

plasma,[63,68] apple juice,[69] carbohydrate-rich foodstuffs,[67] urine[64] and wood-extracts.[70,71]

2.2. EXPERIMENTAL

2.2.1. Materials

For the synthesis of the strong cation-exchange polymers, divinylbenzene-80 (mixture of isomers, 80.0 % grade) and 4-vinylbenzyl chloride (≥ 90.0 %) were purchased from Sigma-Aldrich and purified prior to use by passing through a column of neutral alumina. 2,2'-Azo*bis*(isobutyronitrile), AIBN, (97.0 %) was purchased from BDH and was recrystallised from acetone at low temperature. HPLC grade acetonitrile was purchased from Rathburn Chemicals and was used as received. Iron(III) chloride (97.0 %), anhydrous 1,2-dichloroethane, DCE, (99.8 %), nitric acid (Riedel-de Haën, 65.0 %), acetic anhydride (≥ 99.5 %), sulfuric acid (Riedel-de Haën, > 95.0%), anhydrous dichloromethane (99.8 %), lauric acid (>99.5 %) and tetraethylammonium bromide (98.0 %) were all supplied by Sigma-Aldrich and were used as received. Sodium chloride (≥99.5 %) and sodium hydroxide (> 97.5 %) from BDH and chlorosulfonic acid (98.0 %) from Acros Organics were also used as received.

The solvents employed (toluene, acetone, methanol, propan-2-ol, diethyl ether, petroleum ether [b.p. 60-80 ^{o}C], petroleum ether [b.p. 30-40 ^{o}C] and chloroform) were of standard laboratory reagent grade, and were purchased from Sigma-Aldrich.

The analytes selected for the evaluation of the sorbents were caffeine, trimethoprim, antipyrine, propranolol hydrochloride, salicylic acid, carbamazepine, clofibric acid, diclofenac sodium and ibuprofen, all obtained from Sigma-Aldrich. Standard stock solutions at 1,000 mg/L were prepared for each analyte in methanol. A mixture of all compounds at 100 mg/L was

prepared by diluting the stock solutions in ultra-pure water. All solutions were stored at 4 ^{o}C. Ultra-pure reagent water, purified by a Millipore Milli-Q gradient system, was used throughout. Acetonitrile and methanol (both HPLC grade) were purchased from SDS, and hydrochloric acid was supplied by Probus. Nitrogen of 99.995 % purity was obtained from Carburos Metálicos for use in the evaporation step.

The commercially available SCX SPE sorbents used for comparison were Oasis MCX from Waters, Strata-X-C from Phenomenex, SampliQ SCX from Agilent and Bond Elut PCX from Varian.

Real water samples were obtained from the Ebro river (Catalonia Region, Spain) and from the influent and effluent streams of a waste-water treatment plant (Tarragona, Spain). The samples were filtered through 0.45 μm nylon membranes prior to SPE to eliminate particulate matter. The pH was adjusted to pH 3 with HCl.

2.2.2. Equipment

Precipitation polymerisations were carried out using a Stuart Scientific S160 incubator (Surrey, UK) and a Stovall low-profile roller system (NC, USA). All of the polymerisations were carried out in Nalgene® plastic bottles.

The optical compound microscope employed was a Carl Zeiss Jena (Germany).

Elemental microanalysis was performed by the University of Strathclyde Elemental Microanalysis Service. C, H and N elemental microanalyses were carried out simultaneously using a Perkin Elmer 2400 Series II analyser, while halogen and sulfur contents were determined by standard titration methods.

Scanning electron microscopy (SEM) was carried out by the University of Strathclyde SEM service, using a Cambridge Instruments Stereoscan 90. Samples were coated in gold prior to SEM imaging.

Fourier-Transform Infrared (FT-IR) analyses were carried out using a Perkin-Elmer Spectrum One FT-IR spectrometer. The sample was prepared as a disc with spectroscopic grade KBr in an RIIC press at 10 tons. The sample was scanned over the range 4,000-400 cm^{-1} in transmission mode.

The specific surface area measurements were performed using a Micromeritics ASAP 2000 (samples > 300 mg) or 2020 (samples < 300 mg). Samples were degassed overnight under vacuum at 100 ^{o}C prior to analysis. Analysis was *via* nitrogen sorption, carried out at 77 K.

The ion-exchange capacity was calculated using the following method: 0.050 g of polymer was placed into a beaker with 10 mL of a 2M solution of NaCl (or 0.05 M tetraethyl ammonium bromide solution) and allowed to stir for 30 minutes. The pH was recorded and the solution was then titrated with 0.0098 M NaOH. The volumes added and corresponding pH values were recorded and a pH curve was plotted to allow ion-exchange capacity to be calculated.

The chromatographic experiments were performed using an Agilent 1100 series LC system with UV spectrophotometric detector and an injection valve with a 20 µL loop. The analytical column was a 250 mm × 4.6 mm ID stainless-steel column packed with Kromasil 100 C_{18}, 5 µm, from Scharlau. The mobile phase was a mixture of two solvents: ultra-pure water, adjusted to pH 2.8 with HCl, and acetonitrile. The flow rate was 1 mL min^{-1} and the column oven was set at a temperature of 30 ^{o}C. The gradient profile was 10 % acetonitrile for the initial 10 minutes, then to 25 % acetonitrile in 5 minutes, to 45 % acetonitrile in 13 minutes, to 100% acetonitrile in 9 minutes (held for 1 minute), after which

time the mobile phase was returned to the initial conditions (10 % acetonitrile) in 2 minutes. The wavelength used for detection was 210 nm.

The SPE evaluation was performed in off-line mode using 200 mg of each polymer packed into 6 mL polypropylene cartridges fitted with 2 μm stainless-steel frits (Supelco). The cartridges were connected to a Teknokroma SPE manifold, which was connected to a vacuum pump. The sorbents were conditioned by passing through 15 mL of methanol, followed by 15 mL of ultra-pure water, acidified to pH 3. The analytes were loaded in 5-1,000 mL of ultra-pure or real water samples (all adjusted to pH 3 with HCl). After loading, the cartridge was washed by passing 10 mL of methanol over the sorbent, and then the basic analytes eluted with 10 mL of 5 % NH_4OH in methanol. The eluates from the washing and elution steps were evaporated to dryness under a stream of nitrogen and the respective residues reconstituted in 1 mL of a 1/1 (v/v) mixture of water/methanol.

2.2.3. Typical Preparation of Poly(DVB-co-VBC) Precursors by Precipitation Polymerisation (PP1)

VBC (**7**) (6.925 mL, 7.500 g, 0.058 mol), DVB-80 (**2**) (2.735 mL, 2.500 g, 0.018 mol) and AIBN (**1**) (0.278 g, 1.695 mmol, 2 mol % relative to polymerisable double bonds) were charged to a 1 L Nalgene® bottle with 500 mL of acetonitrile. The bottle was placed into an ultrasonic bath for 10 minutes and was then purged with N_2, whilst on an ice bath, for 10 minutes, before being sealed under N_2. The bottle was placed onto a low profile roller, which was housed in a temperature-controlled incubator. The temperature was ramped from room temperature to 60 ^oC over a period of around 2 hours and then held at 60 ^oC for a further 46 hours. After 46 hours, a representative sample of product was examined under an optical microscope to discern the presence of microspheres. When microspheres could be seen, the product was filtered by vacuum on a 0.2 μm nylon filter membrane and washed with successive 50 mL volumes of acetonitrile, toluene, methanol and acetone. The

product, in the form of a white powder, was dried overnight at 40 °C *in vacuo* (1.721 g, 17 %).

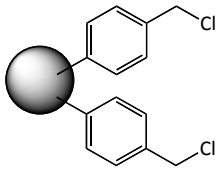

Elemental microanalysis: Expected 76.0 % C, 6.5 % H, 0.5 % N, 17.0 % Cl; Found 76.4 % C, 6.4 % H, 0.5 % N, 16.8 % Cl.

FT-IR $\bar{\nu}/cm^{-1}$ *(KBr): 3022, 2922, 2850, 1605, 1586, 1510, 1445, 1266 (C-H wag of* CH_2*-Cl), 990, 901, 831, 796, 709 (C-Cl str.).*

BET specific surface area: < 5 m^2/g.

An analogous procedure was followed for all DVB/VBC copolymers (Table 2.2.3.1).

Polymer ref.	***DVB (g)***	***VBC (g)***	***AIBN (g)***	***Yield (g)***	***Yield (%)***	***% Cl (w%)***	***Particle Size (μm)***
PP1	2.500	7.500	0.278	1.721	17	16.8	3-5
PP2	5.000	15.000	0.575	4.813	24	14.9	3-5
PP3	2.500	7.500	0.278	2.424	24	14.7	3-5
PP4	2.500	7.500	0.279	2.788	28	14.8	3-5
PP5	2.500	7.500	0.276	2.203	22	14.8	3-5
PP6	2.500	7.500	0.275	2.102	21	14.3	3-5

Table 2.2.3.1. – Feed and analytical data for the DVB/VBC precipitation polymerisations.

2.2.4. Typical Hypercrosslinking Reaction (HXL-PP1)

Precursor particles, PP1, (1.200 g, 5.663 mmol of VBC residues) were charged to a dry, three-necked, round-bottomed flask equipped with a reflux condenser and an overhead mechanical stirrer. Anhydrous DCE (30 mL) was added and the beads were left to swell fully under N_2 at room temperature for 1 hour.

$FeCl_3$ (0.918 g, 5.660 mmol, in a 1:1 mole ratio with respect to the CH_2Cl content of the particles) in DCE (30 mL) was added and the mixture heated at 80 °C for 18 hours. The product particles were recovered from the reaction medium by vacuum filtration on a 0.2 μm nylon filter and washed with successive 50 mL volumes of methanol, aqueous HNO_3 (pH 1) (2 washes), methanol and acetone. The orange-coloured particles were then extracted with acetone overnight in a Soxhlet apparatus and then washed with methanol and diethyl ether before drying *in vacuo* overnight at 40 °C (1.082 g, 73 %).

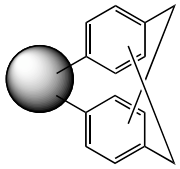

Elemental microanalysis: Expected 92.1 % C, 7.3 % H, 0.6 % N, 0 % Cl; Found 82.8 % C, 7.0 % H, 1.0 % N, 4.5 % Cl.

FT-IR $\bar{\nu}/cm^{-1}$ (KBr): 3021, 2927, 2857, 1604, 1560, 1510, 1448, 1297, 1267 (C-H wag of CH_2-Cl), 894, 826, 710 (C-Cl str.).

Langmuir specific surface area: 1,590 m^2/g.

An analogous procedure was followed for all syntheses of hypercrosslinked materials. The relevant feed and yield data are shown in Table 2.2.4.1.

Polymer ref.	***Precursor (g)***	***$FeCl_3$ (g)***	***Yield (g)***	***Yield (%)***	***% Cl (w%)***	***Langmuir Specific Surface Area (m^2/g)***
HXL-PP1	1.200	0.918	1.082	90	4.5	1,590
HXL-PP2	4.021	3.500	3.498	87	3.9	No data*
HXL-PP3	2.000	1.360	1.646	82	3.4	1,640
HXL-PP4	2.004	1.647	1.712	85	3.9	1,730
HXL-PP5	2.008	1.653	1.751	87	2.9	1,300
HXL-PP6	2.000	1.652	1.631	82	3.6	1,976

Table 2.2.4.1. – Feed and analytical data for hypercrosslinked poly(DVB-*co*-VBC).

*** Insufficient sample remaining thus the specific surface area could not be calculated.**

2.2.5. Typical Sulfonation of Hypercrosslinked Particles Using Acetyl Sulfate (HXL-PP2-SAc1)

Acetyl sulfate (**8**) solution was prepared freshly prior to each experiment as follows: acetic anhydride (0.150 mL, 0.163 g, 1.597 mmol) and anhydrous DCM (1 mL) were charged to a round-bottomed flask, under an N_2 atmosphere. The flask was placed on an ice bath to cool the reaction mixture to 0 ^oC and conc. sulfuric acid (0.066 ml, 0.120 g, 1.293 mmol) added. The flask was removed from the ice bath and allowed to equilibrate to room temperature.

Hypercrosslinked particles, HXL-PP2, (1.010 g, ~8.620 mmol of aromatic residues) were charged to a three-necked, round-bottomed flask fitted with an overhead mechanical stirrer and a reflux condenser, under an N_2 atmosphere. Anhydrous DCM (30 mL) was added and the reaction mixture was left for 1 hour to wet the beads. The acetyl sulfate solution was added to the hypercrosslinked beads *via* syringe. The reaction mixture was then heated to 40 ^oC and held at 40 ^oC with stirring for 2 hours. After 2 hours, propan-2-ol (1 mL) was added. 30 minutes after the propan-2-ol addition, the reaction mixture was cooled to room temperature and the product was filtered on a 0.2 μm nylon filter and washed with water to hydrolyse any remaining acetyl sulfate. The product was extracted with water in a Soxhlet apparatus overnight. The product, in the form of an orange powder, was then dried at 40 ^oC *in vacuo* for 48 hours (0.891 g, 80 %).

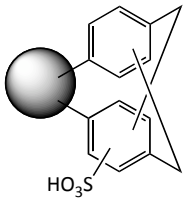

Elemental microanalysis: Expected 81.7 % C, 6.2 % H, 0.3 % N, 3.2 % Cl, 3.3 % S, 4.9 % O; Found 83.9 % C, 6.7 % H, 0.4 % N, 2.9 % Cl, 0.5 % S.

FT-IR $\bar{\nu}$/cm^{-1} (KBr): 3449 (SO_3H O-H str.), 3020, 2927, 2857, 1606, 1511, 1450, 1265 (C-H wag of CH_2-Cl), 1212 (SO_3H S=O asymmetric str.), 1037 (SO_3H S=O symmetric str.), 892, 818, 710 (C-Cl str.).

An analogous procedure was used for the preparation of all materials sulfonated using acetyl sulfate. The relevant feed and yield data is shown in Table 2.2.5.1.

Polymer ref.	***Acetic anhydride (mL)***	***H_2SO_4 (mL)***	***HXL-PP2 (g)***	***Yield (g)***	***Yield (%)***	***% S (w%)***
HXL-PP2-SAc1	0.15	0.066	1.010	0.891	80	0.5
HXL-PP2-SAc2	0.15	0.066	0.501	0.385	64	0.6

Table 2.2.5.1. – Feed and yield data for acetyl sulfate sulfonation reactions.

2.2.6. Typical Sulfonation of Hypercrosslinked Particles Using Lauroyl Sulfate (HXL-PP2-SLau1)

Lauroyl sulfate (**9**) solution was prepared freshly prior to each experiment as follows: lauric acid (0.067 g, 0.323 mmol) was dissolved in cyclohexane (3 mL) in a round-bottomed flask under an N_2 atmosphere. Chlorosulfonic acid (0.022 ml, 0.038 g, 0.323 mmol) was added and the mixture was stirred at room temperature for 1 hour under N_2.

Hypercrosslinked particles, HXL-PP2, (0.252 g, ~2.155 mmol of aromatic residues) were charged to a three-necked, round-bottomed flask fitted with an overhead mechanical stirrer and a reflux condenser, under an N_2 atmosphere. Anhydrous DCE (30 mL) was added. This was left for 1 hour to wet the beads. The lauroyl sulfate solution was added to the hypercrosslinked beads *via* syringe and the reaction was heated to 50 ^oC. The reaction was then held at 50 ^oC with stirring for 24 hours. After 24 hours, the product was recovered by filtration on a 0.2 μm nylon filter and washed with petroleum ether

(b.p. 60-80 °C). The product was extracted in a Soxhlet apparatus overnight with petroleum ether (b.p. 60-80 °C). The product, in the form of a brown powder, was then washed with petroleum ether (b.p. 30-40 °C) and oven-dried *in vacuo* at 40 °C for 24 hours (0.256 g, 92 %).

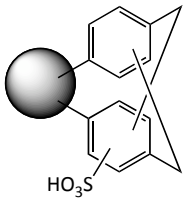

Elemental microanalysis: Expected 81.7 % C, 6.2 % H, 0.3 % N, 3.2 % Cl, 3.3 % S, 4.9 % O; Found 72.3 % C, 6.7 % H, 0.4 % N, 3.2 % Cl, 2.5 % S.
FT-IR $\bar{\nu}/cm^{-1}$ *(KBr): 3406 (SO_3H O-H str.), 3019, 2923, 2852, 1606, 1510, 1449, 1222 (SO_3H S=O asymmetric str.), 1053 (SO_3H S=O symmetric str.), 889, 821, 710 (C-Cl str.)*

An analogous procedure was followed for preparations of all materials sulfonated using lauroyl sulfate as the sulfonating reagent. The mass and yield data for all preparations is shown in Table 2.2.6.1.

Polymer ref.	***Lauric acid (g)***	***$ClHSO_3$ (mL)***	***HXL-PP (g)***	***Time (h)***	***Temp. (°C)***	***Yield (g)***	***Yield (%)***	***%S (w%)***
HXL-PP-SLau1	0.067	0.022	0.252[2]	24	50	0.256	92	2.5
HXL-PP-SLau2	0.066	0.022	0.251[3]	5	50	0.210	76	1.0
HXL-PP-SLau3	0.070	0.022	0.254[3]	2	50	0.225	80	1.8
HXL-PP-SLau4	0.067	0.022	0.254[3]	24	r.t.	0.229	82	2.3
HXL-PP-SLau5	0.065	0.022	0.252[3]	24	80	0.228	82	2.3
HXL-PP-SLau6	0.089	0.029	0.253[1]	24	50	0.279	97	4.5
HXL-PP-SLau7	0.215	0.072	0.250[1]	24	50	0.310	92	5.0
HXL-PP-SCX1	0.390	0.129	1.501[4]	5	80	1.452	88	3.1
HXL-PP-SCX2	0.520	0.172	1.503 [5]	5	80	1.509	88	6.3
HXL-PP-SCX3	1.296	0.430	1.501[6]	5	80	1.658	82	2.8

Table 2.2.6.1. – Feed and yield data for lauroyl sulfate derived sulfonation reactions. The superscripts [1] to [6] indicate which HXL-PP precursor has been sulfonated, *i.e.*, [1]=HXL-PP1.

2.3. RESULTS AND DISCUSSION

While hypercrosslinked materials are extremely interesting and have found use in several applications, the introduction of functional groups will enhance their use in some existing applications, and allow their use in new applications. Previously within our group, addition of both weak anion- and weak cation-exchange functional groups has led to greater selectivity of hypercrosslinked polymer microspheres when applied as solid-phase extraction (SPE) sorbents. Addition of strong ion-exchange functional groups into hypercrosslinked polymer microspheres will provide a complementary material for use in SPE. Thus methods for the introduction of such strong ion-exchange functionality are required.

2.3.1. Synthesis of Hypercrosslinked Particles

Ultra-high specific surface area polymer microspheres were prepared through precipitation copolymerisation of divinylbenzene (DVB) and vinylbenzyl chloride (VBC), followed by a Davankov-type hypercrosslinking reaction.

2.3.1.1. Precipitation Polymerisation

Precipitation polymerisation (PP) can be used to prepare monodisperse polymer microspheres incorporating a range of vinyl monomers in the presence of a multivinyl crosslinker. The higher the level of crosslinker that is included in the precipitation polymerisation, the higher the yield and the more mechanically robust are the microspheres. The microspheres prepared were derived from a 25/75 (w/w) DVB/VBC feed ratio (Figure 2.3.1.1.1). Although the level of DVB was low, this monomer ratio was chosen to ensure that the resultant products would contain a sufficiently high chloromethyl content, and could thus be further reacted in hypercrosslinking reactions. As a consequence of the lower level of DVB, it was expected that the microspheres would not have

smooth surfaces and the particle size distribution of the products would not be as narrow as materials prepared with higher DVB loadings.

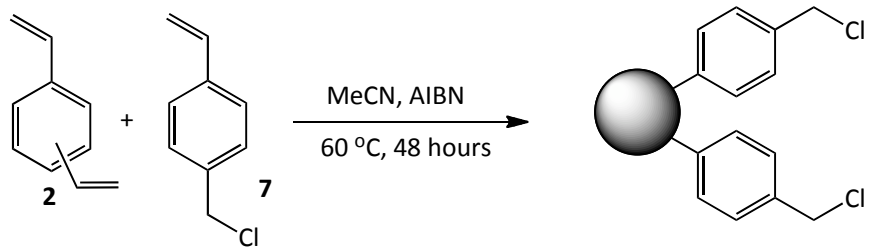

Figure 2.3.1.1.1. – Synthesis of poly(DVB-*co*-VBC) microspheres.

Elemental microanalysis was used to analyse the products, with the results being compared to the expected values to ensure incorporation of both monomers in the products. As the yields of products from such polymerisations involving low crosslinker levels are often ~20 %, it is possible, though unlikely, that the products are composed solely of DVB. However, evidence of Cl present in the products confirms the inclusion of VBC (Table 2.3.1.1.1, where the nitrogen content arises though the incorporation of the AIBN initiator).

Sample	***Elemental microanalysis (%)***			
	C	***H***	***N***	***Cl***
Expected for 25/75 (w/w) DVB/VBC	76.0	6.5	0.5	17.0
Observed (PP1)	**76.4**	**6.4**	**0.5**	**16.8**
Expected for polyDVB only	91.1	8.0	0.9	0.00

Table 2.3.1.1.1. – Elemental microanalysis data for PP1, 25/75 (w/w) DVB/VBC

The elemental microanalysis results for PP1 show clearly that the product is a DVB/VBC copolymer rather than a simple homopolymer, *i.e.*, both DVB and VBC have been incorporated successfully into the product.

FT-IR spectroscopic analysis was also used to show that the PP1 product contained both DVB and VBC, with bands in the FT-IR spectrum ascribed to

chloromethyl groups (~1265 and ~690 cm^{-1}) and unreacted pendent DVB double bonds (~990 and ~901 cm^{-1}) being clearly visible, thereby further verifying the incorporation of both monomers into the product (Figure 2.3.1.1.2).

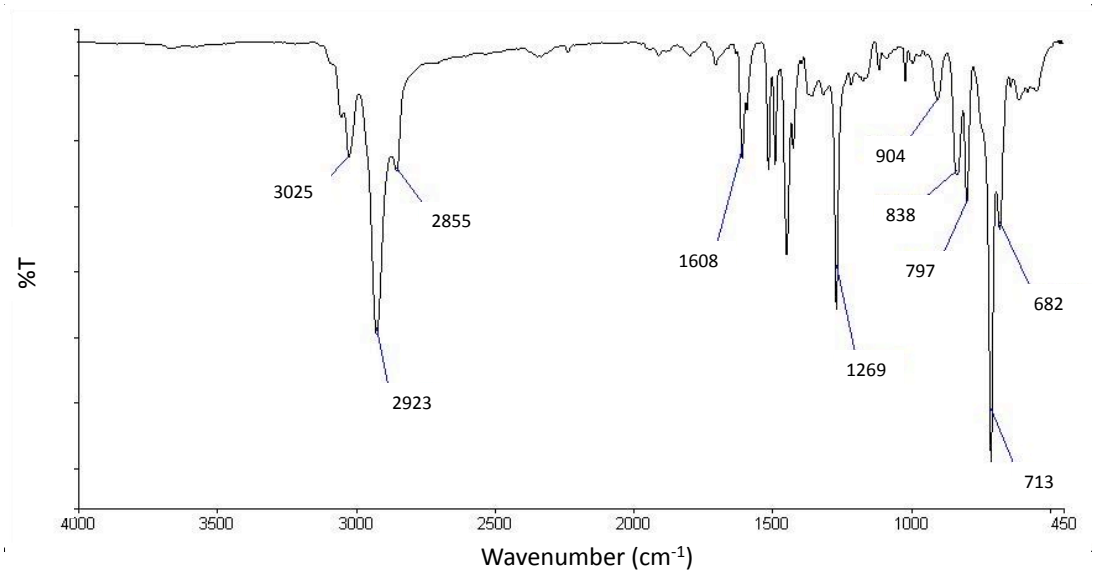

Figure 2.3.1.1.2 – FT-IR spectrum for DVB/VBC copolymer PP1.

Similar elemental microanalysis and FT-IR data was collected for all DVB/VBC copolymers prepared in an analogous fashion.

The shape, size and size distribution of the particles was determined using scanning electron microscopy (SEM). An SEM micrograph for polymer PP1 is presented in Figure 2.3.1.1.3.

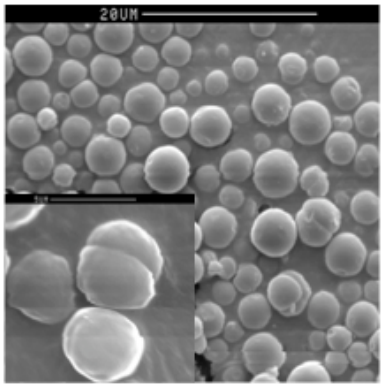

Figure 2.3.1.1.3 – SEM micrograph of PP1.

The SEM micrograph shows that the poly(DVB-*co*-VBC) product consisted primarily of spherical beads, however the surfaces of some of the beads were not entirely smooth, and there was a relatively high occurrence of doublet particles. This may be due to the low level of crosslinker in the monomer feed yielding particles with soft surfaces that readily form doublets on collision. Were the level of crosslinker higher, then collision would have been less likely to result in the formation of doublets as the particles would have been more resistant to aggregation. The majority of the particles had diameters of around 3-5 μm, and the particle size distribution was relatively narrow.

2.3.1.2. Hypercrosslinking

Microporosity can be introduced into polymer microspheres containing high levels of pendent chloromethyl groups using Friedel-Crafts reagents such as $FeCl_3$ and $TiCl_4$ (Figure 2.3.1.2.1). The specific surface area increases from only a few m^2/g to somewhere in the region of 1,000 m^2/g. Ultra-high specific surface area is extremely attractive in view of the potential uses of such microspheres in many applications including hydrogen storage, LC stationary phases and SPE sorbents.

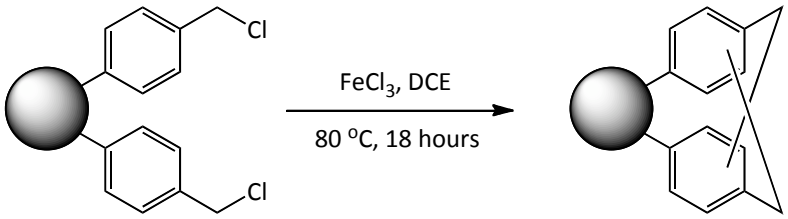

Figure 2.3.1.2.1 – Hypercrosslinking reaction using $FeCl_3$ as the Friedel-Crafts catalyst.

The hypercrosslinked products produced in this manner were extremely hygroscopic, as they were highly strained when dried, and thus they readily sorbed any solvent that they came into contact with, meaning that they took up water on contact with air. This made it difficult to analyse accurately these products by techniques such as elemental microanalysis, as there are always interfering elements present (*e.g.*, oxygen due to water taken up from the air or residual solvent, *etc.*). Nevertheless, elemental microanalysis was carried out and, despite the discrepancies, it was clear that the Cl content had dropped significantly relative to the poly(DVB-*co*-VBC) precursor, clear evidence that the hypercrosslinking reaction was successful (Table 2.3.1.2.1).

	Elemental microanalysis (%)			
Polymer ref.	***C***	***H***	***N***	***Cl***
PP1	76.4	6.4	0.5	16.8
HXL-PP1	82.8	7.2	1.0	4.5

Table 2.3.1.2.1. – Elemental microanalysis data for HXL-PP1 and its swellable precursor PP1.

Nitrogen sorption porosimetry is another useful technique for analysing these beaded products, with the specific surface area being calculated using the Brunauer-Emmett-Teller (BET) isotherm. Upon hypercrosslinking, the surface area should increase from a few m^2/g to somewhere in excess of 1,000 m^2/g. Table 2.3.1.2.2 shows the nitrogen sorption porosimetry data obtained for both

a swellable precursor polymer and its corresponding hypercrosslinked derivative (PP1 and HXL-PP1, respectively).

Polymer ref.	*BET c value*	*Langmuir b value*	*Specific surface area (m^2/g)*		*Specific pore vol. (cm^3/g)*	*Ave. pore diameter (nm)*
			BET	*Langmuir*		
PP1	135	0.036	2	3	0.003	5.522
HXL-PP1	-372	0.018	1166	1587	0.669	2.296

Table 2.3.1.2.2. – Nitrogen sorption porosimetry data for the hypercrosslinked polymer, HXL-PP1, and its precursor, PP1.

The data obtained from nitrogen sorption porosimetry analysis shows that, upon hypercrosslinking, many changes occur to the internal structure of the microspheres. The specific pore volume is greatly increased, while the average pore diameter is decreased from mesoporous levels, towards microporous territory. This is quite intuitive as the hypercrosslinking reaction forms many crosslinks in the microspheres when the microspheres are in a swollen/expanded state. The BET c value, calculated as the gradient of the BET plot, shows a very significant change. In the precursor, PP1, the c value is high and positive. This indicates that the BET plot has taken the correct form and thus nitrogen sorption onto the surfaces of the pores will be in several layers. After hypercrosslinking, however, the c value becomes negative, indicating that the data no longer fits the BET isotherm, and thus the nitrogen does not sorb onto the surface in several distinct layers. Instead, the Langmuir isotherm must be used in order to manipulate the data correctly and calculate the specific surface area. The Langmuir isotherm deals with sorption of the nitrogen onto the surface in a single layer. This change in sorption mode, and thus calculation of specific surface area, can be rationalised from the average pore diameters of the two materials. As the pore size has been greatly reduced, it follows that the amount of nitrogen that can access each pore has been reduced and therefore can only form a single layer in the space provided.

FT-IR spectroscopy was also used to show that the hypercrosslinking reaction had been successful (Figure 2.3.1.2.2). As the starting material contained pendent chloromethyl groups, the FT-IR spectrum contained peaks at ~1265 cm^{-1} (C-H wag of CH_2-Cl) and ~690 cm^{-1} (C-Cl stretch) ascribed to the chloromethyl group; a decline in the intensity, or even disappearance, of these peaks would indicate the loss of chlorine and, by inference, the formation of hypercrosslinks.

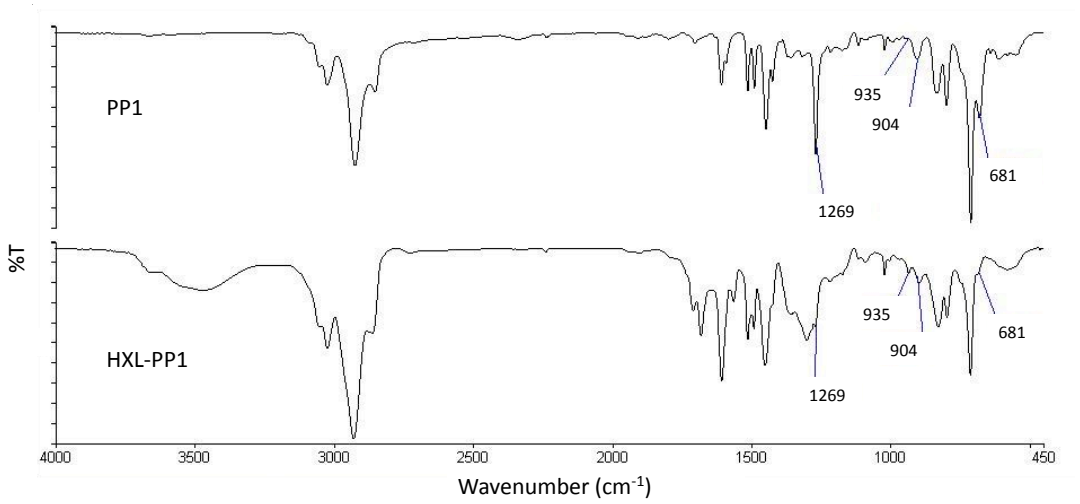

Figure 2.3.1.2.2. – FT-IR spectra of precursor, PP1, and its hypercrosslinked derivative HXL-PP1.

The FT-IR spectrum of the hypercrosslinked product shows a dramatic decrease in intensity of the signal at ~1265 cm^{-1}, which appears in the precursor (PP1) spectrum as a sharp, dominant peak, but appears only as a small peak in the spectrum of HXL-PP1. The signal at ~690 cm^{-1} is much more prominent relative to other signals present in the precursor spectrum compared to the spectrum of the hypercrosslinked material. The changes in intensity of both of these peaks are clear indications that the hypercrosslinking reaction has occurred, however the continued presence of the peaks, albeit at significantly reduced intensity, indicates that there are still some pendent chloromethyl groups present, *i.e.*, the reaction has not gone to completion. This may be due to a portion of the chloromethyl groups being inaccessible to the $FeCl_3$ reagent, however where

these groups are accessible to reagents they may be exploited in subsequent reactions to introduce desirable properties, such as acid/base functionality or polar groups, *etc*.

SEM was used in order to show that the hypercrosslinking reaction conditions did not cause any alteration to the spherical nature of the precursor material (Figure 2.3.1.2.3).

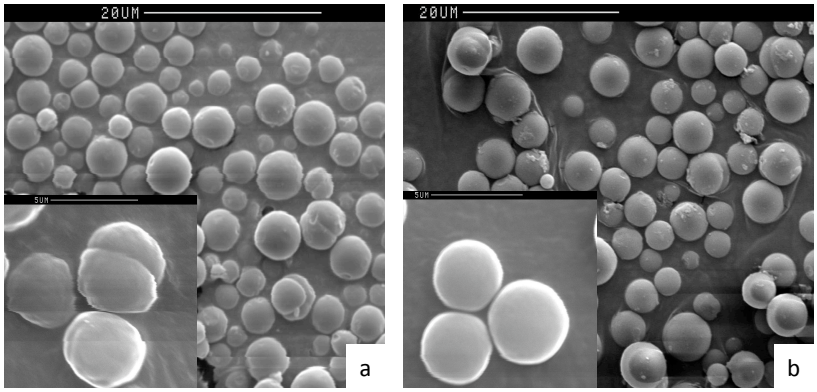

Figure 2.3.1.2.3. – SEM images obtained for: (a) PP1 and (b) HXL-PP1.

The SEM micrographs obtained for the PP1 precursor show that the particles were essentially spherical in shape, however they did have a slightly bumpy surface and there was evidence of the formation of doublet particles. The particle sizes were around 3-5 μm, with a relatively narrow particle size distribution. The SEM micrograph obtained for the hypercrosslinked derivative, HXL-PP1, shows that despite the high temperature (80 ^{o}C) and presence of the powerful Lewis acidic $FeCl_3$ reagent used in the hypercrosslinking reaction, the particles remained spherical in nature and the surface smoothness of the particles had improved. The rough surface present in the poly(DVB-*co*-VBC) precursor arose as a result of the low level of DVB crosslinker in the monomer feed (25/75, w/w, DVB/VBC), which led to soft, collapsible particles. The introduction of methylene bridges during the hypercrosslinking reaction results in an increased stability and therefore increased hardness, which may explain the smoother appearance of the surfaces of the hypercrosslinked material. This

was encouraging, as it showed that the particles were not damaged in any way under the hypercrosslinking conditions. The precursor particles were swollen in DCE prior to hypercrosslinking, thus the particle size of 4-6 μm, observed for the hypercrosslinked particles, is increased relative to that of the precursor particles.

2.3.2. Sulfonation of Hypercrosslinked Materials Using Acetyl Sulfate

The hypercrosslinked polymers have a high abundance of electron rich, aromatic residues. These can be modified readily through electrophilic aromatic substitution reactions to provide new classes of functionalised hypercrosslinked materials, hence opening up a whole new range of applications. In order to impart strong cation-exchange functionality into the hypercrosslinked polymers, sulfonic acid residues must be added into the structure. This can be potentially done in a facile manner, using a variety of sulfonation conditions.

The first sulfonation reaction carried out used acetyl sulfate (Figure 2.3.2.1), a reagent which can be formed through reaction of acetic anhydride and sulfuric acid. The reaction was carried out in such a way as to introduce the acetyl sulfate at a level of 15 mol% relative to the number of aromatic residues present, as in the literature this was shown to be the maximum level of sulfonation which gave SO_3H groups exclusively[11] *i.e.*, which avoids sulfone bridge formation. Sulfone bridge formation should be avoided as, while it may effectively help to increase the degree of hypercrosslinking in the system, this will occur at the expense of the cation-exchange capacity of the material. Nevertheless, a second reaction was carried out using the acetyl sulfate reagent at a level of 30 mol% with respect to the aromatic residues present. The purpose of this reaction was to test the theory of sulfone bridge formation in the context of hypercrosslinked materials, as the original, published methodology used branched polymers whereas the materials used here were highly porous

resins that had had their internal structures locked *via* a hypercrosslinking reaction. The branched polymers would be more flexible and therefore more likely to be able to adopt different conformations during the sulfonation reaction, which would allow the sulfonic acid residues to come into close contact with each other and therefore react together to give sulfone bridges. With the hypercrosslinked resin, however, the structure is much more rigid and there is a distinct possibility that the sulfonic acid groups do not come into contact with one another and are therefore unable to react.

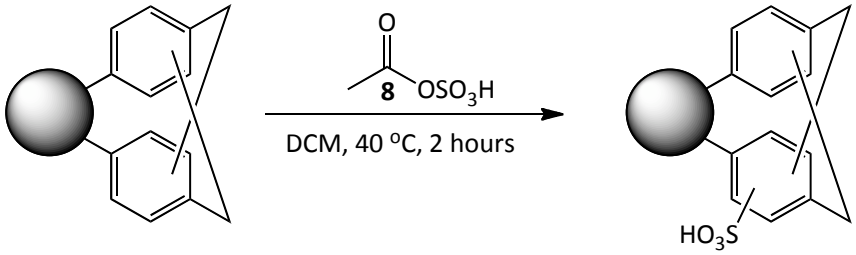

Figure 2.3.2.1. – Sulfonation of hypercrosslinked particles using acetyl sulfate.

The elemental microanalytical data obtained for the products prepared using acetyl sulfate as the sulfonating reagent are shown in Table 2.3.2.1. Data shown includes the mol% of sulfonation reagent used, relative to the number of moles of aromatic rings present in the hypercrosslinked starting material, HXL-PP2, together with reference data for HXL-PP2.

Polymer ref.	***Mol% Sulfate reagent used***	***Elemental microanalysis (%)***				
		C	***H***	***N***	***Cl***	***S***
HXL-PP2	0	82.9	6.3	0.3	3.9	0.0
HXL-PP2-SAc1	15	83.9	6.7	0.4	2.9	0.5
HXL-PP2-SAc2	30	77.7	6.5	0.4	2.9	0.6

Table 2.3.2.1. – Elemental microanalytical data for products obtained through reaction of HXL-PP2 with acetyl sulfate.

The elemental microanalysis results show that sulfur was incorporated successfully into the hypercrosslinked material in both cases. However, the values obtained were much lower than the levels expected assuming 100 % reaction efficiency. For the 15 mol% and 30 mol% sulfonation reactions, it was expected that the level of sulfur present in the sulfonated products would be 3.3 % and 6.1 %, respectively. As both reactions yielded products with only ~0.5 % sulphur, it was clear that the method had not worked as efficiently as intended. Information about the presence of any sulfone bridge formation cannot be ascertained from this data alone.

FT-IR spectroscopy was also used to follow the reactions, however the level of sulfur introduced was sufficiently low that the FT-IR spectra showed only a slight change subsequent to the sulfonation reaction. New signals were introduced at 1213 and 1037 cm^{-1} corresponding to the asymmetric and symmetric stretches of the SO_3H group, respectively, however these signals were extremely weak.

2.3.3. Sulfonation of Hypercrosslinked Materials Using Lauroyl Sulfate

The second sulfonation method employed used lauroyl sulfate in place of acetyl sulfate (Figure 2.3.3.1). This method was used previously by Cameron *et al*.[30] for the sulfonation of poly(styrene-*co*-DVB) polyHIPE® materials which are similar in nature to the hypercrosslinked resins used here (in that they are hydrophobic and highly porous styrenic materials), and gave a higher level of sulfonation than the acetyl sulfate method (2.2 mmol/g *vs.* 4.0 mmol/g for acetyl and lauroyl sulfate, respectively). In this method, the higher hydrophobicity of the lauroyl group compared to the acetyl group should, in theory, be more compatible with the hypercrosslinked material. This should then, in turn, permit a higher degree of sulfonation as the lauroyl sulfate reagent can better penetrate the hypercrosslinked particles and should thus be able to react with a higher percentage of aromatic groups.

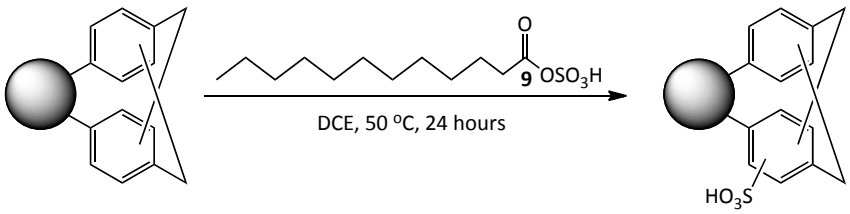

Figure 2.3.3.1. – Sulfonation of hypercrosslinked particles using lauroyl sulfate.

Table 2.3.3.1 shows the results of the experiment carried out using the lauroyl sulfate reagent. Data shown includes reference data for the non-functionalised hypercrosslinked polymer (HXL-PP2). The mol% of lauroyl sulfate was 15 mol%, relative to the number of moles of aromatic rings present in the precursor material.

Polymer ref.	***Elemental microanalysis (%)***				
	C	***H***	***N***	***Cl***	***S***
HXL-PP2	82.9	6.3	0.3	3.9	0.0
HXL-PP2-SLau1	72.3	6.7	0.4	3.2	2.5

Table 3.3.3.1. – Elemental microanalysis results from the sulfonation of HXL-PP2 using lauroyl sulfate.

It can be seen from the elemental microanalysis results that sulfur has been introduced much more successfully into the hypercrosslinked polymer when using lauroyl sulfate as the reagent, compared to the previous use of acetyl sulfate. When the percentage of the lauroyl sulfate reagent added was 15 mol% relative to the aromatic rings available for reaction with the reagent, the expected level of sulfur in the sulfonated product (assuming 100 % reaction) was 3.3 %. The elemental microanalysis results from the product showed a level of sulfur of 2.5 %, which was far closer to the expected level than was obtained previously with the acetyl sulfate reagent.

FT-IR spectroscopy was also used to follow the success of the reaction, and in this case, as the level of sulfur introduced was much greater, the FT-IR spectrum

of the sulfonated product showed new signals at 1228 and 1053 cm^{-1}, ascribed to the asymmetric and symmetric S=O stretch of sulfonic acid groups, respectively, and a new signal at 3406 cm^{-1} which can be ascribed to the O-H stretch of the sulfonic acid groups (Figure 2.3.3.2).

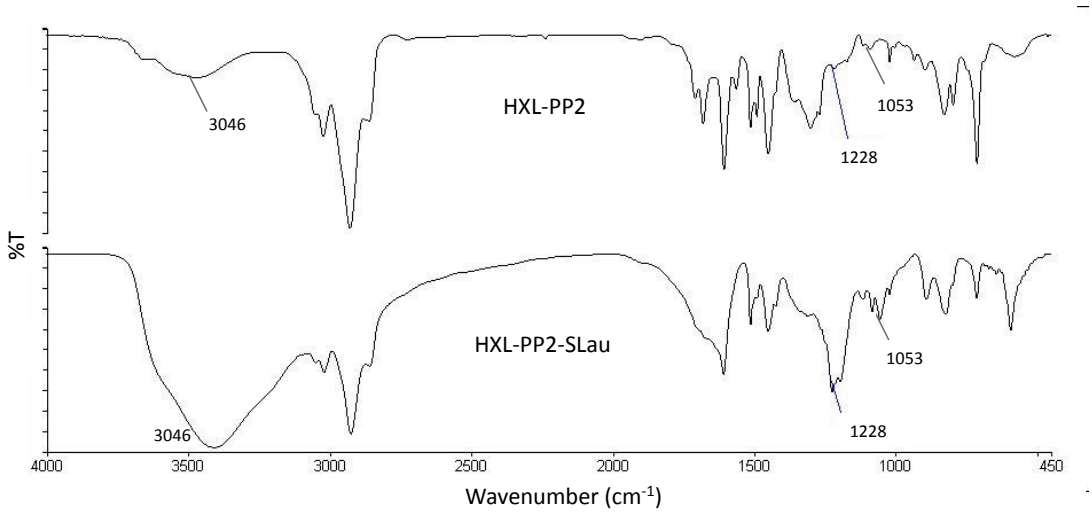

Figure 2.3.3.2. – FT-IR spectra showing the hypercrosslinked polymer HXL-PP2 and the product of the reaction of the HXL-PP2 polymer with lauroyl sulfate, HXL-PP2-SLau.

It has therefore been shown, in practice, that the more hydrophobic reagent does indeed afford a much higher level of sulfur in the final product. This may be due to the better compatibility of the reagent with the hypercrosslinked polymer, although there was a large difference in the reaction time between the two different methods (1 hour *vs.* 24 hours for the acetyl and lauroyl sulfate reagents, respectively), which may also have contributed to the higher degree of sulfonation when using the lauroyl sulfate reagent.

2.3.4. Ion-Exchange Capacity

As was the case with the unmodified hypercrosslinked particles, the sulfonated particles were not straight-forward to analyse accurately by techniques such as elemental microanalysis since their hypercrosslinked character made the

sulfonated materials extremely hygroscopic. This led to variability in the elemental microanalysis data, which meant that it was somewhat hard to interpret the results with complete confidence.

A more accurate method for ascertaining the degree of sulfonation, *i.e.,* the number of moles of sulfonic acid groups introduced through reaction, is titration of the sulfonated material. In this regard, the sulfonated material was first subjected to a cationic-exchange reaction to replace the acidic protons of the sulfonic acid groups with cations of differing size. The two cation-exchange reagents used were aqueous solutions of sodium chloride (NaCl) and tetraethylammonium bromide (TEABr). In order for exchange to occur, the cation had to be able to penetrate the polymeric material and thus reach the sulfonic acid groups. As the cations in these reagents (Na^+ and TEA^+) were of different sizes, a similar IEC result arising from both titrations would indicate that all of the sulfonic acid groups are accessible to large and small cations. A higher degree of sulfonation indicated by titration with NaCl than with TEABr would suggest that some of the sulfonic acid groups are inaccessible to large cations, and that size-exclusion effects are playing a role.

This method of IEC determination was more accurate than elemental microanalysis in showing the number of SO_3H groups, as any sulfone bridges (which would appear as sulfur content in the elemental microanalysis results) would have no acidic character and would therefore not undergo ion-exchange. When coupled with the elemental microanalysis results, this may be able to give an indication of the level of sulfone bridge formation (Table 2.3.4.1).

Polymer ref.	*Mol% Sulfate reagent*	*mmol/g S from elemental microanalysis*	*IEC (mmol/g)*	
			NaCl	*TEABr*
HXL-PP2-SAc1	15	0.2	0.3	0.3
HXL-PP2-SAc2	30	0.2	0.2	0.2
HXL-PP2-SLau1	15	0.8	1.2	1.2

Table 2.3.4.1. – Comparison of sulfur content in mmol/g from titrations and elemental microanalysis.

The data presented in Table 2.3.4.1 shows that in the case of the materials prepared using acetyl sulfate the results obtained from elemental microanalysis and titration are fairly consistent, however where lauroyl sulfate was used the sulfur content calculated using the elemental microanalysis data was lower than that calculated by titration. This confirms that the elemental microanalysis results are not indicative of the true levels of each element present. In the case of the ion-exchange materials, the titration data is more important as the method used to calculate IEC is very close in nature to the method that will be employed in the intended SPE application.

2.3.5. Optimisation of Sulfonation Conditions

As lauroyl sulfate was shown to be the most effective reagent for the sulfonation of the hypercrosslinked particles, a series of experiments was carried out to optimise the reaction conditions. The three main considerations in the method were reaction time, reaction temperature and the number of moles of lauroyl sulfate added. Each of these parameters was varied twice in order to discover how the method was affected by such changes to the reaction conditions. Table 2.3.5.1 shows the results of the experiments carried out using lauroyl sulfate as the sulfonation reagent.

Polymer ref.	*Time (h)*	*Temp. (°C)*	*Mol% Lauroyl Sulfate*	*mmol/g S from elemental microanalysis*	*IEC (mmol/g)*	
					NaCl	*TEABr*
HXL-PP-SLau1	24	50	15	0.8	1.2	1.2
HXL-PP-SLau2	**2**	50	15	0.6	1.3	1.3
HXL-PP-SLau3	**5**	50	15	0.3	1.3	1.0
HXL-PP-SLau4	24	**r.t.**	15	0.7	1.4	1.5
HXL-PP-SLau5	24	**80**	15	0.7	1.5	1.5
HXL-PP-SLau6	24	50	**20**	1.4	2.7	2.7
HXL-PP-SLau7	24	50	**50**	1.6	3.3	3.1

Table 2.3.5.1. – Comparison of sulfur content in mmol/g from titrations and elemental microanalysis, in products obtained under different reaction conditions.

As the original sulfonation method had a long reaction time (24 hours), the initial optimisation experiments used reduced reaction times. The times chosen were 5 hours and 2 hours. In the original method, the IEC was 1.2 mmol/g. When the reaction time was reduced to 5 and 2 hours, the slight variation in the IEC values was insignificant, therefore it would seem that the reaction time is not an especially important factor for the reaction given the timescales investigated and that the reaction is essentially complete in 2 hours or less. This is significant, as a 2 hour reaction time is much more favourable than a 24 hour reaction period. A 2 hour reaction time is also comparable to the conditions employed with the acetyl sulfate reagent, and this therefore confirms that the lauroyl sulfate was indeed a better reagent for the sulfonation of the hypercrosslinked material.

The reaction temperature used in the original sulfonation method was 50 °C. The new temperatures used were room temperature and 80 °C. Again, there was no significant change in the IEC suggesting that temperature is also not a very important variable in this reaction. Reaction at 80 °C did cause more of an increase in the IEC than reaction at room temperature, however not by a

significant amount. The fact that the reaction proceeds efficiently at room temperature is very favourable.

The last parameter changed was the number of moles of lauroyl sulfate reagent used in the reaction. The lauroyl sulfate was added in at levels of 20 mol% and 50 mol%, relative to the number of aromatic rings present in the non-functionalised polymer, in order to further test the theory of sulfone bridge formation. The IEC values obtained were 2.7 and > 3 mmol/g, respectively, which shows that the IEC is greatly increased relative to the materials prepared using 15 mol% of the sulfate reagent. This increase in IEC is not directly correlated to the amount of sulfate reagent used. If it were, it would be expected that on increasing the amount of sulfate reagent by more than double, from 20 mol% to 50 mol%, the IEC should increase more than 2-fold. As this is not the case, it could be inferred that there has been some sulfone bridge formation. This cannot, however, be proven or disproven given the data available.

For all of the experiments carried out, there is a very good correlation between the IEC values measured using the two cation-exchangers. This shows that the polymers are equally accessible to both small and large cations, which makes them very amenable to ion-exchange chromatography or SPE of water samples which can potentially contain a complex mixture of large and small cationic species.

2.3.6. Synthesis of SCX Material for SPE

With a suitable method developed for the production of sulfonated hypercrosslinked particles, the next step was to repeat the synthesis on a larger scale, in order to produce sufficient material to be taken forward for use in SPE. As before, the sulfonation reaction was carried out using 15, 20 and 50 mol% of the lauroyl sulfate reagent relative to aromatic residues in the material. All

reactions were carried out at 80 °C for 5 hours in order to achieve the maximum possible level of sulfonation. The characterisation data for the products are shown in Table 2.3.6.1.

Polymer ref.	*Mol% Sulfate*	*Elemental microanalysis (%)*					*IEC (mmol/g)*	
		C	*H*	*N*	*Cl*	*S*	*NaCl*	*TEABr*
HXL-PP-SCXa	15	62.1	6.6	0.6	3.1	3.1	1.7	1.8
HXL-PP-SCXb	20	52.3	5.8	0.5	7.0	6.3	2.0	1.9
HXL-PP-SCXc	50	63.7	6.1	0.6	3.0	2.8	2.8	2.5

Table 2.3.6.1. – Elemental microanalysis results and ion-exchange capacities for the sulfonated materials.

The elemental microanalysis results (Table 2.3.6.1) suggest a decreased level of sulfonic acid groups at 50 mol% of sulfate reagent. Since the formation of sulfone bridges results in a loss of sulfur and therefore reduced sulfur levels, consideration of the elemental microanalysis results alone suggests that sulfone bridges have formed within the material. However, the ion-exchange capacity as calculated by titration using an ion-exchange methodology contradicts this. As the titration-derived sulfur levels were much more reliable in showing the behaviour of the materials for the intended application, these results help to support the belief that the elemental microanalysis data for the hypercrosslinked materials needs to be treated with caution.

The titration-derived IEC values show that as the level of sulfate reagent used in the reactions was increased, the ion-exchange capacity of the materials also increased. This shows that the lauroyl sulfate method gives good control over the ion-exchange capacity, and that it is thus possible, using this method, to tune the properties of the sulfonated polymers to the specific needs of an application.

Nitrogen sorption porosimetry was employed in order to ensure that the specific surface areas of the sulfonated SCX polymers were sufficiently high, and

that the materials were microporous. The data obtained is presented in Table 2.3.6.2.

Polymer ref.	*Langmuir specific surface area (m^2/g)*	*Single point total pore volume (cm^3/g)*	*Average pore diameter (nm)*
HXL-PP-SCXa	1070	0.416	2.07
HXL-PP-SCXb	1160	0.452	2.08
HXL-PP-SCXc	1370	0.543	2.11

Table 2.3.6.2. – Nitrogen sorption porosimetry analysis results for the HXL-PP-SCX materials.

The nitrogen sorption data shows that the specific surface areas of the polymer are in excess of 1,000 m^2/g and thus these materials are ideal for their intended application, to act as efficient SPE sorbents. The ultra-high specific surface areas coupled with the average pore diameters of around 2 nm, indicate that the materials contain high levels of micropores, with a small number of mesopores also being present.

SEM was also used in order to show that the sulfonation reaction did not alter the size and shape of the particles, as this would potentially hinder the packing of these polymers into columns in the desired applications. Monodisperse, spherical particles are ideal for packing into SPE cartridges and chromatography columns, therefore the sulfonation reaction should ideally not have any detrimental effect on the size or shape of the particles. The SEM images obtained for the sulfonated particles at each level of sulfonation are shown in Figure 2.3.6.1.

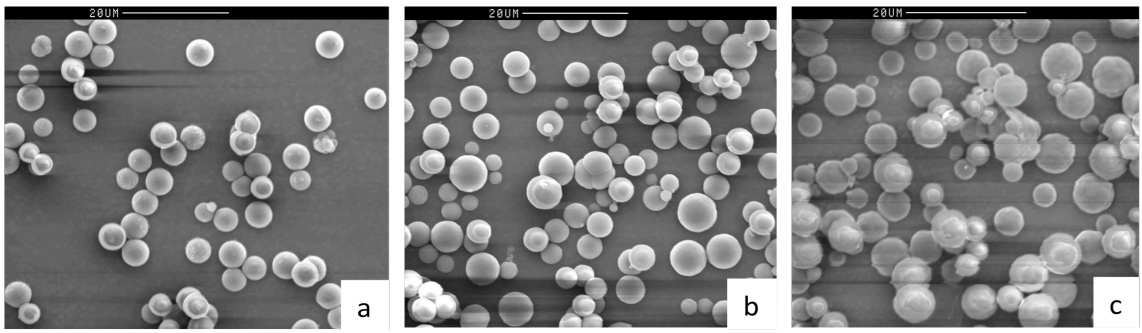

Figure 2.3.6.1. – SEM micrographs obtained for the sulfonated hypercrosslinked polymers: (a) HXL-PP-SCXa, (b) HXL-PP-SCXb, (c) HXL-PP-SCXc.

The SEM micrographs show that the HXL-SCX polymers produced are spherical in nature, with diameters in the range 3-5 μm. While not monodisperse, the size distribution is still relatively narrow and the particles should be able to pack well into SPE cartridges, or chromatography columns. During the SEM analysis the HXL-PP-SCXc sample became highly charged, resulting in a blurred image. This is perhaps due to the higher sulfonic acid content of this polymer. Despite the blurring, it is still clear that the material is composed of spherical particles in the same size range as the other HXL-PP-SCX polymers.

FT-IR spectroscopy was also used to analyse the sulfonated materials; an increase in the breadth of the peak at ~1220 cm^{-1}, ascribed to the asymmetric S=O stretch of sulfonic acid groups, was observed with increasing IEC. This is perhaps due in part to an increase in the number of sulfonic acid groups, but may also be attributed to sulfone bridge formation. The signals are not well resolved, however and thus this can neither be confirmed nor denied. This peak broadening was accompanied by an increase in intensity of both the signal at ~1059 cm^{-1}, which is ascribed to the symmetric S=O stretch of the sulfonic acid groups, and the O-H stretch at ~ 3400 cm^{-1} (Figure 2.3.6.2).

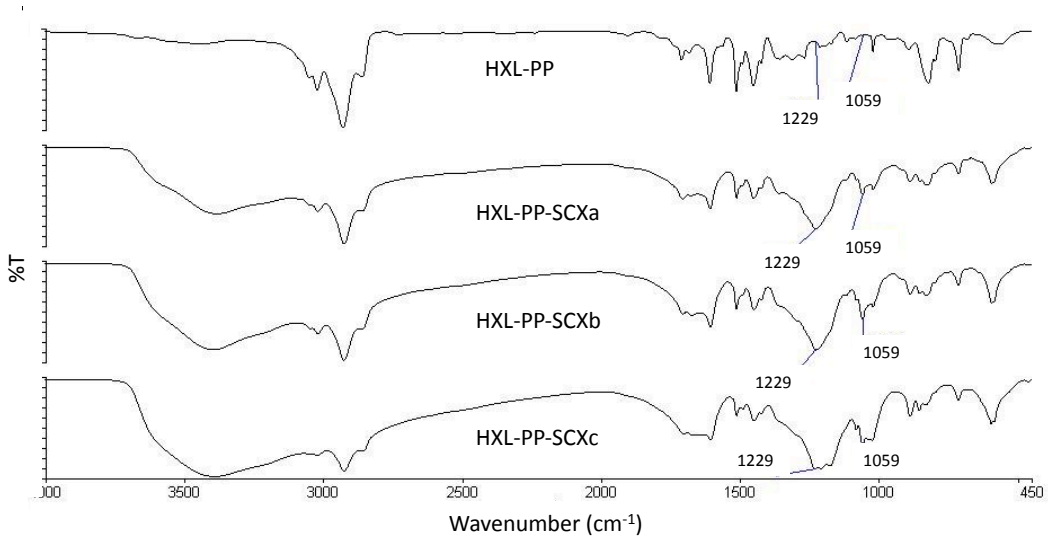

Figure 2.3.6.2. – FT-IR spectra of a non-sulfonated hypercrosslinked polymer and three sulfonated derivatives.

2.3.7. Application of HXL-PP-SCX Materials in Ion-Exchange SPE

In order to test the SPE performance of the polymeric sorbents prepared, a range of anionic and cationic compounds were required. Pharmaceutical compounds were selected as an ideal class of compounds due to their widespread use and thus the high probability of them being present in environmental samples (Table 2.3.7.1). A wide range of pharmaceutical compounds were selected to represent the variety of drug classes available.

Compound	*Therapeutic Use*	*Structure*	*pK_a*
Caffeine (**10**)	Stimulant	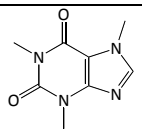	13.4
Trimethoprim (**11**)	Antibacterial	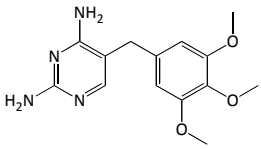	7.2
Antipyrine (**12**)	Analgesic/antipyretic	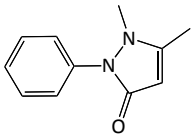	13.3
Propranolol (**13**)	β-blocker	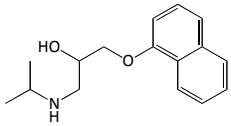	9.5
Carbamazepine (**14**)	Anticonvulsant	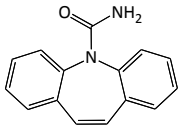	2.5
Salicylic acid (**15**)	Analgesic/antifungal	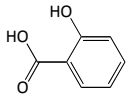	3.0
Clofibric acid (**16**)	Lipid regulator	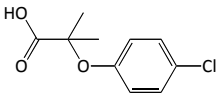	3.6
Diclofenac (**17**)	NSAID/antipyretic	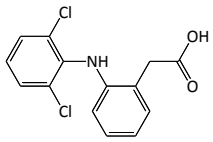	3.9
Ibuprofen (**18**)	NSAID/antipyretic	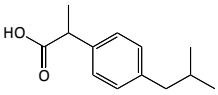	4.6

Table 2.3.7.1. – Pharmaceutical compounds used to test the HXL-PP-SCX sorbents.

All of the compounds shown should be extracted from aqueous samples through hydrophobic interactions with the hydrophobic, hypercrosslinked backbone of the sorbents, however the acidic compounds (salicylic acid (**15**), clofibric acid (**16**), diclofenac (**17**) and ibuprofen (**18**)) should be eluted during washing with an organic solvent, while the basic compounds (caffeine (**10**), trimethoprim (**11**), antipyrine (**12**), propranolol (**13**) and carbamazepine (**14**)) should remain

bound to the sorbent and thus these compounds can be eluted separately from the sorbent thereby giving a more selective extraction.

2.3.7.1. SPE Method Development.

To evaluate the performance of the HXL-PP-SCX sorbents it was necessary to select carefully the SPE conditions, to give maximum retention and elution of the basic compounds of interest. All of the SPE optimisation was carried out using ultra-pure water.

With many analytes able to bind to the sorbent through reversed-phase interactions, a washing step was extremely important to break these interactions and thus remove any interferences, while still leaving behind the basic analytes of interest which were bound to the sorbent through additional ionic interactions. The optimum volume of methanol required for such a washing step was investigated, with volumes from 1 to 10 mL being tested. With the maximum volume tested (10 mL) the basic analytes trimethoprim, antipyrine and propranolol remained completely bound to the sorbent (0 % loss), while the loss of caffeine ranged from 94 % for HXL-PP-SCXa to 10 % for HXL-PP-SCXc *i.e.*, the loss of caffeine decreased with increasing sulfonic acid content of the sorbents. With 10 mL of methanol, carbamazepine was eluted almost completely (>90 %) from all sorbents, however this is consistent with previous studies carried out within our group using commercially available SCX SPE sorbents.[72] For volumes of methanol less than 10 mL, removal of acidic impurities was incomplete. That the HXL-PP-SCXc sorbent can withstand a high volume of washing solvent, while retaining high levels of the basic analytes of interest, is extremely promising, as complex real water samples can contain very high levels of impurities and thus require large volumes of washing solvent to ensure the complete removal of such impurities prior to the elution step.

The next parameters optimised were the volume and composition of the elution solvent. For most of the basic analytes, complete elution was achieved using

5 mL of a solution of NH_4OH in methanol, however only 85 % of propranolol was recovered with this volume. Initially, 5 % of NH_4OH was added to the methanol. This was increased to 10 and 15 % in order to allow the complete removal of propranolol, however the increased concentration of NH_4OH had no significant effect on propranolol recovery. Instead, the volume of the 5 % solution of NH_4OH had to be increased, to 10 mL, before complete elution, and thus recovery, was achieved.

The final parameter investigated was the sample loading volume. The different sample volumes percolated through the sorbent were 100, 250, 500 and 1,000 mL. The volume of analyte mixture spiked into the samples was consistent throughout, thus the concentration of analytes decreased with increasing sample volume. For the sorbents HXL-PP-SCXa and HXL-PP-SCXb, the maximum volume of ultra-pure water that could be tolerated was 500 mL. Above this volume the recoveries were reduced, in particular for HXL-PP-SCXb. HXL-PP-SCXc, however, gave high recoveries even when a 1,000 mL sample was percolated through, which was extremely promising as the analytes were present at a level of only 10 μg/L.

As HXL-PP-SCXc can support the greatest sample loading volume and also provides the best retention of caffeine throughout the loading and washing steps, HXL-PP-SCXc was used for the commercial sorbent comparison and also for the complex, real water sample analysis.

As a control experiment, an unmodified hypercrosslinked polymer was also tested in order to show that the retention of the basic analytes on the HXL-PP-SCX sorbents was in fact due to the presence of sulfonic acid moieties (Table 2.3.7.1.1). As the unmodified sorbent contains no ionic groups, the sole mode of analyte retention will be through hydrophobic interactions and thus all analytes should be removed through an organic solvent wash.

From the data obtained (Table 2.3.7.11), it can be seen that the absence of sulfonic acid residues in the unmodified sorbent does indeed prevent the retention of analytes subsequent to the wash step (with the slight exception of caffeine). For the HXL-PP-SCXc sorbent, it is clear that the acidic analytes are removed by washing with an organic solvent, while basic analytes are retained until elution with a basic solution of NH_4OH in methanol. This demonstrates the effectiveness of the HXL-PP-SCXc sorbent for the selective extraction of basic compounds in the presence of acidic and neutral impurities.

	Recovery (%)			
	HXL-PP-SCXc		***Unmodified HXL-PP***	
Analyte	***Wash***	***Elution***	***Wash***	***Elution***
Caffeine	10	92	80	7
Trimethoprim	-	101	90	-
Antipyrine	-	97	87	-
Propranolol	-	102	86	-
Salicylic acid	109	-	65	-
Carbamazepine	94	5	97	-
Clofibric acid	125	-	84	-
Diclofenac	105	-	64	-
Ibuprofen	140	-	95	-

Table 2.3.7.1.1. – Recovery (%) values obtained for each analyte from the washing and elution steps after percolation of a 1,000 mL sample of ultra-pure water spiked at 10 µg/L through a sulfonated and a non-sulfonated sorbent.

The recoveries obtained for clofibric acid and ibuprofen are higher than would be expected during this anaysis. This is due to the error associated with these compounds during the HPLC anaysis. When calculating the repeatability and reproducibility, the %RSD was higher for both of these compounds, with %RSD for the other compounds being ~1, while the %RSD for these compounds was ~4-5. The limits of detection for these compounds were higher, with values of 0.050 and 0.100 ppm for ibuprofen and clofibric acid, respectively, while the

limits of detection for all of the other compounds were either 0.010 or 0.005 ppm. The limits of quantification for these compounds was also higher, with values of 0.10 and 0.25 ppm for ibuprofen and clofibric acid, respectively, while the limits of quantification for all of the other compounds were either 0.01 or 0.05 ppm. As these compounds are classed in terms of this analysis as impurities and their retention is not due to ionic interaction with the sorbent, that the recoveries are not as accurate is not a huge worry. The smaller errors associated with the compounds of interest allow for a much more accurate recovery to be calculated.

2.3.7.2. Comparison of HXL-PP-SCX with Commercial Sorbents.

As the HXL-PP-SCXc sorbent has been shown to be especially effective in SPE when compared to HXL-PP-SCXa, HXL-PP-SCXb and an unmodified hypercrosslinked sorbent, the next step was to compare it to commercially available SCX SPE sorbents. The commercially available sorbents selected were from the leading companies that supply SPE sorbent technologies. Table 2.3.7.2.1 shows characterisation data for the sorbents being compared.

Sorbent	*Supplier*	*Ion-exchange capacity (mmol/g)*	*Specific surface area (m^2/g)*	*Particle size (µm)*
HXL-PP-SCXc	In-house	2.6	1,370	3-5
Oasis MCX	Waters	1.0	805	31.4
Strata-X-C	Phenomenex	1.0	800	33
SampliQ SCX	Agilent	1.0	600	25-35
Bond Elut PCX	Varian	0.9	550	45

Table 2.3.7.2.1. – Characterisation data for HXL-PP-SCXc and the commercially available SCX sorbents.

From the characterisation data available, it is clear that there are several differences between the sorbents. HXL-PP-SCXc has a much larger specific

surface area than the Oasis MCX sorbent, which is significant as a higher specific surface area (coupled with a microporous structure) has been shown to increase the efficiency of the sorbents.[41,44] The van Deemter equation suggests that smaller particle size should also lead to better efficiency of the sorbents, thus the smaller particle size of the HXL-PP-SCXc sorbent should also be advantageous.[73] HXL-PP-SCXc has the largest recorded IEC at 2.6 mmol/g.

As the HXL-PP-SCXc sorbent was shown to perform well at a sample volume of 1,000 mL, this was the sample volume used for the comparison. 1,000 mL samples of ultra-pure water, spiked with analytes at a concentration of 10 µg/L, were percolated through each of the sorbents in turn, and the eluates from both the wash and elution steps were analysed to assess the analyte recoveries. The recoveries obtained using each of the sorbents are detailed in Table 2.3.7.2.2.

	Recovery (%)									
	HXL-PP-SCXc		***Oasis MCX***		***Strata-X-C***		***SampliQ SCX***		***Bond Elut PCX***	
Analyte	***Wash***	***Elute***	***Wash***	***Elute***	***Wash***	***Elute***	***Wash***	***Elute***	***Wash***	***Elute***
Caffeine	10	92	86	3	78	13	33	37	57	21
Trimethoprim	-	101	-	104	-	99	-	82	-	93
Antipyrine	-	97	-	99	-	89	-	74	-	89
Propranolol	-	102	-	110	-	112	-	97	-	113
Salicylic acid	109	-	102	-	99	4	77	3	82	-
Carbamazepine	94	5	91	-	98	5	79	3	91	-
Clofibric acid	125	-	89	-	131	-	101	-	94	-
Diclofenac	105	-	101	-	125	-	131	-	80	-
Ibuprofen	140	-	96	-	119	-	97	-	98	-

Table 2.3.7.2.2. – Recovery (%) values obtained from the washing and elution steps using each sorbent after percolation of a 1,000 mL sample of ultra-pure water spiked at 10 µg/L.

Perhaps the most striking difference between each of the sorbents (Table 2.3.7.2.2) is the retention of caffeine. Only the HXL-PP-SCXc sorbent can retain

caffeine to any significant level. SampliQ SCX can selectively extract around one third of the caffeine, however the recoveries of the other analytes (in particular antipyrine and, to a lesser extent, trimethoprim) are not as high as obtained with the other sorbents. Another significant point to note is that none of the sorbents can retain the basic carbamazepine, however this is in keeping with previous observations in our group.[72] Overall, each of the commercially available sorbents performs well under the conditions investigated, and the novel HXL-PP-SCXc sorbent compares favourably. The Oasis MCX sorbent was deemed to be the better of the commercial sorbents based on the higher recovery of antipyrine compared to the other sorbents. Thus for the real water sample extractions using HXL-PP-SCXc, Oasis MCX was used for the comparison.

2.3.7.3. Application to Real Samples

In order to assess the applicability of the HXL-PP-SCXc sorbent for the analysis of complex, real samples, three environmental water samples were evaluated: water from the Ebro river, which runs through the Catalonia region in Northern Spain, and water from both the influent and effluent streams of a waste water treatment plant (WWTP) in Reus, Tarragona, Spain. These samples contain very different types and levels of impurities and thus provide for a thorough evaluation of the sorbents.

The first sample matrix used for analysis was water from the Ebro river. This water will potentially contain trace levels of many types of interfering compounds. Table 2.3.7.3.1 shows the recoveries calculated for each sorbent after percolation of 1,000 mL of Ebro river water, spiked with analytes at a level of 2 μg/L.

Analyte	Recovery (%)			
	HXL-PP-SCXc		Oasis MCX	
	Wash	Elution	Wash	Elution
Caffeine	108	1	51	-
Trimethoprim	-	82	-	80
Antipyrine	-	96	-	22
Propranolol	-	36	-	55
Salicylic acid	111	-	64	1
Carbamazepine	90	10	64	-
Clofibric acid	112	-	70	-
Diclofenac	82	-	123	-
Ibuprofen	126	-	95	-

Table 2.3.7.3.1. – Recovery (%) values obtained for HXL-PP-SCXc and Oasis MCX after percolation of 1,000 mL of Ebro river water spiked with analytes at a level of 2 µg/L.

When the analytes are spiked into Ebro river water, the recoveries of all analytes are lower than for ultra-pure water. While the methanol wash successfully removed all of the acidic impurities, it also resulted in almost complete removal of caffeine from both sorbents. While this was expected for the Oasis MCX sorbent, it was very unexpected in the case of the HXL-PP-SCXc sorbent. It is most likely that this difference in behaviour of the sorbent is a consequence of the river water containing an impurity that inhibits the ionic interaction between the caffeine and the sorbent. The recoveries of trimethoprim and antipyrine on the HXL-PP-SCXc sorbent remained high, although the recovery of propranolol was greatly reduced. Again, this may be due to an interaction with another component present within the sample matrix.

On using the Oasis MCX sorbent, the recovery of trimethoprim was high as expected but the propranolol recovery was significantly reduced as was also observed for HXL-PP-SCXc. The most notable result, however, was the extremely low recovery of antipyrine. Despite being recovered at a level of

96 % on the HXL-PP-SCXc sorbent, only 22 % was retained by and thus recovered from, the Oasis MCX sorbent. In this case a matrix component(s) is presumably perturbing the interaction between the antipyrine and the Oasis sorbent, however this component has no apparent effect on the interaction between the antipyrine and the HXL-PP-SCXc sorbent. This is a very surprising result, yet promising in terms of the HXL-PP-SCXc sorbent evaluation and its future potential.

Chromatograms showing the compounds present in washing and elution steps, obtained after percolation of a 2 µg/L spiked sample of Ebro river water through the HXL-PP-SCXc sorbent, are shown in Figure 2.3.7.3.1. The chromatogram obtained from the elution step of a blank sample of Ebro river water is also shown for comparison.

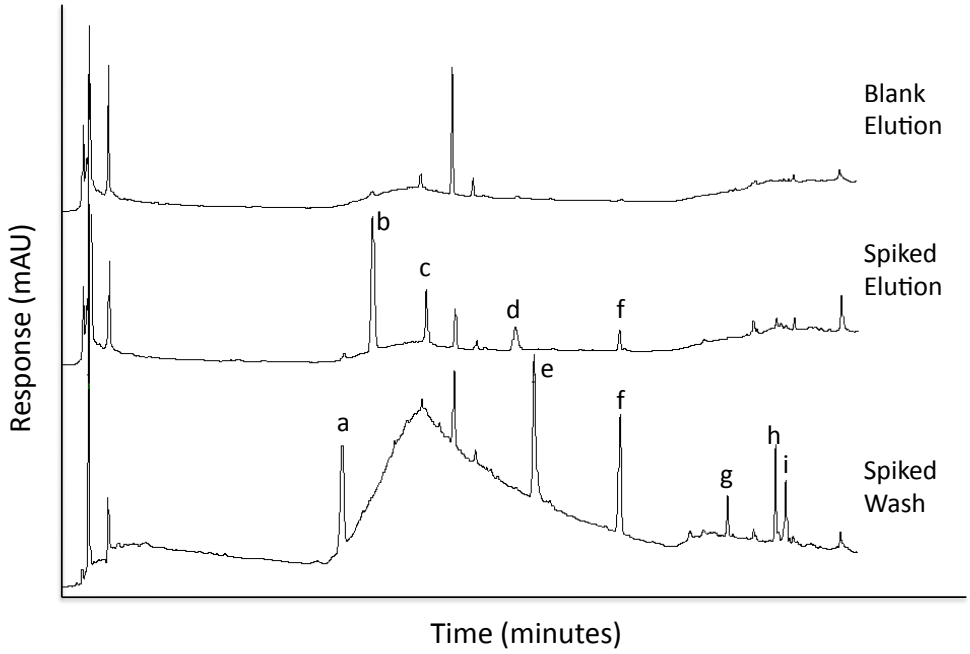

Figure 2.3.7.3.1. – Chromatograms obtained from 1,000 mL spiked (2 µg/L) and blank samples of Ebro river water percolated through the HXL-PP-SCXc sorbent: (a) caffeine, (b) trimethoprim, (c) antipyrine, (d) propranolol, (e) salicylic acid, (f) carbamazepine, (g) clofibric acid, (h) diclofenac and (i) ibuprofen.

The importance of the wash step is clearly highlighted in the chromatograms; a large rise and fall in the baseline, around the area of the analytes of interest, is removed by washing. It can also be clearly seen that the acidic analytes are completely removed by the washing step. The cleanliness of the sample is also apparent, from the lack of impurity peaks in both the wash and elution chromatograms, as well as the blank chromatogram. That the peaks present in the wash and elution chromatograms of the spiked sample are in fact a result of the analytes added is confirmed by the absence of any of these peaks in the blank chromatogram.

The next sample matrix tested was effluent water from a WWTP. This is the water that leaves the WWTP after treatment, and thus should be relatively clean, but may contain interferences introduced through the treatment process. The recoveries obtained from percolation of 250 mL samples of effluent water spiked with the analytes at a level of 8 µg/L are shown in Table 2.3.7.3.2.

	Recovery (%)			
	HXL-PP-SCXc		***Oasis MCX***	
Analyte	***Wash***	***Elution***	***Wash***	***Elution***
Caffeine	105	4	59	-
Trimethoprim	-	95	-	68
Antipyrine	-	46	-	12
Propranolol	-	85	-	56
Salicylic acid	157	-	68	-
Carbamazepine	115	10	55	-
Clofibric acid	153	-	76	-
Diclofenac	125	-	54	-
Ibuprofen	126	-	79	-

Table 2.3.7.3.2. – Recovery (%) values obtained for HXL-PP-SCXc and Oasis MCX after percolation of 250 mL of WWTP effluent water spiked with analytes at a level of 8 µg/L.

On switching to this different sample matrix, recovery of caffeine is still poor. Recovery of trimethoprim is still high and the propranolol recovery has increased again to a very high level. However, recovery of antipyrine has been greatly reduced. The reason for the differences in propranolol and antipyrine recovery, when compared to Ebro river water, is most likely due to differences in the sample matrices and the impurities contained within them. While the 46 % recovery of antipyrine has been reduced relative to previous samples, it is still significantly higher than the 12 % recovery obtained from the Oasis MCX sorbent, which is a pleasing outcome. For each of the basic analytes retained on both sorbents (trimethoprim, antipyrine and propranolol) the recoveries in all cases are approximately 30 % lower for the Oasis MCX sorbent than for the HXL-PP-SCXc sorbent, which is a very promising result in the evaluation of the novel HXL-PP-SCXc sorbent.

The recoveries of the acidic interferents are much higher than expected. This may be due to the presence of these analytes within the sample matrix prior to spiking with the analyte mixture, or indeed it may be a result of similar compounds being present in the matrix that co-elute with the analytes thus giving the appearance of higher levels present in the sample. In order to ascertain whether it is the analytes of interest or co-eluting analytes a more accurate analysis technique, such as mass spectrometry, would be required. Pedrouzo *et al*.[74] have previously noted the presence of trace levels of pharmaceuticals within samples of Ebro river water and indeed from the same WWTP.

Figure 2.3.7.3.2. shows wash and elution step chromatograms obtained for spiked and blank samples of WWTP effluent water.

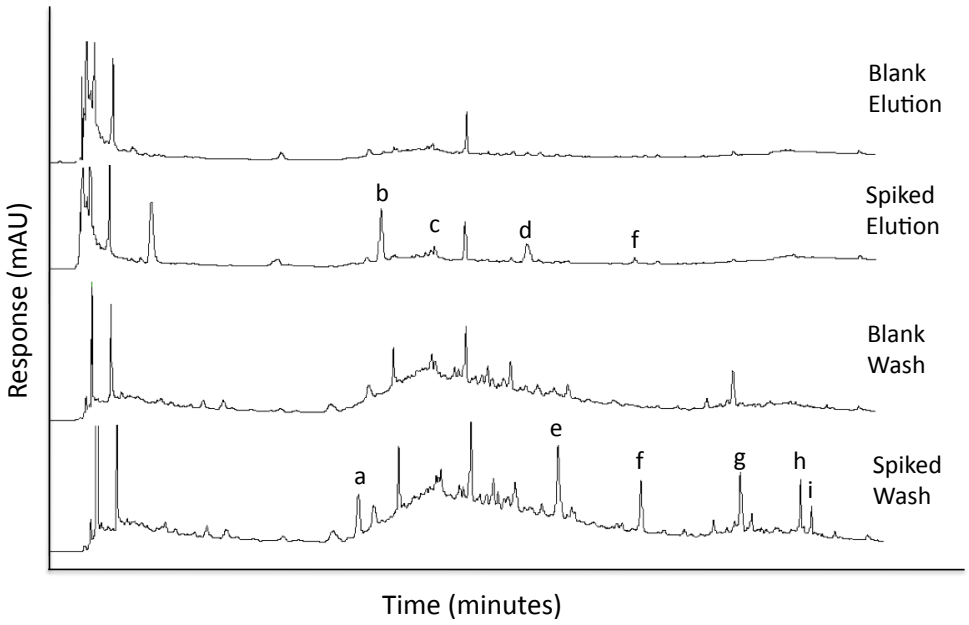

Figure 2.3.7.3.2. – Chromatograms obtained for the washing and elution steps of 250 mL spiked (8 µg/L) and blank samples of WWTP effluent water percolated through the HXL-PP-SCXc sorbent: (a) caffeine, (b) trimethoprim, (c) antipyrine, (d) propranolol, (e) salicylic acid, (f) carbamazepine, (g) clofibric acid, (h) diclofenac and (i) ibuprofen.

The chromatograms show again that the wash step was extremely successful in removing interferences to leave behind a relatively clean chromatogram containing only the basic analytes of interest. In addition, the blank wash chromatogram shows interferences around the area of salicylic acid and clofibric acid, which may help to explain the high recoveries of these analytes as shown in Table 2.3.7.3.2.

The final sample matrix used was water from the influent stream of the same WWTP. As this water had not yet been treated it was expected to contain very high levels of impurities and interferents. 100 mL samples of the influent water spiked at a level of 20 µg/L were passed through both the HXL-PP-SCXc and Oasis MCX sorbents (Table 2.3.7.3.3).

Analyte	Recovery (%)			
	HXL-PP-SCXc		Oasis MCX	
	Wash	Elution	Wash	Elution
Caffeine	No recoveries calculated.	154	No recoveries calculated.	5
Trimethoprim		51		67
Antipyrine		75		67
Propranolol		60		19
Salicylic acid		-		-
Carbamazepine		10		-
Clofibric acid		-		-
Diclofenac		-		-
Ibuprofen		-		-

Table 2.3.7.3.3. – Recovery (%) values obtained for HXL-PP-SCXc and Oasis MCX after percolation of 100 mL of WWTP influent water spiked with analytes at a level of 20 µg/L.

Due to the high level of impurities removed during the wash, recovery values for the compounds present in these eluates could not be calculated. However, such was the success of the wash step, calculation of recoveries from the elution were calculated without difficulty.

Despite the influent sample being the most complex of all the sample matrices tested, the retention, and thus recovery, of caffeine was surprisingly restored for the HXL-PP-SCXc sorbent, suggesting that perhaps the WWTP process introduces a component(s) into the effluent water which causes the poor caffeine retention. The 154 % recovery of caffeine indicates that there was some caffeine present within the influent water prior to the sample being spiked with analytes, or that there is another component within the influent water which co-elutes with the caffeine. While caffeine recovery was extremely successful using the HXL-PP-SCXc sorbent, recovery on the Oasis MCX sorbent was very poor at only 5 %. This is all the more disappointing for the Oasis MCX sorbent considering the enhanced level of caffeine provided by the influent water itself. Propranolol recovery is also significantly different between the

two sorbents. While the 60 % recovery on the HXL-PP-SCXc sorbent is lower than was obtained from the effluent water, it is still significantly higher than the 19 % recovery on the Oasis MCX sorbent. For the other basic analytes; trimethoprim recovery was, for the first time, reduced by quite a significant amount, however this can be seen for both sorbents, and antipyrine recovery is similar on both of the sorbents.

Figure 2.3.7.3.3. shows wash and elution chromatograms for both a blank and a spiked (20 µg/L) sample of WWTP influent water.

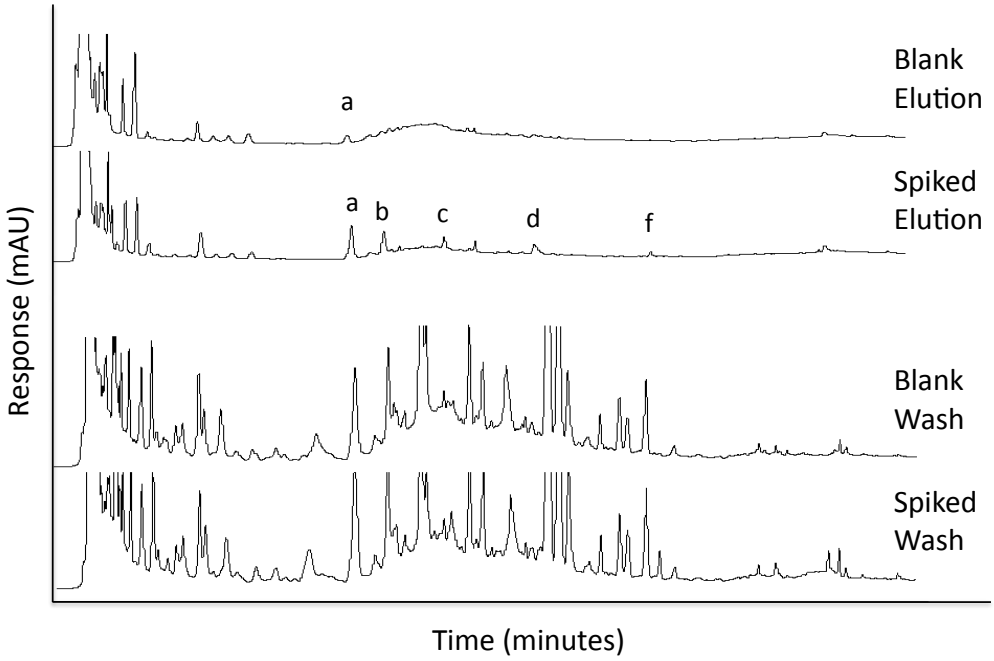

Figure 2.3.7.3.3. – Chromatograms obtained for the washing and elution steps of 100 mL spiked (20 µg/L) and blank samples of WWTP influent water percolated through the HXL-PP-SCXc sorbent: (a) caffeine, (b) trimethoprim, (c) antipyrine, (d) propranolol and (f) carbamazepine.

The high level of impurities present in the wash chromatograms show just how complex and 'dirty' the influent water is. Recovery values for the analytes within the wash chromatogram could not be calculated due to the complexity of the sample. With this in mind, it is really quite remarkable how clean the elution chromatograms are, and how flat the baselines are. This serves to

reinforce just how important the wash step is, and also how selective the ionic interactions between the sorbent and the basic analytes of interest are. In the blank elution chromatogram, a peak is clearly visible which co-elutes with caffeine. This supports the belief that the high level of caffeine recovered from percolation of the spiked sample was perhaps due to caffeine already present within the sample matrix, as previously demonstrated by Pedrouzo *et al*.[74] However, a more powerful and accurate analytical method, such as mass spectrometry, would be required to ensure that this peak is in fact due to caffeine and not another basic compound that co-elutes.

2.4. CHAPTER CONCLUSIONS

It has been demonstrated that sulfonic acid functionality can be introduced into hypercrosslinked polymers in a facile and controlled manner. Lauroyl sulfate was shown to be a more effective sulfonating reagent than acetyl sulfate. With lauroyl sulfate as the sulfonating reagent, the reaction conditions were optimised and a synthetic strategy for the production of hypercrosslinked polymer microspheres functionalised with sulfonic acid groups (and thus strong cation-exchange properties) was developed. This synthetic strategy was used to prepare hypercrosslinked polymer microsphere-based SPE sorbents with three strong cation-exchange loading levels/capacities. These sulfonated hypercrosslinked polymers (HXL-PP-SCX) were then applied to the solid-phase extraction of pharmaceuticals from complex real water samples, with the pharmaceutical recoveries on the novel HXL-PP-SCX sorbents comparing, in some cases, favourably to those obtained using commercially available SPE sorbents.

2.5. REFERENCES

1. G. D. Christian, *Analytical Chemistry*, *Fifth Edition*, J. Wiley and Sons, New York, 1994, p517-522.
2. S. Takamuku, K. Akizuki, M. Abe and H. Kanesaka, *J. Polym. Sci. Part A: Polym. Chem.*, (2009), **47**, 700-712.
3. B. Chakravorty, R. N. Mukherjee and S. Basu, *J. Membrane Sci.*, (1989), **41**, 155-161.
4. Z. Zhang, E. Chalkova, M. Fedkin, C. Wang, S. N. Lvov, S. Komarneni and T. C. M. Chung, *Macromolecules*, (2008), **41**, 9130-9139.
5. K. Matsumoto, T. Higashihara and M. Ueda, *Macromolecules*, (2009), **42**, 1161-1166.
6. B. Bae, T. Hoshi, K. Miyatake and M. Watanabe, *Macromolecules*, (2011), **44**, 3884-3892.
7. H. Baharvand and A. Rabiee, *J. Appl. Polym. Sci*, (2004), **91**, 2973-2979.
8. A. Seubert and A. Klingenberg, *J. Chromatogr. A*, (1997), **782**, 149-157.
9. D. W. Brousmiche, J. E. O'Gara, D. P. Walsh, P. J. Lee, P. C. Iraneta, B. C. Trammell, Y. Xu and C. R. Mallet, *J. Chromatogr. A*, (2008), **1191**, 108-117.
10. L. Rubatat, C. Li, H. Dietsch, A. Nykänen, J. Ruokolainen and R. Mezzenga, *Macromolecules*, **41**, (2008), 8130-8137.
11. C. P. L. Rubinger, C. R. Martins, M.-A. De Paoli and R. M. Rubinger, *Sensors and Actuators B*, (2007), **123**, 42-49.
12. A. Nordborg, F. Limé, A. Shchukarev and K. Irgum, *J. Sep. Sci.*, (2008), **31**, 2143-2150.
13. M. Dieterle, T. Blaschke and H. Hasse, *J. Chromatogr. A*, (2008), **1205**, 1-9.
14. Y. Arakawa, N. Haraguchi and S. Itsuno, *Angew. Chem. Int. Ed.*, (2008), **47**, 8232-8235.
15. N. Haraguchi, Y. Takemura and S. Itsuno, *Tetrahedron Lett.*, (2010), **51**, 1205-1208.
16. S. Itsuno, D. K. Paul and N. Haraguchi, *Chem. Lett.*, (2010), **39**, 86-87.
17. S. Itsuno, D. K. Paul, M. A. Salam and N. Haraguchi, *J. Am. Chem. Soc.*, (2010), **132**, 2864-2865.
18. T. Matsuura, K. Ohnaka, M. Takagi, M. Ohashi, K. Mibu and A. Yuchi, *Anal. Chem.*, (2008), **80**, 9666-9671.
19. N. Sahiner, K. Sel, K. Meral, Y. Onganer, S. Butun, O. Ozay and C. Silan, *Colloids Surfaces A: Physicochem. Eng. Aspects*, (2011), **389**, 6-11.

20. B. Liu, W. Hu, G. P. Robertson and M. D. Guiver, *J. Mater. Chem.*, (2008), **18**, 4675-4682.
21. A. G. Theodoropoulos, V. T. Tsakalos and G. N. Valkanas, *Polymer*, (1993), **34**, 3905-3910.
22. M. M. Nasef and H. Saidi, *J. Membrane Sci.*, (2003), **216**, 27-38.
23. N. A. Peppas and K. P. Staller, *Polym. Bull.*, (1982), **8**, 233-237.
24. R. Neihof, *J. Phys. Chem.*, (1954), **58**, 916-925.
25. M. Kato, T. Nakagawa and H. Akamatu, *Bull. Chem. Soc. Japan*, (1960), **33**, 322-329.
26. N. A. Peppas, W. R. Bussing and K. A. Slight, *Polym. Bull.*, (1981), **4**, 193-198.
27. H. S. Makowski, R. D. Lundberg and G. H. Singhal, *U.S. Patent 3,870,841*, (1975).
28. R. A. Weiss, A. Sen, C. L. Willis and L. A. Pottick, *Polymer*, (1991), **32**, 1867-1874.
29. C. R. Martins, G. Ruggeri and M.-A. De Paoli, *J. Braz. Chem. Soc.*, (2003), **14**, 797-802.
30. N. R. Cameron, D. C. Sherrington, I. Ando and H. Kurosu, *J. Mater. Chem.*, (1996), **6**, 719-726.
31. W. A. Thaler, *Macromolecules*, (1983), **16**, 623-628.
32. K. W. Pepper, D. Reichinberg and D. K. Hale, *J. Chem. Soc.*, (1952), 3129-3136.
33. A. F. Turbak, *Ind. Eng. Chem., Prod. Res. Dev.*, (1962), **1**, 275-278.
34. P. Ergenekon, E. Gürbulak, B. Keskinler, *Chem. Eng. Process.*, (2011), **50**, 16-21.
35. E. Unsal, B. Elmas, B. Çağlayan, M. Tuncel, S. Patir and A. Tuncel, *Anal. Chem.*, (2006), **78**, 5868-5875.
36. G. D. Christian, *Analytical Chemistry*, *Fifth Edition*, J. Wiley and Sons, New York, 1994, p499-501.
37. N. Fontanals, R. M. Marcé and F. Borrull, *Trends Anal. Chem.*, (2005), **24**, 394-406.
38. N. Fontanals, R. M. Marcé and F. Borrull, *J. Chromatogr. A*, (2007), **1152**, 14-31.
39. G. A. Junk, J. J. Richard, M. D. Grieser, D. Witiak, M. D. Arguello, R. Vick, H. J. Svec, J. S. Fritz and G. V. Calder, *J. Chromatogr.*, (1974), **99**, 745-762.
40. J. S. Fritz, P. J. Dumont and L. W. Schmidt, *J. Chromatogr. A*, (1995), **691**, 133-140.
41. N. Fontanals, M. Galia, P. A. G. Cormack, R. M. Marcé, D. C. Sherrington and F. Borrull, *J. Chromatogr. A*, (2005), **1075**, 51-56.
42. K. Bielicka-Daszkiewicz, A. Voelkel, M. Szejner and J. Osypiuk, *Chemosphere*, (2006), **62**, 890-898.
43. N. Fontanals, M. Galia, R. M. Marcé and F. Borrull, *J. Chromatogr. A*, (2004), **1030**, 63-68.

44. V. Davankov, L. Pavlova, M. Tsyurupa, J. Brady, M. Balsamo and E. Yousha, *J. Chromatogr. B*, (2000), **739**, 73-80.
45. X. Liu, J. Li, Z. Zhao, W. Zhang, K. Lin, C, Huang and X. Wang, *J. Chromatogr. A*, (2009), **1216**, 2220-2226.
46. I. G. Casella, G. A. Palladino and M. Contursi, *J. Sep. Sci.*, (2008), **31**, 3718-3726.
47. U. Nilsson, N. Berglund, F. Lindahl, S. Axelsson, T. Redeby, P. Lassen and A.-T. Karlberg, *J. Sep. Sci.*, (2008), **31**, 2784-2790.
48. V. Davankov, L. Pavlova, M. Tsyurupa, J. Brady, M. Balsamo and E. Yousha, *J. Chromatogr. B*, (2000), **739**, 73-80.
49. P. K. Kanaujia, V. Tak, D. Pardasani, A. K. Gupta and D. K. Dubey, *J. Chromatogr. A*, (2008), **1185**, 167-177.
50. N. Fontanals, J. Cortés, M. Galià, R. M. Marcé, P. A. G. Cormack, F. Borrull and D. C. Sherrington, *J. Polym. Sci. Part A: Polym. Chem.*, (2005), **43**, 1718-1728
51. N. Masqué, M. Galia, R. M. Marcé and F. Borrull, *J. Chromatogr. A*, (1997), **771**, 55-61.
52. N. Masqué, M. Galia, R. M. Marcé and F. Borrull, *Analyst*, (1997), **122**, 425-428.
53. N. Masqué, M. Galia, R. M. Marcé and F. Borrull, *J. Chromatogr. A*, (1998), **803**, 147-155.
54. N. Masqué, M. Galia, R. M. Marcé and F. Borrull, *Chromatographia*, (1997), **50**, 21-26.
55. http://www.waters.com/waters/nav.htm?locale=en_US&cid=513209 (accessed on 06 Apr 2009)
56. http://www.phenomenex.com/Products/SPDetail/Strata-X (accessed on 14 Oct 2011)
57. http://www.chem.agilent.com/Library/brochures/5989-9334EN.pdf (accessed on 14 Oct 2011)
58. http://www.chem.agilent.com/Library/brochures/5990-6042EN.pdf (accessed on 14 Oct 2011)
59. B. Kasprzyk-Horden, R. M. Dinsdale and A. J. Guwy, *Anal. Bioanal. Chem.*, (2008), **391**, 1293-1308.
60. M. Lavén, T. Alsberg, Y. Yu, M. Adolfsson-Erici and H. Sun, *J. Chromatogr. A*, (2009), **1216**, 49-62.
61. N. Lindqvist, T. Tuhkanen and L. Kronberg, *Water Res.*, (2005), **39**, 2219-2228.

62. S. Castiglioni, R. Bagnati, D. Calamari, R. Fanelli and E. Zuccato, *J. Chromatogr. A*, (2005), **1092**, 206-215.
63. A. Salvador, D. Dubreuil, J. Denouel and L. Millerioux, *J. Chromatogr. B*, (2005), **820**, 237-242.
64. S. Huq, A. Dixon, K. Kelly and K. M. R. Kallury, *J. Chromatogr. A*, (2005), **1073**, 355-361.
65. S. Zorita, L. Larsson and L. Mathiasson, *J. Sep. Sci.*, (2008), **31**, 3117-3121.
66. V. Balakrishnan, K. A. Terry and J. Toito, *J. Chromatogr. A*, (2006), **1131**, 1-10.
67. E. Bermudo, E. Moyano, L. Puignou and M. T. Galceran, *Anal. Chim. Acta.*, (2006), **559**, 207-214.
68. D. N. Mallet, S. Dayal, G. J. Dear and A. J. Patemen, *J. Pharm. Biomed. Anal.*, (2006), **41**, 510-516.
69. N. Rosales-Conrado, M. E. León-Gonzáles, L. V. Pérez-Arribas and L. M. Polo-Díez, *J. Chromatogr. A*, (2005), **1076**, 202-206.
70. T. Miyauchi, M. Mori and K. Ito, *J. Chromatogr. A*, (2005), **1095**, 74-80.
71. T. Miyauchi, M. Mori and K. Ito, *J. Chromatogr. A*, (2005), **1063**, 137-141.
72. N. Gilart, Final Year Thesis, *Universitat Rovira i Virgili*, Tarragona, Spain, 2009.
73. http://www.restek.com/Technical-Resources/Technical-Library/Pharmaceutical/pharm_A016 (accessed on 07 Nov 2011)
74. M. Pedrouzo, S. Reverté, F. Borrull, E. Pocurull and R. M. Marcé, *J. Sep. Sci.*, (2007), **30**, 297-303.

CHAPTER 3

SYNTHESIS, CHARACTERISATION AND APPLICATION OF HYPERCROSSLINKED POLYMER MICROSPHERES WITH STRONG ANION-EXCHANGE PROPERTIES

3.1. INTRODUCTION

As demonstrated in Chapter 2, addition of sulfonic acid functionality into hypercrosslinked polymers can be achieved in a facile manner, and this allows for more selective extraction of analytes from real water samples to be realised. In order to provide a complementary material, a strong anion-exchange functionality in the hypercrosslinked material is required. This can be achieved through incorporation of quaternary ammonium moieties into the structure of the hypercrosslinked polymer.

3.1.1. Anion-Exchange Resins

In anion-exchange resins, strong anion-exchange (SAX) character arises from the presence of a quaternary ammonium cation on the resin. Amine moieties provide weak anion-exchange (WAX) functionality. It is normally a halogen or hydroxyl anion on these quaternary ammonium groups that is exchanged with anions (Figure 3.1.1.1).[1]

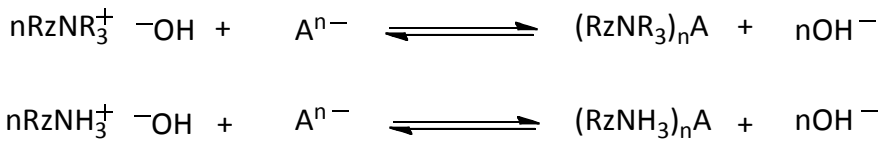

Figure 3.1.1.1. – Exchange of hydroxyl anion on anion-exchange resin (Rz=Resin).

As with cation-exchange resins, the key practical difference between strong and weak anion-exchange resins lies in the pH range over which they can perform. SAX resins work from pH 0 to pH 12, whereas WAX resins work only over the range from 0 to 9. WAX resins are not capable of removing very weak acids, but are the preferred resin in the case of capture of strong acids, such as sulfonic acids, which are so strongly acidic that they are bound very tightly by SAX resins.

3.1.2. Use of Aminated Polymers

Polymers with amine functionality can be used in many applications. Anion-exchange polymers with amine functionality can be prepared in resin,[2,3,4] fibre[5] and monolith[6] forms. Several ion-exchange chromatography supports, based on amine-containing polymers, have also been reported.[7,8,9,10] Other uses reported include solid-phase extraction (SPE) sorbents,[11,12] a fuel cell membrane material[13] and biologically active, antimicrobial polymers.[14]

3.1.3. Amination Reactions

In order to introduce amine functionality into a polystyrene-based polymer, there are many methods that can be employed. One of the most popular routes involves first chloromethylating the aromatic residues present, followed by utilising the newly introduced chloromethyl groups in a subsequent nucleophilic aliphatic substitution reaction with the desired amine.[4,6,9,10,12] The chloromethylation step can be carried out in several ways, with the notoriously toxic[15] stannic chloride often forming part of the synthetic protocol. A safer alternative for laboratory-scale synthesis is to substitute an alkyl chloride containing monomer, such as vinylbenzyl chloride[11,14] (VBC) or 2-chloroethyl vinyl ether,[14] for styrene in the initial polymerisation to introduce the chloromethyl groups in the first step of the reaction. This also has the advantage of reducing the overall preparation time as it removes the chloromethylation step, which can be a very lengthy process. Introduction of chloromethyl groups, be it through post-polymerisation chloromethylation or through inclusion of VBC, then allows for further reaction with an amine to yield the desired functionality.

Other methods for introducing amines into styrenic polymers include inclusion of an amine containing monomer,[3] inclusion of glycidyl methacrylate in the

polymerisation, followed by ring-opening of the epoxide with an amine,[5,7] and first nitrating the aromatic rings, followed by subsequent reduction of the nitro groups using hydrazine hydrate.[2]

Fontanals *et al*.[11] prepared amine-functionalised hypercrosslinked polymer microspheres by exploiting the chloromethyl groups remaining after hypercrosslinking, in a nucleophilic aliphatic substitution reaction with both primary and secondary amines (ethylene diamine and piperazine, respectively). Introduction of primary and secondary amines gave the hypercrosslinked polymers weak anion-exchange (WAX) properties, and these polymers were subsequently applied as WAX SPE sorbents for the selective extraction of acidic pharmaceuticals in the analysis of real water samples.

3.1.4. Anion-Exchange Solid-Phase Extraction

Combining the hydrophobic interactions obtained through the use of polymeric SPE sorbents with additional ionic interactions on the sorbent gives a much more selective extraction. Several SPE sorbents containing amine and ammonium functionalities are commercially available (Table 3.1.4.1).

Use of these polymeric anion-exchange sorbents has allowed the selective extraction of acidic compounds from complex mixtures containing basic and/or neutral interferences. Compounds such as pharmaceuticals,[16,17,18] illicit drugs[18], sunscreen agents,[18] preservatives,[18] disinfectants,[18] phenolic compounds[19] and colophonium components[20] have been extracted from matrices including cosmetics,[20] wastewaters,[16,17,18] river and sea water[16] and aqueous solutions.[19]

Sorbent	*Supplier*	*Sorbent Properties*				*Ref.*
		Polymer base	*Ionic group*	*Ionic mode*	*Meq g^{-1}*	
Oasis MAX	Waters	Oasis HLB [poly(DVB-*co*-*N*-vinyl pyrrolidone)]	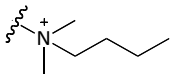	Strong anion	0.25	21
Oasis WAX			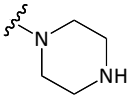	Weak anion	0.60	
Strata-X-C	Phenomenex	Strata X [poly(styrene-*co*-DVB)]	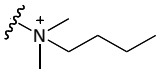	Strong anion	No data	22
Strata-X-CW			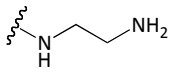	Weak anion	0.60	
SampliQ SAX	Agilent	SampliQ OPT [polyDVB]	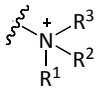	Strong anion	0.09	23
SampliQ WAX			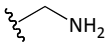	Weak anion	0.67	

Table 3.1.4.1. – Structure and properties of commercially available mixed-mode anion-exchange SPE sorbents.

3.2. EXPERIMENTAL

3.2.1. Materials

Divinylbenzene-80 (mixture of isomers, 80.0 % grade) and 4-vinylbenzyl chloride (≥ 90.0 %) were purchased from Sigma-Aldrich and purified prior to use by passing through a column of neutral alumina. 2,2'-Azo*bis*(isobutyronitrile), AIBN, (97.0 %) was purchased from BDH and was recrystallised from acetone at low temperature. HPLC grade acetonitrile was

purchased from Rathburn Chemicals and was used as received. Iron(III) chloride (97.0 %), anhydrous 1,2-dichloroethane, DCE, (99.8 %), triethylamine (≥99.5 %) and dimethylbutylamine, DMBA, (99 %) were purchased from Sigma-Aldrich and used as received. Sodium hydrogen carbonate (>99.5 %) and sodium chloride (≥99.5 %) were purchased from BDH and were also used as received.

The solvents employed (toluene, acetone, methanol and diethyl ether) were of standard laboratory reagent grade, and were purchased from Sigma-Aldrich.

For the sorbent evaluation through SPE (N.B. this particular body of analytical work was carried out by D. Bratkowska in a collaborating group in Universitat Rovira i Virgili, Tarragona, Spain), the pharmaceutical compounds caffeine, antipyrine, propranolol, carbamazepine, salicylic acid, fenoprofen, ibuprofen and diclofenac, were all obtained from Sigma-Aldrich and used as received. Ultra-pure reagent water, purified using a Milli-Q gradient system from Millipore, was used throughout. Acetonitrile and methanol (both HPLC grade) were purchased from SDS, and hydrochloric acid was supplied by Probus. Standard stock solutions (1,000 mg/L) were prepared for each analyte in methanol. A 100 mg/L mixture of all compounds was prepared by diluting the standard solutions in ultra-pure water. All solutions were stored at 4 ^{o}C.

Real water samples were obtained from the Ebro river (Catalonia Region, Spain) and from the effluent stream of a waste water treatment plant (Tarragona, Spain). The samples were filtered through 0.45 μm nylon membranes (Supelco) prior to SPE to eliminate particulate matter. The pH of the real water samples was adjusted to pH 3 with HCl and stored at 4 ^{o}C prior to analysis.

The commercially available SAX SPE sorbents used for comparison were Oasis MAX from Waters and SampliQ SAX from Agilent.

3.2.2. Equipment

Precipitation polymerisations were carried out using a Stuart Scientific S160 incubator (Surrey, UK) and a Stovall low-profile roller system (NC, USA). All of the polymerisations were carried out in Nalgene® plastic bottles.

The optical compound microscope employed was a Carl Zeiss Jena (Germany).

Elemental microanalysis was carried out by the University of Strathclyde Elemental Microanalysis Service. C, H and N elemental microanalyses were carried out simultaneously using a Perkin Elmer 2400 Series II analyser. Halogen and sulfur contents were determined by standard titration methods.

Scanning electron microscopy (SEM) was carried out by the University of Strathclyde SEM service, using a Cambridge Instruments Stereoscan 90. Samples were coated in gold prior to SEM imaging.

Fourier-Transform Infrared (FT-IR) analysis was carried out using a Perkin-Elmer Spectrum One FT-IR spectrometer. The sample was prepared as a disc with spectroscopic grade KBr in an RIIC press at 10 tons. The sample was scanned over the range 4,000-400 cm^{-1} in transmission mode.

The specific surface area measurements were performed using a Micromeritics ASAP 2000 (sample > 300 mg) or 2020 (samples < 300 mg). Samples were degassed overnight under vacuum at 100 ^{o}C prior to analysis. Analysis was *via* nitrogen sorption, carried out at 77 K.

Solvent uptake data was obtained using centrifuge tubes fitted with 0.2 μm modified nylon 500 μL centrifugal filter inserts (VWR, North America). The centrifuge used was an Eppendorf Centrifuge 5804 (Hamburg, Germany).

The SPE evaluations were performed in an off-line mode using 200 mg of each polymer packed into 6 mL polypropylene cartridges fitted with 2 μm stainless-steel frits (Supelco) below the sorbent bed and a 10 μm pore size polyethylene frit above the sorbent bed. The cartridges were connected to a Teknokroma SPE manifold, which was connected to a vacuum pump. The sorbents were activated using 5 mL of methanol, followed by 5 mL of ultra-pure water acidified to pH 3. The analytes were loaded in 5-1,000 mL of ultra-pure or real water samples (both adjusted to pH 7, with HCl or NaOH as appropriate, prior to analysis). After loading, the cartridge was washed by passing 10 mL of methanol over the sorbent and then basic analytes were eluted with 10 mL of 10 % formic acid in methanol. The eluates from the washing and elution steps were evaporated to dryness under a stream of nitrogen and the respective residues reconstituted in 500 μL of a 1/1 (v/v) mixture of water/methanol.

The chromatographic experiments were performed with an Agilent 1100 series LC system, with a UV spectrophotometric detector and an injection valve with a 20 μL sample loop. The analytical column was a 250 mm × 4.6 mm ID stainless-steel column packed with Kromasil 100 C_{18}, 5 μm, from Teknokroma. The mobile phase was ultra-pure water, adjusted to pH 3 with HCl, and acetonitrile. The flow rate was 1 mL/min and the column oven was set at a temperature of 30 ^{o}C. The gradient profile was initially from 20 % to 25 % acetonitrile in 15 minutes, then to 60 % acetonitrile in 15 minutes, to 100 % acetonitrile in 10 minutes (held for 2 minutes), after which time the mobile phase was returned to the initial conditions (20 % acetonitrile) in 3 minutes. The wavelength used for detection was 210 nm.

3.2.3. Typical Preparation of Poly(DVB-co-VBC) Precursors by PP (PP1)

VBC (**9**) (6.925 mL, 7.500 g, 0.058 mol), DVB-80 (**2**) (2.735 mL, 2.500 g, 0.018 mol) and AIBN (**1**) (0.278 g, 1.695 mmol, 2 mol % relative to polymerisable double bonds) were charged to a 1 L Nalgene® bottle together with 500 mL of acetonitrile. The bottle was placed into an ultrasonic bath for

10 minutes and was then purged with N_2, whilst on an ice bath, for 10 minutes before being sealed under N_2. The bottle was placed onto a low profile roller, which was housed in a temperature-controlled incubator. The temperature was ramped from room temperature to 60 °C over a period of around 2 hours and then held at 60 °C for a further 46 hours. After 46 hours, a representative sample of product was examined under an optical microscope to discern the presence of microspheres. When microspheres could be seen, the product was filtered by vacuum on a 0.2 μm nylon filter membrane and washed with successive 50 mL volumes of acetonitrile, toluene, methanol and acetone. The product, in the form of a white powder, was dried overnight at 40 °C *in vacuo* (1.721 g, 17 %).

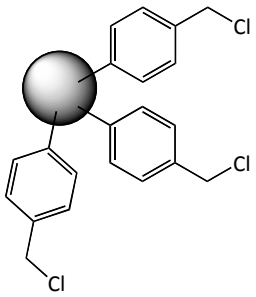

Elemental microanalysis: Expected 76.0 % C, 6.5 % H, 0.5 % N, 17.0 % Cl; Found 76.4 % C, 6.4 % H, 0.5 % N, 16.8 % Cl.

FT-IR $\bar{\nu}$*/cm*$^{-1}$ *(KBr): 3022, 2922, 2850, 1605, 1586, 1510, 1445, 1266 (C-H wag of* CH_2*-Cl), 990, 901, 831, 796, 709 (C-Cl str.).*

BET specific surface area: < 5 m^2/g.

An analogous procedure was followed for all of the DVB/VBC precursors prepared. The relevant masses and yield data are presented in Table 3.2.3.1.

Polymer ref.	*DVB (g)*	*VBC (g)*	*AIBN (g)*	*Yield (g)*	*Yield (%)*	*% Cl (w%)*	*Particle Size (μm)*
PP1	2.500	7.500	0.278	1.721	17	16.8	3-5
PP2	5.000	15.000	0.575	4.813	24	14.9	3-5
PP4	2.500	7.500	0.276	2.203	22	14.8	3-5
PP7	5.000	15.000	0.580	3.514	18	14.8	3-5
PP8	2.500	7.500	0.281	2.789	28	15.2	3-5
PP9	2.500	7.500	0.276	2.307	23	14.6	3-5
PP10	2.500	7.500	0.279	1.961	20	14.4	3-5

Table 3.2.3.1. – Feed and analytical data for the DVB/VBC precipitation polymerisations.

3.2.4. Typical Hypercrosslinking Reaction (HXL-PP7)

Precursor particles, PP7, (2.870 g, 0.014 mol of VBC residues) were charged to a dry, three-necked, round-bottomed flask equipped with a reflux condenser and an overhead mechanical stirrer. Anhydrous DCE (30 mL) was added and the beads were left to swell fully under N_2 at room temperature for 1 hour. $FeCl_3$ (2.269 g, 0.014 mol, in a 1:1 mole ratio with respect to the CH_2Cl content of the particles) in DCE (30 mL) was added and the mixture heated at 80 ^oC for 18 hours. The product particles were recovered from the reaction medium by filtration on a 0.2 μm nylon filter and washed with successive 50 mL volumes of methanol, aqueous HNO_3 (pH 1) (2 washes), methanol and acetone. The orange-coloured particles were then extracted with acetone overnight in a Soxhlet apparatus and were then washed with acetone, methanol and diethyl ether before drying *in vacuo* overnight at 40 ^oC (2.333 g, 81 %).

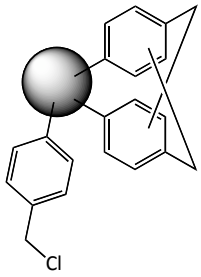

Elemental microanalysis: Expected 92.1 % C, 7.3. % H, 0.6. % N, 0 % Cl; Found 82.8 % C, 7.0 % H, 1.0 %N, 4.5 % Cl.

FT-IR $\bar{\nu}$*/cm*$^{-1}$ *(KBr): 3021, 2927, 2857, 1604, 1560, 1510, 1448, 1297, 1267 (C-H wag of* CH_2*-Cl), 894, 826, 710 (C-Cl str.).*

Langmuir specific surface area: 1,285 m^2/g*.*

An analogous procedure was followed for all syntheses of hypercrosslinked polymer microspheres. The relevant feed and analytical data are shown in Table 3.2.4.1.

Polymer ref.	*Precursor (g)*	*$FeCl_3$ (g)*	*Time (mins)*	*Yield (g)*	*Yield (%)*	*% Cl (w%)*	*Specific Surface Area* (m^2/g)*
HXL-PP2	4.021	3.500	1080	3.498	87	3.9	< 5
HXL-PP7	2.870	2.406	1080	2.333	81	3.0	1,285
HXL-PP4-5mins	0.198	0.135	5	0.119	60	5.3	1,240
HXL-PP4-10mins	0.199	0.140	10	0.125	63	4.0	1,530
HXL-PP4-15mins	0.199	0.139	15	0.111	58	3.9	1,500

Table 3.2.4.1. – Feed and yield data for hypercrosslinking reactions of poly(DVB-*co*-VBC). *Specific surface areas calculated using the Langmuir isotherm.

3.2.5. Typical Amination of Hypercrosslinked Particles Using Triethylamine (HXL-PP7-AT1)

Hypercrosslinked particles, HXL-PP7, (0.250 g, 0.208 mmol of Cl residues) were charged to a two-necked, round-bottomed flask fitted with an overhead mechanical stirrer. A 50/50 (v/v) mixture of toluene/methanol (40 mL) was added and left for 1 hour to wet the beads. After 1 hour, triethylamine (**19**)

(0.145 mL, 0.105 g, 4.155 mmol, a 5-fold excess relative to the number of moles of Cl present in the hypercrosslinked material) was added dropwise using a syringe and the reaction was left to stir at room temperature for 24 hours. After 24 hours, the resultant particles were filtered using a 0.2 μm nylon filter and washed with 50 mL volumes of toluene, methanol, 50/50 (v/v) methanol/water, water, 5 % $NaHCO_3$, water and acetone. The product was then extracted overnight in a Soxhlet apparatus with acetone. The product, in the form of an orange powder, was then dried overnight at 40 °C *in vacuo* (0.185 g, 68 %).

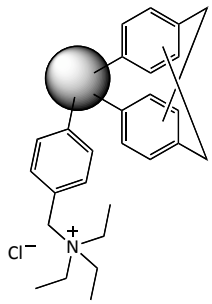

Elemental microanalysis: Expected 87.7 % C, 7.1 % H, 2.3 % N, 2.9 % Cl; Found 81.2 % C, 6.6 % H, 1.0 % N, 3.2 % Cl.

FT-IR $\bar{\nu}/cm^{-1}$ *(KBr): 3021, 2928, 2857, 1606, 1560, 1511, 1449, 1305, 892, 824, 710 (C-Cl str.)*

3.2.6. Typical Amination of Hypercrosslinked Particles using Dimethlybutylamine (HXL-PP7-AD1)

Hypercrosslinked particles, HXL-PP7, (0.500 g, 0.416 mmol of Cl residues) were charged to a three-necked, round-bottomed flask equipped with a reflux condenser and mechanical stirrer, under an N_2 atmosphere. Dimethylbutylamine (**20**) (30 mL) was added and the reaction was heated to reflux (95 °C) for 2 hours. The product particles were washed with deionized water until the washings became neutral. The product was then washed with

methanol (100 mL) and oven-dried under vacuum at 40 °C for 24 hours to give HXL-PP7-AD1 as an orange powder (0.448 g, 77 %).

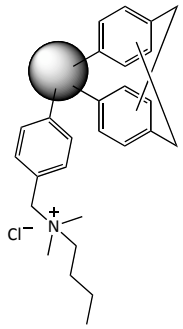

Elemental microanalysis: Expected 87.7 % C, 7.1 % H, 2.3 % N, 2.9 % Cl; Found 81.2 % C, 6.4 % H, 1.4 % N, 2.2 % Cl.
FT-IR $\bar{\nu}/cm^{-1}$ *(KBr): 3020, 2927, 2863, 1605, 1558, 1511, 1449, 1304, 892, 823, 710 (C-Cl str.).*

An analogous synthetic procedure was used to prepare all materials aminated using DMBA. The relevant synthetic detail is shown in Table 3.2.6.1.

Polymer ref.	*Precursor (g)*	*DMBA (mL)*	*DCE (mL)*	*Time (h)*	*Yield (g)*	*Yield (%)*
HXL-PP7-AD1	0.500	30	0	2	0.448	77
HXL-PP2-AD2	0.252	30	0	24	0.243	87
HXL-PP2-AD3	0.251	30	30	24	0.246	88

Table 3.2.6.1 – Feed and analytical data for the DMBA aminated hypercrosslinked materials.

3.2.7. Amination of Precursor Particles Prior to Hypercrosslinking

3.2.7.1. Amination of Precursor Particles (PP8-AD)

Precursor particles, PP8, (0.300 g, 1.416 mmol Cl residues) were charged to a three-necked, round-bottomed flask equipped with a reflux condenser and

mechanical stirrer, under an N_2 atmosphere. Anhydrous DCE (30 mL) was added to swell the beads, and the reaction mixture was left to equilibrate under N_2 at room temperature for 1 hour. DMBA (19.86 μL, 0.142 mmol) in DCE (5 mL) was added and the reaction was heated to reflux (95 °C) for 24 hours. The product particles were then filtered and washed with deionized water until the washings became neutral. The product was then washed with methanol (100 mL) and oven-dried under vacuum at 40 °C for 24 hours to give PP8-AD as a cream-coloured powder (0.297 g, 95 %).

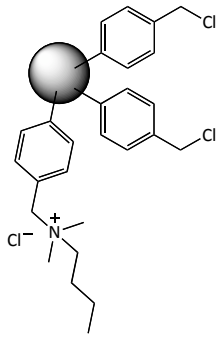

Elemental microanalysis: Expected 75.8 % C, 6.9 % H, 1.0 % N, 16.3 % Cl; Found 76.5 % C, 7.0 % H, 1.0 % N, 13.8 % Cl.

FT-IR $\bar{\nu}/cm^{-1}$ (KBr): 3020, 2922, 2852, 1605, 1586, 1510, 1445, 1266 (CH_2 wag of CH_2-Cl), 990, 901, 829, 797, 709 (C-Cl str.).

An analogous synthetic procedure was used to prepare all precursor materials aminated using DMBA. The relevant synthetic detail is shown in Table 3.2.7.1.1.

Polymer ref.	***Precursor (g)***	***DMBA (mL)***	***DCE (mL)***	***Time (h)***	***Yield (g)***	***Yield (%)***
PP8-AD	0.300	0.018	30	24	0.297	95
PP9-AD	2.015	0.067	40	24	2.008	97
PP10-AD	1.802	0.103	40	24	1.845	98

Table 3.2.7.1.1. – Feed and analytical data for the precursor polymers aminated using DMBA.

3.2.7.2. Hypercrosslinking of Aminated Precursor Particles (HXL-PP8-AD)

Aminated precursor particles, PP8-AD, (0.197 g, 0.926 mmol of VBC residues) were charged to a dry, three-necked, round-bottomed flask equipped with a reflux condenser and an overhead mechanical stirrer. Anhydrous DCE (30 mL) was added and the beads were left to swell fully under N_2 at room temperature for 1 hour. $FeCl_3$ (0.144 g, 0.926 mmol, in a 1:1 mole ratio with respect to the CH_2Cl content of the particles) in DCE (30 mL) was added and the mixture heated at 80 ^oC for 18 hours. The product particles were recovered from the reaction medium by filtration on a 0.2 μm nylon filter and washed with successive 50 mL volumes of methanol, aqueous HNO_3 (pH 1) (2 washes), methanol and acetone. The orange-coloured particles were then extracted with acetone overnight in a Soxhlet apparatus and were then washed with acetone, methanol and diethyl ether before drying *in vacuo* overnight at 40 ^oC (0.121 g, 75 %).

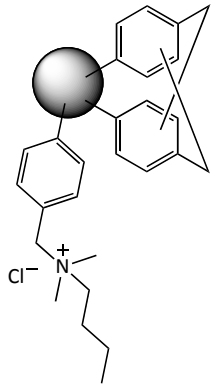

Elemental microanalysis: Expected 91.0 % C, 7.8 % H, 1.1 % N, 0 % Cl; Found 81.6 % C, 7.6 % H, 1.8 % N, 3.4 % Cl.

FT-IR $\bar{\nu}/cm^{-1}$ (KBr): 3019, 2924, 2974, 1627, 1604, 1510, 1447, 1384, 878, 829, 710 (C-Cl str.).

Langmuir specific surface area: 870 m^2/g.

An analogous synthetic procedure was used to hypercrosslink all precursor materials aminated using DMBA. The relevant synthetic detail is shown in Table 3.2.7.2.1.

Polymer ref.	*Precursor (g)*	*$FeCl_3$ (g)*	*Time (hours)*	*Yield (g)*	*Yield (%)*	*% Cl (w%)*	*Specific Surface Area* (m^2/g)*
HXL-PP8-AD	0.197	0.144	1	0.121	61	3.4	870
HXL-PP-SAX1	1.901[1]	1.495	2	1.658	87	3.8	1,470
HXL-PP-SAX2	1.502[2]	0.986	2	1.162	77	4.6	1,290

Table 3.2.7.2.1. – Feed and analytical data for the hypercrosslinked aminated particles. * Specific surface areas calculated using the Langmuir isotherm. [1] and [2] indicate that the precursor particles used were PP9-AD and PP10-AD, respectively.

3.2.8. Aminated Precursor Particle Solvent Uptake Tests.

Aminated precursor particles, PP8-AD (0.025 g) were charged to a centrifugal filter (small filter cartridge which can then be inserted into a centrifuge tube) and the filter weighed. 0.30 mL of DCE was added and the solvent and polymer were left to equilibrate for 3 hours. The sample was placed into a centrifuge at 3,000 rpm for 3 minutes. The insert was then re-weighed.

An analogous procedure was used for all solvents (Table 3.2.8.1).

Solvent	*Mass of polymer (g)*	*Mass of solvent uptaken (g)*	*g/g solvent sorbed*	*mL/g solvent sorbed*
DCE	0.025	0.067	2.67	2.13
Toluene	0.024	0.044	1.85	2.13
Methanol	0.026	0.034	1.31	1.65
THF	0.026	0.053	2.01	2.26
Water	0.025	0.012	0.48	0.48

Table 3.2.8.1. – Solvent uptake data for aminated precursor PP8-AD.

3.3. RESULTS AND DISCUSSION

Hypercrosslinked particles were synthesised and characterised as described in Chapter 2, Section 2.3.1. It was shown through both elemental microanalysis and FT-IR spectroscopic analysis that while the majority of the chloromethyl groups were consumed by the hypercrosslinking reaction, a portion remained unreacted. With this in mind, substitution of the remaining pendent chloromethyl groups with nucleophiles, *e.g.*, amines, can be carried out. The amines used can be primary, secondary or tertiary, with the final properties of the products being dependent on the nature of the amine and the degree of substitution. Such a reaction introduces new functionality that will further the potential for application of the, already extremely interesting, hypercrosslinked materials. For example, when a tertiary amine is reacted with the chloromethyl groups, the polymeric product will contain a permanent positive charge arising from the quaternary nitrogen centre, and this can be utilised in many ways, including as a strong anion-exchange (SAX) moiety in SPE or ion chromatography.

3.3.1. Amination of Hypercrosslinked Materials Using Triethylamine

The first amination reaction carried out used triethylamine (TEA) in a 5-fold excess relative to the number of moles of chlorine present in the hypercrosslinked polymer (Figure 3.3.1.1).

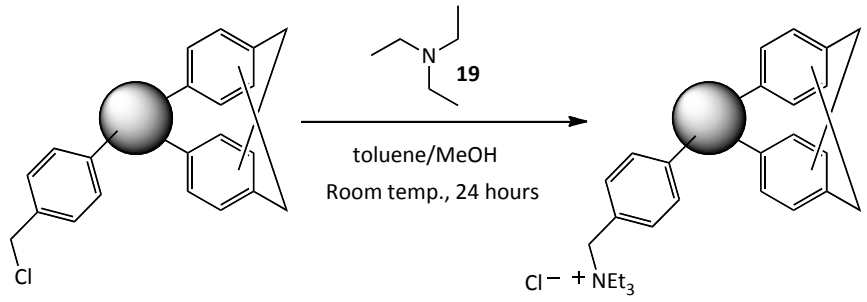

Figure 3.3.1.1. – Amination of pendent chloromethyl groups on the hypercrosslinked polymer, using TEA as the amine.

Elemental microanalytical data obtained for the product isolated from this reaction is shown in Table 3.3.1.1. Data is also shown for the HXL polymer.

Polymer	***Elemental microanalysis (%)***			
ref.	***C***	***H***	***N***	***Cl***
HXL-PP7	82.9	6.7	1.2	3.0
HXL-PP7-AT1	81.2	6.6	1.0	3.2

Table 3.3.1.1. – Results for amination reaction of HXL-PP7 using TEA as the amine.

The results from the elemental microanalysis (Table 3.3.1.1) show that after amination there was little change in the content of each element, with the small changes observed most likely being within experimental error. Overall, the values obtained for the 'aminated' product were very close to those measured for the hypercrosslinked starting material. This suggested that the reaction was unsuccessful, as the expected level of nitrogen, assuming a 100 % efficient reaction, was 2.3 %.

FT-IR spectroscopy was also used to follow the success or otherwise of the nucleophilic substitution reaction. Had the substitution been successful, a relative increase in intensity of the aliphatic signals in the FT-IR spectrum would have been observed, since the amine contains three ethyl groups. As the chlorine directly attached to the chloromethyl group would be replaced by the amine, the intensity of the peaks ascribed to the C-Cl bond would also be expected to be reduced in intensity if the reaction had worked. Since these signals are already quite weak in the spectrum of the hypercrosslinked polymer, changes are hard to ascertain. The signals corresponding to aliphatic C-H stretches (~2925 cm^{-1}) and aliphatic C-H bends (~1449 cm^{-1}) showed no significant changes in intensity suggesting that the substitution reaction was unsuccessful.

3.3.2. Amination of Hypercrosslinked Materials Using Dimethylbutylamine

Aminated products were also generated using neat dimethylbutylamine (DMBA) (Figure 3.3.2.1). DMBA was used as it was shown in the literature to be a more effective amine than triethylamine for this substitution reaction.[12] In addition, DMBA is the amine of choice for commercial SAX SPE sorbents, and thus HXL-PP-SAX sorbents prepared using DMBA will allow for a more accurate and fair comparison of the novel sorbents with commercially available sorbents.

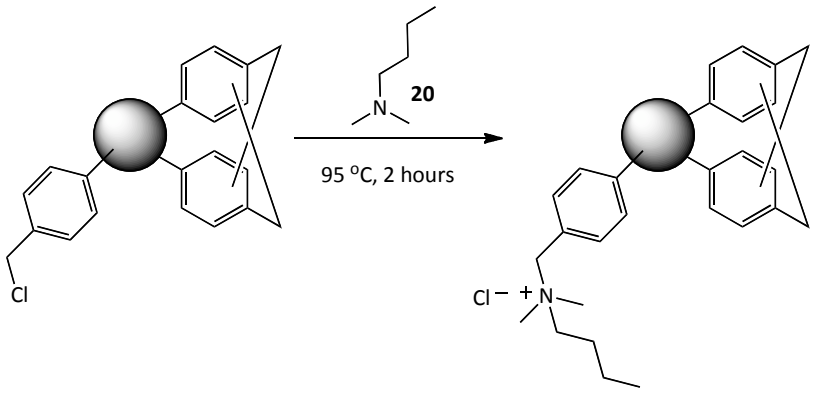

Figure 3.3.2.1. – Amination of pendent chloromethyl groups on the hypercrosslinked polymer using DMBA.

Neat DMBA was heated at reflux with the hypercrosslinked polymer for two hours, as per the literature,[12] where two hours was found to give maximum levels of amination for this reaction. This reaction was then repeated at reflux for 24 hours in order to see if a longer reaction time would lead to a higher nitrogen content in the final product. Although two hours reaction time was found in the literature to be sufficient to yield products with maximum levels of amination, the starting materials used in the literature were not hypercrosslinked materials and contained a polar comonomer, therefore it could be that the hypercrosslinked materials used here have different reactivity. It is also possible that the chloromethyl moieties that remained after the hypercrosslinking reaction were those residing in positions that were hard for the $FeCl_3$ to access, therefore these positions would also have been difficult for

DMBA to access. If this was the case, a longer reaction time would be extremely beneficial. A third reaction was carried out which involved wetting the hypercrosslinked polymer in DCE before addition of excess DMBA to see if this would have any effect on the reaction outcome.

Table 3.3.2.1 shows the elemental microanalytical data obtained for each of the DMBA based products. Also included in the table are details of the analogous non-functionalised hypercrosslinked polymers.

	Elemental microanalysis (%)			
Polymer ref.	***C***	***H***	***N***	***Cl***
HXL-PP7	82.9	6.7	1.2	3.0
HXL-PP7-AD1	81.2	6.4	1.4	2.2
HXL-PP2	82.9	6.3	0.3	3.9
HXL-PP2-AD2	81.8	7.3	1.3	2.7
HXL-PP2-AD3	81.0	6.6	1.0	3.1

Table 3.3.2.1. – Elemental microanalytical data for hypercrosslinked polymers and their DMBA aminated derivatives.

The elemental microanalysis data (Table 3.3.2.1) shows that the nitrogen content of the material generated through amination of HXL-PP7 has increased relative to the precursor, however, the observed increase was much less than the expected increase; if all of the chlorine groups were exchanged with amine groups then it was expected that there would be ~2.3 % nitrogen, taking into account the nitrogen that was present in HXL-PP7 before amination (most likely to be AIBN-derived). Overall, the results from the unmodified material were very similar to those for the aminated material which would suggest that only a small amount of amine had been added to the material, if any.

The elemental microanalysis results (Table 3.3.2.1) also show that for the aminated products derived from HXL-PP2, the observed values of N are getting

closer to the expected value of 1.7 %, however the results observed for the other elements are quite different from those expected for C (87.1 %), H (7.7 %) and Cl (3.5 %), which could be an indication that, as was the case for those hypercrosslinked polymers which had been sulfonated, the elemental microanalysis results are somewhat unreliable and tricky to interpret due to the hygroscopic nature of hypercrosslinked materials.

As FT-IR spectroscopy can potentially give a good indication of the success of this reaction through changes in the relative intensity of the C-Cl bond-derived signals, FT-IR spectra were obtained for each product. However, again the spectra obtained showed that, upon amination, there did not seem to be any significant change in the relative intensity of the C-Cl signals compared to the other signals present in the spectrum. This indicates that relatively few or no C-Cl bonds have been broken under these reaction conditions. Therefore, the reaction did not appear to have worked to any notable degree.

As neither HXL-PP2 nor HXL-PP7 could be successfully aminated, yet the literature suggested that this method ought to readily produce the desired products, speculation as to why this method may have failed led to the hypothesis that the residual pendent chloromethyl groups left over from the hypercrosslinking reaction were in sterically congested locations and therefore unable to react with bulky tertiary amines, as opposed to being in locations which are hard to access but not completely unreactive. However, it is important to note that these locations have been shown previously in our group to be accessible and able to react with both primary (ethylene diamine) and secondary (piperazine) amines to yield weak anion-exchange materials.

3.3.3. Investigation of Pendent Chlorine Groups From Hypercrosslinking Reactions

If it is true that the residual chloromethyl groups present in the hypercrosslinked polymers are unreactive because they are inaccessible to the

$FeCl_3$ reagent, then it is more than likely that these chloromethyl moieties are also inaccessible to DMBA. It may therefore be advantageous to produce hypercrosslinked polymers in which a higher proportion of the VBC-derived chloromethyl residues have not been consumed in the hypercrosslinking reaction and the polymers are less heavily hypercrosslinked; such pendent groups thus remain available for subsequent chemical modification. A study by Fontanals *et al.*[24] demonstrated that for polymer beads prepared by non-aqueous dispersion (NAD) and precipitation polymerisations, at least 50 % of the monomer feed must be VBC (the balance being DVB) in order to prepare a polymeric material that can be hypercrosslinked to give specific surface areas in excess of 1,000 m^2/g. 50 % of VBC should theoretically crosslink 100 % of the aromatic residues (*i.e.,* one Cl atom is lost in joining two aromatic rings together), therefore in the present study, where the precursor polymers contain 75 % VBC, not all of the VBC has to be utilised in order to yield ultra-high specific surface area products.

Hypercrosslinked polymers containing unreacted, accessible VBC-derived chloromethyl groups can be prepared in two ways, either by reducing the reaction time of the hypercrosslinking reaction or by reducing the amount of $FeCl_3$ used.

Ahn *et al.*[25] showed that for the hypercrosslinking of their suspension polymerisation-derived precursors, the fall in chlorine content was most dramatic within the first 15 minutes of the reaction. Further reaction, for up to 18 hours, resulted in a much reduced rate of chlorine loss compared to the first 15 minutes, to give "measureable but minor" loss of chlorine over the extra time period. With this in mind, hypercrosslinking reactions were carried out on precursor PP4, for 5, 10 and 15 minutes in order to establish how the Cl content and specific surface area vary with time. The results from each of these experiments are presented in Table 3.3.3.1, along with the results for the reaction carried out previously on PP4 for 18 hours (1,080 minutes).

From the elemental microanalysis results (Table 3.3.3.1) it can be seen that when the hypercrosslinking reaction was carried out for just 5 minutes, a higher level of Cl remained in the product than in the products obtained after a reaction time of 10 minutes or more. For the 10 and 15 minute hypercrosslinking reactions, the level of residual Cl was almost identical to that of the 18 hour reaction time. This suggests that the hypercrosslinking reaction must be carried out for less than 10 minutes in order to leave behind chloromethyl groups that are both accessible to $FeCl_3$ and to DMBA in subsequent amination reactions.

Polymer ref.	***Reaction Time (mins.)***	***Elemental microanalysis (%)***				***Langmuir specific surface area (m^2/g)***
		C	***H***	***N***	***Cl***	
PP4	0	77.6	6.7	0.5	14.8	< 5
HXL-PP4-5mins	5	85.4	6.7	0.6	5.3	1,236
HXL-PP4-10mins	10	85.7	7.0	0.4	4.0	1,530
HXL-PP4-15mins	15	85.2	6.8	0.5	3.9	1,497
HXL-PP4	1,080	85.2	7.0	0.7	3.9	1,730

Table 3.3.3.1. – Hypercrosslinking with different reaction times.

The nitrogen sorption porosimetry data for the hypercrosslinked polymer, HXL-PP4 and the short reaction time products HXL-PP4-5mins, -10 mins and -15mins (Table 3.3.3.1) show that shorter reaction times lead to lower specific surface areas than for the 18 hour reaction, however the specific surface areas obtained are still high such that the materials would be potentially useful in SPE or chromatography. These results support the claim by Ahn *et al.*[25] that the hypercrosslinking reaction proceeds very rapidly indeed, resulting in ultra-high specific surface area materials in a short period of time.

The loss of chlorine and simultaneous increase in Langmuir specific surface area was plotted to illustrate the relationship between the two properties (Figure 3.3.3.1).

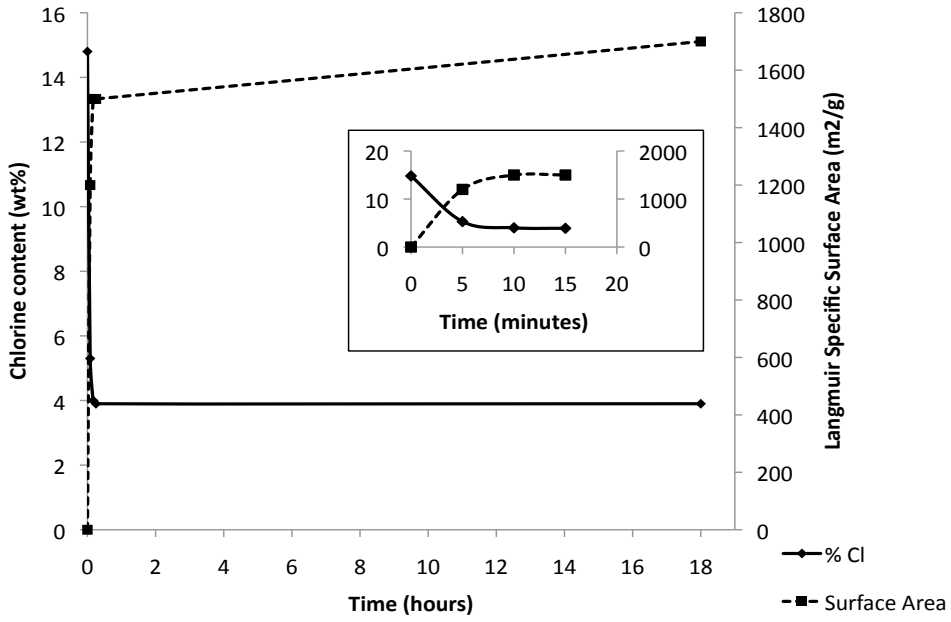

Figure 3.3.3.1. – Time study graph showing a decrease in chlorine content and simultaneous increase in Langmuir specific surface area with respect to time.

FT-IR spectra were obtained for these products (Figures 3.3.3.2 and 3.3.3.3), with the signals of interest being the chloromethyl group-derived signals at ~690 cm^{-1} (C-Cl stretch) and ~1265 cm^{-1} (C-H wag of CH_2-Cl), which should decrease significantly in intensity upon hypercrosslinking.

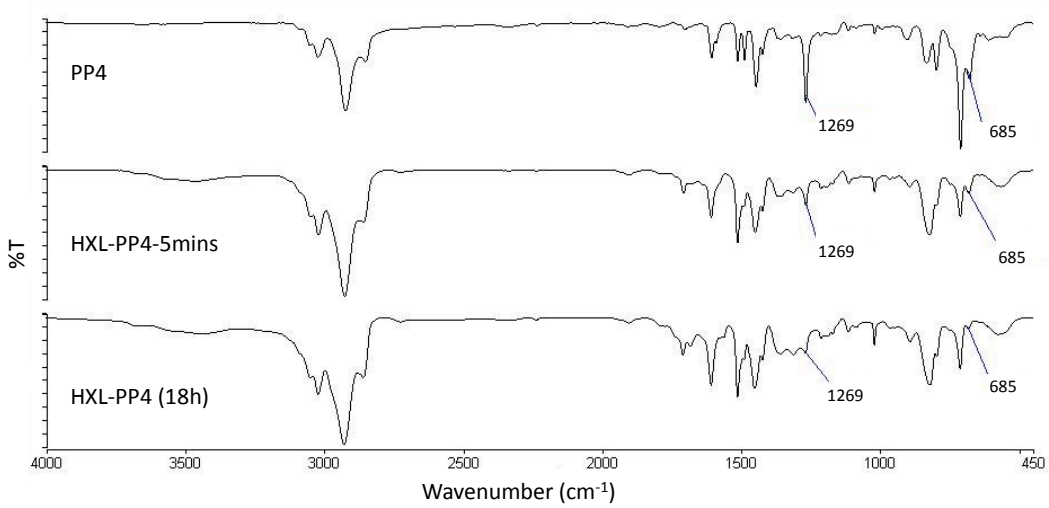

Figure 3.3.3.2. – Comparison of FT-IR spectra for the hypercrosslinked polymers formed after 5 minutes and 18 hours of reaction with the non-hypercrosslinked precursor material.

The spectra presented in Figure 3.3.3.2 show that after 5 minutes and 18 hours the hypercrosslinked reaction is well advanced. The intensity of the signal assigned to the C-H wag of CH_2-Cl, at ~1265 cm^{-1}, which is one of the dominant signals in the precursor spectrum, is substantially reduced in intensity in the spectrum of the product obtained after 18 hours. This shows that the majority of the chloromethyl groups have been consumed in the production of methylene bridges. The C-Cl stretch at ~690 cm^{-1} has also diminished in intensity.

It is also clear from these spectra, however, that the reaction carried out over 18 hours is more advanced than the analogous reaction after 5 minutes. The C-H wag at ~1265 cm^{-1} has practically disappeared in the spectrum of the product from the 18 hour reaction, however it is a more significant feature in the spectrum of the product from the 5 minute reaction, although this signal is still significantly reduced in intensity relative to the same band in the spectrum of the precursor. The fact that the spectra acquired after 18 hours and 5 minutes of reaction are quite similar helps to support the literature evidence

that the hypercrosslinking reaction occurs rapidly within the first 15 minutes and that the rate of reaction slows thereafter.

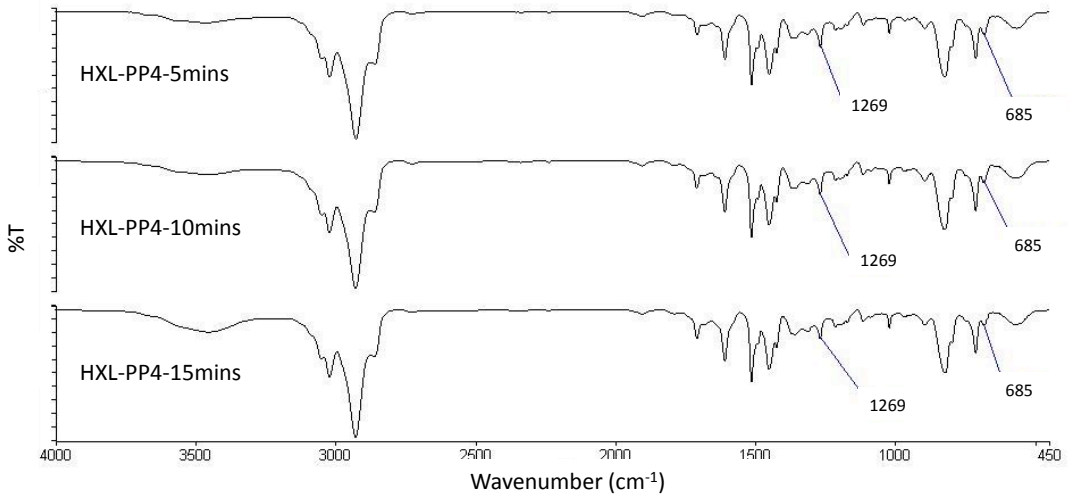

Figure 3.3.3.3. – FT-IR spectra for thehypercrosslinked products formed after 5, 10 and 15 minutes of reaction.

The spectra in Figure 3.3.3.3 show the similarities between the reactions carried out over 5, 10 and 15 minutes. In all cases, it is clear that the C-Cl derived signals at ~690 cm^{-1} and ~1265 cm^{-1} are weak, therefore it would certainly appear that the products have been hypercrosslinked in all cases, albeit to a lesser extent than the product hypercrosslinked for 18 hours.

3.3.4 Amination of the Hypercrosslinked Polymers Produced Using Short Hypercrosslinking Reaction Times

Since the product from the 5 minute hypercrosslinking reaction contained a higher level of pendent chloromethyl groups than the products obtained after longer reaction times, this material was then subjected to an amination reaction to try to utilise some of these pendent groups. This was done by first wetting the material with DCE then adding a 5-fold molar excess of DMBA relative to the

residual chloromethyl groups. The elemental microanalysis results for the resultant 'aminated' material are shown in Table 3.3.4.1

Polymer ref.	*Elemental microanalysis (%)*			
	C	***H***	***N***	***Cl***
HXL-PP4-5min	85.4	6.7	0.6	5.3
HXL-PP4-5min-AD1	83.0	7.7	1.0	3.5

Table 3.3.4.1. – Elemental microanalysis results for DMBA aminated HXL-PP4-5min.

The elemental microanalysis results (Table 3.3.4.1) show that the level of nitrogen has almost doubled upon amination, from 0.6 % in the precursor to 1.0 % in the aminated material. This nitrogen content value is not particularly close to the theoretical maximum value of 2.3 %, however this theoretical value was calculated assuming 100 % reaction, which was never realistically going to be achieved because of the presence of inaccessible chloromethyl groups (a more accurate expected value for N could not be ascertained as the level of accessible Cl could not be distinguished from inaccessible Cl). The levels of C, H and Cl, however, are very close to their expected values (83.5, 7.7 and 4.6 % respectively). Overall, this method did appear to be a potential route to the desired aminated products, however only limited control could be exerted over the level of amination where this synthetic route was employed.

FT-IR spectroscopy was used to analyse the aminated product, with the signals of interest being those ascribed to the chloromethyl group (~1265 and ~690 cm^{-1}). Any decrease in the relative intensity of these bands would indicate that reaction with the amine had occurred. The FT-IR spectra of the hypercrosslinked polymer and the aminated hypercrosslinked polymer derived therefrom showed that upon amination there was a decrease in the relative intensity of the C-H wag at ~1265 cm^{-1}, which is consistent with a successful reaction. There was no obvious decrease in the relative intensity of the C-Cl stretch at ~690 cm^{-1}, however.

3.3.5 Amination Prior to Hypercrosslinking

3.3.5.1. Amination of Precursor Particles

An alternative way to ensure that the amination reaction can take place in a facile manner is to aminate the swellable poly(DVB-*co*-VBC) precursor particles before carrying out the hypercrosslinking reaction. In this instance, the chloromethyl groups present in the material should be readily accessible and reactive to DMBA, provided that the polymer is swollen under the reaction conditions employed. Following amination, the residual chloromethyl groups can then be consumed in the hypercrosslinking reaction to form methylene bridges (Figure 3.3.5.1.1).

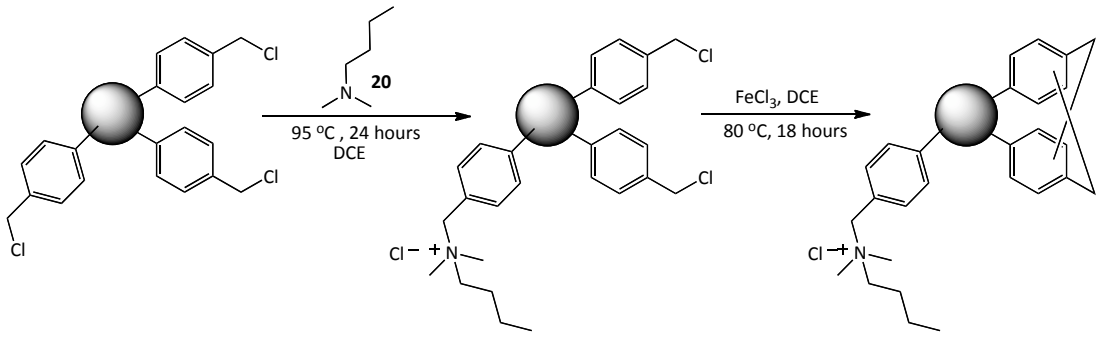

Figure 3.3.5.1.1. – Amination of poly(DVB-*co*-VBC) precursors followed by hypercrosslinking.

In order to assess the viability of this approach as a possible route into the desired products, reactions were carried out in such a way as to give a level of amination in the precursor of 10 % relative to the number of chloromethyl groups present in the precursor prior to reaction. This would still leave behind a considerable percentage of chloromethyl moieties that could then be reacted further in the hypercrosslinking reaction to give the aminated, ultra-high specific surface area products of interest. These reactions were carried out by first swelling the precursor in DCE then adding the DMBA and allowing the

reaction to proceed at 95 °C for 24 hours. The elemental microanalytical data obtained for the precursor and product can be seen in Table 3.3.5.1.1.

Polymer ref.	***Elemental microanalysis (%)***			
	C	***H***	***N***	***Cl***
PP8	77.7	6.3	0.4	15.2
PP8-AD	76.5	7.0	1.0	13.8

Table 3.3.5.1.1. – Elemental microanalytical data for PP8 and its aminated derivative PP8-AD.

The elemental microanalytical data (Table 3.3.5.1.1) shows that after 24 hours the level of nitrogen introduced was slightly higher than the expected value of 0.9 %, with the slightly higher value being within experimental error. These results are extremely promising. Amination prior to hypercrosslinking would be arguably the most advantageous method of preparing these anion-exchange materials, as there is a high level of accessible chloromethyl groups making the reaction very efficient. It also means that a controlled amount of amine can be introduced into the material, in turn meaning that the degree of amination can be varied and thus tailored to the needs of the application, *i.e.*, the materials can be fine-tuned with respect to the analytes requiring extraction or separation. With the other methods, the level of accessible chloromethyl groups remaining after the hypercrosslinking reaction cannot be controlled easily and thus the level of amination in the final product cannot be controlled very well at all.

FT-IR spectra were obtained for these products to show that the reaction had occurred. A decrease in the relative intensity of the chloromethyl derived signals at ~1265 and ~690 cm^{-1} would indicate a successful reaction (Figure 3.3.5.1.2).

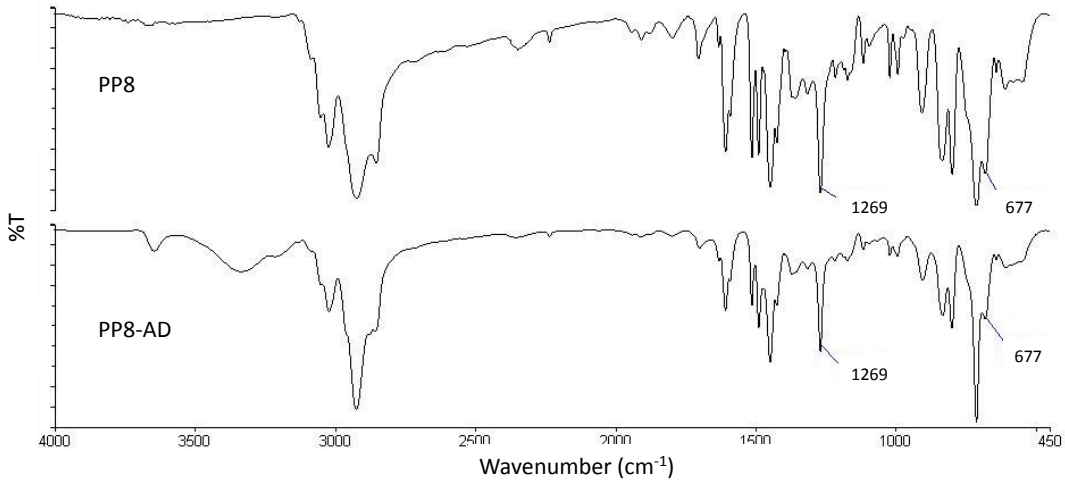

Figure 3.3.5.1.2. – FT-IR spectra for the poly(DVB-*co*-VBC) precursor, PP8, and the corresponding aminated material, PP8-AD.

In the FT-IR spectrum of the aminated material PP8-AD (Figure 3.3.5.1.2) the C-H wag (of a CH_2-Cl, chloromethyl, group) at ~1265 cm^{-1} and the C-Cl stretch (~690 cm^{-1}) are both reduced in intensity upon going from precursor to aminated product. The C-Cl bond content decreased while the aliphatic C-H bond content increased with the introduction of the aliphatic amine group. The FT-IR spectra were useful for confirming a successful reaction, although the extent of the reaction which had taken place (*i.e.*, quantitative analysis) could not be ascertained easily using these spectra.

3.3.5.2. Hypercrosslinking of Aminated Precursor Particles

Since the elemental microanalysis of the aminated precursors showed a level of nitrogen close to the values expected, the aminated precursors were then taken forward and hypercrosslinked to yield their ultra-high specific surface area derivatives since a high level of chloromethyl groups remained in the aminated precursor, the hypercrosslinking reaction ought to result in materials with specific surface areas in excess of 1,000 m^2/g, which will then be well-suited for use in SPE or chromatography.

As the hypercrosslinking experiments carried out over restricted time periods showed that the hypercrosslinking reaction was nearing completion after only 15 minutes, for the present case the hypercrosslinking reaction was carried out for one hour rather than 18 hours. The product was then analysed using elemental microanalysis and nitrogen sorption porosimetry (Table 3.3.5.2.1).

Polymer ref.	***Elemental microanalysis (%)***				***Langmuir specific surface area (m^2/g)***
	C	***H***	***N***	***Cl***	
PP8-AD	76.5	7.0	1.0	13.8	< 5
HXL-PP8-AD*	81.6	7.6	1.8	3.4	870

Table 3.3.5.2.1 – Elemental microanalysis and nitrogen sorption porosimetry results for the aminated precursor and the corresponding hypercrosslinked polymer (N.B. where the nomenclature HXL-PP8-AD* is used, the * indicates that amination reaction was carried out prior to hypercrosslinking).

The elemental microanalysis results (Table 3.3.5.2.1) show that the hypercrosslinking reaction worked well, with the level of Cl in the hypercrosslinked polymer being very much reduced relative to the aminated precursor. The residual chlorine is presumably due in part to inaccessible chloromethyl groups with which the $FeCl_3$ could not react, however the Cl content is also attributable to the Cl^- ions that counter-balance the positively charged nitrogen centre. The level of Cl was expected to be higher than that actually obtained, due to the extra Cl^- ions in the quaternary ammonium group. For previous hypercrosslinking reactions on non-aminated precursors, the level of Cl was typically between 3 and 4 %; with the extra Cl^- ions this should lead to a product with about 5-6 % Cl. This suggests that either more of the chloromethyl groups than normal had reacted in the hypercrosslinking reaction, or that the Cl^- counter ions had been affected in some way by the hypercrosslinking reaction or work-up conditions. This is entirely feasible, as the material is designed to be an ion-exchange resin, therefore any ions introduced during the hypercrosslinking reaction or work-up should in theory

exchange with the Cl^- counter ion, providing that the material does indeed behave as intended.

The specific surface area of 870 m^2/g is not as high as perhaps could be expected, however, it is still sufficiently high to act as a useful material for SPE. This lower specific surface area could be due to the different polarity of the aminated precursor (with respect to the non-aminated precursor) resulting in a different affinity for the DCE swelling solvent used in the hypercrosslinking reaction. The better a solvent is for swelling the precursor, the higher the specific surface area expected after the hypercrosslinking reaction. Thus if DCE does not swell the aminated precursor as much as it does the non-aminated precursor, the specific surface area of the hypercrosslinked aminated precursor will be lower than that of a hypercrosslinked non-aminated precursor material. A series of swelling tests were carried out in order to ensure that DCE was in fact the optimal solvent for swelling the aminated material. A range of solvents with differing polarities were employed (Table 3.3.5.2.2).

Solvent	*Dielectric constant (ε_o)*	*Mass of polymer (g)*	*Mass of solvent uptaken (g)*	*g/g solvent sorbed*	*mL/g solvent sorbed*
Toluene	2.4 @ 25 °C	0.024	0.044	1.85	2.13
THF	7.5 @ 22 °C	0.026	0.053	2.01	2.26
DCE	10.5 @ 20 °C	0.025	0.067	2.67	2.13
Methanol	32.7 @ 20 °C	0.026	0.034	1.31	1.65
Water	80.4 @ 20 °C	0.025	0.012	0.48	0.48

Table 3.3.5.2.2 – Data obtained for the swelling tests carried out on aminated precursor PP8-AD.

The swelling tests (Table 3.3.5.2.2) showed that DCE was in fact the solvent most sorbed by the aminated precursor material. The volume of DCE sorbed by the aminated precursor polymer particle (2.13 mL/g) is extremely close to the volume sorbed by an analogous non-aminated polymer microsphere

(2.44 mL/g).[26] This is not entirely unexpected, because although a charged nitrogen moiety has been introduced to the precursor material, this is surrounded by alkyl chains that shield the ionic charge, thus giving the appearance of a non-polar species similar to the precursor material. This is similar in nature to a quaternary ammonium salt phase-transfer catalyst which is soluble in aqueous media due to its hydrophilic nitrogen centre but which can also transfer anions to an organic medium because of the solubility induced in organic solvents by the catalyst's hydrophobic exterior.[27,28] Thus, it is quite intuitive that the solvent best capable of swelling the precursor should also be the most appropriate for swelling the aminated precursor.

FT-IR spectra were obtained for the aminated precursor and its corresponding hypercrosslinked product to show the success or otherwise of the hypercrosslinking reaction. Any decrease in intensity of the signals ascribed to the chloromethyl group, relative to the precursor, would give an indication that this reaction was successful. The spectra show that the hypercrosslinking reaction was successful; a decrease in the intensity of the signals arising due to the chloromethyl group (at ~1265 and ~690 cm^{-1}) was observed.

After hypercrosslinking, a signal was found in the spectrum of the hypercrosslinked product, at ~1360 cm^{-1}, which did not appear in either of the aminated precursor spectra or in any spectra of hypercrosslinked materials which had been aminated post-hypercrosslinking. This could be due to the chloride ion from the anion-exchange group exchanging with a nitrate (NO_3^-) ion from the aqueous HNO_3 used to wash the hypercrosslinked product. The chloride ion was not present during any of the other hypercrosslinking reactions, thus this exchange would not have occurred. Nitrate ions give a strong signal at 1380-1350 cm^{-1}, which ties in with the spectroscopic observations. In order to test this theory, the aminated hypercrosslinked polymer was stirred for 2 hours in a solution of 2M $NaCl_{(aq)}$ to exchange the nitrate ion back to chloride. An FT-IR spectrum was then obtained of the material after NaCl exchange (Figure 3.3.5.2.3).

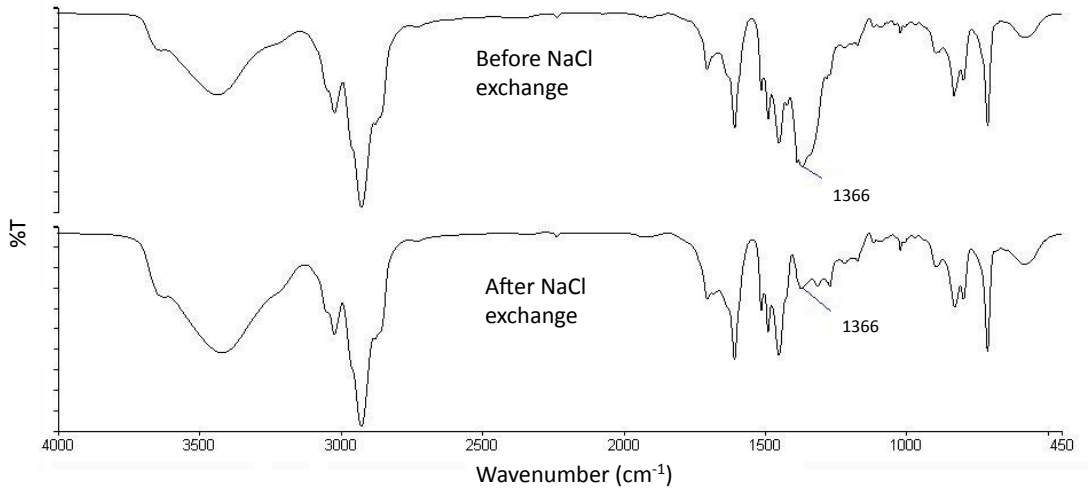

Figure 3.3.5.2.3. – FT-IR spectra of HXL-PP8-AD* before and after NaCl exchange.

The spectra (Figure 3.3.5.2.3) show that the nitrate ion introduced through the HNO_3 wash after the hypercrosslinking step could be easily exchanged back to a chloride ion using a 2M solution of NaCl. This means that in future hypercrosslinking reactions involving aminated precursors, a NaCl wash step should be employed after the HNO_3 wash in order to keep the quaternary ammonium group as its chloride salt. The fact that the NO_3^- ion was present in place of Cl^- in the product provides a perfect explanation for the low level of Cl in the elemental microanalysis. It also shows the potential of these materials to act as anion-exchangers, which is extremely promising considering their intended application.

3.3.6. Synthesis of Hypercrosslinked SAX Materials for SPE

Amination of precursor particles prior to hypercrosslinking has been shown to be the best method for the preparation of HXL-PP-SAX materials. While HXL-PP-WAX materials were prepared by amination of hypercrosslinked polymer microspheres, this method was not suitable for the preparation of HXL-PP-SAX polymers. The former method is perhaps a more suitable alternative, as

amination of the precursor can be carried out in such a way as to target a specific level of amination, while amination subsequent to the hypercrosslinking reaction relies on accessible chloromethyl groups remaining after hypercrosslinking, which cannot be controlled accurately. Thus, the new method will allow for materials to be tuned to the levels required for the intended applications.

In order to generate HXL-PP-SAX materials with differing IEC, poly(DVB-*co*-VBC) precursor particles were aminated by introducing DMBA at levels of 5 and 10 mol% relative to the chloromethyl groups present. Elemental microanalysis (Table 3.3.6.1) and FT-IR spectroscopy were used to analyse the products obtained.

Polymer ref.	***Mol% DMBA added (relative to Cl)***	***Elemental microanalysis (%)***			
		C	***H***	***N***	***Cl***
PP9	n/a	77.1	6.8	0.5	14.6
PP9-AD	5	76.6	6.8	0.7	13.5
PP10	n/a	77.4	6.7	0.5	14.4
PP10-AD	10	76.1	7.1	0.9	14.4

Table 3.3.6.1. – Elemental microanalysis results obtained for the aminated polymers PP9-AD and PP10-AD.

The elemental microanalysis results show that, upon amination, the level of nitrogen present in the polymers has increased by 0.2 and 0.4 % for 5 and 10 mol% of DMBA, respectively. This is entirely as expected, since the higher the level of DMBA introduced the higher the amine content in the product. This further demonstrates the ability of this synthetic method to produce polymers with tunable amine content.

FT-IR spectra were obtained and showed, as before, that upon amination, the C-H wag at ~1265 cm^{-1} was reduced in intensity, due to cleavage of the C-Cl bond.

The aminated precursors were then hypercrosslinked in order to introduce microporosity and ultra-high specific surface area. The elemental microanalysis and nitrogen sorption data obtained for the polymers are shown in Table 3.3.6.2.

Polymer ref.	***Elemental microanalysis (%)***				***IEC* (mmol/g)***	***Langmuir specific surface area (m^2/g)***
	C	***H***	***N***	***Cl***		
HXL-PP-SAXa	82.3	6.7	1.1	3.8	0.2	1,470
HXL-PP-SAXb	81.4	7.6	1.0	4.6	0.4	1,290

Table 3.3.6.2. – Elemental microanalytical and nitrogen sorption data for HXL-PP-SAX polymers. *IEC calculated from elemental microanalysis data.

The elemental microanalytical data shows a drop in Cl relative to the precursors (from 14.4 % and 13.5 % Cl for PP9-AD and PP10-AD, respectively.) This is as expected for hypercrosslinked polymers. The Langmuir specific surface areas are extremely high, as expected for hypercrosslinked polymers, which makes these products ideal for the intended SPE applications. The average pore sizes measured for HXL-PP-SAXa and HXL-PP-SAXb were 2.28 and 2.31 nm, respectively. This coupled with the extremely high specific surface area indicates that the materials do indeed contain a high micropore content (*i.e.*, pores <2 nm), however they are not exclusively microporous, there must also be a small percentage of mesopores present within the material.

SEM was used to determine the shape, size and size distribution of the products, in order to ensure their suitability for packing into SPE cartridges (Figure 3.3.6.2).

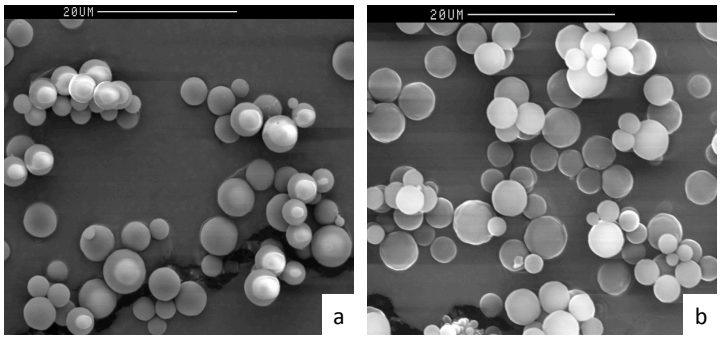

Figure 3.3.6.2. – SEM micrographs for the HXL-PP-SAX materials; (a) HXL-PP-SAXa, (b) HXL-PP-SAXb.

The SEM micrographs show that the particles are spherical and that the particles are around 3-5 μm in diameter. The particles are not monodisperse, however the size distribution is relatively narrow and entirely appropriate for these materials to pack well into SPE cartridges.

3.3.7. Application of HXL-PP-SAX in Ion-Exchange SPE

Application of the HXL-PP-SAX sorbents was carried out in a collaborating group at the Universitat Rovira i Virgili in Tarragona, Spain, thus although all of the polymers were synthesised in Glasgow, *all* of the analytical data presented in Section 3.3.7 has been generated by D. Bratkowska. A summary of the findings is presented. Since pharmaceuticals allowed for a thorough evaluation of the HXL-PP-SCX sorbents, pharmaceutical compounds were also used in the evaluation of the HXL-PP-SAX sorbents. The same set of analytes was selected, with one alteration. The basic trimethoprim was substituted for acidic fenoprofen. (Table 3.3.7.1).

Analyte	*Use*	*Structure*	*pK_a*
Caffeine (**10**)	Stimulant	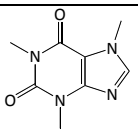	13.4
Antipyrine (**12**)	Analgesic/antipyretic	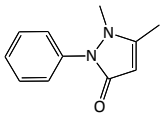	13.3
Propranolol (**13**)	β-blocker	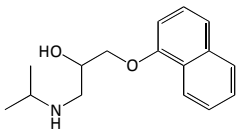	9.5
Salicylic acid (**15**)	Analgesic/antifungal	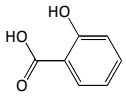	3.0
Carbamazepine (**14**)	Anticonvulsant	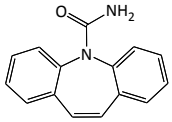	2.5
Clofibric acid (**16**)	Lipid regulator	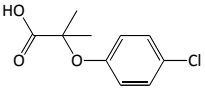	3.6
Fenoprofen (**21**)	NSAID	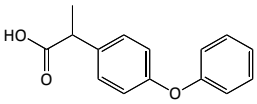	4.5
Diclofenac (**17**)	NSAID/antipyretic	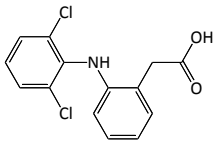	3.9
Ibuprofen (**18**)	NSAID/antipyretic	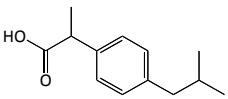	4.6

Table 3.3.7.1. – Analytes used for evaluation of the HLX-PP-SAX sorbents.

These compounds represent a wide range of pharmaceutical drug classes that can easily find their way into environmental water systems. The behaviour of the HXL-PP-SAX sorbents is expected to be the opposite to that of the HXL-PP-SCX sorbents; that is, the basic analytes (caffeine, antipyrine, propranolol and carbamazepine) should be removed by an organic wash solvent, while the acidic analytes (salicylic acid, clofibric acid, fenoprofen, diclofenac and ibuprofen) should be retained throughout the wash due to their additional ionic interaction

with the quaternary ammonium moieties on the HXL-PP-SAX sorbents, thus allowing for a more selective extraction.

3.3.7.1. SPE Method Development.

In order to give maximum retention and elution of the acidic compounds of interest, several parameters of the SPE procedure had to first be optimised. All of the SPE optimisation experiments were carried out using 100 mL of ultra-pure water, spiked with the analyte mixture at a level of 100 µg/L. The parameters optimised were the pH of the sample, loading volume and the composition and volume of the washing and eluting solvents.

The first parameter optimised was the pH of the sample during loading. Both acidic (pH 5) and neutral (pH 7) conditions were considered. The pH of the sample loading will have no effect on the sorbent, as it is permenantly charged due to the quaternary nature of the amine. The results were much more promising when the samples were adjusted to pH 7 prior to loading than when they were loaded at pH 5, thus the optimum sample pH was set at pH 7.

As the method is intended for use in the analysis of complex real water samples, a wash step that can successfully remove impurities is extremely important. Both acetonitrile and methanol were evaluated as prospective washing solvents, with methanol deemed the better of the two. The volume of methanol required was also optimised. While it was found that 5 mL of methanol was insufficient for complete removal of basic and neutral interferences, increasing this to 10 mL resulted in their complete removal. At volumes above 10 mL, however, the retention of the acidic analytes of interest was affected, thus the washing conditions were set at 10 mL of methanol.

The final parameter investigated was the nature and volume of the elution solvent. The nature of the elution solvent is extremely important; in order to break the ionic interaction and thus remove the acidic analytes, the elution solvent must contain an acidic component. Methanol with varying levels of formic acid was investigated. 2, 5 and 10 % solutions were tested, with the 10 % solution providing the highest recoveries, in particular for salicylic acid. The volume of this elution solvent required was also assessed. 5 mL gave recoveries of only ~70 %, however complete elution of all acidic analytes was achieved using 10 mL. Thus the elution conditions were set at 10 mL of a 10 % solution of formic acid in methanol.

The optimum conditions for the SPE were set using only HXL-PP-SAXa, as the behaviour of the two sorbents under those conditions was expected to be very similar. Next, both sorbents were tested at two different loading volumes, to determine which would perform better and thus be taken forward for use in the analysis of real samples. The volumes tested were 100 mL and 500 mL, with the same volume of analyte mixture added each time (thus with increasing sample volume the concentration of analytes decreased). The recoveries obtained using both sorbents under the optimised conditions at both volumes are shown in Table 3.3.7.1.1.

	Recovery (%)							
	HXL-PP-SAXa				HXL-PP-SAXb			
	100 mL		500 mL		100 mL		500 mL	
Analyte	Wash	Elute	Wash	Elute	Wash	Elute	Wash	Elute
Caffeine	102	-	92	-	102	-	103	-
Antipyrine	101	-	97	-	103	-	104	-
Propranolol	100	-	88	-	101	-	83	-
Carbamazepine	100	-	97	-	100	-	104	-
Salicylic acid	-	100	-	92	-	88	-	89
Clofibric Acid	-	96	-	91	-	100	-	90
Fenoprofen	-	99	-	98	-	98	-	103
Diclofenac	-	102	-	93	-	87	-	81
Ibuprofen	-	95	-	94	-	102	-	102

Table 3.3.7.1.1. – Recoveries (%) obtained for both HXL-PP-SAX sorbents at different loading volumes.

From the recovery values shown in Table 3.3.7.1.1 it can be seen just how effective the washing step is at removing the basic interferences while leaving the acidic analytes of interest bound to the sorbent. At both volumes, both sorbents give high recoveries, however the recovery of diclofenac on the HXL-PP-SAXb sorbent is particularly low and thus HXL-PP-SAXa was chosen for the studies using complex, real water sample matrices.

3.3.7.2. Comparison of HXL-PP-SAX with Commercial Sorbents.

As the HXL-PP-SAXa sorbent had been shown to be extremely effective under the optimised SPE conditions, the next step was to compare it to commercially available SAX SPE sorbents. The commercially available sorbents selected were from the leading companies that supply SPE sorbent technologies. Table 3.3.7.2.1 shows characterisation data for the sorbents being compared.

Resin	*Supplier*	*Ion-exchange capacity (mmol/g)*	*Specific surface area (m^2/g)*	*Particle size (μm)*
HXL-PP-SAXa	In-house	0.2	1,470	3-5
Oasis MAX	Waters	0.3	~800	25-35
SampliQ SAX	Agilent	0.1	~600	25-35

Table 3.3.7.2.1. – Characterisation data for HXL-PP-SAXa and the commercially available SAX sorbents.

From the characterisation data available, it is clear that there are several differences between the sorbents. HXL-PP-SAXa has a much higher specific surface area than the commercially available sorbents, which is significant as a higher specific surface area (coupled with a microporous structure) has been shown to increase the efficiency of sorbents.[29,30] The van Deemter equation suggests that smaller particle size should also lead to better performance of the sorbents, thus the smaller particle size of the HXL-PP-SAXa sorbent should also be advantageous.[31] HXL-PP-SAXa has an intermediate IEC compared to the commercial sorbents.

As the HXL-PP-SAXa sorbent was shown to perform favourably at a sample volume of 500 mL, this was the sample volume used for the comparison. 500 mL samples of ultra-pure water, spiked with analytes at a concentration of 20 μg/L, were percolated through each of the sorbents and the eluates from both the wash and elution steps were analysed to assess the analyte recoveries. The recoveries obtained using each of the sorbents are detailed in Table 3.3.7.2.2.

Analyte	Recovery (%)					
	HXL-PP-SAXa		*Oasis MAX*		*SampliQ SAX*	
	Wash	***Elute***	***Wash***	***Elute***	***Wash***	***Elute***
Caffeine	92	-	74	-	87	-
Antipyrine	97	-	95	-	92	-
Propranolol	88	-	90	-	68	-
Carbamazepine	97	-	94	2	94	-
Salicylic acid	-	92	-	90	-	100
Clofibric acid	-	91	-	93	-	95
Fenoprofen	-	98	-	99	-	98
Diclofenac	-	93	-	99	-	99
Ibuprofen	-	94	-	94	-	98

Table 3.3.7.2.2. – Recovery (%) values obtained for the washing and elution steps using HXL-PP-SAXa and the two commercial sorbents with 500 mL samples of ultra-pure water spiked at 20 µg/L.

For each of the sorbents tested, it is clear that the polymeric backbone of the sorbent allows the extraction of organic components from an aqueous sample matrix, while the additional SAX nature allows the selective separation of acidic analytes from the organic compounds retained. Overall, the recovery values of the acidic analytes are fairly similar between the sorbents, indicating that the performance of the novel HXL-PP-SAXa sorbent is on a par with commercially available materials. This is an extremely promising result indeed.

3.3.7.3. Application to Real Samples

In order to assess the applicability of the HXL-PP-SAXa sorbent for the analysis of complex, real samples, two environmental water samples were evaluated; water from the Ebro river which runs through the Catalonia region in Northern Spain, and water from the effluent stream of a waste water treatment plant (WWTP) in Reus, Tarragona, Spain. These samples will contain very different

types and levels of impurities and will thus provide a thorough evaluation of the novel sorbent.

	Recovery (%) *HXL-PP-SAXa*	
Analyte	***Wash***	***Elution***
Caffeine	96	-
Antipyrine	101	-
Propranolol	80	-
Carbamazepine	103	-
Salicylic acid	-	80
Clofibric acid	-	90
Fenoprofen	-	90
Diclofenac	-	74
Ibuprofen	28	66

Table 3.3.7.3.1. – Recovery (%) values obtained for HXL-PP-SAXa after percolation of 500 mL of Ebro river water spiked with analytes at a level of 0.5 µg/L.

From the recovery values presented in Table 3.3.7.3.1 it can be seen that introduction of a complex, real water sample still allowed high recoveries of the acidic analytes of interest. The main effects of this matrix change were some fractionation between the washing and elution steps observed for ibuprofen (28 % lost during washing, leaving only 66 % bound through ionic interaction with the sorbent) and the recovery of diclofenac has decreased significantly in river water relative to the ultra-pure water (74 % *vs.* 93 %, respectively). These effects are most likely a consequence of acidic interferents within the sample matrix inhibiting the interaction of these analytes with the sorbent.

The next sample matrix tested was the effluent water from a WWTP. This is the water that leaves the WWTP after treatment, and thus should be relatively clean, but may contain additional interferences introduced as a result of the treatment process. The recoveries obtained from percolation of 100 mL

samples of effluent water spiked with the analytes at a level of 5 µg/L through the hypercrosslinked sorbent and the commercial sorbents are shown in Table 3.3.7.3.2.

	Recovery (%)					
	HXL-PP-SAXa		***Oasis MAX***		***SampliQ SAX***	
Analyte	***Wash***	***Elution***	***Wash***	***Elution***	***Wash***	***Elution***
Caffeine	82	-	86	-	91	-
Antipyrine	110	-	81	-	85	-
Propranolol	66	-	73	-	80	-
Carbamazepine	99	-	64	-	70	-
Salicylic acid	-	85	-	75	-	88
Clofibric acid	-	74	-	76	-	79
Fenoprofen	4	90	-	75	-	82
Diclofenac	-	85	-	66	-	67
Ibuprofen	11	60	-	58	-	66

Table 3.3.7.3.2. – Recovery (%) values obtained for HXL-PP-SAXa, Oasis MAX and SampliQ SAX after percolation of 100 mL of WWTP effluent water spiked with analytes at a level of 5 µg/L.

Again, high recoveries were obtained for all of the analytes present in the sample. Fractionation was once again observed for ibuprofen, albeit to a lesser extent, using the HXL-PP-SAXa sorbent (11 % lost early during the wash step), but despite this the recovery observed in the elution step was still very close to the recoveries observed using the commercial sorbents. The same is true of fenoprofen, with a higher recovery using the HXL-PP-SAXa sorbent, despite a slight loss during washing. Clofibric acid recovery was reduced, however this effect was the same for all three sorbents. Again, it was surmised that these results were due to interferences present within the sample matrix itself causing disruption of the ionic interactions of the analytes and sorbents. Additionally, the recovery of diclofenac was reduced when using the

commercial sorbents, however recovery using HXL-PP-SAXa was significantly higher.

Overall, the effectiveness of the SPE sorbents for extraction and preconcentration of acidic pharmaceuticals from complex real environmental samples was demonstrated, with the novel HXL-PP-SAXa sorbent comparing favourably to the best sorbents available commercially.

3.4 CHAPTER CONCLUSION

It has been demonstrated in this Chapter that the introduction of a quaternary ammonium species into hypercrosslinked polymer particles can be achieved in a controlled and facile manner. While primary and secondary amines can be introduced into hypercrosslinked polymers relatively easily, it has been shown that amination using tertiary amines compound required the amination reaction to be carried out prior to hypercrosslinking. However, this modification of the synthetic strategy relative to that developed for primary and secondary amines, is arguably advantageous in the respect that it allowed for greater control of the level of quaternary ammonium species present. The resulting hypercrosslinked, functionalised polymers were shown to perform successfully as an anion-exchange SPE sorbents, with the results gained from the application comparing favourable to commercially available SAX SPE sorbents for the selective extraction of acidic pharmaceutical compounds from complex real water samples.

3.5. REFERENCES

1. G. D. Christian, *Analytical Chemistry*, *Fifth Edition*, J. Wiley and Sons, New York, 1994, p517-522.
2. N. Jayaswal, S. Sinha and A. Kumar, *J. Appl. Polym. Sci.*, (2001), **79**, 1735-1748.
3. C. F. Jasso-Gastinel, S. García-Enriquez and L. J. González-Ortiz, *Polym. Bull.*, (2008), **59**, 777-785.

4. A. Ghaderi, M. Abbasian, S. Rahmani, H. Namazi, H. Baharvand and A. A. Entezami, *Iranian Polym. J.*, (2006), **15**, 497-504.
5. V. Frankovič, A. Podgornik, N. L. Krajnc, F. Smrekar, P. Krajnc and A. Štrancar, *J. Chromatogr. A.*, (2008), **1207**, 84-93.
6. Q. Zhang, S. Zhang, S. Chen, P. Li, T. Qin and S. Yuan, *J. Colloid Interface Sci.*, (2008), **322**, 421-428.
7. C. Pohl and C. Saini, *J. Chromatogr. A*, (2008), **1213**, 37-44.
8. R. J. Whitfield, S. E. Battom, M. Barut, D. E. Gilham and P. D. Ball, *J. Chromatogr. A*, (2009), **1216**, 2725-2729.
9. J. Li and J. S. Fritz, *J. Chromatogr. A*, (1998), **793**, 231-238.
10. R. Füßler, H. Schäfer and A. Seubert, *Anal. Bioanal. Chem.*, (2002), **372**, 705-711.
11. N. Fontanals, P. A. G. Cormack and D. C. Sherrington, *J. Chromatogr. A*, (2008), **1215**, 21-29.
12. D. Brousmiche, J. E. O'Gara, D. P. Walsh, P. J. Lee, P. C. Iraneta, B. C. Trammell, Y. Xu and C. R. Mallet, *J. Chromatogr. A*, (2008), **1191**, 108-117.
13. X. Kong, K. Wadhwa, J. G. Verkade and K. Schmidt-Rohr, *Macromolecules*, (2009), **42**, 1659-1664.
14. E.-R. Kenawy, F. I. Abdel-Hay, A. A. El-Magd and Y. Mahmoud, *React. Funct. Polym.*, (2006), **66**, 419-429.
15. http://msds.chem.ox.ac.uk/TI/tin_IV_chloride.html (accessed on 07 Nov 2011)
16. A. R. M. Silva, F. C. M. Portugal and J. M. F. Nogueira, *J. Chromatogr. A*, (2008), **1209**, 10-16.
17. M. Lavén, T. Alsberg, Y. Yu, M. Adolfsson-Erici and H. Sun, *J. Chromatogr. A*, (2009), **1216**, 49-62.
18. A. Kasprzyk-Hordern, R. M. Dinsdale and A. J. Guwy, *Anal. Bioanal. Chem.*, (2008), **391**, 1293-1308.
19. J. Fan, W. Yang and A. Li, *React. Funct. Polym.*, (2011), **71**, 994-1000.
20. U. Nilsson, N. Berglund, F. Lindahl, S. Axelsson, T. Redeby, P. Lassen and A.-T. Karlberg, *J. Sep. Sci.*, (2008), **31**, 2784-2790.
21. http://www.waters.com/waters/nav.htm?cid=513209&locale=en_US (accessed on 07 Nov 2011)
22. http://www.phenomenex.com/Products/SPDetail/Strata-X/X-A,%20Strong%20Anion%20Mixed%20Mode (accessed on 07 Nov 2011)

23. http://www.chem.agilent.com/Library/brochures/5989-9334EN.pdf (accessed on 07 Nov 2011)
24. N. Fontanals, P. Manesiotis, D. C. Sherrington and P. A. G. Cormack, *Adv. Mater.*, (2008), **20**, 1298-1303.
25. J.-H. Ahn, J.-E. Jang, C.-G. Oh, S.-K. Ihm, J. Cortez and D. C. Sherrington, *Macromolecules*, (2006), **39**, 627-632.
26. Unpublished data obtained during PhD of author.
27. C. M. Starks, *J. Am. Chem. Soc.*, (1971), **93**, 195-199.
28. http://www.scs.uiuc.edu/denmark/presentations/2004/gm-2004-11_16%20(b).pdf (accessed on 07 Nov 2011)
29. V. Davankov, L. Pavlova, M. Tsyurupa, J. Brady, M. Balsamo and E. Yousha, *J. Chromatogr. B*, (2000), **739**, 73-80.
30. N. Fontanals, M. Galia, P. A. G. Cormack, R. M. Marcé, D. C. Sherrington and F. Borrull, *J. Chromatogr. A*, (2005), **1075**, 51-56.
31. http://www.restek.com/Technical-Resources/Technical-Library/Pharmaceutical/pharm_A016 (accessed on 07 Nov 2011)

CHAPTER 4

FUNCTIONALISATION OF HYPERCROSSLINKED POLYMER MICROSPHERES USING CLICK CHEMISTRY

4.1. INTRODUCTION

4.1.1. Click Chemistry Definition and Criteria

The concept of 'click chemistry' was first introduced in 2001 by K. Barry Sharpless.[1] It defines a set of powerful, selective and highly reliable reactions that can facilitate the rapid synthesis of combinatorial libraries of useful compounds containing heteroatom links (C-X-C). The ease with which these bonds can be formed in nature (*i.e.*, in polysaccharides, polynucleotides and proteins) formed the basis of the Sharpless click chemistry ideology.

In order for a reaction to earn click chemistry status it must meet a set of stringent criteria defined by the Sharpless group: the reaction must be modular, wide in scope, stereospecific and be very high yielding, while generating only inoffensive by-products, which can be removed in a facile manner without the need for chromatographic techniques. Reaction conditions should be simple (preferably with no water or oxygen sensitivity) and either use no solvent or else a solvent that can be easily removed or one that is benign, such as water. All starting materials and reagents should be readily available and product isolation should be easy to effect. Where purification is required, this should involve only crystallisation or distillation. The final product obtained must also be stable under physiological conditions.[1]

Reactions that are able to satisfy this list of requirements will have a high thermodynamic driving force, allowing the reaction to proceed to completion quickly and efficiently, whilst also exhibiting selectivity for a single product.[1]

With environmental issues at the forefront of many world leaders' agendas, any reactions that can be shown to be environmentally friendly are extremely promising. Consequently, the ability of chemical reactions to proceed readily in water is perhaps one of the most desirable properties of the click chemistry

strategy. Indeed, many click reactions have been found to proceed better in water than in organic solvents. Sharpless proposed that this superior reaction potential in water is a result of the exceptional hydrogen bonding capabilities of water,[2] the large heat capacity and/or the fact that water will not compete or interfere in reactions involving polarisable nucleophiles or electrophiles.[3] It has also been suggested that the free energies of organic molecules are significantly greater when they are poorly solvated in water compared to a more compatible solvent and thus they experience greater reactivity in water. This effect is known as the hydrophobic effect, as described by Breslow[4,5] and Gajewski.[6]

4.1.2. Click Chemistry Reactions

The most common examples of click chemistry reactions, as defined by Sharpless, are carbon-heteratom bond forming reactions that can be split into four classes of transformation: cycloadditions of unsaturated species, such as 1,3-dipolar cycloadditions and Diels-Alder reactions; nucleophilic substitution chemistry, in particular ring-opening reactions of strained heterocyclic electrophiles; 'non-Aldol' type carbonyl chemistry; and oxidative additions to carbon-carbon double bonds (Figure 4.1.2.1).[1]

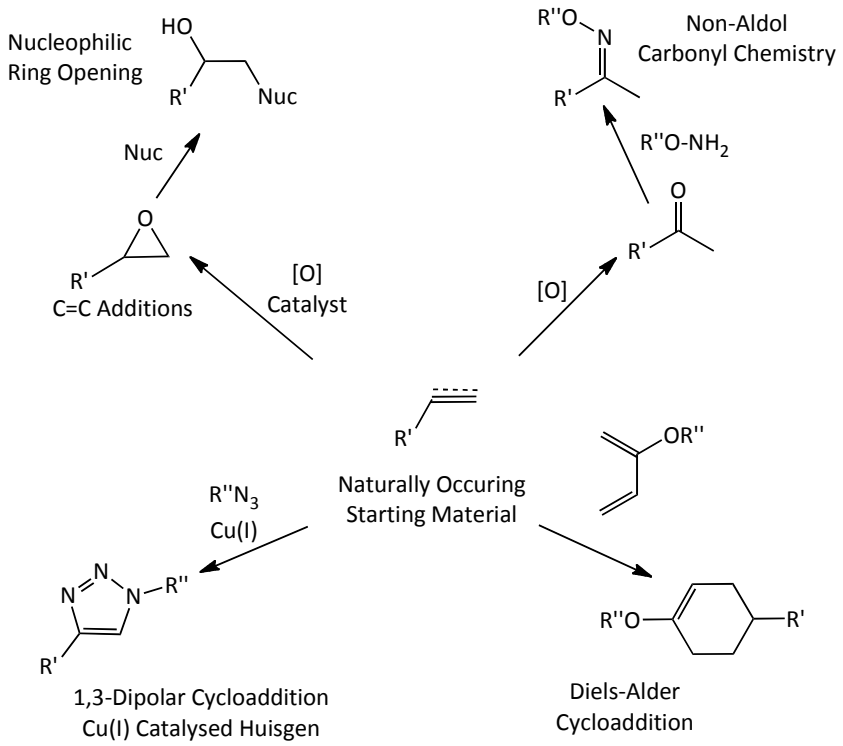

Figure 4.1.2.1. Different types of click chemistry reaction.[1]

4.1.3. Azide-Alkyne Cycloaddition

The most common reaction associated with the term click chemistry is the copper catalysed 1,3-dipolar cycloaddition of an alkyne and an azide to afford [1,2,3]-triazoles. This reaction was first reported by Huisgen in 1967,[7] with high temperatures giving rise to a mixture of 1,4- and 1,5-disubstituted triazole products. This reaction, as described, does not meet the click chemistry criteria, since a high temperature is required and a mixture of products is obtained. In 2002, however, the groups of Meldal[8] and Sharpless[9] reported independently that the addition of a copper catalyst allowed the reaction to proceed at room temperature, while also exhibiting selectivity for a single product, the 1,4-regioisomer.

Meldal and co-workers utilised a copper(I) catalyst, copper iodide, to facilitate cycloaddition of a solid-supported terminal alkyne with primary, secondary,

tertiary and aryl azides to yield diversely substituted [1,2,3]-triazoles.[8] It was demonstrated that sterically hindered azide groups were unreactive, even at high temperatures and with long reaction times. In addition, electron-deficient alkynes were shown to be more reactive. Where the alkyne was tethered to the polymer support, the product obtained was exclusively the intended triazole product, however when the alkyne was present in solution and the azide compound was tethered to the support, cross-coupling between the alkynes was observed, resulting in low reaction efficiencies.[8] This reaction is known as the Glaser coupling reaction, discovered in 1869 by Glaser,[10] when a copper phenylacetylide compound coupled unexpectedly to give diphenyl diacetylene.

Sharpless and co-workers[9] also found evidence of Glaser coupling, however they noted that addition of a nitrogen base, in particular 2,6-lutidine, helped to prevent alkyne cross-coupling. In addition, the Sharpless group discovered that substituting the copper(I) catalyst for a copper(II)/reductant catalyst system inhibited the alkyne cross-coupling reaction. The copper(II)/reductant catalyst system used was copper(II) sulfate pentahydrate and sodium ascorbate, which allowed the formation of a copper(I) species *in situ*. Matyjaszewski *et al*.[11] also noted that hydrazine could be used effectively for the regeneration of a copper(I) species from copper(II).

4.1.3.1. Azide Alkyne Cycloaddition Reaction Mechanism

Initially, Meldal *et al*.[8] believed that the role of the copper catalyst in the azide-alkyne cycloaddition was similar to that of the copper catalyst in Sonogashira coupling reactions,[12] in that the copper would bind covalently to the terminal alkyne, inducing polarisation of the alkyne, which would in turn allow the reaction to proceed in a concerted manner.

Sharpless studied the mechanism in a little more detail and proposed a mechanism in which the reaction begins with formation of a copper(I) acetylide species (Figure 4.1.3.1.1, **1**). Density functional theory (DFT) calculations then

undeniably pointed towards a stepwise cycloaddition of the acetylide and an azide compound involving a six-membered intermediate containing copper (**3**), rather than *via* a concerted [2+3] cycloaddition (*i.e.*, **1** directly to **4**).[13]

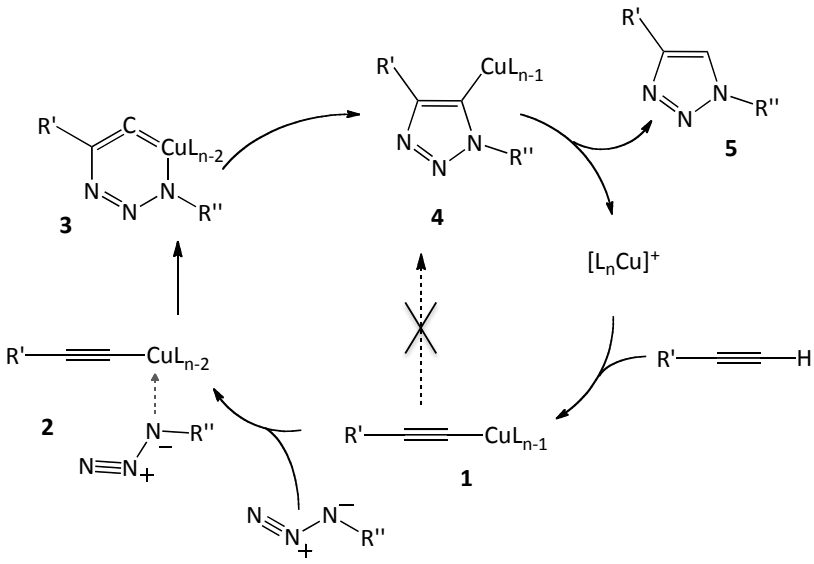

Figure 4.1.3.1.1. – Mechanism proposed by Sharpless for copper(I) catalysed azide-alkyne cycloaddition.[13]

In 2005, Rodionov *et al*.[14] carried out a series of kinetic experiments which led to the proposal of a mechanism in which two copper centres form an ordered interaction with one or two alkyne units but only one azide (Figure 4.1.3.1.2). This is similar to the ordered interaction of two copper centres in the mechanism proposed by Fomina *et al*.[15] for the Glaser coupling reaction, a side reaction sometimes observed during the azide-alkyne coupling reaction.

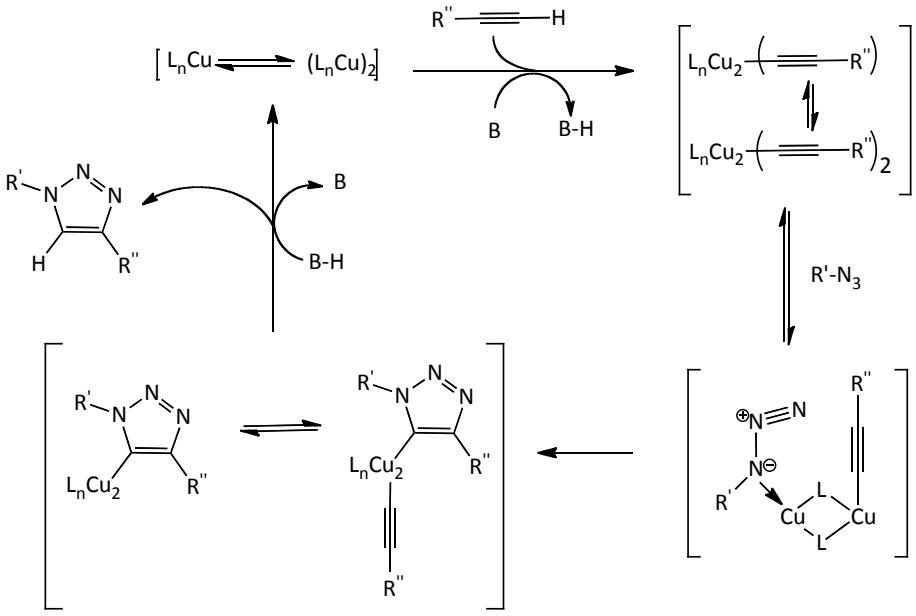

Figure 4.1.3.1.2. – Mechanism proposed by Rodionov for copper(I) catalysed azide-alkyne cycloaddition.[14]

In the same study, Rodionov also investigated the reactivity of diazides in order to gain an even better understanding of the click process. When a large excess of diazide was reacted with a single alkyne, it was expected that the predominant product would be a monotriazole compound with an unreacted azide moiety, however, the major product observed was, in fact, a ditriazole compound. It was found that the second triazole ring was formed faster than the first, suggesting that formation of the first triazole ring can induce an acceleration in the reaction rate of the second azide. It was surmised that this was due to the copper(I) catalyst directing the second alkyne compound into place for reaction with the second azide moiety before it was cleaved from the triazole ring (Figure 4.1.3.1.3). When a monotriazole with free azide moiety, from which the copper(I) catalyst had been removed, was reacted alongside a single azide, it was found that both azides were consumed at equal rate, thus supporting the role of the copper catalyst in the rate enhancement.[14]

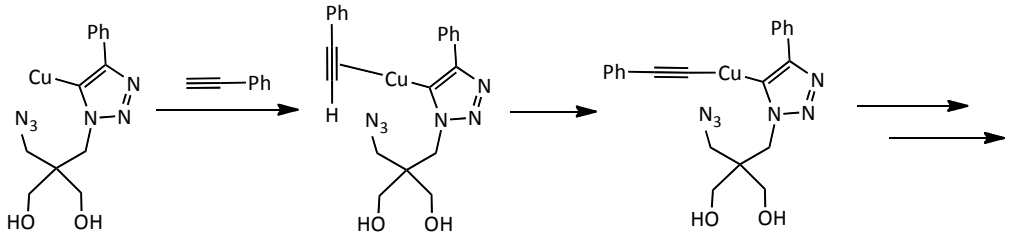

Figure 4.1.3.1.3. – Proposed mechanism of ditriazole formation.[14]

4.1.3.2. Addition of Ligands to the Copper Catalyst

As copper(I) compounds are generally unstable, reaction conditions for reactions involving copper(I) catalysts have to be tightly controlled, *i.e.*, an inert atmosphere and anhydrous solvents are often employed. In order to bring copper(I) catalysts in line with the easier to handle copper(II) catalysts, Chan *et al*.[16] explored a series of triazole containing ligands to stabilise the copper(I) centres. Of several oligotriazole derivatives investigated, one compound was notably successful: *tris*-(benzyltriazolylmethyl)amine, TBTA. It was hypothesised that TBTA was able to completely envelop the copper(I) centre leaving behind no free binding sites for destabilizing interactions. The tertiary amine and the [1,2,3]-triazole functionalities are believed to work in unison to provide the high efficiency observed. The more basic, sterically hindered nitrogen centre provides electron density to the metal centre, thus accelerating the catalysis, while the more labile triazole functionalities can temporarily vacate binding sites to allow for formation of the copper(I) acetylide complex. Rodionov *et al*.[17,18] went on to explore similar compounds, with a tertiary amine motif surrounded by benzimidazole heterocycles, which compared favourably to TBTA. Kinetic studies also revealed that addition of the chelating ligand results in faster cleavage of the copper catalyst from the triazole product.

Matyjaszewski and co-workers studied the effects of a series of aliphatic and pyridine-based amine ligands to determine the effects of both electronic properties and denticity of the ligands in the rate of the click reaction; a series of

bi-, tri- and tetradentate ligands of each type were investigated. It was found that the rates observed for the aliphatic ligands were significantly higher than those observed for the pyridine-based ligands, while the number of coordination sites available also played an important role, with tridentate ligands leading to the most enhanced reaction rates.[11]

4.1.3.3. Azide-Alkyne Cycloaddition with Internal Alkynes

While copper(I) and copper(II) catalysts have been shown to be extremely efficient thus far, only terminal alkynes have been addressed. Further research has led to improved copper(I) catalysts that show high efficiencies for click reactions involving both terminal and internal alkynes.

Nolan and co-workers[19] put forward a series of *N*-heterocyclic carbene (NHC)-containing copper catalysts that showed affinity for both terminal and internal alkynes. As the mechanism proposed for terminal alkynes involves a covalently bound copper, the mechanism for internal alkynes must differ. Nolan therefore investigated the mechanism through use of DFT studies, and subsequently proposed a mechanism for internal alkynes involving π-complexation of the copper and alkyne species (Figure 4.1.3.3.1).

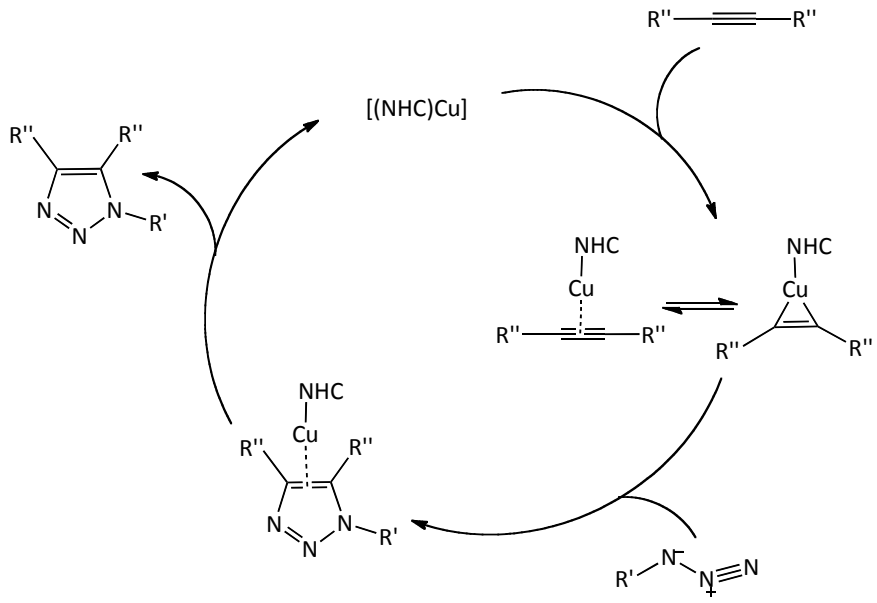

Figure 4.1.3.3.1. – Click mechanism for internal alkynes as proposed by Nolan.[19]

In addition, Nolan found that during the click reaction, organic azides could be generated *in situ* from an organic halide and sodium azide with no competition for the alkyne arising from the inorganic azide. This allows reactions involving difficult to handle, low molecular weight azides to be carried out in a more facile manner.

Candelon *et al*.[20] introduced a copper(I) complex, [Cu(C18$_6$TREN)]Br, which was shown to be highly reactive and efficient for both terminal and internal alkynes. The mechanism by which the TREN ligand coordinates to the copper centre is similar to that of the TBTA ligand mentioned previously.

As well as ligand acceleration, the copper(I)-catalysed click reaction can also undergo rate enhancement when microwaves are applied, as demonstrated by Appukkuttan *et al*.[21] It was shown that both *in situ* azide formation and the azide-alkyne cycloaddition reaction could be carried out in less than 15 minutes under microwave irradiation, with the 1,4-regioisomer formed exclusively.

4.1.3.4. Alternative Azide-Alkyne Cycloaddition Conditions

So far, copper compounds appear to be in vogue as catalysts for the azide-alkyne cycloaddition reaction, however other metals have also been utilised to give access to different products. While copper catalysis leads exclusively to 1,4-disubstituted triazoles, ruthenium catalysis under certain conditions can give rise to the complementary 1,5-disubstituted regioisomer. Sharpless and co-workers[22] found that varying the ligands on the ruthenium centre can have a profound effect on the regiochemical outcome of the reaction (Figure 4.1.3.4.1).

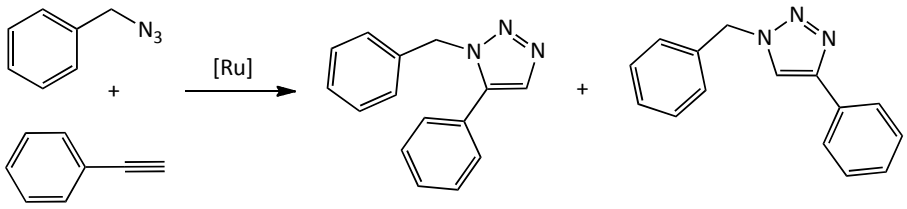

$Ru(OAc)_2(PPh_3)_2$	-	100 %
$CpRuCl(PPh_3)_2$	85 %	15 %
$Cp^*RuCl(PPh_3)_2$	100 %	-
$Cp^*RuCl(NBD)$	100%	-

Figure 4.1.3.4.1. – Ru-catalysed cycloaddition of benzyl azide and phenylacetylene.[22]

Ruthenium catalysis was also shown to be extremely effective for the reaction of both internal and external alkynes. This means that the accepted mechanism for copper catalysis, involving a metal acetylide, becomes impossible. Instead, oxidative coupling of an alkyne and azide on ruthenium is expected to proceed *via* a six-membered ruthenacycle, with the product being released from the ruthenium centre through a reductive elimination. Reaction intermediates were thus proposed to show how the regioselectivity arises in the products of a reaction between an azide and a terminal alkyne (Figure 4.1.3.4.2).

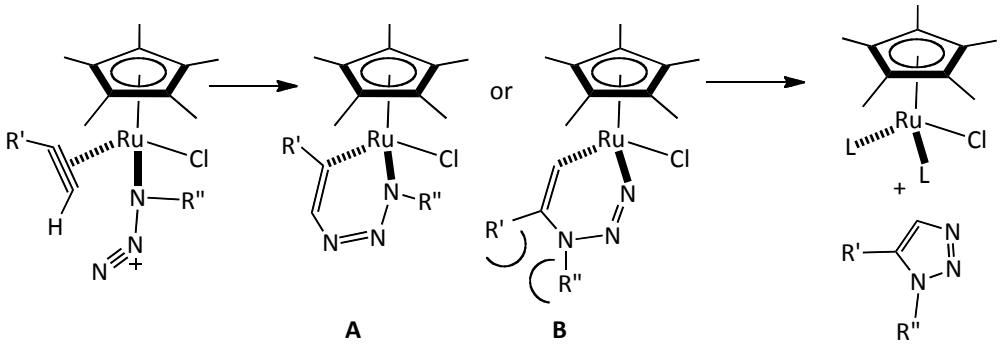

Figure 4.1.3.4.2. – Proposed reaction intermediates for the ruthenium-catalysed reaction of an azide and a terminal alkyne.[22]

Majireck and Weinreb[23] also investigated ruthenium catalysis of the alkyne-azide cycloaddition, but used internal alkynes exclusively. They proposed a similar set of reaction intermediates (Figure 4.1.3.4.3) to those presented by Sharpless and co-workers for internal alkynes.

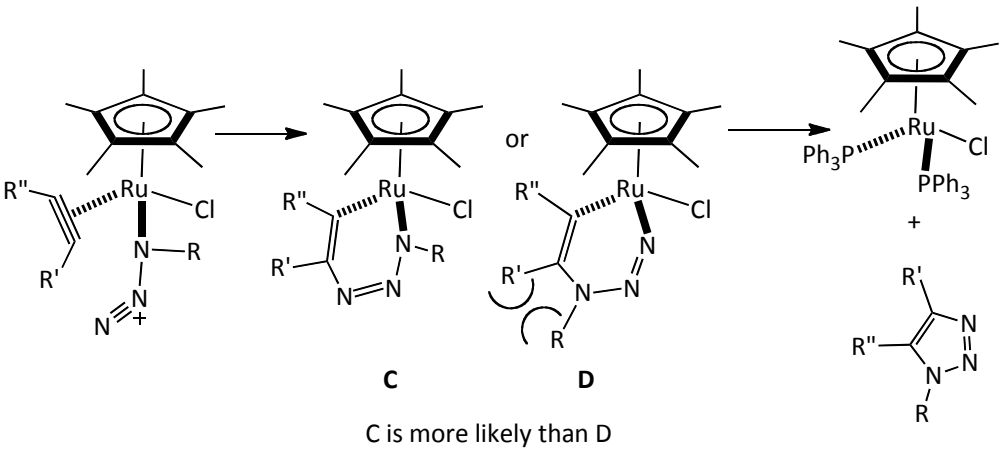

Figure 4.1.3.4.3. – Proposed reaction intermediates for the ruthenium-catalysed reaction of an azide and an internal alkyne.[23]

Matyjaszewski *et al.*[11] also studied nickel, palladium and platinum as alternatives for the catalysis of azide-alkyne cycloadditions. These metals were selected as potential catalysts as they had been previously shown to coordinate

to alkynes in a manner similar to that of copper. The platinum(II) compound, $PtCl_2$, showed the highest catalytic activity of the metals studied. However, the rate of reaction with $PtCl_2$ was still ~10 times slower than with the already well-established catalyst, CuBr.

Where biocompatibility is important in triazole products, the use of transition metal catalysts can lead to potential toxicity issues. Thus, being able to perform azide-alkyne cycloadditions effectively in the absence of metal catalysts is extremely beneficial. Bertozzi and co-workers[24,25] considered ring strain as an alternative means of activating alkynes to accelerate the azide-alkyne reaction thus negating the need for metals. A series of strained-ring substrates with differing side chains were prepared (Figure 4.1.3.4.3). It was shown that the presence of an electron-withdrawing fluorine on the carbon adjacent to the alkyne (cyclooctyne 3) resulted in an enhanced reactivity with benzyl azide relative to the other cyclooctyne substrates (cyclooctynes 1 and 2). Both triazole regioisomers were observed in a ~1:1 ratio. The mechanism and kinetics associated with the use of cyclooctynes to activate alkynes for click chemistry has also been subject to study.[26,27]

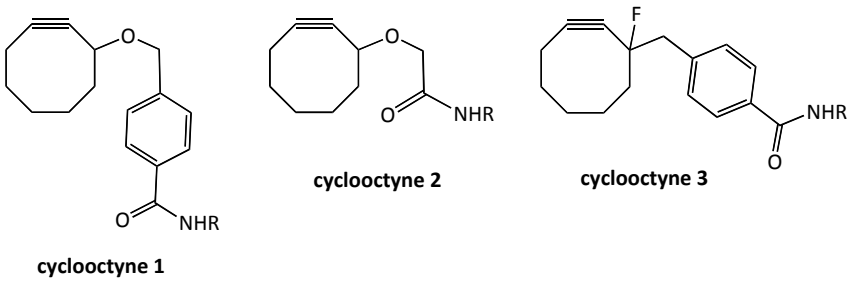

Figure 4.1.3.4.3. – Bertozzi strained-ring alkyne compounds.[24,25]

A photoinitiated cyclooctyne click reaction has also proved successful. Poloukhtine *et al.*[28] converted cyclopropenones to strained cyclooctynes by a photochemical initiation reaction. The cyclopropenones themselves were inactive towards azides, however when irradiated with light they formed the strained compounds and became reactive. When the cyclopropenone was

linked to biotin, this chemistry was used successfully to label cells expressing glycoproteins containing *N*-azidoacetylsialic acid.

Shi *et al.*[29] described the synthesis of substituted benzotriazoles using [3+2] cycloaddition of azides to benzynes, termed 'benzyne click chemistry'. This provides a facile route to substituted, functionalised benzotriazoles, which are renowned as important biologically active species. The reaction was carried out using benzyl azide and *o*-(trimethylsilyl)phenyl triflate under various conditions. A variety of azides were screened with the reaction being tolerant of many functional groups while requiring only mild conditions.

Cornelissen and co-workers[30] developed a novel method to convert alkynes into oxanorbornadienes, through a Diels-Alder reaction with furan, which can then undergo tandem [3+2] cycloaddition-retro-Diels-Alder ligations to furnish stable [1,2,3]-triazole linkages. The reactivity of the oxanorbornadienes was compared to that of the corresponding alkynes and and it was found that the oxanorbornadienes reacted approximately 5 times quicker than the alkynes. Additionally, it was found that for both the oxaborbornadienes and alkyne systems, addition of a trifluoromethyl substituent resulted in an increased reaction rate.

Reaction of oxanorbornadienes and azides can take one of two possible routes (Figure 4.1.3.4.4), however it was found that the cycloaddition occurred preferentially at the most electron-deficient double bond, thus leading to predominantly the products from reaction path A, *i.e.*, products **A1** and **A2**.

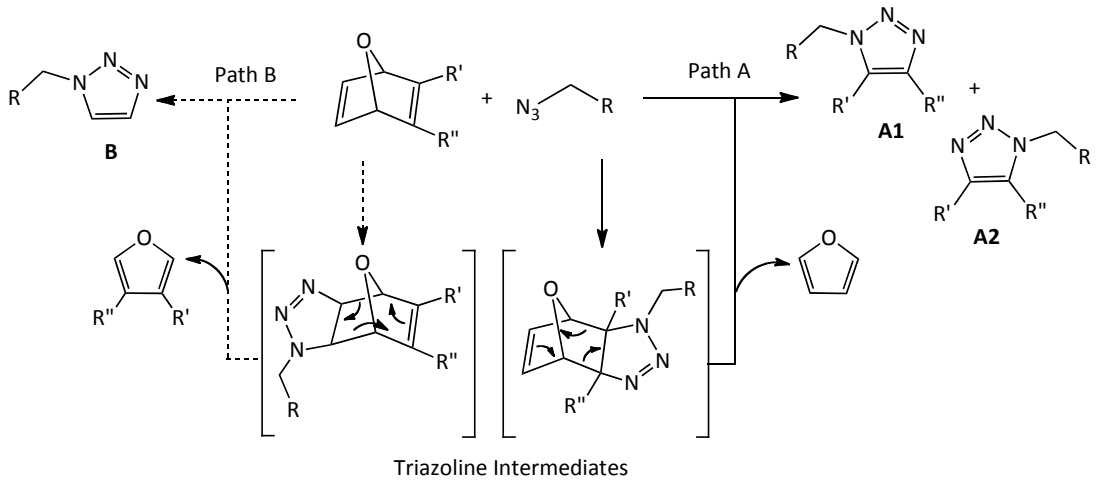

Figure 4.1.3.4.4. – Possible reaction pathways for reaction of oxanorbornadienes and azides.[30]

4.1.4. Use of Click Chemistry in Polymer Synthesis

Click chemistry has been used widely for the preparation of copolymers and dendritic structures. Matyjaszewski and co-workers[31] carried out a study of model azide compounds that bore a structural similarity to the end groups of common polymers, polystyrene, poly(methyl acrylate), poly(methyl methacrylate) and polyacrylonitrile, in order to determine the effects of the polymeric substituents on the reactivity of the azides in the click reaction (Figure 4.1.4.1). It was found that the azide reactivity was influenced by the electronic properties and steric hindrance surrounding the azide moiety. Electron-withdrawing substituents resulted in faster reactions than those of similar compounds with electron rich aromatic rings attached to the azide. A rate decrease was observed on moving from a primary azide to a secondary azide, with a further reduction still observed on moving to a tertiary azide analogue. Coordination of the nitrile group of the nitrile-containing azide to the copper catalyst provided a much reduced reaction rate compared to the other compounds that did not coordinate to the catalyst, thus further demonstrating the importance of the copper acetylide in the click mechanism.

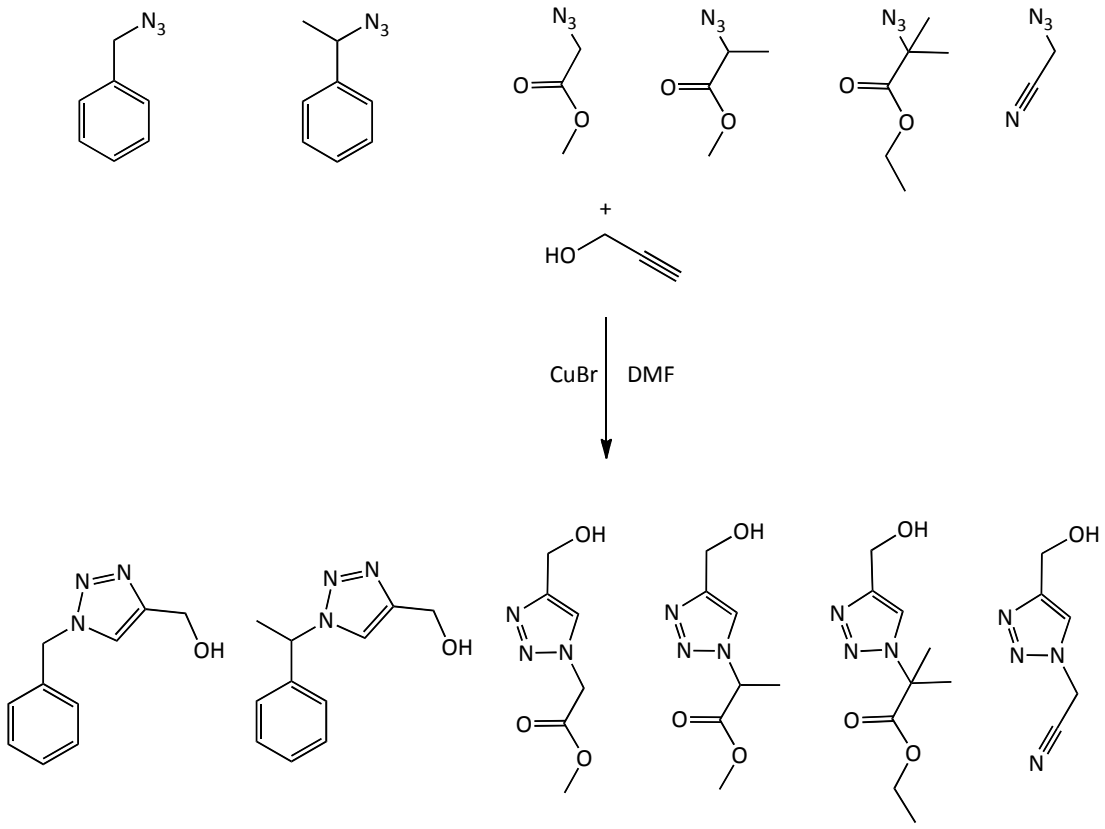

Figure 4.1.4.1. – Model azides investigated by Matyjaszewski and co-workers.[31]

Copolymers can be prepared in a facile manner by incorporating azide and alkyne moieties into the chain ends of polymeric chains. Matyjaszewski and co-workers[32] coupled polystyrene, prepared by atom transfer radical polymerisation (ATRP), using two synthetic protocols. In the first synthesis, an α-alkyne-ω-azido-terminated polystyrene was prepared and then homocoupled. The second synthesis involved preparation of a diazo-terminated polystyrene coupled with propargyl ether. While synthesising the α-alkyne-ω-azido-terminated polystyrene, a one-pot ATRP-nucleophilic substitution-click coupling process was attempted, however this showed limited success. Mantovani *et al.*,[33] on the other hand, were able to successfully combine ATRP and click functionalisation in one-pot by employing *N*-ethyl-2-pyridylmethanimine ligands, with two copper catalysts, Cu(I)Br and Cu(II)Br_2. The polymers were prepared successfully and functionalised with diaza and coumarin dyes using this method.

Opsteen and van Hest[34] prepared polystyrene and poly(methyl methacrylate) by ATRP with click functionality introduced through functional initiators and post-poymerisation end-group modification. End-group modification of commercially available poly(ethylene glycol) was also used to yield clickable polymer blocks. Subsequent click-coupling of the polymers gave both homopolymers and diblock copolymers joined through the formation of triazole rings.

Stenzel and co-workers[35] polymerised propargyl methacrylate using RAFT polymerisation and functionalised it using click chemistry and an azide terminated poly(vinyl acetate) to yield a comb polymer. Similarly, van Camp *et al*.[36] synthesised a comb polymer by first preparing a copolymer of methyl methacrylate and 3-azidopropyl methacrylate, followed by modification using an alkyne-terminated poly(1-ethoxyethyl acrylate).

Kyerematenge *et al*.[37] used click chemistry to develop a simple method for the preparation of triphilic block copolymers. Combining hydrophilic, oleophilic and fluorophilic molecules can be tricky due to the differing reactivity and physical chemistry of each block. Diazo-terminated amphiphilic, AB diblock and ABA triblock copolymers were synthesised using ATRP, where block A was composed of poly(propylene oxide) and block B contained solketal methacrylate which could later be deprotected fully by hydrolysis to yield glycerol monomethacrylate units. These azido-terminated hydro- and oleophilic block copolymers were then reacted with an α-alkyne fluorinated compound to provide the third, fluorophilic, functionality.

The synthesis of other, more exotic, types of polymer has also been facilitated through the use click chemistry. Star polymers can be prepared *via* synthesis of a multi alkyne- or azide-containing core and complementary azide- or alkyne-terminated arms. Many polymers have been synthesised in this way, from three-arm[38,39] to eight-arm[40] star copolymers, and three-miktoarm star

terpolymers.[38,41,42] Other polymer types that have been formed with the help of click chemistry include H-shaped ABCDE type quintopolymers[43] and a 'molecular charm bracelet' formed by catenation of a polymer, followed by cyclisation using click chemistry.[44]

Dendritic species can also be accessed easily through use of clickable components. Dendrimers are well-defined macromolecules with a large number of peripheral functional groups that define the properties, and hence applications, of the dendrimer. As click chemistry is tolerant of many functional groups that are used in dendritic species, synthetic strategies involving versatile 1,3-dipolar cycloadditions are very attractive and have thus received much attention.

Fréchet and co-workers[45] synthesied dendrimers using a combination of click chemistry and a convergent synthesis approach. The branches were built using monomers containing both a dialkyne functionality and a chloromethyl group. The chloromethyl group was then converted to an azide to allow coupling to one of the alkyne groups of a second monomer, and so on. Fréchet and co-workers[46] also 'dendronised' linear poly(vinyl acetylene) *via* reaction with azide-containing dendrimers. It was found that first-generation dendrimers could be added quantitatively in just a few hours, while reactions of second- and third-generation dendrimers took progressively longer. Fourth generation dendrimers did not react due to the inaccessibility of the azide groups. Katritzky *et al*.[47] prepared a series of dendrimers from an alkyne-functionalised core and azido-functionalised dendrons.

4.1.5. Use of Click Chemistry for Polymer Modification

4.1.5.1. Soluble Polymers

The versatility and ease of click chemistry has resulted in its use in a variety of applications. As some polymerisation techniques are intolerant to certain functional groups during the polymerisation, post-polymerisation reactions can be utilised instead to introduce problematic functionalities subsequent to the sensitive polymerisation reaction. Equally, where existing polymerisation methods with easily modifiable monomers are in place, polymerisation prior to introduction of click functionality may be preferable.

Xu *et al*.[48] utilised an already well-established ring-opening polymerisation (ROP) method to prepare a poly(ε-caprolactone) (PCL). The macroinitiator derived from this polymer was then used to initiate a second ROP of 2-bromo-ε-caprolactone (BrCL) to give a block copolymer, PCL-*b*-PBrCL. The bromine moieties of the PBrCL block were then converted to azide groups, which were in turn reacted with alkynyl sugars. The resulting polymers displayed amphiphilic behaviour and were able to self-assemble into spherical aggregates with surface saccharide groups.

A more common synthetic approach, however, appears to be incorporation of functional monomers into polymerisations in order to set in place a reactive handle that can then be exploited in post-polymerisation reactions. Scarpaci *et al*.[49] made use of propargyl methacrylate as an alkyne containing monomer to produce polymers that could be functionalised with chromophores and chromophore insulators to yield novel optic materials, while Yin *et al*.[50] opted for the azide-containing monomer 4-vinylbenzyl azide (VBAz), included in a copolymerisation with *N*-[2-(2-bromoisobutyryloxy)ethyl] maleimide to form an alternating copolymer. An alkyne-terminated poly(*N*-isopropy acrylamide) (polyNIPAM) was then clicked on to furnish a thermoresponsive polymer.

Damiron *et al*.[51] incorporated the azide- and alkyne-containing monomers 11-azido-1-undecanoyl and propargyl methacrylate, respectively, into copolymerisations with methyl methacrylate to furnish polymers that could be modified in the same pot *via* click chemistry, with the CuBr/bipy catalyst system allowing the ATRP and the click reaction to be carried out simultaneously.

Cornelissen and co-workers[52,53,54] prepared alkyne- and azide-functionalised isocyanide monomers, and polymerised them to give helical polymers that could be further modified with a variety of compounds to yield biomimetic materials. Chen and Han[55] prepared an azide-functionalised monomer, 3,6-dibromo-9-(6'-azidohexyl)carbazole, and clicked on a propargyl-terminated *D*-glucofuranose to the monomer unit in both pre- and post-polymerisation reactions, both of which gave rise to the desired glycopolymer product.

Click chemistry can also be used to change the functionality present at polymer chain ends, in order to introduce an alternative functionality into the polymer. Polymers prepared *via* controlled radical polymerisations are ideal in this respect, as they are synthesised in such a way as to contain a 'dormant' end unit, which can be transformed in a fast and efficient manner. Lutz *et al*.[56] converted bromine chain ends, present subsequent to ATRP of styrene, to azide moieties that were then functionalised with propargyl alcohol, propiolic acid and 2-methyl-1-buten-3-yne using click chemistry. The click reaction was successfully catalysed by a common ATRP catalyst system, CuBr/4,4'-di-(5-nonyl)-2,2'-bipyridine, which had previously been untested as a click chemistry catalyst.

Kakuchi and co-workers[57] modified the halogen end groups of polyNIPAM, synthesised using ATRP, to provide an ω-azido-polymer that could be further reacted using alkyne-containing molecules. Alkyne-containing phenyl, 4-phenoxy, butyl, octyl, carboxylic acid and hydroxymethyl groups were introduced in this manner, giving rise to polyNIPAM with differing lower critical

solution temperatures, thus providing a facile route to thermoresponsive polymers that can be fine-tuned for specific applications.

Tong *et al*.[58] synthesised an azide-functionalised xanthate for use as a RAFT polymerisation agent, and used it for preparation of poly(vinyl alcohol). This set in place azide groups at the ends of the polymer chains ready for subsequent click chemistry reactions. Alkyne-containing mannose, pyrene and PCL were added to the polymer in this manner.

Hawker and co-workers[59] utilised the ease and versatility of click chemistry for the preparation of a new class of monomers that were prepared with the desired click modification prior to polymerisation. The 1,4-vinyl-1,2,3,-triazole monomers that were prepared combined the aromaticity of styrene, the polar H-bonding capacity of vinyl pyridines and the functionality of acrylates in a single structure. The functionalities incorporated into the monomer family include alkyls, aryls, esters, acids, ethylene oxides and protected heteroatom groups. These monomers were then polymerised and copolymerised using RAFT polymerisation to yield appropriately functionalised polymers.

4.1.5.2. Polymer Microspheres

Polymer microspheres can also be modified using click chemistry. As with the soluble polymers, 'clickable' polymer microspheres can be prepared through reaction of functional groups present in the microspheres, or directly *via* incorporation of an azide or alkyne monomer. Löber *et al*.[60] prepared an azide-containing resin through reaction of a conventional Merrifield resin with sodium azide. Alkyne-containing aldehyde compounds were then clicked on and the resin used in solid-phase organic synthesis.

Breed *et al*.[61] prepared microspheres with surface chlorine groups *via* emulsion polymerisation, and converted the chlorine to azide by reaction with sodium azide. This allowed introduction of an alkyne-containing molecule that was able

to fluoresce, but only when conjugation was induced through formation of the triazole ring. In a similar approach, Karagoz *et al*.[62] prepared bromine functionalised microspheres that could be substituted with azide in the same way. The bromine groups were introduced into the precipitation polymerisation derived microspheres through conversion of residual vinyl groups in a hydrobromination reaction.

Goldmann *et al*.[63] used both the thiol-ene and azide-alkyne click chemistry methodologies in order to modify DVB-based microspheres prepared *via* distillation precipitation polymerisation. The residual vinyl groups present in the microspheres were first reacted in a thiol-ene reaction with the thiol group of 1-azidoundecane-11-thiol, to afford azide-modified microspheres. The azide groups introduced were then utilised in a second reaction with alkyne-terminated polyHEMA.

Welser *et al*.[64] opted for click-functional monomers to prepare microspheres using micro-emulsion polymerisation. The azide and alkyne functionalities were introduced through *N*-(11-azido-3,6,9-trioxaundecanyl)acrylamide and propargyl acrylamide, respectively. The group of Fréchet also prepared alkyne-functionalised microspheres through incorporation of propargyl acrylate in a suspension polymerisation reaction.[65]

4.1.6. Previous Work Within Our Group

4.1.6.1. Jonathan Chua – Nuffield Summer Student

Chua prepared an azide-containing, vinyl monomer, vinylbenzyl azide (VBAz), by reacting inhibitor-free vinylbenzyl chloride (VBC) (**7**) with sodium azide in a 1/1 (v/v) mixture of water and ethanol at reflux (Figure 4.1.6.1.1).

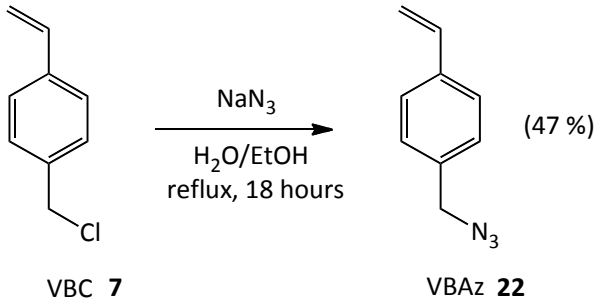

Figure 4.1.6.1.1. – Reaction of VBC and sodium azide to yield VBAz.

The reaction was carried out overnight to afford VBAz (**22**) in a yield of 47 %, however the product, initially a yellow oil, soon developed a sticky constituency, possibly due to polymerisation of the monomer. The reaction was repeated by heating at reflux for a reduced reaction time of 5 hours, without the removal of inhibitors, and the resultant VBAz (**22**) product stored at low temperature to avoid premature polymerisation. This monomer was then incorporated into a precipitation polymerisation, with DVB (**2**) and VBC (**7**) as comonomers (feed ratio 25/65/10, w/w/w, DVB/VBC/VBAz), to yield clickable beaded polymers (Figure 4.1.6.1.2).

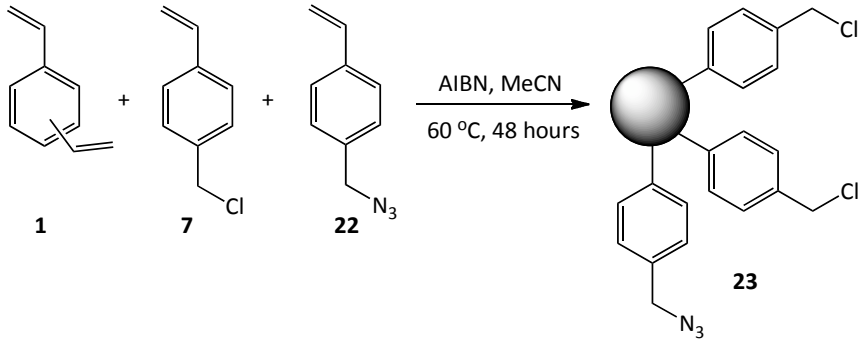

Figure 4.1.6.1.2. – Precipitation polymerisation incorporating 'clickable' monomer VBAz.

FT-IR spectroscopy and elemental microanalysis were used to confirm the inclusion of each of the monomers into the polymeric products.

Chua also investigated the preparation of clickable polymers by synthesising hypercrosslinked polymers followed by reaction of residual pendent chloromethyl groups with sodium azide (Figure 4.1.6.1.3).

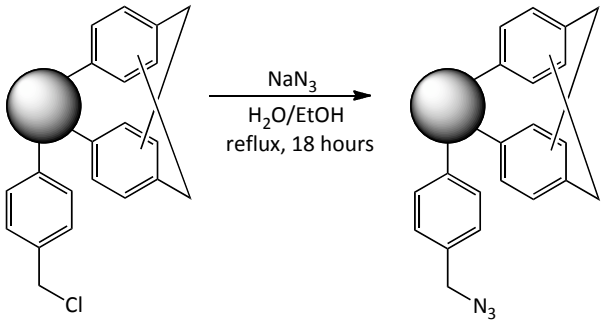

Figure 4.1.6.1.3. – Conversion of pendent Cl moieties to N_3.

The appearance of a weak azide band in the FT-IR spectrum of the product indicated that the reaction had been successful to some extent, however the extent of reaction was not quantified. No attempts were made by Chua to click onto either of the azide-containing polymers prepared, due to time constraints.

4.1.6.2. Rachel Mark – Final Year MSci Undergraduate Student

Mark[66] prepared a series of highly crosslinked polymer microspheres composed primarily of DVB, with 5 or 10 wt% of VBC (**7**) or VBAz (**22**) incorporated in the feed to allow for subsequent click functionalisation. The VBAz(**22**)-containing polymers were clicked directly with propargyl alcohol, while the VBC-containing polymers had the chloromethyl moieties converted to azide prior to click functionalisation with propargyl alcohol (Figure 4.1.6.2.1).

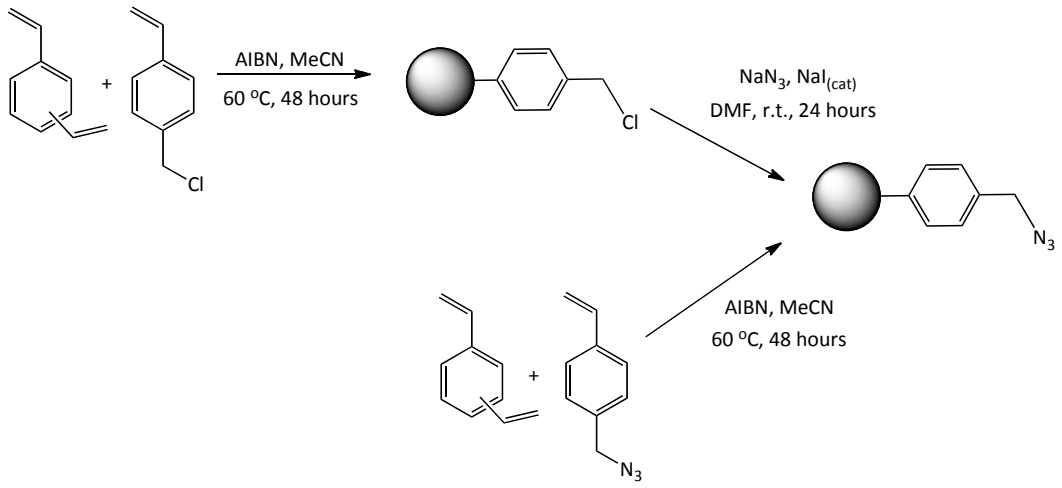

Figure 4.1.6.2.1. – Synthesis of azide-containing polymer microspheres.

Model click reactions between VBAz (**22**) and propargyl alcohol (**24**), carried out in solution, indicated that where a copper(II) catalyst and reductant system were employed ($CuSO_4.5H_2O$ and sodium ascorbate, respectively), DCE was not suitable for use as the solvent, with 0 % conversion to triazole being observed after 24 hours of reaction at room temperature. This was unfortunate, since DCE is considered to be a good solvent for reactions using the beaded polymers of interest, due to the remarkable swelling properties of DVB materials in DCE, which thus allow good access to the polymeric materials for the reagents. Instead, DMF or water/ethanol mixes (both 1/1, v/v and 1/2, v/v) were shown to be effective solvents for the click reaction at room temperature, thus DMF was selected as the preferred solvent for reaction of the polymers due to its compatibility with both the azide-containing polymer and the alkyne-containing alcohol used for the click reaction.

While the click reaction was shown to be effective at room temperature for the small molecules VBAz (**22**) and propargyl alcohol (**24**), reaction of the polymer bound azide groups was not observed under the same conditions. An increase in the reaction temperature to 80 °C, however, resulted in a successful click reaction (Figure 4.1.6.2.2). A decrease in intensity of the azide band in the FT-IR

spectra of the products was used to provide evidence that the click reaction was proceeding.

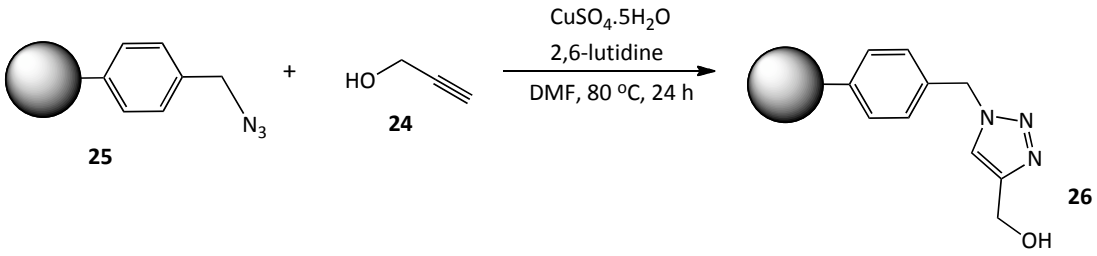

Figure 4.1.6.2.2. – Click reaction of propargyl alcohol and azide-containing polymer microspheres.

With the reaction of azide-containing polymers showing such promise, the reaction was inverted, *i.e.*, an alkyne-containing polymer was synthesised, onto which azide-containing molecules could be clicked. The polymers were prepared by incorporation of 5 or 10 % (w/w) of propargyl methacrylate into the feed of a DVB precipitation polymerisation (Figure 4.1.6.2.3).

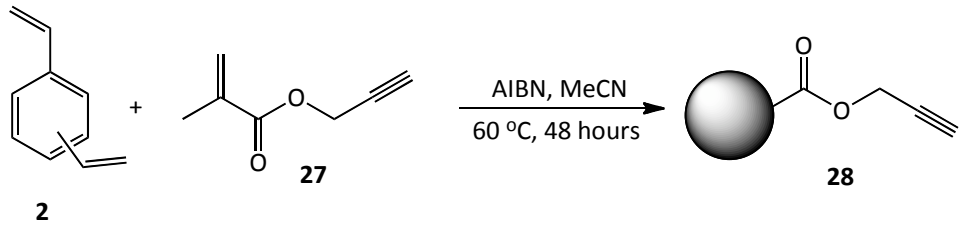

Figure 4.1.6.2.3. – Preparation of alkyne-containing polymer microspheres by precipitation polymerisation.

These alkyne-containing polymer microspheres were then modified under click chemistry conditions using the VBAz (**22**) monomer (Figure 4.1.6.2.4).

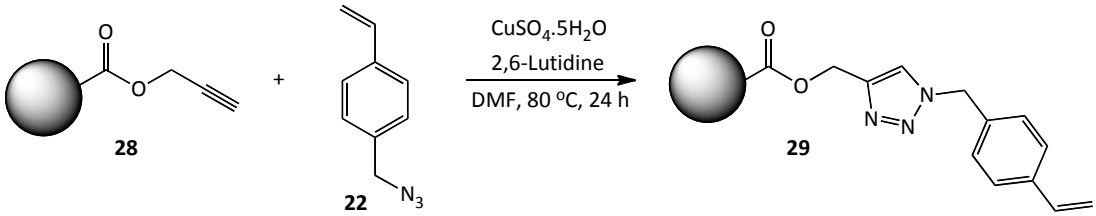

Figure 4.1.6.2.4. – Click reaction of alkyne-containing polymer microspheres and VBAz (22).

FT-IR spectroscopy was used to show that the reaction was proceeding; in particular, there was a reduction in intensity of the bands corresponding to the polymer-bound alkyne groups. However, the alkyne bands of the spectra were weak, thus it was harder to gauge the extent of this reaction compared to the complementary reactions with the azide-containing polymers, due to the higher intrinsic intensity of the azide signal.

Finally, the potential to join together alkyne- and azide-containing beads, using click chemistry, was explored (Figure 4.1.6.2.5).

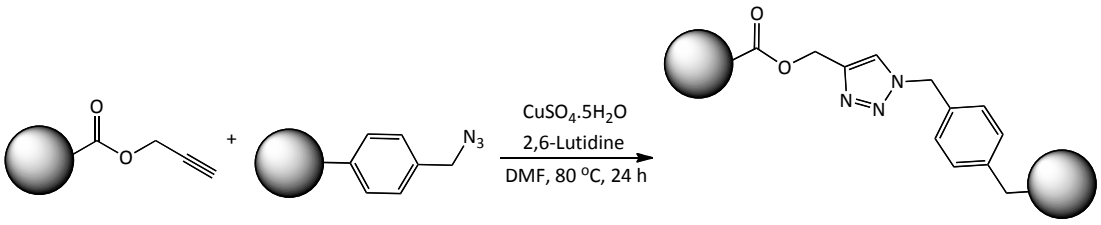

Figure 4.1.6.2.5. – Coupling of alkyne- and azide-containing beads.

The initial findings were extremely encouraging. Representative SEM images obtained, which suggest bead-bead coupling, are shown in Figure 4.1.6.2.6.

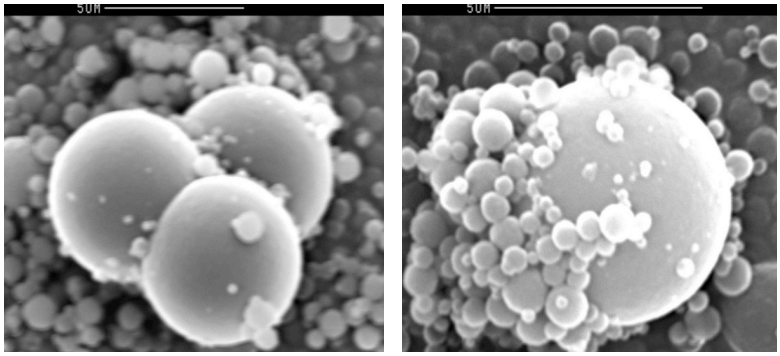

Figure 4.1.6.2.6. – SEM images obtained for RM14, the product arising from reaction of alkyne- and azide-containing beads.

It was unclear at this stage whether the aggregation observed was due to physical forces or if it was in fact due to chemical bonds formed between the beads, however the FT-IR spectra acquired indicated that the azide and alkyne groups were reduced in relative intensity subsequent to reaction, thus inferring triazole formation between the beads.

4.2. EXPERIMENTAL

4.2.1. Materials

Divinylbenzene-80 (80.0 %) and 4-vinylbenzyl chloride (≥ 90.0 %) were purchased from Sigma-Aldrich and purified prior to use by passing through a column of neutral alumina. 2,2'-Azo*bis*(isobutyronitrile), AIBN, (97.0 %) was purchased from BDH and was recrystallised from acetone at low temperature. Iron(III) chloride (97.0 %), anhydrous 1,2-dichloroethane, DCE, (99.8 %), nitric acid (Riedel-de Haën, 65.0 %), anhydrous dichloromethane (99.8 %), copper(I) bromide (98 %), 2,6-lutidine (99 %), copper(II) sulfate pentahydrate (98 + %), dicyclohexyl carbodiimide, DCC, (99 %), 4-dimethylaminopyridine, DMAP, (99 %), propargyl alcohol (99 %), sodium iodide (99 %) and *L*-phenylalanine (98 %) were all supplied by Sigma-Aldrich and were used as received. Methacryloyl chloride (> 97 %), triethylamine (≥ 99.5 %) and triflic anhydride (≥ 98 %), were purchased from Fluka and used as received. Fmoc-glycine

(≥ 98 %), from Bachem and sodium azide (99 %) from Acros Organics were also used as received.

The solvents employed (toluene, acetone, methanol, diethyl ether and dichloromethane [DCM]) were of standard laboratory grade and were obtained from Sigma-Aldrich. HPLC grade acetonitrile and peptide synthesis grade *N*-*N*-dimethylformamide (DMF) were obtained from Rathburn Chemicals Ltd.

4.2.2. Equipment

Precipitation polymerisations were carried out using a Stuart Scientific S160 incubator (Surrey, UK) and a Stovall low-profile roller system (NC, USA). All of the polymerisations were carried out in Nalgene® plastic bottles.

The optical compound microscope employed was a Carl Zeiss Jena (Germany).

Elemental microanalysis was performed by the University of Strathclyde Elemental Microanalysis Service. C, H and N elemental microanalyses were carried out simultaneously using a Perkin Elmer 2400 Series II analyser, while halogen contents were determined by standard titration methods.

Scanning electron microscopy (SEM) was carried out by the University of Strathclyde SEM Service, using a Cambridge Instruments Stereoscan 90. Samples were coated in gold prior to SEM imaging.

Fourier-Transform Infrared (FT-IR) analysis was carried out using a Perkin-Elmer Spectrum One FT-IR spectrometer. The samples were prepared as discs with spectroscopic grade KBr in an RIIC press at 10 tons. The samples were scanned over the range 4,000-400 cm^{-1} in transmission mode.

Electrospray mass spectrometry was performed in the positive ion mode using a LCQ DUO Thermo Finnigan ion trap with a spray voltage of 4.5 kV and capillary temperature of 230 °C. Methanol was used as the solvent. The analyses were carried out by the University of Strathclyde Mass Spectrometry Service.

^{1}H NMR spectra were obtained at 400.13 MHz on a Bruker DPX400 spectrometer or at 500.16 MHz on a Bruker DRX500 spectrometer. The chemical shifts (δ) are quoted in parts per million (ppm) relative to TMS. Multiplicities are abbreviated as: s, singlet; d, doublet; t, triplet; q, quartet; m, multiplet for the ^{1}H NMR spectra. The coupling constants (J) are reported in Hertz (Hz). In cases where superimposition two or more singnals occurred, the signals have been reported as multiplets (m), unless the coupling constants of each signal could be ascertained. All ^{13}C NMR spectra were recorded on a Bruker DRX500 spectrometer at 125.76 MHz.

The specific surface area measurements were performed using a Micromeritics ASAP 2000 (samples > 300 mg) or 2020 (samples < 300 mg) nitrogen sorption porosimeter. Samples were degassed overnight under vacuum at 100 ^{o}C prior to analysis. Analysis was *via* nitrogen sorption, carried out at 77 K.

Solvent uptake data was obtained using centrifuge tubes fitted with 0.2 μm modified nylon 500 μL centrifugal filter inserts (VWR, North America). The centrifuge used was an Eppendorf Centrifuge 5804 (Hamburg, Germany).

4.2.3. Synthesis of Fmoc-Glycine Propargyl Ester

Fmoc-glycine (**30**) (1.004 g, 3.363 mmol), propargyl alcohol (**24**) (0.250 mL, 0.243 g, 4.332 mmol) and DMAP (0.1087 g, 0.673 mmol) were charged to a round-bottomed flask under an N_2 atmosphere. 50 mL of dry dichloromethane (DCM) was added, and the reaction mixture was left stirring for 1 hour. An ice bath was used to cool the reaction mixture to 0 ^{o}C and DCC (0.7212 g,

3.441 mmol, slight excess relative to Fmoc-glycine (**30**)) in a DCM solution (6 mL) was added slowly over 5 minutes. The flask was removed from the ice bath, allowed to equilibrate to room temperature and then stirred at room temperature for 24 hours. DCU formed during the reaction was removed by filtration, and the filtrate washed with 5 % acetic acid (2 × 20 mL), followed by successive 20 mL volumes of water, 5 % $NaHCO_3$ and brine. The organic phase was dried over anhydrous sodium sulfate, filtered and the DCM removed by rotary evaporation to yield the product as a cream-coloured solid (0.737 g, 62 %). No further purification was performed.

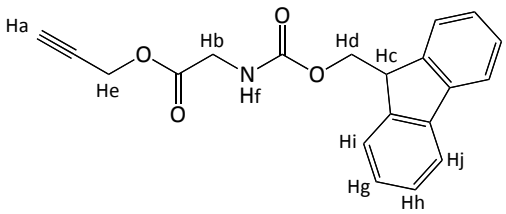

^{1}H NMR (500 MHz, $CDCl_3$) ppm: 2.52 (t, J=2.0 Hz, 1H, Ha), 4.07 (d, J=6.0 Hz, 2H, Hb), 4.25 (t, J=7.0 Hz, 1H, Hc), 4.43 (d, J=7.0 Hz, 2H, Hd), 4.78 (d, J=2.0 Hz, 2H, He), 5.27 (s, 1H, Hf), 7.31-7.35 (m, 2H, Hg), 7.42 (t, J=7.5 Hz, 2H, Hh), 7.61 (d, J=7.5 Hz, 2H, Hi), 7.78 (d, J=7.5 Hz, 2H, Hj).

^{13}C NMR (126 MHz, $CDCl_3$) ppm: 42.5, 47.1, 52.6, 66.3, 78.4, 78.7, 120.6, 125.7, 127.6, 128.1, 141.2, 144.3, 157.0, 170.1.

FT-IR: $\bar{\nu}$/cm^{-1} (KBr), 3320 (alkyne C-H stretch), 3064 (amide, N-H stretch), 3018, 2933, 2851, 2131 (alkyne C-C stretch), 1770 (ester C=O stretch), 1690 (urethane C=O str.), 1542, 1451, 1288 and 1182 (C-O stretch).

Mass spectrometry: (ESI$^+$), Expected 335.4; Found $(M+Na)^+$ 358.4.

An analogous procedure was followed for all further syntheses of Fmoc-glycine propargyl ester (Table 4.2.3.1).

Sample Ref.	*Glycine (g)*	*Propargyl alcohol (mL)*	*DMAP (g)*	*DCC (g)*	*DCM (mL)*	*Product mass (g)*	*Product yield (%)*
Fmoc-Gly-1	1.004	0.250	0.109	0.721	50	0.737	62
Fmoc-Gly-2	1.001	0.250	0.110	0.740	50	0.960	81

Table 4.2.3.1. – Synthesis and yield data for all preparations of Fmoc-glycine propargyl ester.

4.2.4. Synthesis of α-Azido Phenylalanine (34) (Azido-Phe)[72]

Triflyl azide (**31**) was prepared freshly prior to use as follows: NaN_3 (3.968 g, 0.061 mol) was charged to a round-bottomed flask with 9 mL of water. 15 mL of DCM was added and the reaction mixture cooled on an ice bath. Triflic anhydride (2.040 mL, 3.416 g, 0.012 mol) was added slowly over *ca.* 5 minutes and the reaction was stirred for 2 hours. The organic layer was removed and the aqueous layer was extracted with 2 × 10 mL DCM. The organic fractions were pooled and washed once with saturated Na_2CO_3. The triflyl azide product was not isolatd from solution and used directly without further purification.

L-Phenylalanine (**32**) (0.999 g, 6.054 mmol), K_2CO_3 (1.691 g, 0.012 mol) and copper(II) sulfate pentahydrate (0.157 g, 0.605 mmol) were charged to a round-bottomed flask with 20 mL water and 40 mL methanol. The triflyl azide (**31**) in DCM was added and the mixture stirred overnight at ambient temperature. The volatiles were removed under reduced pressure. The aqueous slurry remaining was diluted with water (50 mL) and acidified to pH 6 with conc. HCl. 50 mL of 0.25 M, pH 6.2, phosphate buffer was added and the sulfonamide by-product was removed by 4 × extraction with EtOAc. The aqueous phase was then acidified to pH 2 with conc. HCl and the azide-protected amino acid product was obtained from 3 × EtOAc extractions. The organic portions were combined and dried over anhydrous sodium sulfate, filtered and the EtOAc removed by rotary

evaporation to yield the product as a pale yellow oil (0.690 g, 69 %). No further purification was performed.

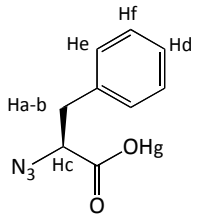

^{1}H NMR (500 MHz, $CDCl_3$) ppm: 3.06 (dd, J=14.0, 9.0 Hz, 1H, Ha), 3.26 (dd, J=14.0, 5.0 Hz, 1H, Hb), 4.19 (dd, J=9.0, 5.0, 1H, Hc), 7.28-7.36 (m, 5H, Hd-f), no signal detected for Hg.
^{13}C NMR (126 MHz, $CDCl_3$) ppm: 37.5, 63.1, 127.5, 128.8, 129.2, 135.6, 175.7.
FT-IR: $\bar{\nu}/cm^{-1}$ (KBr), 3032, 2859, 2116 (N_3 stretch), 1720 (carboxylic acid C=O str.), 1605, 1586, 1456, 1264 (O-H bending), 751 and 700 (mono subst. aromatic ring).
Mass spectrometry: (ESI^-), expected 191.1; found $(M-H)^-$ 190.1.

4.2.5. Typical Vinylbenzyl Azide (22) (VBAz) Synthesis

Vinylbenzyl chloride (**7**) (VBC) (9.234 mL 10.000 g, 0.065 mol), sodium azide (12.796 g, 0.197 mol, 3 × molar excess relative to VBC), sodium iodide (0.982 g, 6.550 mmol) and hydroquinone were charged to a round-bottomed flask and 50 mL of anhydrous DMF added. The reaction mixture was left stirring for 24 hours at room temperature under an N_2 atmosphere. The reaction mixture was extracted with water (30 mL) and diethyl ether (50 mL). The aqueous portion was washed with 2 × 25 mL portions of diethyl ether. The organic fractions were combined and washed with 4 × 25 mL portions of water. The washed organic fraction was then dried over anhydrous sodium sulfate and the ether removed by rotary evaporation to give the product as a bright yellow oil (7.600 g, 76 %). No further purification was performed.

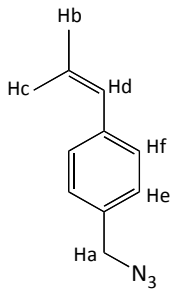

^{1}H NMR (500 MHz, $CDCl_3$) ppm: 4.34 (s, 2H, Ha), 5.29 (dd, J=11.0, 0.5 Hz, 1H, Hb), 5.78 (dd, J=18.0, 0.5 Hz, 1H, Hc), 6.73 (dd, J=18.0, 11.0 Hz, 1H, Hd), 7.29 (d, J=8.0 Hz, 2H, He), 7.44 (d, J=8.0 Hz, 2H, Hf).

^{13}C NMR (126 MHz, $CDCl_3$) ppm: 54.6, 114.5, 126.7, 128.5, 134.9, 136.3, 137.7.

FT-IR: $\bar{\nu}/cm^{-1}$ (KBr), 3025, 2930, 2876, 2098 (N_3 stretch), 1630, 1569, 1512, 1443, 991 and 912 ($R_2C=CH_2$), 824 (para-subst. aromatic ring).

Mass spectrometry: (ESI^+), Expected 158.2; Found dimer $[(M)_2+Na]^+$ 339.4.

An analogous procedure was followed for all further preparations of the vinylbenzyl azide monomer (Table 4.2.5.1).

Sample ref.	***VBC (g)***	***NaN_3 (g)***	***NaI (g)***	***Solvent (mL)***	***Product mass (g)***	***Product yield (%)***
VBAz-1	10.000	12.796	0.982	50	7.600	76
VBAz-2	21.660	25.976	1.996	100	19.710	91

Table 4.2.5.1. – Synthesis and yield data for all preparations of VBAz.

4.2.6. Propargyl Methacrylate (27) (PMA) Synthesis

Propargyl alcohol (**24**) (11.040 mL, 10.726 g, 0.191 mol) and triethylamine (34.845 mL, 25.298 g, 0.250 mol) were charged to a round-bottomed flask with 100 mL of diethyl ether. The reaction was cooled to –20 ^{o}C and a solution of methacryloyl chloride (**33**) (18.939 mL, 20.000 g, 0.191 mol in 100 mL of diethyl ether) was added dropwise over *ca*. 1 hour. The mixture was then stirred at room temperature overnight. The triethylammonium chloride

precipitate was filtered off and the volatiles removed by rotary evaporation. The crude product was then distilled under reduced pressure to give propargyl methacrylate monomer as a colourless oil.

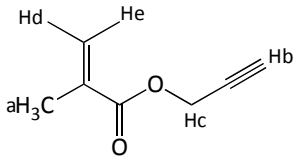

^{1}H NMR (500 MHz, DMSO) ppm: 1.89 (s, 3H, Ha), 3.50 (t, J=2.5 Hz, 1H, Hb), 4.77 (d, J=2.5 Hz, 2H, Hc), 5.72 (t, J=2.0 Hz, 1H, Hd), 6.06 (d, J=1.0 Hz, 1H, He).

^{13}C NMR (126 MHz, $CDCl_3$) ppm: 18.4, 52.6, 78.2, 78.9, 127.1, 135.8, 166.2.

FT-IR: $\bar{\nu}/cm^{-1}$ (KBr), 3284 (alkyne C-H stretch), 2960, 2131 (alkyne C-C stretch), 1724 (ester C=O stretch), 1437, 1178 (ester C-O stretch), 954 ($R_2C=CH_2$).

Mass spectrometry: Advised by Mass Spectrometry Service that this will not be observed by MS.

4.2.7. Typical Synthesis of Poly(DVB-co-VBC-co-VBAz) by PP (PPAz-1)

VBC (**7**) (6.518 mL, 7.000 g, 0.046 mol), DVB-80 (**2**) (2.735 mL, 2.500 g, 0.018 mol), VBAz (**22**) (0.509 g, 3.140 mmol) and AIBN (0.275 g, 1.670 mmol, 2 mol % relative to polymerisable double bonds) were charged to a 1 L Nalgene® bottle with 500 mL of acetonitrile. The bottle was placed into an ultrasonic bath for 10 minutes, then purged with N_2, whilst on an ice bath, for 10 minutes, before being sealed under N_2. The bottle was placed onto a low profile roller, which was housed in a temperature-controlled incubator. The temperature was ramped from room temperature to 60 ^{o}C over a period of around 2 hours and then held at 60 ^{o}C for a further 46 hours. After 46 hours, a representative sample of product was examined under an optical microscope to discern the presence of microspheres. When microspheres could be seen, the product was filtered under vacuum on a 0.2 μm nylon filter membrane and washed with successive 50 mL volumes of acetonitrile, toluene, methanol and

acetone. The product, in the form of a white powder, was oven-dried overnight at 40 °C *in vacuo* (2.492 g, 25 %).

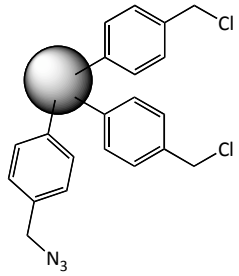

Elemental microanalysis: Expected 75.8 % C, 6.5 % H, 1.8 % N, 15.9 % Cl; Found 77.4 % C, 6.4 % H, 1.3 % N, 14.1 % Cl.

FT-IR: $\bar{\nu}/cm^{-1}$ (KBr): 3022, 2923, 2853, 2097 (N_3 stretch), 1605, 1511, 1444, 1265 (CH wag of CH_2-Cl), 990 and 908 ($R_2C=CH_2$), 833 (para-subst. aromatic ring), 677 (C-Cl stretch).

BET specific surface area: < 5 m^2/g.

An analogous procedure was followed for all of the DVB/VBC/VBAz copolymers obtained. The relevant masses and yield data are presented in Table 4.2.7.1.

Polymer ref.	***DVB (g)***	***VBC (g)***	***VBAz (g)***	***AIBN (g)***	***Yield (g)***	***Yield (%)***	***Particle Size (µm)***
PPAz-1	2.500	7.000	0.509	0.275	2.492	25	4-6
PPAz-2	2.500	7.000	0.501	0.271	1.436	14	4-6

Table 4.2.7.1. – Feed and analytical data for the DVB/VBC/VBAz precipitation polymerisations.

4.2.8. Click Chemistry Modification of Poly(DVB-co-VBC-co-VBAz) (PPAz-CC1)

Azide-containing polymer microspheres, PPAz-1, (0.209g, 6.282 x 10^{-5} mol of VBAz residues) were charged to a dry, three-necked round-bottomed flask

equipped with a reflux condenser and an overhead mechanical stirrer. Anhydrous DCE (30 mL) was added and the beads were left to swell fully under N_2 at room temperature for 1 hour. 2,6-Lutidine (7.25 μL, 6.282 x 10^{-5} mol), copper bromide (2.1 mg, 1.256 x 10^{-5} mol) and propargyl alcohol (3.60 μL, 3.52 mg, 6.282 x 10^{-5} mol) were added to a round-bottomed flask with 10 mL of DCE and left to stir for 10 minutes; the solution was added to the swollen beads *via* syringe and the mixture left to react for 24 hours at ambient temperature.

The polymer product was filtered on a 0.2 μm nylon filter and washed with successive 50 mL volumes of *t*-amyl alcohol, glacial acetic acid (×2), *t*-amyl alcohol, DCM (×3) and diethyl ether. The cream coloured, powdered product was then dried *in vacuo* at 40 ^{o}C overnight (0.205 g, 97 %).

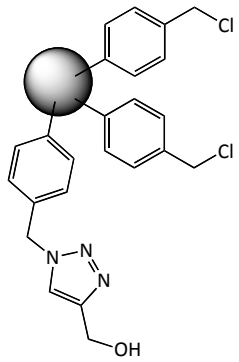

Elemental microanalysis: Expected 77.2 % C, 6.5 % H, 1.3 % N, 13.9 % Cl, 0.4 % O; Found 77.0 % C, 6.4 % H, 1.3 % N, 13.8 % Cl.
FT-IR: $\bar{\nu}$/cm^{-1} (KBr), 3446, 3022, 2923, 2852, 2097 (N_3 stretch), 1607, 1511, 1444, 1266 (CH wag of CH_2-Cl), 990 and 909 ($R_2C=CH_2$), 833 (para-subst. aromatic ring), 677 (C-Cl stretch).

An analogous procedure was followed for all propargyl alcohol click chemistry modifications of poly(DVB-*co*-VBC-*co*-VBAz). The relevant feed and yield data is detailed in Table 4.2.8.1.

Polymer ref.	*Solvent*	*Temp. (°C)*	*PPAz (g)*	*Propargyl alcohol (µL)*	*2,6-lutidine (µL)*	*CuBr (mg)*	*Yield (g)*	*Yield (%)*
PPAz-CC1	DCE	r.t.	0.209[1]	3.6	7.3	2.1	0.205	97
PPAz-CC2	H_2O/MeOH	r.t.	0.198[1]	3.6	7.3	5.4	0.192	95
PPAz-CC3	DMF	r.t.	0.200[1]	3.6	7.3	10.4	0.206	102
PPAz-CC4	DMF	80	0.204[1]	3.6	7.3	8.9	0.214	103
PPAz-CC5	H_2O/MeOH	80	0.205[2]	3.6	7.3	7.4	0.191	92
PPAz-CC6	DCE	80	0.202[2]	3.6	7.3	7.1	0.201	98

Table 4.2.8.1. – Feed and yield data for the propargyl alcohol click modified polymers. [1] and [2] denote that the preursor particles used were PPAz-1 and PPAz-2, respectively.

Click chemistry modifications of poly(DVB-*co*-VBC-*co*-VBAz) with Fmoc-glycine propargyl ester were carried out in an analogous fashion, with a direct substitution of propargyl alcohol with Fmoc-glycine propargyl ester. All of these modifications were carried out using DMF as the solvent. Feed and yield data are presented in Table 4.2.8.2.

Polymer ref.	*Temp. (°C)*	*PPAz (g)*	*Fmoc-glycine propargyl ester (mg)*	*2,6-lutidine (µL)*	*CuBr (mg)*	*Yield (g)*	*Yield (%)*
PPAz-CC7	80	0.205[1]	44.1	7.3	6.4	0.209	93
PPAz-CC8	120	0.203[2]	47.3	7.3	4.4	0.200	89
PPAz-CC9*	80	0.204[2]	42.9	7.3	11.3	0.205	91
PPAz-CC10	80	0.205[2]	92.1	7.3	5.2	0.200	88
PPAz-CC11	r.t.	0.200[2]	41.0	7.3	9.8	0.195	88

Table 4.2.8.2. – Feed and yield data for the Fmoc-glycine propargyl ester click modified polymers. * denotes a 48 hour reaction time rather than the 24 hours used for all other reactions. [1] and [2] denote that the preursor particles used were PPAz-1 and PPAz-2, respectively.

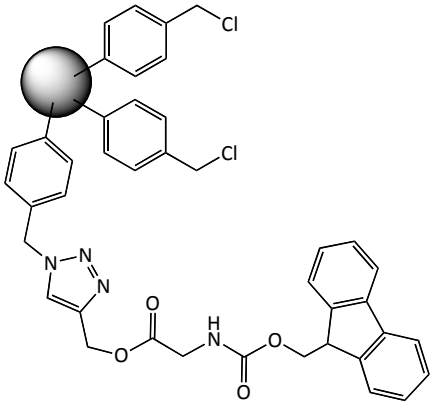

Results for PPAz-CC7:

Elemental microanalysis: Expected 77.0 % C, 6.3 % H, 1.2 % N, 12.9 % Cl, 1.5 % O; Found 76.1 % C, 6.5 % H, 1.4 % N, 13.8 % Cl.

FT-IR: $\bar{\nu}/cm^{-1}$ (KBr), 3022, 2923, 2853, 2097 (N_3 stretch), 1726 (ester C=O stretch), 1606, 1511, 1445, 1266 (CH wag of CH_2-Cl), 991 and 909 ($R_2C=CH_2$), 830 (para-subst. aromatic ring), 677 (C-Cl stretch).

4.2.9. Hypercrosslinking Reaction of Poly(DVB-co-VBC-co-VBAz) (HXL-PPAz)

Poly(DVB-*co*-VBC-*co*-VBAz) microspheres, PPAz-1, (1.006 g, 4.456 mmol of VBC residues) were charged to a dry, three-necked round-bottomed flask equipped with a reflux condenser and an overhead mechanical stirrer. Anhydrous DCE (30 mL) was added and the beads were left to swell fully under N_2 at room temperature for 1 hour. $FeCl_3$ (0.753 g, 4.456 mmol, in a 1:1 mole ratio with respect to the CH_2Cl content of the particles) in DCE (30 mL) was added and the mixture heated at 80 ^oC for 18 hours. The product particles were recovered from the reaction medium by filtration on a 0.2 μm nylon filter and washed with successive 50 mL volumes of methanol, aqueous HNO_3 (pH 1) (2 washes), methanol and acetone. The orange-coloured particles were then extracted with acetone overnight in a Soxhlet apparatus and then washed with methanol and diethyl ether before drying *in vacuo* overnight at 40 ^oC (0.797 g, 79 %).

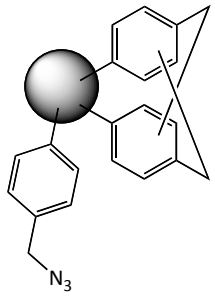

Elemental microanalysis: Expected 90.2 % C, 7.7 % H, 2.1 % N, 0 % Cl; Found 84.6 % C, 6.8 % H, 0.9 % N, 3.5 % Cl.

FT-IR: $\bar{\nu}$*/cm^{-1} (KBr), 3019, 2925, 2857, 1606, 1511, 1448, 1267 (CH wag of CH_2-Cl), 891, 819 (para-subst. aromatic ring), 680 (C-Cl stretch).*

Langmuir specific surface area: 1,295 m^2/g.

4.2.10. Typical Synthesis of Poly(DVB-co-VBC-co-PMA) by PP (PPAlk-1)

VBC (**7**) (6.518 mL, 7.000 g, 0.046 mol), DVB-80 (**2**) (2.735 mL, 2.500 g, 0.018 mol), PMA (**27**) (0.525 g, 4.030 mmol) and AIBN (0.284 g, 1.670 mmol, 2 mol % relative to polymerisable double bonds) were charged to a 1 L Nalgene® bottle with 500 mL of acetonitrile. The bottle was placed into an ultrasonic bath for 10 minutes and was then purged with N_2, whilst on an ice bath, for 10 minutes, before being sealed under N_2. The bottle was placed onto a low profile roller, which was housed in a temperature-controlled incubator. The temperature was ramped from room temperature to 60 ^{o}C over a period of around 2 hours and then held at 60 ^{o}C for a further 46 hours. After 46 hours, a representative sample of product was examined under an optical microscope to discern the presence of microspheres. The product was filtered by vacuum on a 0.2 μm nylon filter membrane and washed with successive 50 mL volumes of acetonitrile, toluene, methanol and acetone. The product, in the form of a white powder, was oven-dried overnight at 40 ^{o}C *in vacuo* (1.110 g, 11 %).

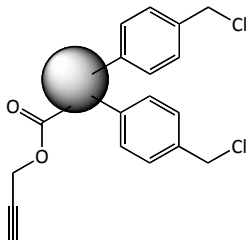

Elemental microanalysis: Expected 75.8 % C, 6.5 % H, 0.5 % N, 15.8 % Cl; Found 78.5 % C, 7.0 % H, 0.4 % N, 15.4 % Cl.

FT-IR: $\bar{\nu}/cm^{-1}$ *(KBr), 3295 (alkyne C-H stretch), 3021, 2922, 2852, 2120 (alkyne C-C stretch), 1732 (ester C=O stretch), 1604, 1511, 1444, 1265 (CH wag of* CH_2*-Cl), 990 and 907 (*$R_2C=CH_2$*), 827 (para-subst. aromatic ring), 676 (C-Cl stretch).*

BET Specific surface area: < 5 m^2/g.

An analogous procedure was followed for all of the DVB/VBC/PMA copolymers obtained. The relevant masses and yield data are presented in Table 4.2.10.1.

Polymer ref.	***DVB (g)***	***VBC (g)***	***PMA (g)***	***AIBN (g)***	***Yield (g)***	***Yield (%)***	***Particle Size (μm)***
PPAlk-1	2.500	7.500	0.525	0.284	1.110	11	4-6
PPAlk-2	2.500	7.500	0.523	0.278	1.424	14	4-6

Table 4.2.10.1. – Feed and yield data for the DVB/VBC/PMA precipitation polymerisations.

4.2.11. Click Chemistry Modification of Poly(DVB-co-VBC-co-PMA) (PPAlk-CC1)

Alkyne-containing microspheres, PPAlk-1, (0.204 g, 8.055 x 10^{-5} mol of PMA residues) were charged to a dry, three-necked round-bottomed flask equipped with a reflux condenser and an overhead mechanical stirrer. Peptide synthesis grade DMF (30 mL) was added and the beads were left to swell fully under N_2 at room temperature for 1 hour. 2,6-Lutidine (9.32 μL, 8.055 x 10^{-5} mol), copper bromide (8.2 mg, 1.611 x 10^{-5} mol) and VBAz (**22**) (13.3 mg, 8.055 x 10^{-5} mol) were added to a round-bottomed flask with 10 mL of DMF and left stirring for

10 minutes; this solution was then added to the swollen beads *via* syringe and the mixture left to react for 24 hours at ambient temperature.

The modified polymer product was filtered on a 0.2 μm nylon filter and washed with successive 50 mL volumes of *t*-amyl alcohol, glacial acetic acid (×2), *t*-amyl alcohol, DCM (×3) and diethyl ether. The cream coloured, powdered product was then dried *in vacuo* at 40 °C overnight (0.204 g, 94 %).

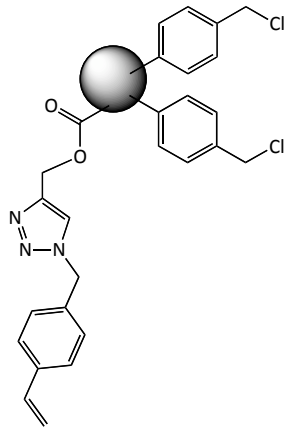

Elemental microanalysis: Expected 75.4 % C, 6.5 % H, 2.0 % N, 14.9 % Cl; Found 75.7 % C, 6.5 % H, 1.2 % N, 12.4 % Cl.

FT-IR: $\bar{\nu}/cm^{-1}$ *(KBr), 3296 (alkyne C-H stretch), 3021, 2923, 2852, 1727 (ester C=O stretch), 1605, 1511, 1444, 1266 (CH wag of* CH_2*-Cl), 991 and 909 (*$R_2C=CH_2$*), 827 (para-subst. aromatic ring), 677 (C-Cl stretch).*

Click chemistry modifications of poly(DVB-*co*-VBC-*co*-PMA) with α-azido-*L*-phenylalanine were carried out in an analogous fashion, with a direct substitution of VBAz (**22**) for α-azido-*L*-phenylalanine (**34**) in the synthetic protocol. Feed and yield data are presented in Table 4.2.11.1.

Polymer ref.	*PPAlk-1 (g)*	*Azido-Phe (mg)*	*2,6-lutidine (μL)*	*CuBr (mg)*	*Yield (g)*	*Yield (%)*
PPAlk-CC2	0.203	23.4	9.32	5.8	0.197	87

Table 4.2.11.1. – Feed and yield data for the azide-protected *L*-phenylalanine click chemistry modification of Poly(DVB-*co*-VBC-*co*-PMA).

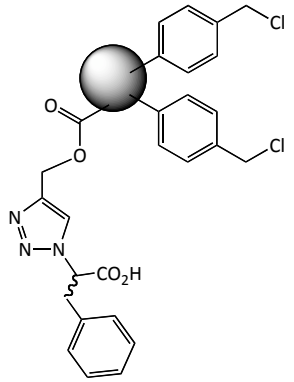

Results for PPAlk-CC2:

Elemental microanalysis: Expected 74.5 % C, 6.4 % H, 2.0 % N, 14.7 % Cl; Found 76.8 % C, 6.3 % H, 0.8 % N, 12.8 % Cl.

FT-IR: $\bar{\nu}/cm^{-1}$ (KBr), 3296 (alkyne C-H stretch), 3022, 2923, 2852, 2107 (alkyne C-C stretch) 1730 (ester C=O stretch), 1605, 1511, 1444, 1266 (CH wag of CH_2-Cl), 991 and 908 ($R_2C=CH_2$), 828 (para-subst. aromatic ring), 677 (C-Cl stretch).

4.2.12. Hypercrosslinking Reaction of Poly(DVB-co-VBC-co-PMA) (HXL-PPAlk)

Poly(DVB-*co*-VBC-*co*-PMA) microspheres, PPAlk-1, (1.011 g, 4.586 mmol of VBC residues) were charged to a dry, three-necked round-bottomed flask equipped with a reflux condenser and an overhead mechanical stirrer. Anhydrous DCE (30 mL) was added and the beads were left to swell fully under N_2 at room temperature for 1 hour. $FeCl_3$ (0.756 g, 4.586 mmol, in a 1:1 mole ratio with respect to the CH_2Cl content of the particles) in DCE (50 mL) was added and the

mixture was heated at 80 °C for 18 hours. The product particles were recovered from the reaction medium by vacuum filtration on a 0.2 μm nylon filter and washed with successive 50 mL volumes of methanol, aqueous HNO_3 (pH 1) (2 washes), methanol and acetone. The orange-coloured particles were then extracted with acetone overnight in a Soxhlet apparatus and then washed with methanol and diethyl ether before drying *in vacuo* overnight at 40 °C (0.641 g, 63 %).

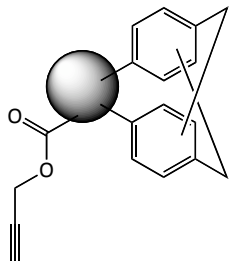

Elemental microanalysis: Expected 90.6 % C, 7.3 % H, 0.6 % N, 0 % Cl; Found 84.8 % C, 6.8 % H, 0.9 % N, 5.2 % Cl.

FT-IR: $\bar{\nu}/cm^{-1}$ (KBr), 3021, 2928, 2107 (alkyne C-C stretch), 1726 (ester C=O stretch), 1608, 1511, 1450, 1266 (CH wag of CH_2-Cl), 890, 817 (para-subst. aromatic ring), 677 (C-Cl stretch).

Langmuir specific surface area: 1,440 m^2/g.

4.2.13. Typical Synthesis of Poly(DVB-co-VBC) by PP (PP11)

VBC (**7**) (6.925 mL, 7.500 g, 0.058 mmol), DVB-80 (**2**) (2.735 mL, 2.500 g, 0.018 mol) and AIBN (0.266 g, 1.674 mmol, 2 mol % relative to polymerisable double bonds) were charged to a 1 L Nalgene® bottle with 500 mL of acetonitrile. The bottle was placed into an ultrasonic bath for 10 minutes and was then purged with N_2, whilst on an ice bath, for 10 minutes, before being sealed under N_2. The bottle was placed onto a low profile roller, which was housed in a temperature-controlled incubator. The temperature was ramped from room temperature to 60 °C over a period of around 2 hours and then held at 60 °C for a further

46 hours. After 46 hours, a representative sample of product was examined under an optical microscope to discern the presence of microspheres. The product was filtered by vacuum on a 0.2 μm nylon filter membrane and washed with successive 50 mL volumes of acetonitrile, toluene, methanol and acetone. The product, in the form of a white powder, was oven-dried overnight at 40 °C *in vacuo* (2.648 g, 26 %).

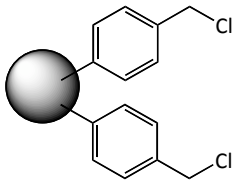

Elemental microanalysis: Expected 76.0 % C, 6.5 % H, 0.5 % N, 17.0 % Cl; Found 77.7 % C, 6.5 % H, 0.4 % N, 11.1 % Cl.
FT-IR: $\bar{\nu}$*/cm^{-1} (KBr), 3021, 2922, 2852, 1605, 1511, 1444, 1265 (CH wag of CH_2-Cl), 990 and 908 ($R_2C=CH_2$), 832 (para-subst. aromatic ring), 677 (C-Cl stretch).*
Specific surface area: <5 m^2/g.

4.2.14. Hypercrosslinking Reaction of Poly(DVB-co-VBC) (HXL-PP11)

Precursor particles, PP11, (2.024 g, 9.828 mmol of VBC residues) were charged to a dry, three-necked round-bottomed flask equipped with a reflux condenser and an overhead mechanical stirrer. Anhydrous DCE (30 mL) was added and the beads were left to swell fully under N_2 at room temperature for 1 hour. $FeCl_3$ (1.587 g, 9.828 mmol, 1:1 mole ratio with respect to the CH_2Cl content of the particles) in DCE (100 mL) was added and the mixture heated at 80 °C for 18 hours. The product particles were recovered from the reaction medium by vacuum filtration on a 0.2 μm nylon filter and washed with successive 50 mL volumes of methanol, aqueous HNO_3 (pH 1) (2 washes), methanol and acetone. The orange-coloured particles were then extracted with acetone overnight in a Soxhlet apparatus and then washed with methanol and diethyl ether before drying *in vacuo* overnight at 40 °C (1.723 g, 85 %).

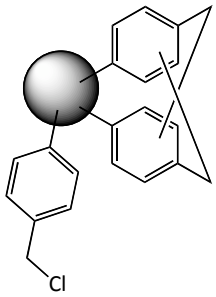

Elemental microanalysis: Expected 92.1 % C, 7.32 % H, 0.6 % N, 0 % Cl; Found 82.7 % C, 6.3 % H, 0.9 % N, 5.0 % Cl.

FT-IR: $\bar{\nu}$*/cm*$^{-1}$ *(KBr), 3022, 2929, 2857, 1607, 1511, 1449, 1265 (CH wag of* CH_2*-Cl), 889, 820 (para-subst. aromatic ring), 680 (C-Cl stretch).*

Langmuir specific surface area: 1,810 m^2/g.

4.2.15. Azidation of Hypercrosslinked Poly(DVB-co-VBC) Residual Chlorine (HXL-PP11-Az1)

Hypercrosslinked polymer microspheres, HXL-PP11, (0.497 g, *ca.* 0.070 mmol Cl) were charged to a round-bottomed flask, 50 mL of anhydrous DMF added to wet the microspheres and the mixture then left for 1 hour. Sodium azide (0.138 g, 0.210 mmol) and sodium iodide (0.011 g, 0.007 mmol) were dissolved in 7 mL of DMF and 1 mL of water and added to the hypercrosslinked microspheres *via* syringe. The reaction mixture was left for 24 hours at 50 ^{o}C under an N_2 atmosphere. The polymer product was filtered by vacuum on a 0.2 μm nylon filter and washed with successive 50 mL volumes of *t*-amyl alcohol, glacial acetic acid (×2), *t*-amyl alcohol, DCM (×3) and diethyl ether. The orange-coloured powdered product was then dried *in vacuo* at 40 ^{o}C overnight (0.477 g, 96 %).

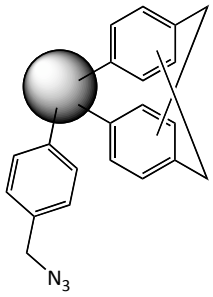

Elemental microanalysis: Expected 87.0 % C, 6.9 % H, 6.1 % N, 0 % Cl; Found 84.0 % C, 6.4 % H, 2.0 % N, 1.4 % Cl.

FT-IR: $\bar{\nu}$*/cm^{-1} (KBr), 3022, 2929, 2100 (N_3 stretch), 1606, 1511, 1449, 889, 820 (para-subst. aromatic ring).*

Langmuir specific surface area: 1,645 m^2/g.

4.2.16. Click Chemistry Modification of Azide-Containing Hypercrosslinked Microspheres (HXL-PP11-Az-CC1)

Azide-containing hypercrosslinked polymer microspheres, HXL-PP11-Az (0.202 g, *ca*. 0.282 mmol of azide residues) were charged to a dry, three-necked, round-bottomed flask equipped with a reflux condenser and an overhead mechanical stirrer. Peptide synthesis grade DMF (30 mL) was added to wet the beads and the mixture then left under N_2 at room temperature for 1 hour. 2,6-Lutidine (32.6 μL, 0.282 mmol), copper bromide (9.7 mg, 0.056 mmol) and propargyl alcohol (0.033 mL, 0.016 g, 0.282 mmol) in 10 mL of DMF was added to the beads *via* syringe and the mixture left to react for 24 hours at ambient temperature.

The polymer product was vacuum filtered on a 0.2 μm nylon filter and washed with successive 50 mL volumes of *t*-amyl alcohol, glacial acetic acid (×2), *t*-amyl alcohol, DCM (×3) and diethyl ether. The cream coloured powdered product was then dried *in vacuo* at 40 ^{o}C overnight (0.187 g, 86 %).

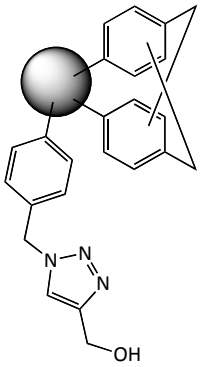

Elemental microanalysis: Expected 85.3 % C, 6.9 % H, 5.6 % N, 0 % Cl; Found 82.0 % C, 6.3 % H, 2.0 % N, 2.7 % Cl.

FT-IR: $\bar{\nu}/cm^{-1}$ *(KBr), 3020, 2926, 2863, 2093 (N_3 stretch), 1606, 1511, 1449, 892, 817 (para-subst. aromatic ring).*

A click chemistry modification of azide-containing hypercrosslinked poly(DVB-*co*-VBC) microspheres with Fmoc-glycine propargyl ester was carried out in an analogous fashion, with a direct substitution of propargyl alcohol for Fmoc-glycine propargyl ester in the synthetic protocol. Feed and yield data are presented in Table 4.2.16.1.

Polymer ref.	***HXL-PP11-Az (g)***	***Fmoc-Gly propargyl ester (mg)***	***2,6-lutidine (μL)***	***CuBr (mg)***	***Yield (g)***	***Yield (%)***
HXL-PP11-Az-CC2	0.201	0.095	32.6	0.012	0.205	69

Table 4.2.16.1. – Feed and yield data for the Fmoc-glycine propargyl ester click modification of azide-containing hypercrosslinked microspheres.

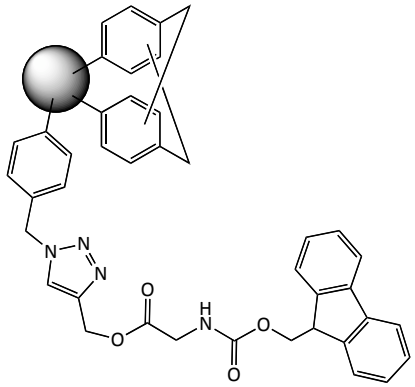

Results for HXL-PP11-Az-CC2:

Elemental microanalysis: Expected 82.1 % C, 6.3 % H, 5.5 % N, 0 % Cl; Found 81.9 % C, 6.2 % H, 2.2 % N, 2.5 % Cl.

FT-IR: $\bar{\nu}/cm^{-1}$ *(KBr), 3020, 2926, 2857, 2093 (N_3 stretch), 1725 (ester C=O stretch), 1606, 1511, 1450, 889, 818 (para-subst. aromatic ring).*

A click chemistry modification of azide-containing hypercrosslinked poly(DVB-*co*-VBC) microspheres with propargyl amine (**35**) was carried out in an analogous fashion, with a direct substitution of propargyl alcohol for propargyl amine in the synthetic protocol. Feed and yield data are presented in Table 4.2.16.2.

Polymer ref.	***HXL-PP11-Az (g)***	***Propargyl amine (µL)***	***2,6-lutidine (µL)***	***CuBr (mg)***	***Yield (g)***	***Yield (%)***
HXL-PP11-Az-CC3	0.203	36.0	32.6	0.018	0.211	96

Table 4.2.16.2. – Feed and yield data for the propargyl amine click modification of azide-containing hypercrosslinked microspheres.

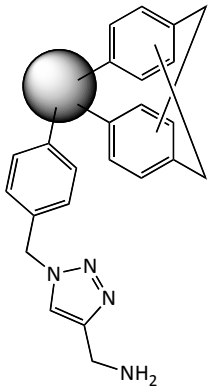

Results for HXL-PP11-Az-CC3:

Elemental microanalysis: Expected 84.8 % C, 6.8 % H, 8.3 % N, 0 % Cl; Found 78.0 % C, 6.2 % H, 3.5 % N, 2.6 % Cl.

FT-IR: $\bar{\nu}/cm^{-1}$ *(KBr), 3020, 2926, 2857, 2093 (N_3 stretch), 1606, 1511, 1450, 889, 818 (para-subst. aromatic ring).*

A click chemistry modification of azide-containing hypercrosslinked poly(DVB-*co*-VBC) microspheres with 4-pentynoic acid (**36**) was carried out in an analogous fashion, with a direct substitution of propargyl alcohol for 4-pentynoic acid in the synthetic protocol. Feed and yield data are presented in Table 4.2.16.3.

Polymer ref.	***HXL-PP11-Az (g)***	***4-pentynoic acid (mg)***	***2,6-lutidine (μL)***	***CuBr (mg)***	***Yield (g)***	***Yield (%)***
HXL-PP11-Az-CC4	0.199	0.041	32.6	0.017	0.199	88

Table 4.2.16.3. – Feed and yield data for the pentynoic acid click modification of azide-containing hypercrosslinked microspheres.

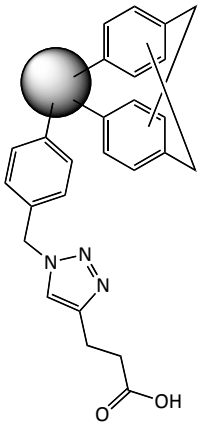

Results for HXL-PP11-Az-CC4:

Elemental microanalysis: Expected 82.3 % C, 6.6 % H, 6.2 % N, 0 % Cl; Found 74.1 % C, 5.8 % H, 2.0 % N, 1.8 % Cl.

FT-IR: $\bar{\nu}$*/cm*$^{-1}$ *(KBr), 3020, 2926, 2857, 2093 (*N_3 *stretch), 1710 (acid C=O stretch), 1606, 1511, 1450, 889, 818 (para-subst. aromatic ring).*

4.2.17. Synthesis by Precipitation Polymerisation of Poly(DVB-co-VBAz) (PPAz-75)

DVB-80 (**2**) (2.735 mL, 2.500 g, 0.018 mol), VBAz (**22**) (7.452 g, 0.047 mmol) and AIBN (0.266 g, 1.670 mmol, 2 mol % relative to polymerisable double bonds) were charged to a 1 L Nalgene® bottle with 500 mL of acetonitrile. The bottle was placed into an ultrasonic bath for 10 minutes, then purged with N_2, whilst on an ice bath, for 10 minutes, before being sealed under N_2. The bottle was placed onto a low profile roller, which was housed in a temperature-controlled incubator. The temperature was ramped from room temperature to 60 °C over a period of around 2 hours and then held at 60 °C for a further 46 hours. After 46 hours, a representative sample of product was examined under an optical microscope to discern the presence of microspheres. The product was filtered by vacuum on a 0.2 μm nylon filter membrane and washed with successive 50 mL volumes of acetonitrile, toluene, methanol and acetone. The product, in the form of a white powder, was oven-dried overnight at 40 °C *in vacuo* (1.773 g, 18 %).

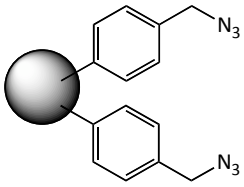

Elemental microanalysis: Expected 73.8 % C, 6.3 % H, 19.8 % N; Found 77.8 % C, 6.4 % H, 13.7 % N.

FT-IR: $\bar{\nu}$*/cm^{-1} (KBr), 3022, 2925, 2852, 2098 (N_3 stretch), 1606, 1511, 1447, 991 and 905 ($R_2C=CH_2$), 818 (para-subst. aromatic ring).*

Specific surface area: <5 m^2/g.

4.2.18. Click Chemistry Hypercrosslinking of Poly(DVB-co-VBAz) (PPAz-75-CCHXL-1)

PPAz-75 (0.200 g, 0.942 mmol of VBAz residues) was charged to a dry, three-necked round-bottomed flask equipped with a reflux condenser and an overhead mechanical stirrer. Peptide synthesis grade DMF (30 mL) was added and the beads were left to swell fully under N_2 at room temperature for 1 hour. 2,6-Lutidine (0.109 mL, 0.942 mmol), copper bromide (27.3 mg, 0.189 mmol) and 1,3-diethynyl benzene (**37**) (0.063 mL, 0.059 g, 0.471 mmol) in a 20 mL solution of DMF was added to the swollen beads *via* syringe and the mixture was left to react for 24 hours at 80 ^{o}C. The polymer product was vacuum filtered on a 0.2 μm nylon filter and washed with successive 50 mL volumes of *t*-amyl alcohol, glacial acetic acid (×2), *t*-amyl alcohol, DCM (×3) and diethyl ether. The cream coloured, powdered product was then dried *in vacuo* at 40 ^{o}C overnight (0.234 g, 78 %).

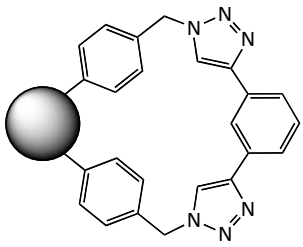

Elemental microanalysis: Expected 81.0 % C, 5.8 % H, 13.2 % N; Found 73.1 % C, 5.8 % H, 9.5 % N.

FT-IR: $\bar{\nu}/cm^{-1}$ *(KBr), 3021, 2925, 2857, 2225 (alkyne C-C stretch), 2097 (*N_3 *stretch), 1606, 1512, 1449, 791 (1,3-subst. aromatic ring).*

Langmuir specific surface area: 30 m^2/g.

All click chemistry hypercrosslinking reactions were carried out in an analogous fashion. Feed and yield data are presented in Table 4.2.18.1.

Polymer ref.	***Solvent***	***PPAz-75 (g)***	***Dialkyne (mL)***	***2,6-lutidine (mL)***	***CuBr (mg)***	***Yield (g)***	***Yield (%)***
CCHXL-PPAz-75-1	DMF	0.200	0.063	0.109	27.3	0.234	78
CCHXL-PPAz-75-2	DCE	0.204	0.063	0.109	33.7	0.251	82

Table 4.2.18.1 – Feed and yield data for click hypercrosslinking reaction of Poly(DVB-*co*-VBA) with 1,3-diethynyl benzene.

4.2.19. Poly(DVB-co-VBAz) Solvent Uptake Tests

Poly(DVB-*co*-VBAz) microspheres (0.025 g) were charged to a centrifugal filter (small filter cartridge which can then be inserted into a centrifuge tube) and the filter weighed. 0.30 mL of solvent was added and the solvent and polymer were left to equilibrate for 3 hours. The sample was placed into a centrifuge at 3,000 rpm for 3 minutes. The insert was then re-weighed.

An analogous procedure was used for all solvents (Table 4.2.19.1).

Solvent	*Mass of polymer (g)*	*Mass of solvent uptaken (g)*	*g/g solvent sorbed*	*mL/g solvent sorbed*
THF	0.026	0.038	1.49	1.68
DCE	0.025	0.041	1.65	1.32
DMF	0.025	0.029	1.17	1.23
Acetonitrile	0.014	0.020	1.41	1.80

Table 4.2.19.1 – Solvent uptake data for 25/75 (w/w) DVB/VBAz copolymer (click hypercrosslinking precursor).

4.3. RESULTS AND DISCUSSION

4.3.1. Synthesis of Azide-Containing 'Clickable' Polymer Microspheres

In order for a polymer to be modified by click chemistry, it must contain a functional group compatible with the chosen click chemistry reaction. For the 1,3-dipolar cycloaddition click reaction, the polymer must bear either an alkyne or azide functionality on which the click reaction can be performed. Azide functional groups can be incorporated into the polymer by means of copolymerisation of a functionalised monomer, or can be introduced subsequent to polymerisation in a post-polymerisation chemical modification reaction. Incorporation of functional monomers into a polymerisation can allow more control over the level of functionality present in the polymeric product. In some cases, it can also be easier to prepare functional monomers from existing monomeric compounds in solution rather than carrying out a polymer analogous reaction on the monomer residue when it is incorporated into a polymer.

An azide-containing, vinyl monomer (vinylbenzyl azide, VBAz (**22**)) was synthesised by reaction of vinylbenzyl chloride (**7**) (VBC) with sodium azide, whereby the azide displaces the chlorine of the VBC (**7**) in a nucleophilic

substitution reaction (Figure 4.3.1.1). The reaction conditions avoid the need for high temperatures which can lead to premature polymerisation of the monomer.

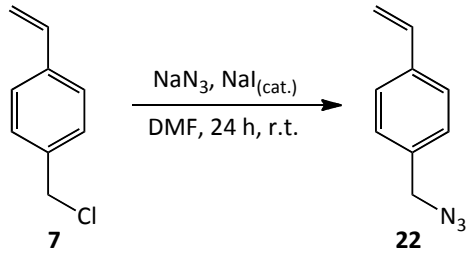

Figure 4.3.1.1. – Conversion of VBC into VBAz.

In order to synthesise a clickable polymer containing an azide group, the VBAz monomer was incorporated into a precipitation polymerisation, with divinylbenzene (**2**) (DVB) and vinylbenzyl chloride (**7**) (VBC) as comonomers (Figure 4.3.1.2). Once formed, this polymer can potentially be functionalised through click chemistry by reaction with molecules bearing a terminal alkyne moiety.

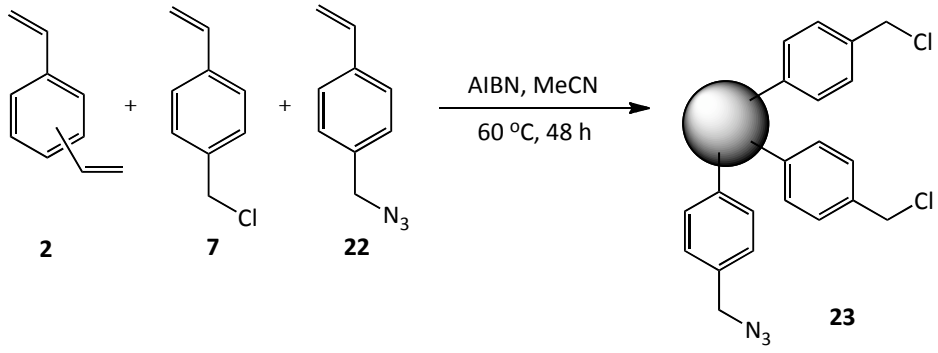

Figure 4.3.1.2. – Synthesis of poly(DVB-*co*-VBC-*co*-VBAz) microspheres using precipitation polymerisation conditions.

The monomers were fed into the polymerisation in the ratio 25/70/5 (w/w/w) DVB(**2**)/VBC(**7**)/VBAz(**22**), with a low DVB (**2**) content and high percentage of

VBC (**7**) being used to set the polymeric product up for subsequent hypercrosslinking.

The yield of polymeric product was low (25 %), however elemental microanalysis was used to ensure that all monomers had been incorporated into the polymeric product. Table 4.3.1.1 shows the expected elemental microanalysis results for a DVB(**2**)/VBC(**7**) copolymer (no VBAz (**22**) present), for a copolymer including all three monomers in a 25/70/5 ratio, as well as the observed results.

Sample	***Observed Microanalysis (%)***			
	C	***H***	***N***	***Cl***
Expected for 25/70/5 (w/w/w) DVB/VBC/VBAz	75.8	6.5	1.8	15.9
Observed (PPAz-1)	**77.4**	**6.4**	**1.3**	**14.1**
Expected for 25/75 (w/w) DVB/VBC only	76.1	6.5	0.5	17.1

Table 4.3.1.1. – Expected and observed elemental microanalysis results for poly(DVB-*co*-VBC-*co*-VBAz), PPAz-1.

From the elemental microanalysis results it can be seen that the observed results are not in perfect agreement with the expected result for a 25/70/5 (w/w/w) copolymer of DVB(**2**)/VBC(**7**)/VBAz(**22**), however they are in reasonably good agreement for a polymer. When compared to the expected result for a 25/75 (w/w) DVB(**2**)/VBC(**7**) copolymer with no VBAz (**22**) included, it is clear from the higher nitrogen content observed for copolymer PPAz-1 that the VBAz (**22**) has indeed been incorporated into the polymer. The nitrogen content of 1.3 % is slightly lower than expected, but not by a significant amount.

FT-IR spectroscopy was also used to ensure incorporation of all monomers in the polymer product. Regions of interest in the FT-IR spectrum include the bands at ~1265 and ~677 cm^{-1}, ascribed to the chloromethyl group in VBC (**7**)

residues (CH_2 wag of CH_2-Cl and C-Cl stretch, respectively), the band at ~2096 cm^{-1} assigned to the azide stretch of VBAz (**22**) residues, and the bands at ~990 and ~901 cm^{-1} corresponding to unreacted pendent double bonds from DVB (**2**). Figure 4.3.1.3 shows the FT-IR spectra obtained for PPAz-1.

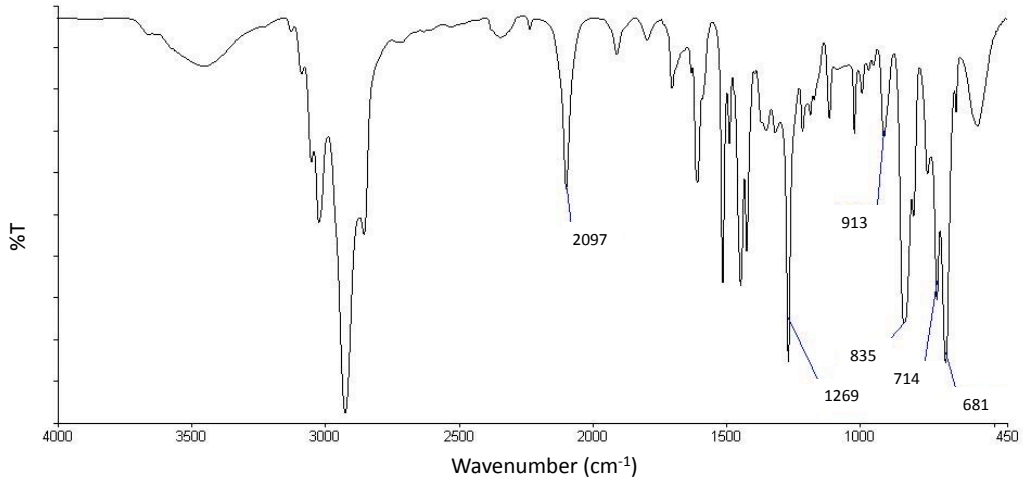

Figure 4.3.1.3. – FT-IR spectrum of PPAz-1.

SEM was also used to assess the particle size, particle size distribution and particle shape. Ideally, precipitation polymerisation products are expected to be microspheres with average particle diameters in the 0.1-10 μm range, and preferably with narrow particle size distributions, thus the particle size, shape and size distribution are important features. Figure 4.3.1.4 shows the SEM images obtained for PPAz-1.

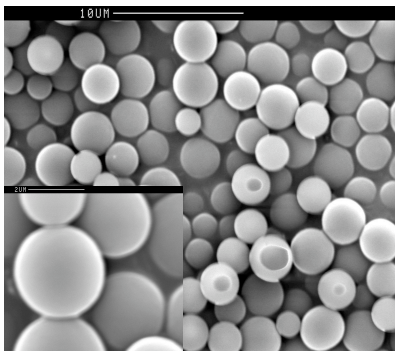

Figure 4.3.1.4. – SEM micrographs for PPAz-1.

The SEM micrographs show that the microspheres produced were spherical in shape and had smooth surfaces. The particles were not monodisperse, however most of the particles had diameters in the region of 2-4 μm, giving the sample a relatively narrow size distribution.

Analogous data was observed for all further 25/70/5 (w/w/w) DVB/VBC/VBAz particles synthesised in this manner.

4.3.2. Hypercrosslinking of Poly(DVB-co-VBC-co-VBAz)

In order to introduce ultra-high specific surface area into the azide-containing polymer, the VBC residues present were subjected to a hypercrosslinking reaction. Hypercrosslinking should, in theory, allow different solvent systems to be used for the click reaction due to the amphipathic nature of HXL polymers.

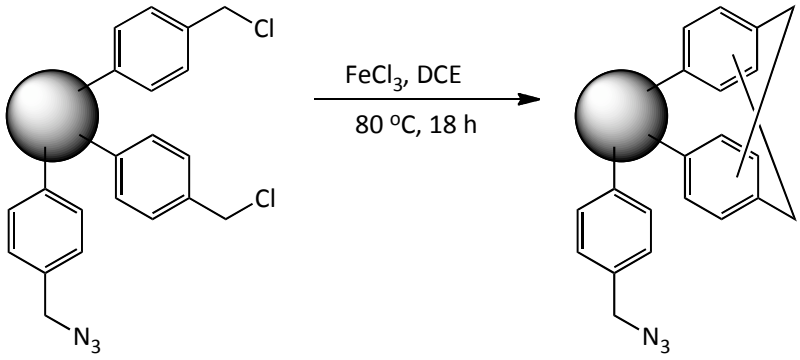

Figure 4.3.2.1. – Hypercrosslinking of the azide-containing polymer, PPAz-1.

Analysis of the hypercrosslinked polymer formed was carried out using elemental microanalysis and FT-IR spectroscopy, with nitrogen sorption porosimetry (using the Langmuir isotherm) being used for specific surface area measurements. The elemental microanalysis and nitrogen sorption data are detailed in Table 4.3.2.1.

Polymer ref.	*Elemental microanalysis (%)*				*Langmuir specific surface area (m^2/g)*
	C	*H*	*N*	*Cl*	
PPAz-1	77.4	6.4	1.3	14.1	< 5
HXL-PPAz-1	84.6	6.8	0.9	3.5	1,295

Table 4.3.2.1. – Elemental microanalysis and Langmuir specific surface area data for the azide-containing polymer before and after hypercrosslinking.

From the elemental microanalysis results it can be seen that upon reaction with $FeCl_3$ the chlorine content of the microspheres has dropped significantly, indicating that the hypercrosslinking reaction has been successful. The nitrogen content has also been reduced from 1.3 to 0.9 %, however an increase in nitrogen content to 2.1 % would have been expected upon hypercrosslinking due to the loss of chlorine from the polymer. This suggests that the azide group may be somewhat labile under the hypercrosslinking conditions. A more detailed study would be required to gain insight into this possibility.

The Langmuir surface area data shows that despite the effects that the hypercrosslinking reaction may have on the azide functionality, the hypercrosslinking reaction has indeed resulted in the introduction of ultra-high specific surface area into the polymer, as intended, with the specific surface area soaring from less than 5 m^2/g to 1,295 m^2/g.

FT-IR spectroscopy was also used to confirm whether the hypercrosslinking reaction had been successful (Figure 4.3.2.2). For successful hypercrosslinking reactions, the bands ascribed to the chloromethyl moiety in VBC (1265 and 677 cm^{-1}) should be reduced considerably in intensity.

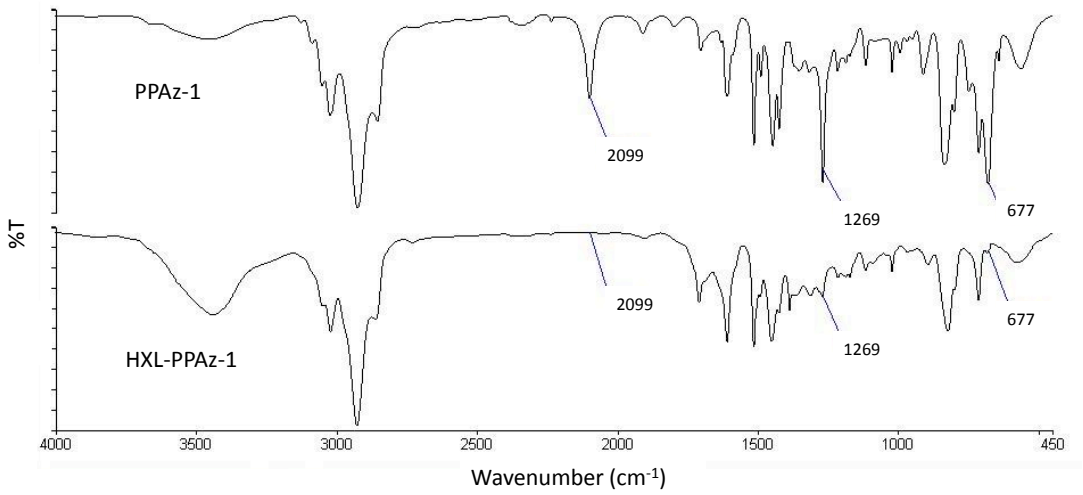

Figure 4.3.2.2. – FT-IR spectra of the azide-containing polymer PPAz-1 and its hypercrosslinked derivative.

From the FT-IR spectra it is clear that the hypercrosslinking reaction has resulted in a significant loss of chloromethyl groups, as expected. However, it also appears that the hypercrosslinking reaction has had a detrimental effect on the azide moieties within the polymer, as the azide band (2096 cm^{-1}) has disappeared completely. This supports the earlier elemental microanalysis results.

Since the hypercrosslinking reaction apparently destroys the azide functionality, no chemical modification of the polymer *via* click chemistry is possible after the hypercrosslinking step, thus all hypercrosslinking should be carried out subsequent to click functionalisation.

4.3.3. Click Chemistry Modification of Azide-Containing Polymer Microspheres

Previously in the group, model click reactions of the azide monomer, VBAz (**22**), and alkyne-containing compounds were shown to be successful in solution.[66] The observations made were that the reactions could proceed in DCE where copper(I) bromide was used directly as catalyst, however where a copper(II)

sulfate/sodium ascorbate catalyst system was employed, DCE was not a suitable solvent. Both catalysts gave promising results where DMF was used as the solvent. As DCE is the solvent of choice for reactions involving swellable polymer microspheres, the copper(I) bromide catalyst was selected. Although the reactions were shown to proceed well for the free azide monomer, the reactivity of the azide group may be different when it is chemically bound to a porous, insoluble polymeric bead, as indicated by the work of Mark[66] (Section 4.1.6.2), where a reaction temperature of 80 ^{o}C was required in order for the reaction of a polymer bound azide to proceed using copper(II) sulfate in DMF, despite the analogous free azide reacting at room temperature.

The solvents employed for the reaction were DCE and DMF. A 1/1 (v/v) mixture of water and ethanol was also considered as a solvent as the click reaction has been shown to occur favourably under such conditions. Water/ethanol was not expected to be compatible with the polymer but was nevertheless included in the solvent study to assess the effect it would have on the click reaction. Propargyl alcohol was studied as the initial alkyne source.

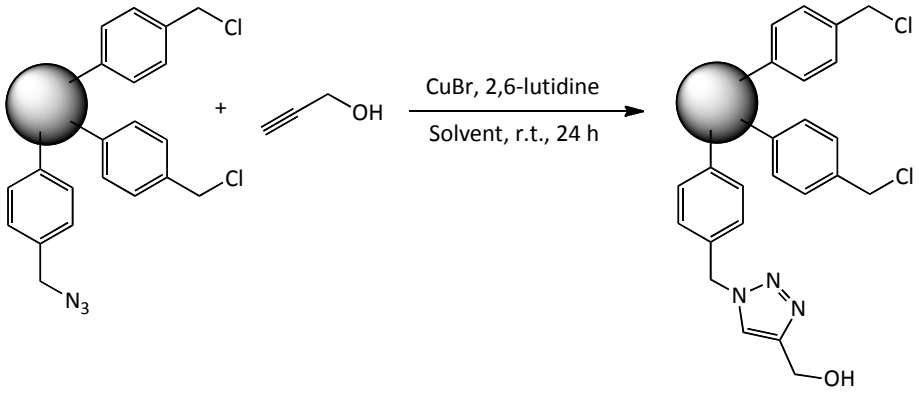

Figure 4.3.3.1. – Click chemistry modification of the azide-containing polymers (PPAz-1, PPAz-2 and PPAz-3) with propargyl alcohol.

As the amount of propargyl alcohol being added to the polymer was very small, and no new elements were being added to the polymer, elemental microanalysis does not, in this instance, offer the same analytical assistance as with the

previous methods of functionalisation (since it is too insensitive). For the purposes of this reaction, a different analytical technique, such as FT-IR, was expected to give more useful data. FT-IR spectroscopy was thus used to monitor the degree to which the click reaction had occurred, with the signal at ~2096 cm^{-1}, corresponding to the azide, being the region of the FT-IR spectrum of most interest.

The FT-IR spectrum obtained for the product of the reaction in DCE showed that the reaction had not occurred to a very great extent as the band corresponding to the azide group, at ~2096 cm^{-1}, did not diminish noticeably in intensity. Since DCE is known to be a good solvent for swelling of the polymer particles, the failure of the reaction is most likely due to solubility issues concerning the propargyl alcohol and/or the copper(I) bromide catalyst in DCE.

The spectrum obtained after reaction of the azide-functionalised polymer with propargyl alcohol in water/methanol indicates, again, a largely unsuccessful reaction. This is most likely as a result of the solvent system being unfavourable for the polymer and thus not allowing the particles to swell and the reagents to penetrate the polymer and reach the azide groups for reaction to occur.

The spectrum obtained for the product of the reaction between propargyl alcohol and the azide-containing polymer in DMF, a solvent which is compatible with both the alcohol and polymer starting materials, is however much more promising than those obtained from reactions in DCE or a mixture of water/methanol. The FT-IR spectrum for the product has an azide band at 2093 cm^{-1} that is much reduced in intensity relative to the same band in the precursor polymer. This suggests that the azide group has been converted into the corresponding triazole ring. Although a small azide band still remains in the spectrum, this is most likely due to some of the azide moieties being located in regions of the polymer that are inaccessible to the propargyl alcohol and or the copper(I) catalyst, thus these azide groups are unavailable for reaction.

The next click reaction was carried out in DMF at 80 °C. The purpose of this experiment was to investigate whether or not increasing the reaction temperature would have any beneficial effect on the reaction, as previous work has shown that an increase in temperature is favourable for the reaction (Section 4.1.6.2). The FT-IR spectra for the products arising from reactions in DMF at different temperatures, and for the precursor polymer, are shown in Figure 4.3.3.3.

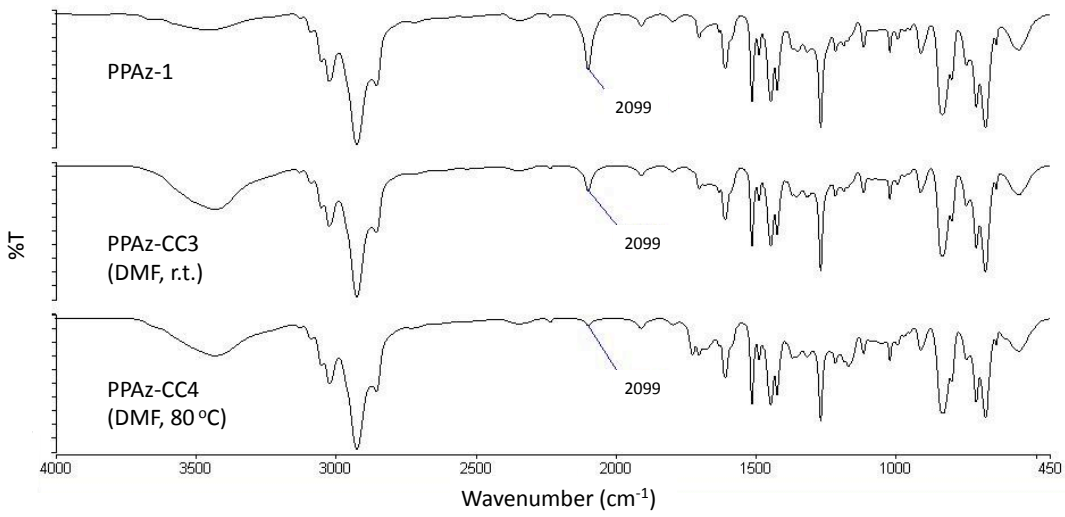

Figure 4.3.3.3. – FT-IR spectra for an azide-containing polymer, PPAz-1, and the products of click reactions of PPAz-1 and propargyl alcohol carried out in DMF at different temperatures.

The FT-IR spectra show that upon reaction in DMF at higher temperature the azide band is reduced further still in intensity. This suggests that the increase in temperature allows the reaction to occur to a greater extent.

As increased temperature had such a profound effect on the reaction, the reactions in DCE and water/methanol (1/1, v/v) were also carried out at elevated temperature.

The FT-IR spectra showed that increasing the temperature of the reaction in DCE resulted in a decrease in the intensity of the azide band. This would

suggest that the click reaction between the azide-containing polymer and the propargyl alcohol was successful. This is a significant result, as the reaction did not occur in DCE at room temperature, thus the increased temperature seems to provide the driving force required for the reaction to proceed. An alternative interpretation of this result is that as a result of the higher temperature there is thermal degradation of the azide group, however further work would be required before a definitive conclusion about this can be drawn.

The FT-IR spectrum from the product of the reaction carried out in water/ethanol at 80 ^{o}C showed a slight decrease in intensity of the azide band, however this was to a lesser extent than the reactions carried out in DMF and DCE at 80 ^{o}C, thus suggesting that the reductions in intensity of the azide band observed under the other solvent conditions tested are not solely induced by the reaction temperature *i.e.*, thermal stability of the azide under these solvent conditions is not an issue. That the reaction has been less successful than those performed in the other solvents is, again, most likely as a result of the incompatibility of the polymer with the water, thus penetration of the polymer by reagents is hindered. Despite this incompatibility, however, the reaction has still occurred at such a level as to lead to a slight change in intensity of the azide band. This could involve the azide moieties close to the surfaces of the microspheres being able to react, with introduction of the propargyl alcohol potentially reducing the hydrophobicity of the microspheres at their surfaces and thus allowing the water to penetrate the polymer layer by layer as the reaction proceeds.

Overall, it has been shown that the click modification of an azide-containing polymer with propargyl alcohol can be carried out most effectively in DMF using a copper(I) bromide catalyst, for reaction at room temperature. Increased reaction temperature has also been shown to exert an effect on the reaction, in particular for DCE and DMF as reaction solvents.

SEM was used to reveal how the click reaction influenced the size and shape of the microspheres, if at all. Figure 4.3.3.4 shows the SEM micrographs obtained for the azide-containing polymer and the corresponding product obtained after click reaction with propargyl alcohol in DMF at 80 ^{o}C.

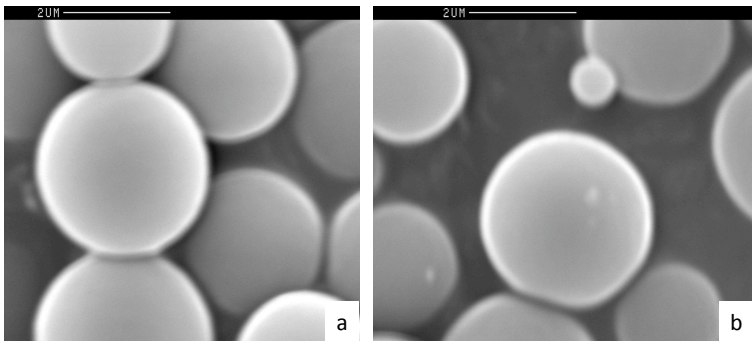

Figure 4.3.3.4. – SEM micrographs obtained for: (a) the azide-containing polymer PPAz-1, and (b) the product of its click reaction with propargyl alcohol, PPAz-CC4.

From the SEM micrographs obtained it is clear that the click reaction has not changed the shape, size or surface morphology of the particles. The particles are smooth and spherical and most have diameters in the range 2-3 μm.

After the propargyl alcohol had been clicked successfully onto the azide-containing polymers, a second alkyne-containing compound, Fmoc-glycine propargyl ester (**38**), was synthesised to be clicked onto the polymers. Addition of an amino acid to the polymers helps to demonstrate the diversity of the click reaction for functionalisation of the microspheres, thus opening up a wide range of properties and hence potential applications. The Fmoc-glycine propargyl ester (**38**) was synthesised by reaction of Fmoc-glycine (**30**) with propargyl alcohol (**24**) under Stieglich esterification reaction conditions[67] (Figure 4.3.3.5) as shown by Castelhano *et al.*[68] Click modification of the azide-containing polymer (**25**) with the Fmoc-glycine propargyl ester (**38**) was carried out in DMF at 80 ^{o}C for 24 hours, the same reaction conditions that proved to be the most successful for the click reactions involving propargyl alcohol (**24**).

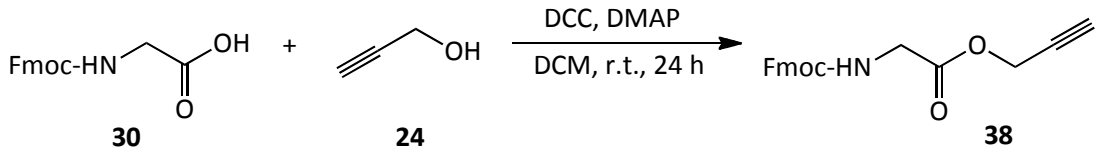

Figure 4.3.3.5. – Synthesis of Fmoc-glycine propargyl ester.

The FT-IR spectrum of the clicked product obtained after reaction in DMF at 80 ^{o}C for 24 hours showed a decrease in the intensity of the azide band (~2096 cm^{-1}) relative to the precursor, suggesting that the reaction had occurred, albeit to a lesser extent than with propargyl alcohol (Figure 4.3.3.6). Further evidence for successful reaction was provided by the appearance of a new signal at ~1723 cm^{-1}, which can be assigned to an ester carbonyl group (*i.e.*, from Fmoc-glycine propargyl ester). While only a small percentage of the azide groups appear to have reacted, the conditions could be optimised. Increased reaction times and increased reaction temperatures were thus investigated and the outcome of these reactions assessed by FT-IR spectroscopy.

Since the reaction of the Fmoc-glycine propargyl ester (**38**) was shown to occur to only a small extent in DMF at 80 ^{O}C over a reaction period of 24 hours, the reaction time was increased to 48 hours to investigate whether this would result in an increase in conversion, which would most likely manifest itself as a further reduction in intensity of the azide band in the FT-IR spectrum of the product relative to the spectrum of the reaction product isolated from the reaction carried out over 24 hours. The azide band does not appear to be any less intense after 48 hours than it is after 24 hours, suggesting that after 24 hours the reaction is essentially complete. This would suggest that the reaction is not being limited by slow diffusion of the amino acid into the polymer. It is perhaps more likely that the amino acid cannot penetrate further into the polymer, perhaps due to its size. That the azide band has not been

reduced further in intensity after an additional 24 hours at 80 °C, indicates that the reaction temperature is not adversely affecting the azide moieties through thermolysis.

Since an increase in reaction temperature from room temperature to 80 °C gave an improved reaction outcome, a further increase in reaction temperature to 120 °C was next investigated to see if this would enhance further the reaction between the Fmoc-glycine propargyl ester and the azide group. Again, these reactions were followed by FT-IR spectroscopy (Figure 4.3.3.6).

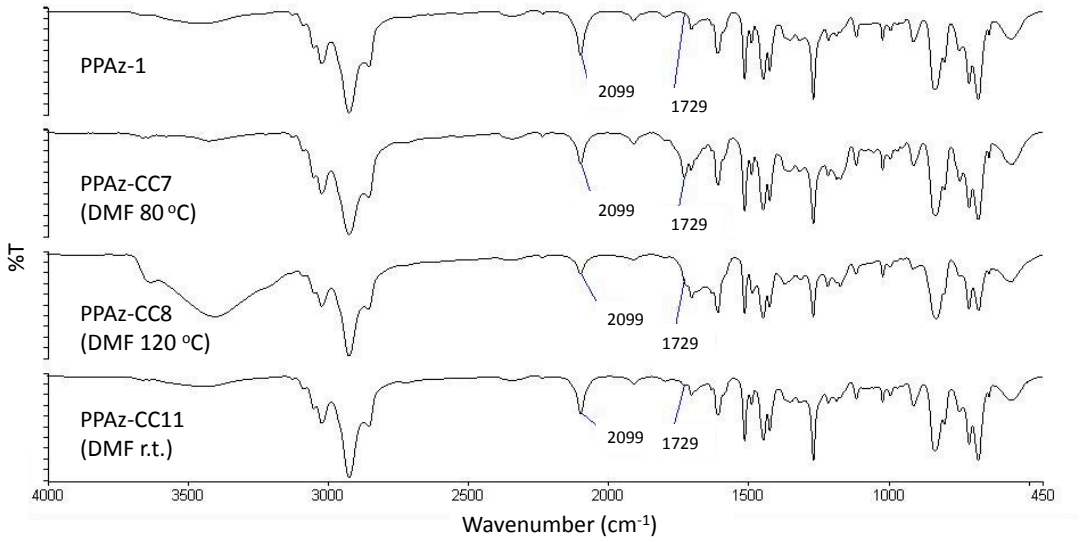

Figure 4.3.3.6. – FT-IR spectra obtained for the products collected after reaction of PPAz-1 with Fmoc-glycine propargyl ester in DMF for 24 hours at different temperatures.

The FT-IR spectra show that the yet higher reaction temperature (120 °C) has indeed resulted in a further decrease in the intensity of the azide peak, however the carbonyl peak introduced is not as intense as that introduced through reaction at 80 °C. After reaction at 120 °C, only a small shoulder of a second peak is present at 1720 cm^{-1}, while the carbonyl peaks introduced at lower temperatures are much more prominent. This would suggest that the higher temperature results in a slight loss of the azide functionality through thermolysis, and thus the reaction at 120 °C is less efficient than the reaction at

80 ^{0}C. The FT-IR spectra also show that the higher temperature has resulted in a reduction in intensity of the bands assigned to chloromethyl groups *i.e.*, those at 1265 and 675 cm^{-1}. This loss of pendent chlorine functionality means that any hypercrosslinking carried out after the click reaction is likely to become less efficient.

Finally, a reaction of the azide-containing polymer with Fmoc-glycine propargyl ester (**38**) was carried out at room temperature in order to show that an increased reaction temperature was indeed required for successful reaction. The FT-IR spectrum of the product showed that after 24 hours at room temperature the azide band had been reduced only slightly in intensity, and a small signal, corresponding to an ester carbonyl, was beginning to appear at 1725 cm^{-1}. This supports the belief that an increase in reaction temperature is essential for click modification of the polymer microspheres, despite high conversions being achieved at room temperature when the substrates are in solution. This reaction also serves to support the earlier observation that the higher reaction temperature does not adversely affect the azide group to a significant extent. When the reaction is carried out at a higher temperature then the azide peak is further diminished in intensity, however this is accompanied by a simultaneous increase in the ester carbonyl peak intensity indicating that the reduction in intensity of the azide band is caused by reaction with Fmoc-glycine propargyl ester (**38**) rather than by a thermal degradation of the azide group.

SEM was used to ensure that reaction with Fmoc-glycine propargyl ester (**38**) using click chemistry was not having any detrimental affect on the particle surface morphology, shape or size. Figure 4.3.3.7 shows the SEM micrographs obtained for both the precursor and the product of the click reaction performed at 80 ^{o}C for 24 hours. Again, it is clear that the click reaction does not have any obvious detrimental effects on the microspheres.

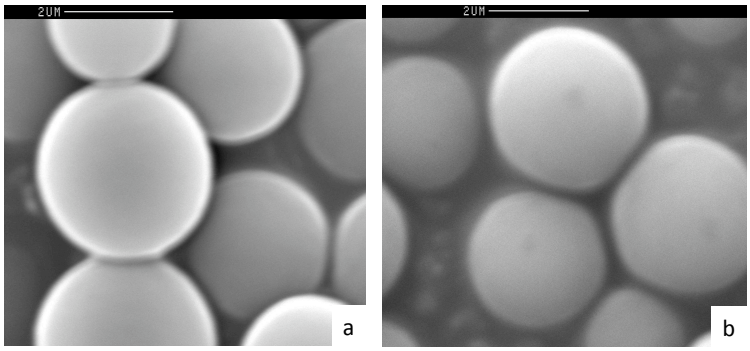

Figure 4.3.3.7. – SEM micrographs obtained for: (a) the azide-containing polymer PPAz-1, and (b) the product of its click reaction with propargyl alcohol, PPAz-CC7.

4.3.4. Hypercrosslinking of Click Chemistry Modified Polymer Microspheres

When polymers are hypercrosslinked subsequent to click chemistry functionalisation reactions, the azide functionality has been converted already to triazole rings and thus can no longer be lost during hypercrosslinking. Two swellable polymers, one functionalised with propargyl alcohol (PPAz-CC4) and one functionalised with Fmoc-glycine propargyl ester (PPAz-CC7) were hypercrosslinked and characterised to ascertain whether the presence of the different functional groups affected the hypercrosslinking reaction.

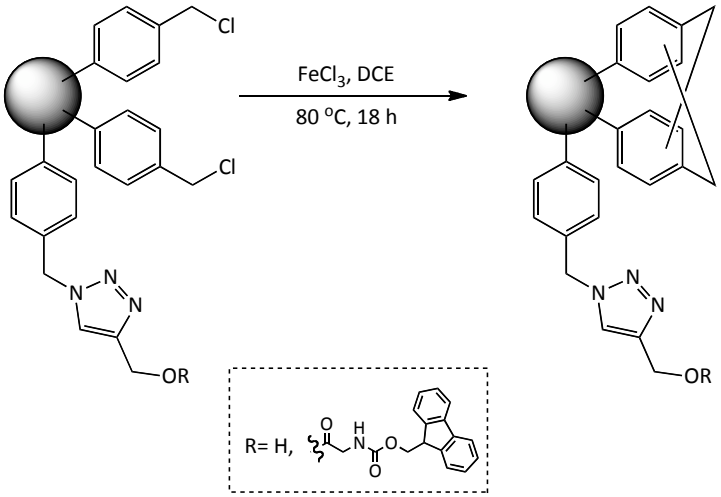

Figure 4.3.4.1. – Hypercrosslinking of the polymer microspheres modified using click chemistry.

Elemental microanalysis, nitrogen sorption porosimetry and FT-IR spectroscopy were used to characterise the hypercrosslinked products. The elemental microanalysis and Langmuir specific surface areas for each sample are detailed in Table 4.3.4.1.

Polymer ref.	***Elemental microanalysis (%)***				***Langmuir specific surface area (m^2/g)***
	C	***H***	***N***	***Cl***	
HXL-PPAz-CC4	81.5	6.9	1.6	2.1	860
HXL-PPAz-CC7	83.7	6.9	1.3	2.9	1,120

Table 4.3.4.1. – Elemental microanalysis and Langmuir specific surface area data for the pre-functionalised hypercrosslinked polymers.

The elemental microanalysis data (Table 4.3.4.1) shows that subsequent to the hypercrosslinking reaction, both the propargyl alcohol and Fmoc-glycine propargyl ester functionalised polymers showed a considerable decrease in the level of chlorine present relative to their precursors (13.1 and 13.8 % Cl for PPAz-CC4 and PPAz-CC7, respectively). This is as expected from hypercrosslinking reactions. The nitrogen content was expected to have increased slightly due to mass loss, however this has remained fairly constant which would suggest again that the azide groups remaining following the click reaction have been lost under the hypercrosslinking reaction conditions. The Langmuir specific surface areas show that the hypercrosslinking reaction leads to ultra-high specific surface area, functionalised materials.

FT-IR spectra were obtained for both of the hypercrosslinked polymers. For both of the hypercrosslinked products, it could be seen that the chloromethyl group-derived signals in the spectra (1265 and 672 cm^{-1}) had been substantially diminished in intensity, as expected. Additionally, the small azide band that remained after the click reaction was completely lost. For the hypercrosslinked material modified with propargyl alcohol, there were no obvious signals arising from the propargyl alcohol moieties or the triazole rings, thus it was not

possible to tell how these residues fared under the hypercrosslinking conditions. In the case of the material functionalised with the propargyl ester of Fmoc-glycine, the signal attributed to the ester carbonyl in the non-hypercrosslinked precursor polymer seemed to have been diminished slightly in intensity, however this is in accordance with previous observations when a methacrylic acid-containing polymer was hypercrosslinked resulting in a reduction in intensity of the carbonyl band ascribed to the methacrylic acid group.[69] Materials prepared in this way were subsequently applied as weak cation-exchangers by utilising the carboxylic acid moieties in the polymer, confirming that the hypercrosslinking reaction did not destroy the carboxylic acid groups.[70]

SEM was used to demonstrate that the hypercrosslinking reaction did not alter the surface morphology of the particles that had been modified by click reactions prior to hypercrosslinking. The SEM micrographs for the hypercrosslinked polymers are shown in Figure 4.3.4.2.

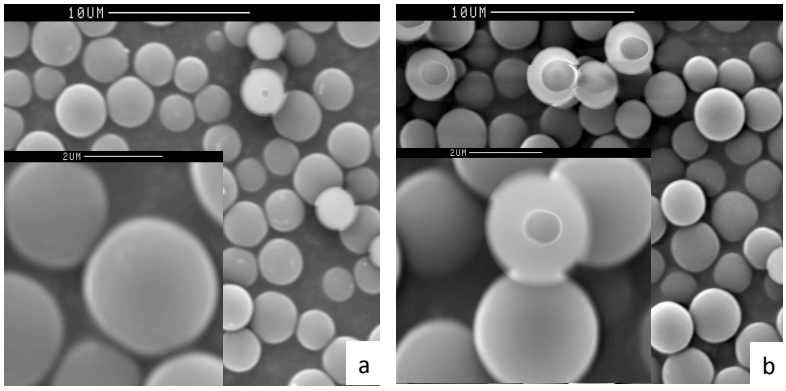

Figure 4.3.4.2. – SEM micrographs obtained for hypercrosslinked functionalised polymers: (a) HXL-PPAz-CC4 (b) HXL-PPAz-CC7.

From the SEM micrographs it can be seen that the hypercrosslinking chemistry has not obviously changed the particles in terms of their size and shape. The particles are still spherical and smooth, while the size of the majority of the particles remains unchanged.

4.3.5. Synthesis of Alkyne-Containing 'Clickable' Polymer Microspheres

After the click chemistry modification of the azide-containing polymers was shown to be successful, the concept of click chemistry modification of polymers was then carried forward to the click chemistry modification of alkyne-containing polymers, *i.e.*, clicking an azide-containing molecule onto an alkyne-containing polymer. An alkyne-containing polymer was thus required, and so an alkyne-containing monomer was synthesised. A methacrylate monomer containing a propargyl group (propargyl methacrylate, PMA (**27**)) was prepared using a method reported by Haddleton *et al.*[71] The synthesis involves a simple reaction between an acid chloride and an alcohol to furnish an ester (Figure 4.3.5.1).

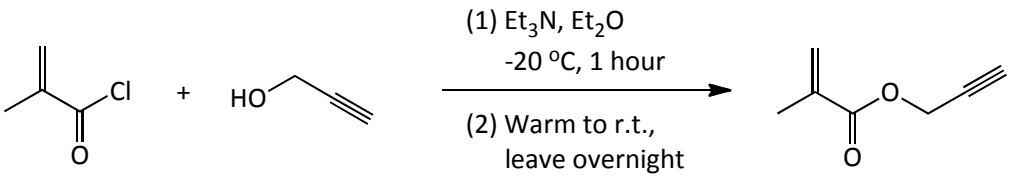

Figure 4.3.5.1. – Reaction of methacryloyl chloride with propargyl alcohol to give the methacrylate ester propargyl methacrylate (PMA).

The PMA monomer (**27**) was then incorporated into a precipitation polymerisation at a level of 5 wt% relative to the other monomers, with 25 wt% DVB (**2**) crosslinker used to give stable particles and 70 wt% VBC (**7**) for the subsequent hypercrosslinking reaction (Figure 4.3.5.2).

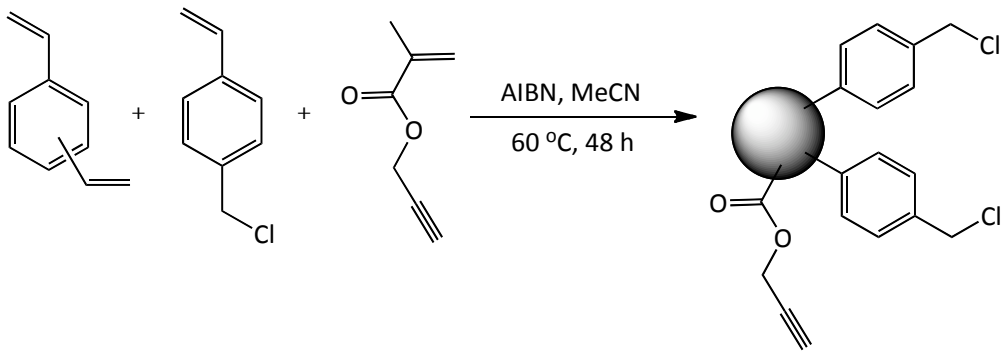

Figure 4.3.5.2. – Synthesis of 25/70/5 (w/w/w) DVB/VBC/PMA polymer microspheres under precipitation polymerisation conditions.

The yield of product was unexpectedly low (11 %), however elemental microanalysis was used gather evidence that all three monomers had been incorporated into the final product. Table 4.3.5.1 shows the expected elemental microanalysis results for a copolymer containing DVB and VBC only, as well as for a copolymer including all three monomers in the ratio 25/70/5, for comparison with the observed result.

Sample	***Observed Microanalysis (%)***			
	C	***H***	***N***	***Cl***
Expected for 25/70/5 (w/w/w) DVB/VBC/PMA	75.8	6.5	0.5	15.8
Observed (PPAlk-1)	**78.5**	**7.0**	**0.4**	**15.4**
Expected for 25/75 (w/w) DVB/VBC only	76.1	6.5	0.5	17.1

Table 4.3.5.1. – Expected and observed microanalysis results for poly(DVB-*co*-VBC-*co*-PMA), PPAlk-1.

From the elemental microanalysis results it can be seen that the main difference between a copolymer that has the PMA (**27**) incorporated and one that does not, is the chlorine content. The copolymer isolated contained a lower level of chlorine than would be expected had the PMA (**27**) not been incorporated. Analysis of the oxygen content would be a better way to confirm inclusion of the

PMA (**27**) monomer, however this analysis could not be carried out with the equipment available.

FT-IR spectroscopy was also used to ensure incorporation of all three monomers in the polymer product. Regions of interest in the FT-IR spectrum included the bands at ~1265 and ~677 cm^{-1}, ascribed to the chloromethyl group from VBC residues, the band at ~1731 cm^{-1} corresponding to the ester carbonyl of the methacrylate monomer PMA, the bands at ~3295 cm^{-1} and ~2121 cm^{-1} (very weak signal) which indicate the presence of an alkyne in the polymer and, finally, the bands at ~990 and ~901 cm^{-1} corresponding to unreacted pendent double bonds from DVB. Figure 4.3.5.3 shows the FT-IR spectrum obtained for the poly(DVB-*co*-VBC-*co*-PMA) product.

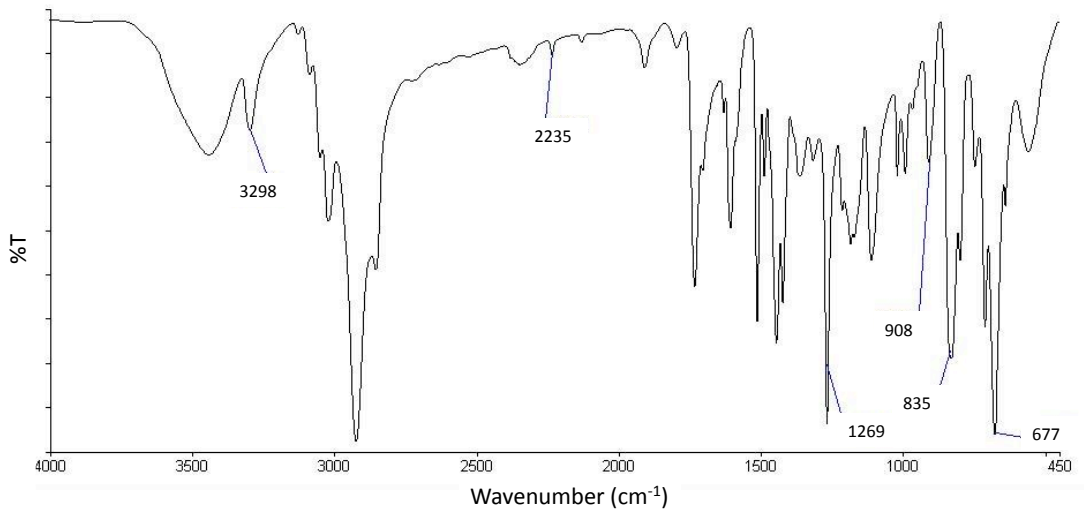

Figure 4.3.5.3. – FT-IR spectrum for copolymer PPAlk-1 prepared using 25/70/5 (w/w/w) DVB/VBC/PMA in the feed.

SEM (Figure 4.3.5.4) was also used to assess the particle quality of the product, with spherical, monodisperse particles being desirable.

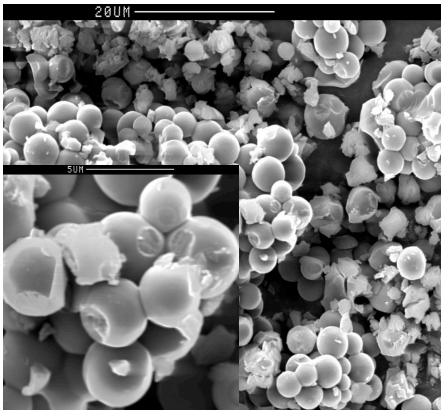

Figure 4.3.5.4. – SEM images of poly(DVB-*co*-VBC-*co*-PMA) (PPAlk-1).

From the SEM micrographs obtained it can clearly be seen that the product contained spherical particles that have aggregated and which contain many surface defects. This is not ideal in terms of the desired particle quality for some potential applications, with the azide-containing microspheres described previously showing much better particle quality. Nevertheless, the alkyne-containing polymer can still be subjected to the click chemistry modification reactions, with improvements in particle quality potentially being investigated further at a later date.

4.3.6. Hypercrosslinking of Poly(DVB-co-VBC-co-PMA) Microspheres (PPAlk-2)

As was the case for the azide-containing polymers, ultra-high specific surface areas can be introduced into alkyne-containing polymers through exploitation of the pendent chloromethyl moieties present arising from the inclusion of VBC in the polymer microsphere synthesis. An analogous copolymer prepared from a feed containing 25/70/5 (w/w/w) DVB/VBC/PMA, PPAlk-2, was hypercrosslinked to determine whether or not the pendent alkyne-moieties would be stable under the hypercrosslinking conditions (the second copolymer was synthesised since there was not enough of the first copolymer left for the hypercrosslinking reaction).

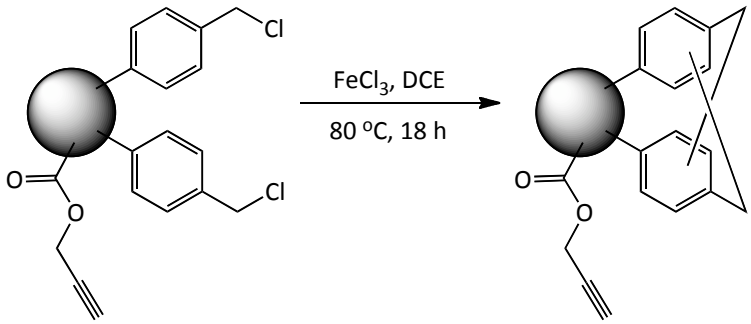

Figure 4.3.6.1. – Hypercrosslinking of the alkyne-containing polymer microspheres PPAlk-2 prior to functionalisation.

The hypercrosslinked polymer was analysed by elemental microanalysis, and nitrogen sorption porosimetry was used to measure the specific surface areas of the polymers (Table 4.3.6.1.).

Polymer ref.	***Elemental microanalysis (%)***				***Langmuir specific surface area (m^2/g)***
	C	***H***	***N***	***Cl***	
PPAlk-2	77.0	6.6	0.4	14.7	< 5
HXL-PPAlk-2	84.8	6.8	0.9	5.2	1,440

Table 4.3.6.1. – Elemental microanalytical and nitrogen sorption porosimetry data for the alkyne-containing polymer PPAlk-2 and its hypercrosslinked derivative HXL-PPAlk-2.

From the elemental microanalysis data it can be seen that after hypercrosslinking the chlorine content of the microspheres was reduced significantly, indicating that the hypercrosslinking reaction had been successful. The nitrogen sorption porosimetry data confirmed this through an increase in the specific surface area from a negligible value (< 5 m^2/g) to 1,440 m^2/g, thus hypercrosslinking of the alkyne-containing polymer leads to the intended ultra-high specific surface area product. The stability of the alkyne-containing residue cannot be determined from this data.

FT-IR spectroscopy was then used to demonstrate that the reaction had been successful, through the disappearance of the chloromethyl derived signals (1265 and 675 cm^{-1}) as the methylene bridges are formed. From the FT-IR spectra it was clear that the hypercrosslinking reaction had been successful through the disappearance of the chloromethyl derived signals. However, the alkyne signal at 2231 cm^{-1} also appeared to have been reduced slightly in intensity, while the alkyne signal at 3291 cm^{-1} could no longer be observed. This may be a consequence of the hygroscopic nature of the hypercrosslinked polymer resulting in water being absorbed (hence the increased intensity and broadening of the –OH peak at ~3400 cm^{-1}) thus masking the alkyne band, however it may be a result of cleavage of the alkyne-containing group. It was also noted that the signal at 1726 cm^{-1}, which can be attributed to the ester carbonyl group from the propargyl methacrylate, is no longer present as a sharp peak, but instead appears reduced in intensity and it has merged with the adjacent signal. As mentioned previously for the hypercrosslinking of the azide-containing polymer clicked with Fmoc-glycine propargyl ester, this is most likely not caused by degradation of the carbonyl group. As the fate of the alkyne-containing group is unclear, the preferred route of synthesis of functionalised hypercrosslinked materials will be *via* a 'click prior to hypercrosslinking' method, as was discussed previously for the azide-containing polymers.

4.3.7. Click Chemistry Modification of Alkyne-Containing Polymer Microspheres

Since polymers containing the azide monomer VBAz (**22**) were modified successfully with alkyne-containing compounds using click chemistry, as outlined earlier, analogous reaction conditions can be used for modification of the alkyne-containing polymers with azide compounds. 2,6-Lutidine, included previously to prevent alkyne-alkyne coupling reactions from taking place, will most likely be an unnecessary additive to these reactions as the alkyne groups present on the polymer are unlikely to couple due to the fact that they are likely

to be site-isolated on the polymers, however 2,6-lutidine was used nevertheless to keep the reaction conditions constant and thus comparable to the analogous reactions of the azide-containing polymers.

As the VBAz monomer (**22**) was readily available it was used for the initial modification reactions (Figure 4.3.7.1).

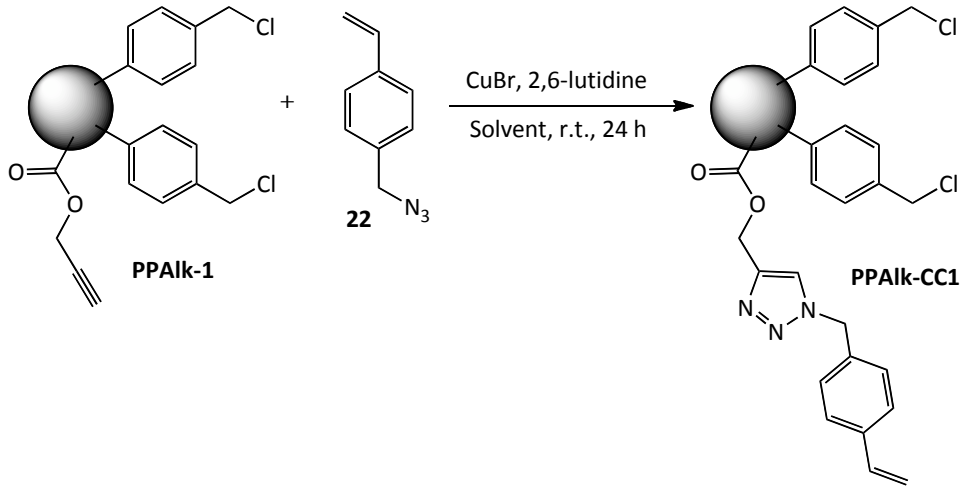

Figure 4.3.7.1. – Click chemistry modification of alkyne-containing polymer microspheres PPAlk-1 with the azide VBAz.

In this instance, elemental microanalysis was much more useful than before in monitoring the click reaction, with an increase in nitrogen content on formation of the triazole ring being the most obvious indicator of a successful reaction (Table 4.3.7.1).

Polymer	***Observed Microanalysis (%)***			
ref.	***C***	***H***	***N***	***Cl***
PPAlk-1	78.5	7.0	0.4	15.4
PPAlk-CC1	75.7	6.5	1.2	12.4

Table 4.3.7.1. – Elemental microanalysis results for the alkyne-containing polymer PPAlk-1 and the corresponding click product PPAlk-CC1.

From the elemental microanalysis results it can be seen that upon reaction with an azide-containing compound, the nitrogen content has increased from 0.4 % to 1.2 %, and the chlorine content has decreased. The observed values for carbon and hydrogen are remarkably similar to the expected values (75.4 and 6.5 %, respectively), while the nitrogen and chlorine values are not as close to their expected values (2.0 and 14.9 %, respectively). Although the nitrogen content has not increased to the 2.0 % level, the increase that was observed still serves to confirm that the reaction has taken place to some extent. It is possible that some of the alkyne groups are located in positions that are inaccessible to the catalyst or are unable to adopt an appropriate conformation for reaction to occur.

FT-IR spectroscopy was also used to demonstrate that the click reaction had taken place, with a decrease in intensity of the signals at ~3295 cm^{-1} and ~2121 cm^{-1}, attributed to the alkyne group of the precursor, implying success of the reaction. Figure 4.3.7.2 shows the FT-IR spectra of the alkyne-containing precursor polymer PPAlk-1 and the product obtained from reaction of PPAlk-1 with VBAz (**22**) carried out in DMF at 80 ^{o}C for 24 hours, PPAlk-CC1.

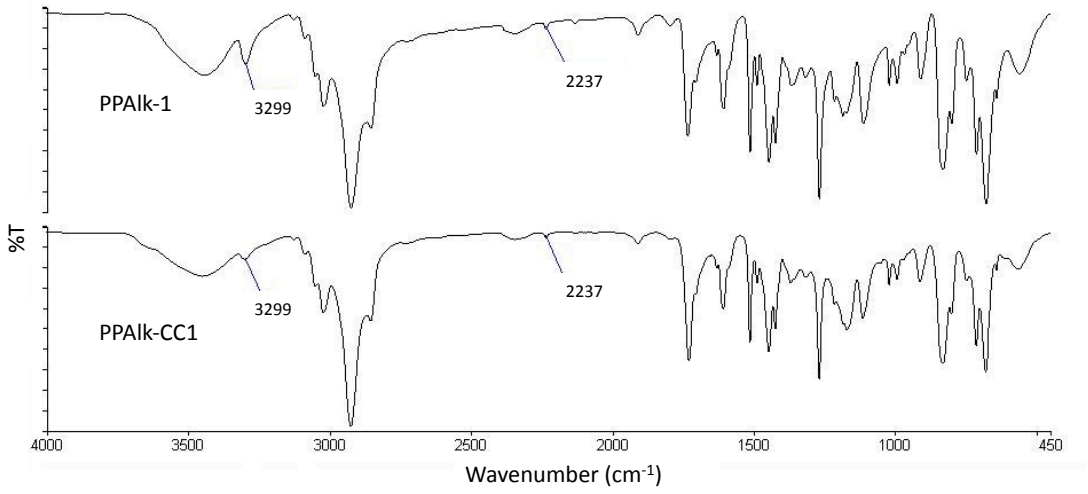

Figure 4.3.7.2. – FT-IR spectra of the alkyne-containing precursor polymer PPAlk-1 and the product obtained from reaction of PPAlk-1 with VBAz in DMF at 80 ^{o}C for 24 hours, PPAlk-CC1.

The FT-IR spectra reveal a decrease in intensity of the alkyne band at 3291 cm^{-1} and a concomitant decrease in the weaker signal at 2126 cm^{-1}, indicating that the reaction has been successful to some extent. The remaining alkyne groups are potentially present in positions that are inaccessible to the azide monomer and/or catalyst, which would thus render them unreactive. As the alkyne signal is partly obscured, however, it would be beneficial to click on a compound containing a functional group not already present, but which also shows strong absorption bands in FT-IR spectra in order to introduce a new signal and facilitate analysis. Another possibility in this regard is to click on a substrate which fluoresces.

SEM was used to determine whether the click reaction affected the particles in terms of their size, shape and surface morphology (Figure 4.3.7.3).

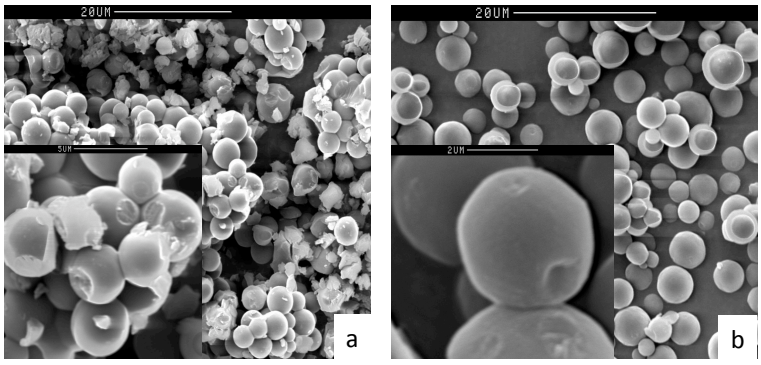

Figure 4.3.7.3. – SEM micrographs obtained for (a) PPAlk-1 and (b) PPAlk-CC1.

From the SEM micrographs shown it can be seen that after the click reaction the particle quality is much improved relative to the precursor. This would suggest that the aggregation observed for the AD123 particles was physical rather than chemical. The surface appearance of the particles also appears to have been improved.

Since an alkyne-containing amino acid (Fmoc-glycine propargyl ester) was clicked onto azide-containing polymers in the manner described previously, a complementary reaction was carried out on the alkyne-containing polymer by clicking on an α-azido amino acid.

In order to synthesise an azide containing amino acid, the free amine of an amino acid can be readily converted to an azide group, to yield an α-azido acid, by reaction of the amino acid with triflyl azide (prepared in turn *via* reaction of NaN_3 and triflyl anhydride) and a copper(II) catalyst, as shown in Figure 4.3.7.4. This method was shown by Lunquist *et al*.[72] to be effective as an alternative protecting group for amino acids, which could then be converted back to the free amine. However this azide group can also be left in place and utilised as a reactive handle in the amino acid, for example in click chemistry reactions.

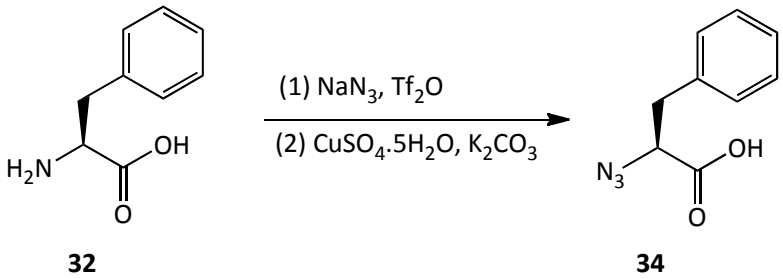

32 **34**

Figure 4.3.7.4. – α-Azido amino acid synthesis (34), with phenylalanine (32) as the amino acid.

The α-azido-*L*-phenylalanine (**34**) synthesised, was clicked onto the alkyne-containing polymer using the same conditions used for click with VBAz (**22**) (Figure 4.3.7.2).

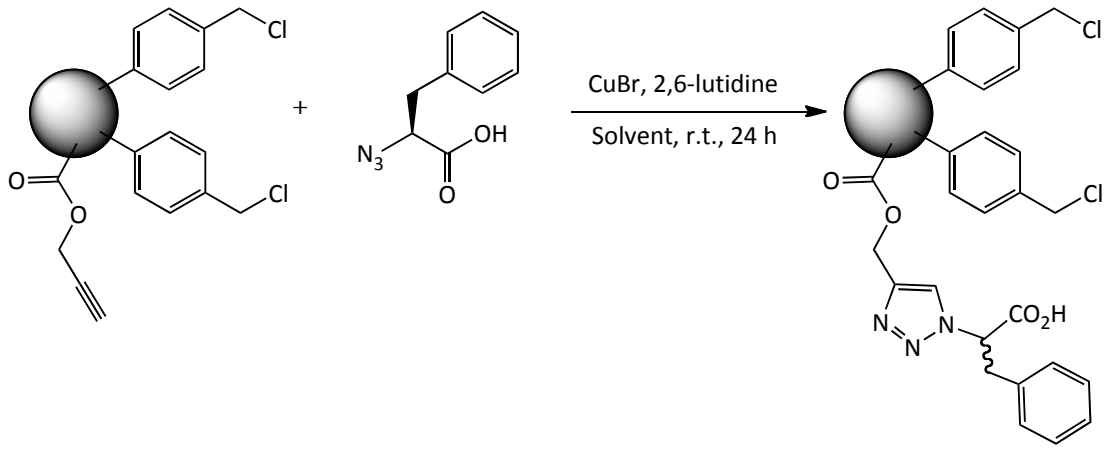

Figure 4.3.7.5. – Reaction of α-azido-*L*-phenylalanine with alkyne-containing polymer microspheres PPAlk-1 *via* click chemistry.

Elemental microanalysis was used to ascertain if reaction has occurred, with an increase in nitrogen content inferring some success (Table 4.3.7.2).

Polymer	***Observed Microanalysis (%)***			
ref.	***C***	***H***	***N***	***Cl***
PPAlk-1	78.5	7.0	0.4	15.4
PPAlk-CC2	76.8	6.3	0.8	12.8

Table 4.3.7.2. – Elemental microanalytical data for the alkyne-containing polymer PPAlk-1 and the corresponding amino acid-modified polymer PPAlk-CC2.

From the elemental microanalysis results it can be seen that upon reaction with α-azido-*L*-phenylalanine (**34**) the nitrogen content of the polymer has doubled. This nitrogen content falls short of the 2.0 % expected for complete reaction, however the observed increase suggests that the reaction has been partially successful.

Due to the weak nature of the alkyne signals in the FT-IR spectrum, as well as the presence of overlapping signals, FT-IR spectroscopy was not particularly useful in this instance. The SEM micrographs obtained, once again showed that the quality of the particles was greatly improved after the click reaction.

4.3.8. Hypercrosslinking of Click Chemistry Modified Polymer Microspheres

The alkyne-containing polymer modified with VBAz (**22**) (PPAlk-CC1) was hypercrosslinked to find out if the hypercrosslinking reaction is possible in cases where the alkyne-containing functionality has been replaced by a functional group containing a triazole ring (Figure 4.3.8.1).

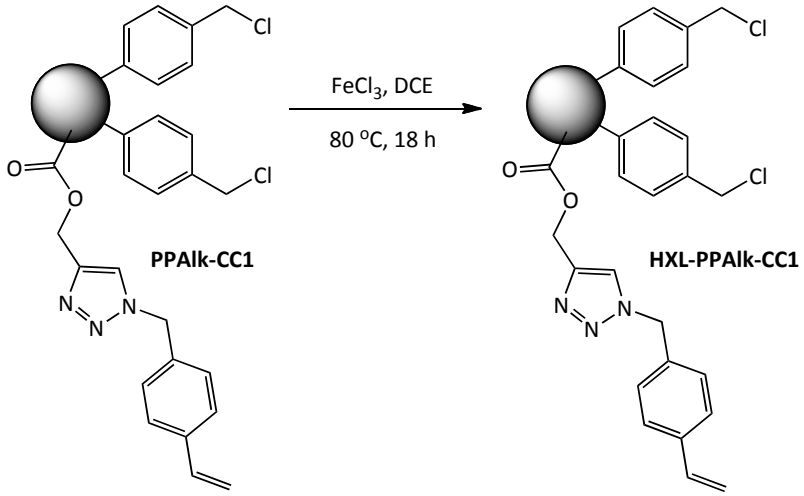

Figure 4.3.8.1. – Hypercrosslinking reaction of the click chemistry modified polymer PPAlk-CC1.

The product of the hypercrosslinking reaction, HXL-PPAlk-CC1, was analysed using elemental microanalysis and nitrogen sorption porosimetry, the results of which are detailed in Table 4.3.8.1.

Polymer ref.	***Elemental microanalysis (%)***				***Langmuir specific surface area (m^2/g)***
	C	***H***	***N***	***Cl***	
PPAlk-CC1	75.7	6.5	1.2	12.4	< 5
HXL-PPAlk-CC1	81.9	6.7	1.4	3.3	1,725

Table 4.3.8.1. – Elemental microanalytical and nitrogen sorption porosimetry data for the VBAz-modified polymer PPAlk-CC1 and its hypercrosslinked derivative HXL-PPAlk-CC1.

From the elemental microanalysis data it can be seen that subsequent to the hypercrosslinking reaction the chlorine content of the polymer microspheres has dropped dramatically as expected. Additionally, the Langmuir specific surface areas obtained show that the hypercrosslinking reaction has resulted in a significant increase in the specific surface area, showing that the presence of the triazole ring does not hinder the hypercrosslinking reaction, and thus clicking on desired functional groups prior to hypercrosslinking still allows the facile preparation of functionalised particles with ultra-high specific surface areas.

FT-IR spectroscopy was used to monitor the hypercrosslinking reaction, with the signals that arise due to the presence of chloromethyl groups (1265 and 675 cm^{-1}) being the signals of particular interest. It was shown that, after reaction under hypercrosslinking conditions, the bands assigned to the chloromethyl groups were reduced in intensity as expected. As was the case for the non-functionalised alkyne-containing polymer, there seems to be a change in the carbonyl region of the FT-IR spectrum (*i.e.*, 1726 cm^{-1}).

SEM was used to assess the particle size, shape and surface morphology after the hypercrosslinking reaction (Figure 4.3.8.2).

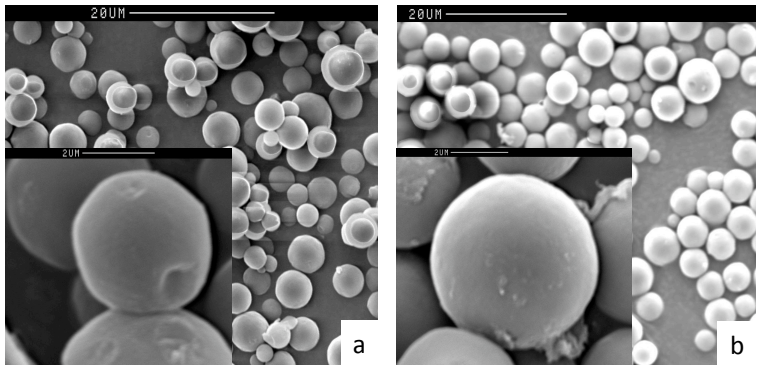

Figure 4.3.8.2. – SEM micrographs obtained for: (a) PPAlk-CC1 and (b) HXL-PPAlk-CC1.

From the SEM micrographs it is clear that the hypercrosslinking reaction has not damaged the particles in any obvious way. The particles appear to have grown slightly in size upon hypercrosslinking from ~ 3-5 μm to ~ 4-6 μm. This is most likely a consequence of the particles being swollen prior to the hypercrosslinking reaction and being hypercrosslinked in this swollen state.

4.3.9. Post-Hypercrosslinking Azidation and Subsequent Click Chemistry Functionalisation

While the incorporation of functional monomers into a polymerisation delivers functional polymers set up immediately for click chemistry, these functional click-ready polymers can also be accessed through post-polymerisation chemical reactions on the hypercrosslinked material. As discussed in Chapter 3, while the hypercrosslinking reaction is extremely successful in generating ultra-high specific surface area particles, there normally remains a small number of chloromethyl groups that do not participate in the hypercrosslinking reaction, and which can thus can be utilised in further reactions. The residual chloromethyl groups in the hypercrosslinked material can be modified with sodium azide to afford pendent benzyl azide groups for click chemistry modification of the polymers. The two main advantages of this synthetic route are that the azide groups are introduced subsequent to the hypercrosslinking chemistry and thus cannot interfere with, or be destroyed by, the hypercrosslinking step, such as they were in the materials prepared using the VBAz monomer. Furthermore, if the azide groups can be formed through reaction of the residual chloromethyl groups, then they must be present in regions of the porous polymer that are accessible and hence they should be readily reactive to click chemistry.

A hypercrosslinked precursor polymer was prepared *via* a precipitation polymerisation reaction of DVB (**2**) and VBC (**7**) (25 and 75 wt%, respectively) followed by hypercrosslinking using $FeCl_3$, as detailed in Chapter 2. This

polymer was then treated with an excess of sodium azide to install pendent azide moieties (Figure 4.3.9.1).

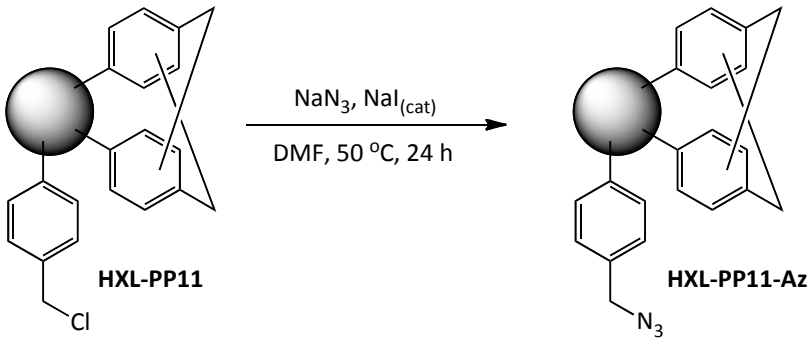

Figure 4.3.9.1. – Synthesis of clickable polymer microspheres with high specific surface area *via* the post-polymerisation modification of a hypercrosslinked polymer (PP11).

Elemental microanalysis was carried out to establish the effectiveness of the chlorine displacement by the azide. Table 4.3.9.1 shows the elemental microanalysis data obtained for the precursor (PP11), the hypercrosslinked material (HXL-PP11) and the azide-modified hypercrosslinked polymer (HXL-PP11-Az).

Polymer ref.	***Elemental microanalysis (%)***				***Langmuir specific surface area (m^2/g)***
	C	***H***	***N***	***Cl***	
PP11	77.7	6.5	1.0	16.9	< 5
HXL-PP11	82.7	6.3	0.9	5.0	1,805
HXL-PP11-Az	84.0	6.4	2.0	1.4	1,645

Table 4.3.9.1. – Elemental microanalysis and specific surface area data for the precursor PP11, corresponding hypercrosslinked polymer HXL-PP11 and the azide-modified hypercrosslinked polymer derived therefrom, HXL-PP11-Az.

From the elemental microanalysis results (Table 4.3.9.1) it can be clearly seen that the hypercrosslinking reaction has resulted in a significant drop in the chlorine content of the microspheres, as expected. Introduction of the azide moieties has been successful, as shown by the simultaneous drop in chlorine

content and increase in nitrogen content of the microspheres. From the nitrogen sorption porosimetry data presented it is clear that the hypercrosslinking reaction has been successful in generating an ultra-high specific surface area polymer. It is also shown that when the remaining chloromethyl groups present in this polymer are treated with sodium azide, to give pendent azide groups, the specific surface area remains extremely high. Therefore, this method does indeed provide a viable route to clickable polymers with ultra-high specific surface areas already in place prior to click chemistry reactions.

FT-IR spectroscopic analysis was then used to ascertain whether or not the azide group had been successfully installed into the hypercrosslinked polymer (Figure 4.3.9.2).

The appearance of a new band at ~2103 cm^{-1} in the FT-IR spectrum confirms the introduction of the azide group. This therefore gives a hypercrosslinked polymer with clickable functionality on which a wide variety of click modification reactions can be performed, resulting in wide-ranging functionalities and thus opening the hypercrosslinked materials up to a whole new world of application.

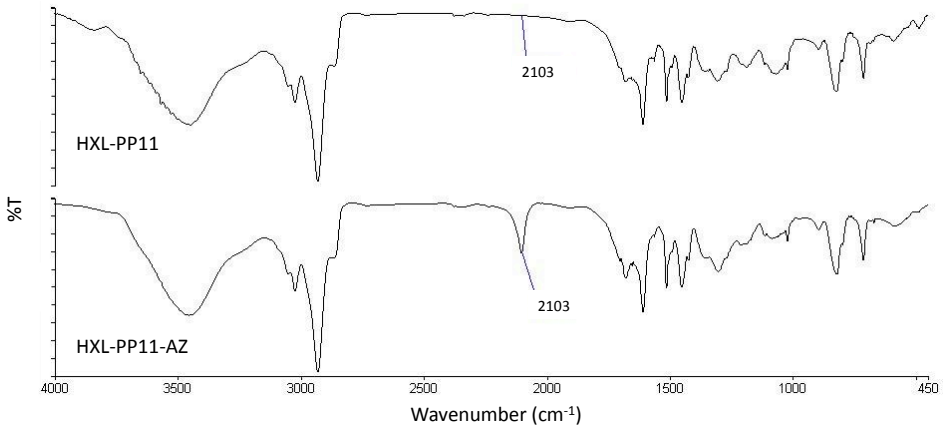

Figure 4.3.9.2. – FT-IR spectra of the hypercrosslinked polymer HXL-PP11 and the corresponding azide-modified hypercrosslinked material HXL-PP11-Az.

SEM was used to gauge whether or not the azidation reaction affected the particles in terms of their size, shape and surface morphology (Figure 4.3.9.3). The resulting images suggest that the hypercrosslinking and azidation reactions do not affect the surface morphology, shape or size of the particles.

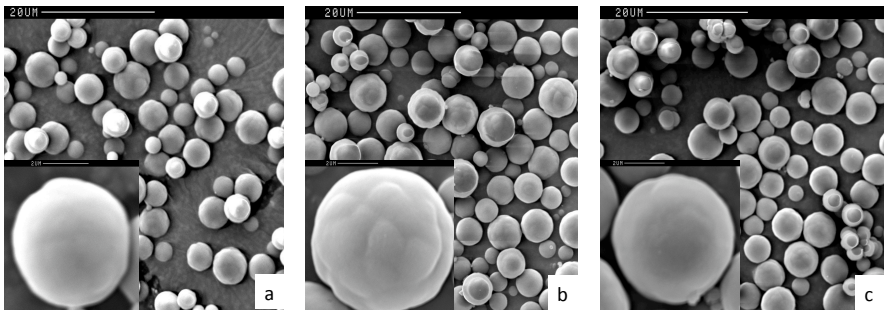

Figure 4.3.9.3 – SEM images obtained for: (a) the precursor PP11, (b) the hypercrosslinked polymer HXL-PP11 and (c) the azide-modified hypercrosslinked polymer HXL-PP11-Az.

The azide-containing hypercrosslinked polymer, HXL-PP11-Az was then modified *via* click chemistry reactions with propargyl alcohol (**24**) and Fmoc-glycine propargyl ester (**38**), as per the azide-containing polymer prepared with VBAz (**22**).

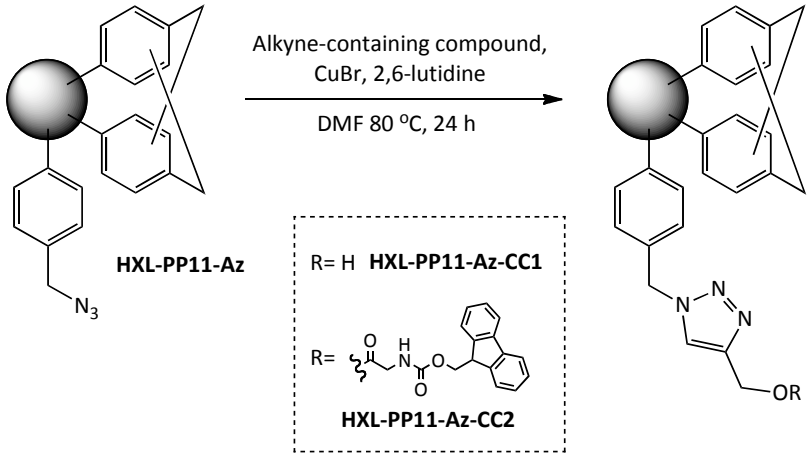

Figure – 4.3.9.4. – Modification of the azide-containing hypercrosslinked polymer HXL-PP11-Az microspheres using propargyl alcohol and Fmoc-glycine propargyl ester to give the products HXL-PP11-Az-CC1 and HXL-PP11-Az-CC2, respectively.

As discussed in Section 4.3.3, in this instance elemental microanalysis does not offer the same assistance in determining the inclusion or otherwise of propargyl alcohol and Fmoc-glycine propargyl ester within the azide-containing hypercrosslinked product through the click chemistry reaction. Again, FT-IR spectroscopy offers more useful data. FT-IR spectra were obtained for each of the products, as shown in Figure 4.3.9.5.

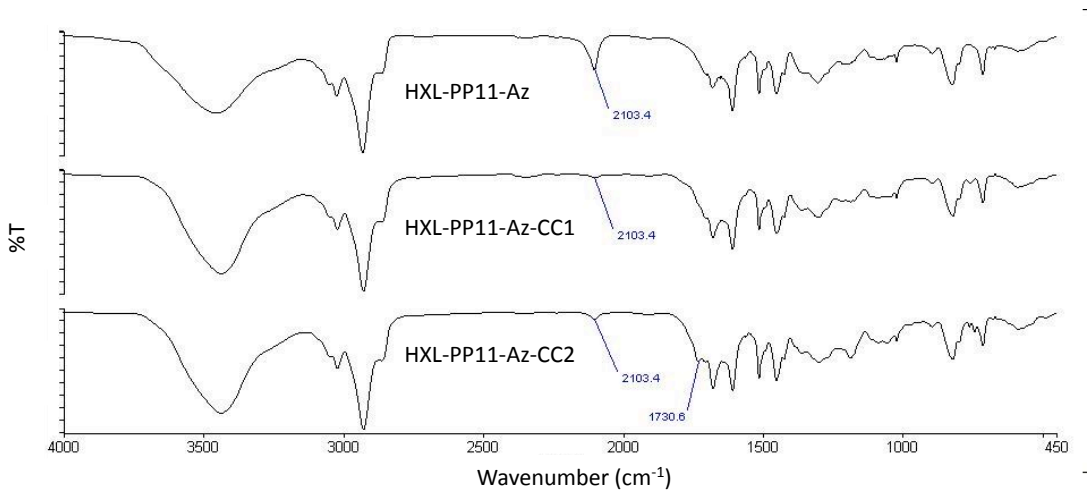

Figure 4.3.9.5. – FT-IR spectra for the azide-modified hypercrosslinked polymer HXL-PP11-Az and the subsequent products derived from its click reactions with propargyl alcohol and Fmoc-glycine propargyl ester (HXL-PP11-Az-CC1 and HXL-PP11-Az-CC2, respectively).

From the FT-IR spectra obtained it is clear that the azide band has been reduced significantly in intensity upon reaction with propargyl alcohol (**24**), suggesting that the reaction has been successful. The addition of propargyl alcohol (**24**) does not appear to result in the introduction of any unambiguous, characteristic signals in the spectrum of the product; while the –OH stretch (> 3300 cm^{-1}) appears to have increased in intensity subsequent to the reaction, it is unclear whether this is in fact due to the introduction of propargyl alcohol residues into the polymer or if it is a consequence of the hygroscopic nature of the hypercrosslinked polymer leading to water uptake.

From the FT-IR spectrum obtained for the Fmoc-glycine modified polymer, HXL-PP11-Az-CC2, it can be seen yet again that the azide band (2099 cm^{-1}) has been reduced considerably in intensity upon reaction, indicating that reaction has taken place. Unlike the propargyl alcohol example, addition of the Fmoc-glycine propargyl ester (**38**) is supported by the appearance of a small band at 1728 cm^{-1}, which is consistent with an ester carbonyl group. Two carbonyl groups are present in the Fmoc-glycine propargyl ester, one in the Fmoc fragment and one in the propargyl ester fragment at the C-terminus of the glycine.

SEM images obtained (Figure 4.3.9.6) showed that the click reaction did not change the particle shape and there was no damage to the surface of the microspheres. The particle size has also remained constant.

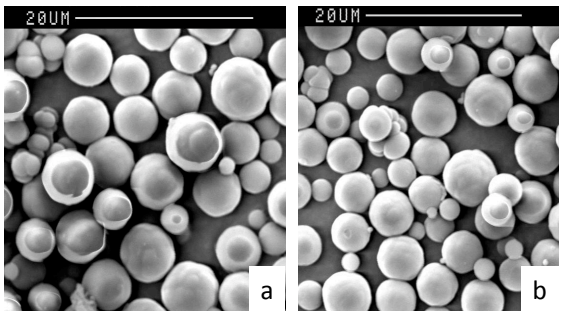

Figure 4.3.9.6. – SEM micrographs obtained for (a) HXL-PP1-Az-CC1 and (b) HXL-PP1-Az-CC2.

In addition to the polar alcohol and the amino acid, alkyne-containing compounds that contained weak ion-exchange functionality were clicked onto the azide-modified hypercrosslinked microspheres (Figure 4.3.9.7). Propargyl amine (**35**) was used to provide a primary amine functionality (WAX), while 4-pentynoic acid (**36**) was used to provide a carboxylic acid moiety (WCX), thus providing a complementary set of materials to the strong ion-exchangers described in Chapters 2 and 3. This further shows the potential of click

chemistry for the introduction of many types of functional group into the hypercrosslinked materials in an extremely facile manner, to allow their use in a variety of applications.

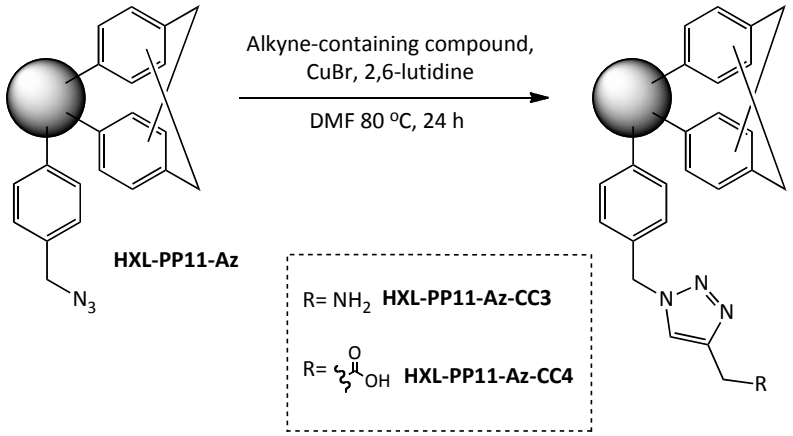

Figure 4.3.9.7. - Modification of the azide-containing hypercrosslinked polymer HXL-PP11-Az microspheres using propargyl amine and 4-pentynoic acid to give the products HXL-PP11-Az-CC3 and HXL-PP11-Az-CC4, respectively.

Elemental microanalysis was used to show that these amine and carboxylic acid moieties had been incorporated into the polymer successfully *via* the click chemistry reaction. Table 4.3.9.2 shows the elemental microanalysis data for the azide-containing hypercrosslinked polymer HXL-PP11-Az and the products of its reaction with propargyl amine (**35**), HXL-PP11-Az-CC3, and 4-pentynoic acid (**36**), HXL-PP11-Az-CC4.

Polymer ref.	***Observed Microanalysis (%)***			
	C	***H***	***N***	***Cl***
HXL-PP11-Az	86.3	6.6	2.4	2.0
HXL-PP11-Az-CC3	78.0	6.2	3.5	2.6
HXL-PP11-Az-CC4	74.1	5.8	2.0	1.8

Table 4.3.9.2. – Elemental microanalysis data for the azide-containing hypercrosslinked polymer HXL-PP11-Az and the products of its reaction with propargyl amine and 4-pentynoic acid, HXL-PP11-Az-CC3 and HXL-PP11-Az-CC4, respectively.

Comparison of the elemental microanalytical data for the azide-containing hypercrosslinked polymer, HXL-PP11-Az, and the product obtained after the click reaction with propargyl amine, HXL-PP11-Az-CC3, indicates that the reaction has been successful, by way of the increase in nitrogen content in the product relative to the azide-containing hypercrosslinked polymer. This is very promising indeed. The elemental microanalysis data cannot, however, be used to assess whether or not the carboxylic acid has been clicked onto the azide-containing hypercrosslinked polymer. An increase in oxygen content of the polmer would be best placed to indicate if this reaction had been successful, however oxygen content cannot currently be ascertained by the elemental analysis.

FT-IR spectroscopy was used to show that the introduction of these functional groups into the hypercrosslinked polymer had been successful (Figure 4.3.9.8).

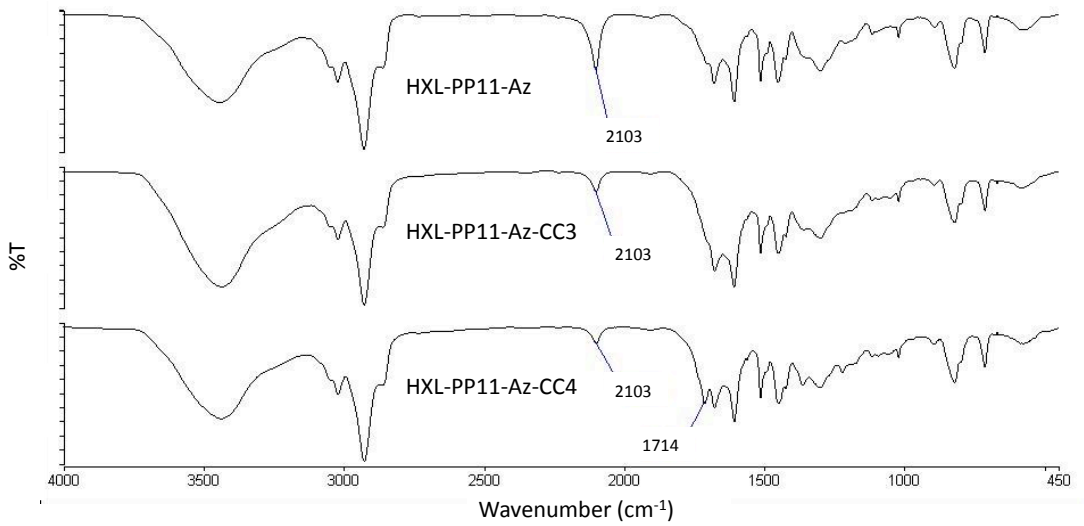

Figure 4.3.9.8. – FT-IR spectra obtained for the azide modified hypercrosslinked polymer HXL-PP11-Az and the subsequent products derived from its click reactions with propargyl amine and 4-pentynoic acid (HXL-PP11-Az-CC3 and HXL-PP11-Az-CC4, respectively).

From the FT-IR spectra obtained it is clear that the azide band has been reduced significantly in intensity upon reaction with propargyl amine (**35**), suggesting that the reaction has been successful. The addition of propargyl amine (**35**) does not appear to result in the introduction of additional signals, however any amine stretches present would be masked due to the the hygroscopic nature of the hypercrosslinked polymer, while any amine bends will be masked by the aliphatic and aromatic bend region of the spectra.

From the FT-IR spectrum obtained for the 4-pentynoic acid modified polymer, HXL-PP11-Az-CC4, it can be seen that yet again the azide band (2099 cm^{-1}) has been reduced considerably in intensity upon reaction, indicating that reaction has taken place. Addition of the acid is supported by the appearance of a small band at 1714 cm^{-1}, which is consistent with a carbonyl group.

4.3.10. Hypercrosslinking Using Click Chemistry

While the hypercrosslinking reactions carried out thus far have utilised reactive chloromethyl moieties incorporated into the polymer through copolymerisation of VBC, alternative methods of preparing ultra-high specific surface area polymers are also of interest.

4.3.10.1. Synthesis of Poly(DVB-*co*-VBAz) Precursor Polymer

In order to prepare ultra-high specific surface area polymers *via* click chemistry, a polymer precursor containing a sufficient level of azide or alkyne functional groups is required. A polymer was thus synthesised using DVB (**2**) and VBAz (**22**) (25 and 75 wt%, respectively) as comonomers (Figure 4.3.10.1.1).

Figure 4.3.10.1.1. – Synthesis by precipitation polymerisation of 25/75 (w/w) DVB/VBAz copolymer, PPAz-75.

As was the case for the conventional, Friedel-Crafts mediated hypercrosslinking chemistry, the precursor was synthesised in such a way as to contain 75 wt% of functional monomer. The precursor was analysed using elemental microanalysis, FT-IR spectroscopy and SEM. Table 4.3.10.1.1 shows the expected and observed elemental microanalysis results for the precursor.

	Observed Microanalysis (%)		
Sample	***C***	***H***	***N***
Expected for 25/75 DVB/VBAz	73.9	6.3	19.8
Observed (PPAz-75)	**77.8**	**6.4**	**13.7**
Expected for polyDVB only	91.1	8.1	0.8

Table 4.3.10.1.1. – Elemental microanalysis results expected and observed for PPAz-75.

From the elemental microanalysis results (Table 4.3.10.1.1) it can be seen that both the azide monomer VBAz (**22**) and the DVB (**2**) have been incorporated into the polymer at a significant level from the high nitrogen content observed.

FT-IR spectroscopy was also used to show the incorporation of both monomers in the polymer product, with bands of interest being those ascribed to residual double bonds from the DVB (~910 cm^{-1}) and the azide group of VBAz (2097 cm^{-1}). Figure 5.11.1.2 shows the FT-IR spectrum obtained for PPAz-75.

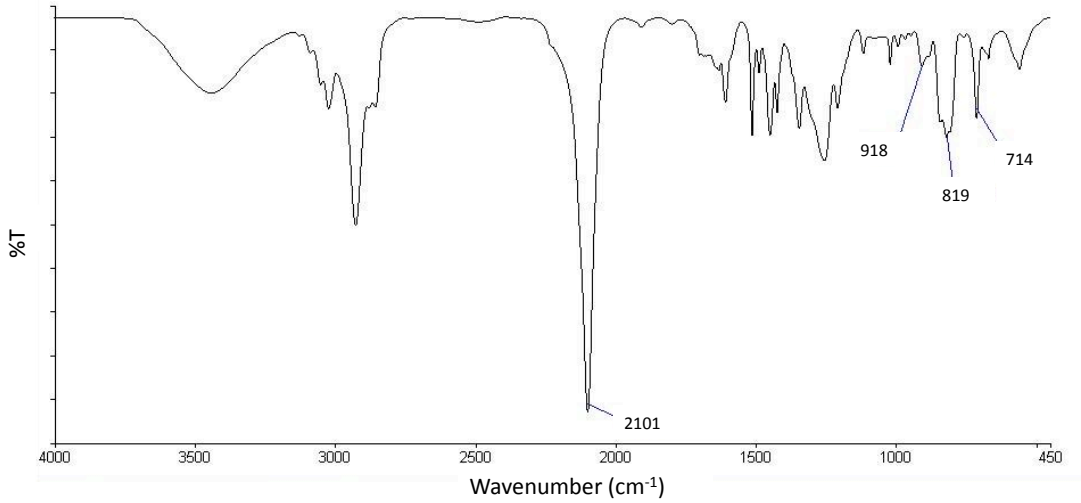

Figure 4.3.10.1.2. – FT-IR spectrum for the copolymer prepared from a feed of 25/75 (w/w) DVB/VBAz (PPAz-75).

From the FT-IR spectrum (Figure 4.3.10.1.2) it can be seen that the polymer contains a high level of the azide monomer, as the predominant signal in the spectrum can be ascribed to the azide group (2101 cm^{-1}). A band that can be ascribed to the residual double bonds of DVB can also be seen, confirming the inclusion of DVB in the product.

SEM was used to assess the size, shape and size distribution of the particles. The SEM micrographs obtained are presented in Figure 4.3.10.1.3.

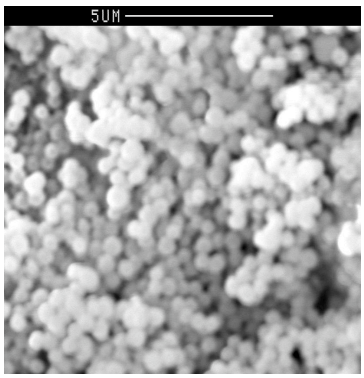

Figure 4.3.10.1.3. – SEM image obtained for PPAz-75.

From the SEM micrograph obtained (Figure 4.3.10.1.3) it can be seen that the use of large amounts of VBAz relative to DVB in the precipitation polymerisation has resulted in smooth, round (albeit extremely small) polymer microspheres (all < 1 μm in diameter). The particle quality is good, however particles of this size may prove to be problematic in certain applications, for example, in SPE it would be difficult to contain such microspheres within the SPE cartridge. Nevertheless, the material can still be used for click chemistry hypercrosslinking reactions, with optimisation of the particle synthesis potentially being investigated at a later time.

4.3.10.2. Hypercrosslinking of Poly(DVB-*co*-VBAz) Using Dialkyne and Click Chemistry

With a precursor polymer in place that contains a high loading of azide functionality, an alternative hypercrosslinking reaction can be carried out using a dialkyne compound to bridge between two azide moieties. An ideal dialkyne for this purpose is expected to possess a short or rigid group between the alkynes in order to produce short, stable linkages. The dialkyne selected for this role was 1,3-diethynylbenzene (**37**) (Figure 4.3.10.2.1).

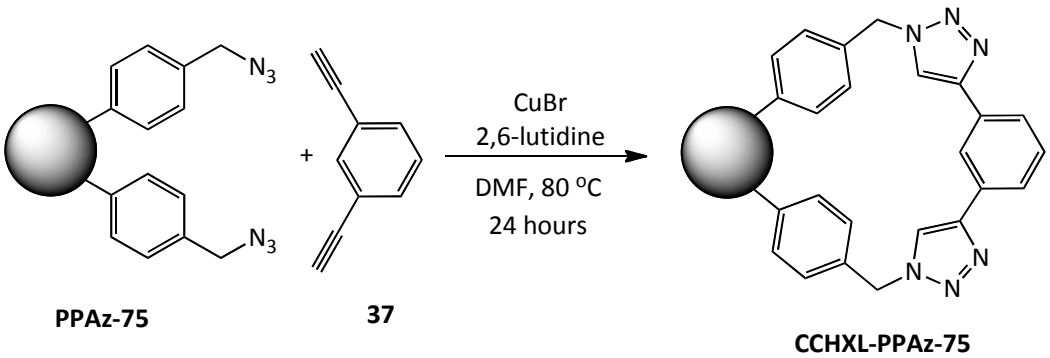

Figure 4.3.10.2.1. – Click-based hypercrosslinking reaction of PPAz-75.

The degree to which a solvent can swell the precursor polymer can influence the resulting surface area displayed by the hypercrosslinked product. In principle, the more a solvent can swell a polymer, the higher the resultant specific surface area will be for the same level of hypercrosslinking. In order to assess which solvent would be best for the swelling of the PPAz-75 polymer containing high levels of the azide monomer, a series of solvents of differing polarity were used to conduct swelling tests (Table 4.3.10.2.1).

Solvent	*Dielectric constant (ε_o)*	*Mass of polymer (g)*	*Mass of solvent uptaken (g)*	*g/g solvent sorbed*	*mL/g solvent sorbed*
THF	7.52 @ 22 ^oC	0.026	0.038	1.49	1.68
DCE	10.5 @ 20 ^oC	0.025	0.041	1.65	1.32
DMF	36.7 @ 20 ^oC	0.025	0.029	1.17	1.23
MeCN	37.5 @ 20 ^oC	0.014	0.020	1.41	1.80

Table 4.3.10.2.1. – Data obtained for the swelling tests carried out on the polymer prepared using 25/75 (w/w) DVB/VBAz.

The data from the swelling tests show that THF, DCE, DMF and MeCN are all suitable solvents for swelling the precursor polymer, however the extent to which they swell the polymer is slightly lower than the 2.44 mL/g of DCE sorbed by the polymer precursors used in conventional, Friedel-Crafts mediated hypercrosslinking. Thus the specific surface areas introduced through a click chemistry hypercrosslinking protocol may not be as high as those observed using a conventional hypercrosslinking strategy. As DCE is the solvent of choice for the $FeCl_3$ catalysed, conventional hypercroslinking reaction, due to the exceptional swelling capability of DCE for VBC-containing polymers, DCE was investigated for the click chemistry hypercrosslinking method. DMF was also used as this was shown previously to be the optimal solvent for the click reaction to take place on polymer beads.

Elemental microanalysis was used to assess the reaction progress, with increases in C and H content (hence, decrease in N content) indicating the incorporation of the dialkyne. The elemental microanalysis results obtained for the products prepared in both DCE and DMF are shown in Table 4.3.10.2.2, with reference data for the precursor (PPAz-75).

Polymer ref.	***Solvent***	***Temp. (°C)***	***Observed Microanalysis (%)***		
			C	***H***	***N***
PPAz-75	n/a	n/a	77.8	6.4	13.7
CCHXL-PPAz-75-1	DMF	80	73.2	5.8	9.5
CCHXL-PPAz-75-2	DCE	80	73.4	5.8	9.6

Table 4.3.10.2.2. - Elemental microanalytical data for the polymers hypercrosslinked using click chemistry.

The elemental microanalysis results (Table 4.3.10.2.2) show that, after reaction with the dialkyne species, the nitrogen and hydrogen contents of the polymers decreased. Had all of the azide groups reacted, it would be expected that the nitrogen content would be reduced to 9.1 % while the hydrogen content should be reduced slightly to 5.9 %, thus it is clear from the elemental microanalysis data that the reactions have been relatively successful. The decrease in nitrogen and hydrogen contents should however be accompanied by an increase in carbon content to 83.7 %, which is not observed. The reason for this is unclear.

Nitrogen sorption porosimetry was used to assess the specific surface areas of the hypercrosslinked polymers using both BET and Langmuir isotherms. Specific surface areas, total pore volumes and pore sizes are detailed in Table 4.3.10.2.3 for each of the polymers.

Polymer ref.	BET c value	Specific surface area (m^2/g)		Total pore volume (cm^3/g)	Pore size (nm)
		BET	Langmuir		
CCHXL-PPAz-75 -1	136	30	48	0.054	12.850
CCHXL-PPAz-75 -2	300	19	30	0.039	13.560

Table 4.3.10.2.3. – Nitrogen sorption porosimetry data for the polymers hypercrosslinked *via* click chemistry.

From the nitrogen sorption porosimetry data (Table 4.3.10.2.3) it is clear that the HXL reaction has not been successful in generating ultra-high specific surface area polymers. The BET c values for CCHXL-PPAz-75-1 and CCHXL-PPAz-75-2 are high and positive, indicating that for these samples more than one layer of nitrogen is able to sorb onto the surfaces of the pores and thus the correct specific surface areas to quote for these samples are the ones calculated using the BET isotherm (30 and 19 $m^2\ g^{-1}$ for CCHXL-PPAz-75-1 and CCHXL-PPAz-75-2, respectively). The large pore diameter of these polymers (13.56 and 12.85 nm for CCHXL-PPAz-75-1 and CCHXL-PPAz-75-2, respectively) supports the assumption that microporosity has not been introduced and helps to rationalise the BET surface area allowing for the absorption of several layers of nitrogen in each pore. Thus the polymers are mesoporous. Whilst porosity has been imparted into the particles through this hypercrosslinking strategy, it has only been possible to a modest level.

FT-IR spectroscopy was also used to determine whether the reactions were successful, with the main difference expected upon reaction being a decrease in the intensity of the azide signal at 2096 cm^{-1}. The reaction was carried out in different solvents to see how the surface areas differed with the different swelling capabilities of the solvents. The first solvent used was DMF, as this had been shown previously to be a good solvent for the click reaction of interest. The next solvent used was DCE due to its swelling capabilities. The reactions

were carried out at 80 °C to give maximum conversion to triazole. The FT-IR spectra obtained for the products are presented in Figure 4.3.10.2.2.

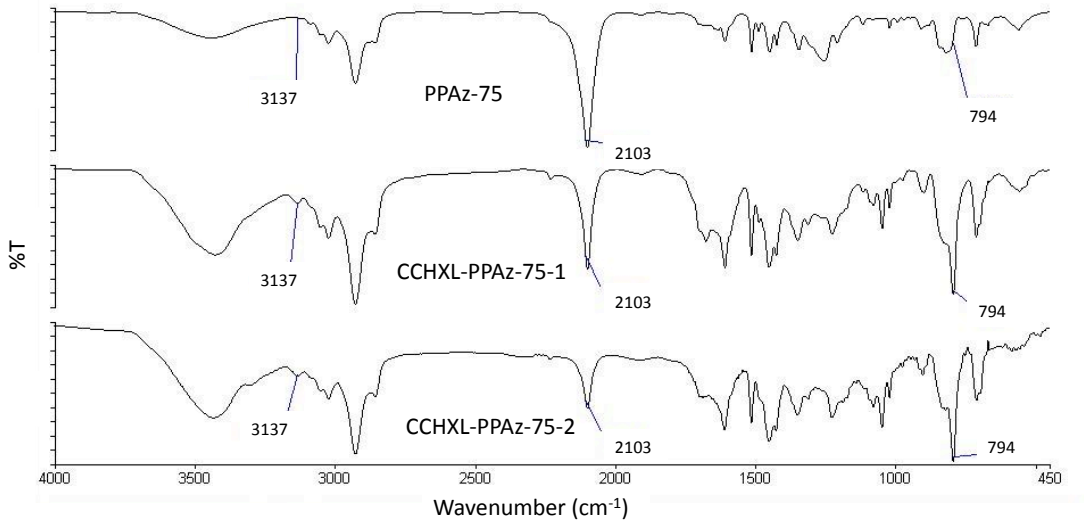

Figure 4.3.10.2.2. – FT-IR spectra obtained for azide-containing precursor polymer (PPAz-75) and the corresponding hypercrosslinked click products CCHXL-PPAz-75-1 and CCHXL-PPAz-75-2.

From the FT-IR spectra (Figure 4.3.10.2.2) it can be seen that the azide-derived signals at 2093 cm^{-1} have been reduced significantly in intensity subsequent to the click reaction. This is accompanied by the introduction of peaks corresponding to a 1,3-disubstituted aromatic ring (790 cm^{-1}) and an alkyne moiety (3297 cm^{-1}). This suggests that in some cases either the azide groups closer to the surface are all reacting first, resulting in alkyne groups with no adjacent azide to react with, or, alternatively, that the dialkyne cannot get into the correct orientation to react with a second azide group. This is not true of all the dialkyne groups however, as the introduction of porosity, albeit to a modest extent, suggests that some of the dialkyne groups have indeed formed bridges.

SEM micrographs were obtained to determine the effects of the hypercrosslinking reaction on the particle size and shape. Figure 4.3.10.2.4 shows the product obtained from the reaction in DMF at 80 °C.

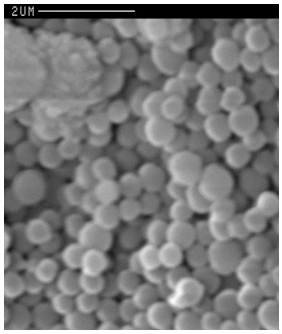

Figure 4.3.10.2.4. – SEM micrograph obtained for CCHXL-PPAz-75-1.

From the SEM micrograph obtained (Figure 4.3.10.2.4) it is clear that the hypercrosslinking reaction has not adversely affected the particle size and shape to any noteable degree relative to the non-hypercrosslinked precursor PPAz-75, as presented in Figure 4.3.10.1.3.

4.4. CHAPTER CONCLUSIONS

Azide-alkyne cycloaddition click chemistry has been used successfully in the preparation of functionalised hypercrosslinked microspheres. Two synthetic strategies have been developed: copolymerisation of azide- and alkyne-containing monomers to give "clickable" polymers, functionalised *via* click chemistry followed by subsequent hypercrosslinking; and azidation of the pendent chloromethyl groups present within hypercrosslinked poly(DVB-*co*-VBC) microspheres followed by click chemistry functionalisation. The latter method has been used to deliver polymer microspheres with weak ion-exchange functionality.

A click chemistry-based hypercrosslinking strategy has also been investigated. While this did not produce polymer microspheres with the desired microporosity, mesopores and modest specific surface areas have successfully been introduced, which is promising preliminary data nonetheless.

4.5. REFERENCES

1. H. C. Kolb, M. G. Finn and K. B. Sharpless, *Angew. Chem. Int. Ed.*, (2001), **40**, 2004-2021.
2. F. Fringuelli, O. Piermatti, F. Pizzo and L. Vaccaro, *J. Org. Chem.*, (1999), **64**, 6094-6096.
3. D. van Mersbergen, J. W. Wijnen and J. B. F. N. Engberts, *J. Org. Chem.*, (1998), **63**, 8801-8805.
4. R. Breslow, *Acc. Chem. Res.*, (1991), **24**, 159-164.
5. R. Breslow, K. Groves and M. U. Mayer, *Pure. Appl. Chem.*, (1998), **70**, 1933-1938.
6. J. J. Gajewski, *Acc. Chem. Res.*, (1997), **30**, 219-225.
7. R. Huisgen, G. Szeimies and L. Moebius, *Chem. Ber.*, (1967), **100**, 2494.
8. C. W. Tornøe, C. Christensen and M. Meldal, *J. Org. Chem.*, (2002), **67**, 3057-3064.
9. V. V. Rostovtsev, L. G. Green, V. V. Fokin and K. B. Sharpless, *Angew. Chem. Int. Ed.*, (2002), **41**, 2596-2599.
10. C. Glaser, *Ber. Deutschen Chemischen Gesellschaft*, (1869), **2**, 422-424.
11. P. L. Golas, N. V. Tsarevsky, B. S. Sumerlin and K. Matyjaszewski, *Macromolecules*, (2006), **39**, 6451-6457.
12. K. Sonogashira, Y. Tohda and N. Hagihara, *Tetrahedron Lett.*, (1975), **16**, 4467-4470.
13. F. Himo, T. Lovell, R. Hilgraf, V. V. Rostovtsev, L. Noodleman, K. B. Sharpless and V. V. Fokin, *J. Am. Chem. Soc.*, (2005), **127**, 210-216.
14. V. O. Rodionov, V. V. Fokin and M. G. Finn, *Angew. Chem. Int. Ed.*, (2005), **44**, 2210-2215.
15. L. Fomina, B. Vasquez, E. Tkatchouk and S. Fomine, *Tetrahedron*, (2002), **58**, 6741-6747.
16. T. R. Chan, R. Hilgraf, K. B. Sharpless and V. V. Fokin, *Org. Lett.*, (2004), **6**, 2853-2855.
17. V. O. Rodionov, S. I. Presolski, S. Gardinier, Y.-H. Lim and M. G. Finn, *J. Am. Chem. Soc.*, (2007), **129**, 12696-12704.
18. V. O. Rodionov, S. I. Presolski, D. Díaz Díaz, V. V. Fokin and M. G. Finn, *J. Am. Chem. Soc.*, (2007), **129**, 12705-12712.
19. S. Díez-González, A. Correa, L. Cavallo and S. P. Nolan, *Chem. Eur. J.*, (2006), **12**, 7558-7564.

20. N. Candelon, D. Lastécouères, A. K. Diallo, J. R. Aranzaes, D. Astruc and J.-M. Vincent, *Chem. Commun.*, (2008), 741-743.
21. P. Appukkuttan, W. Dehaen, V. V. Fokin and E. Van der Eycken, *Org. Lett.*, (2004), **6**, 4223-4225.
22. L. Zhang, X. Chen, P. Xue, H. H. Y. Sun, I. D. Williams, K. B. Sharpless, V. V. Fokin and G. Jia, *J. Am. Chem. Soc.*, (2005), **127**, 15998-15999.
23. M. M. Majireck and S. M. Weinreb, *J. Org. Chem.*, (2006), **71**, 8680-8683.
24. N. J. Agard, J. A. Prescher and C. R. Bertozzi, *J. Am. Chem. Soc.*, (2004), **126**, 15046-15047.
25. N. J. Agard, J. M. Baskin, J. A. Prescher. A. Lo and C. R. Bertozzi, *ACS Chem. Biol*., (2006), **1**, 644-648.
26. R. D. Bach, *J. Am. Chem. Soc.*, (2009), **131**, 5233-5234.
27. F. Schoenebeck, D. H. Ess, G. O. Jones and K. N. Houk, *J. Am. Chem. Soc.*, (2009), **131**, 8121-8133.
28. A. A. Poloukhtine, N. E. Mbua, M. A. Wolfert, G.-J. Boons and V. V. Popik, *J. Am. Chem. Soc.*, (2009), **131**, 15769-15776.
29. F. Shi, J. P. Waldo, Y. Chen and R. C. Larock, *Org. Lett.*, (2008), **10**, 2409-2412.
30. S. S. van Berkel, A. J. Dirks, M. F. Debets, F. L. van Delft, J. J. L. M. Cornelissen, R. J. M. Nolte and F. P. J. T. Rutjes, *Chem. Bio. Chem.*, (2007), **8**, 1504-1508.
31. P. L. Golas, N. V. Tsarevsky and K. Matyjaszewski, *Macromol. Rapid Commun.*, (2008), **29**, 1167-1171.
32. N. V. Tsarevsky, B. S. Summerlin and K. Matyjaszewski, *Macromolecules*, (2005), **38**, 3558-3561.
33. G. Mantovani, V. Ladmiral, L. Tao and D. M. Haddleton, *Chem. Commun.*, (2005), 2089-2091.
34. J. A. Opsteen and J. C. M. van Hest, *Chem. Commun.*, (2005), 57-59.
35. D. Quémener, M. Le Hellaye, C. Bissett, T. P. Davis, C. Barner-Kowollik and M. H. Stenzel, *J. Polym. Sci. Part A: Polym. Chem.*, (2008), **46**, 155-173.
36. W. van Camp, V. Germonpré, L. Mespouille, P. Dubois, E. J. Goethals and F. E. Du Prez, *React. Funct. Polym.*, (2007), **67**, 1168-1180.
37. S. O. Kyerematen, E. Amado, A. Blume and J. Kressler, *Macromol. Rapid Commun.*, (2008), **29**, 1140-1146.
38. E. Gungor, C. Bilir, H. Durmaz, G. Hizal and U. Tunca, *J. Polym. Sci. Part A: Polym. Chem.*, (2009), **47**, 5947-5953.

39. S. Sinnwell, A. J. Inglis, M. H. Stenzel and C. Barner-Kowollik, *Macromol. Rapid Commun.*, (2008), **29**, 1090-1096.
40. P.-F. Gou, W.-P. Zhu and Z.-Q. Shen, *J. Polym. Sci. Part A: Polym. Chem.*, (2009), **47**, 2905-2916.
41. Y. Zhang, C. Li and S. Liu, *J. Polym. Sci. Part A: Polym. Chem.*, (2009), **47**, 3066-3077.
42. C. Li, Z. Ge, H. Liu and S. Liu, *J. Polym. Sci. Part A: Polym. Chem.*, (2009), **47**, 4001-4013.
43. E. Gungor, G. Hizal and U. Tunca, *J. Polym. Sci. Part A: Polym. Chem.*, (2009), **47**, 3409-3418.
44. P. G. Clark, E. N. Guidry, W. Y. Chan, W. E. Steinmetz and R. H. Grubbs, *J. Am. Chem. Soc.*, (2010), **132**, 3405-3412.
45. P. Wu, A. K. Feldman, A. K. Nugent, C. J. Hawker, A. Scheel, B. Voit, J. Pyun, J. M. J. Fréchet, K. B. Sharpless and V. V. Fokin, *Angew. Chem. Int. Ed.*, (2004), **43**, 3928-3932.
46. B. Helms, J. L. Mynar, C. J. Hawker and J. M. J. Fréchet, *J. Am. Chem. Soc.*, (2004), **126**, 10520-10521.
47. A. R. Katritzky, Y. Song, R. Sakhuja, R. Gyanda, N. K. Meher, L. Wang, R. S. Duran, D. A. Ciaramitaro and C. D. Bedford, *J. Polym. Sci. Part A: Polym. Chem.*, (2009), **47**, 3748-3756.
48. N. Xu, R. Wang, F.-S. Du and Z.-C. Li, *J. Polym. Sci. Part A: Polym. Chem.*, (2009), **47**, 3583-3594.
49. A. Scarpaci, C. Cabanetos, E. Blart, V. Montembault, L. Fontaine, V. Rodriguez and F. Odobel, *J. Polym. Sci. Part A: Polym. Chem.*, (2009), **47**, 5652-5660.
50. J. Yin, Z. Gem H. Liu and S. Liu, *J. Polym. Sci. Part A: Polym. Chem.*, (2009), **47**, 2608-2691.
51. D. Damiron, M. Desorme, R.-V. Ostaci, S. A. Akhrass, T. Hamaide and E. Drockenmuller, *J. Polym. Sci. Part A: Polym. Chem.*, (2009), **47**, 3803-3813.
52. E. Schwartz, H. J. Kitto, R. De Gelder, R. J. M. Nolte, A. E. Rowan, and J. J. L. M. Cornelissen, *J. Mater. Chem.*, (2007), **17**, 1876-1884.
53. H. J. Kitto, E. Schwartz, M. Nijemeisland, M. Koepf, J. J. L. M. Cornelissen, A. E. Rowan and R. J. M. Nolte, *J. Mater. Chem.*, (2008), **18**, 5615-5624.
54. E. Schwartz, M. Koepf, H. J. Kitto, M. Espelt, V. J. Nebot-Carda, R. De Gelder, R. J. M. Nolte, J. J. L. M. Cornelissen and A. E. Rowan, *J. Polym. Sci. Part A: Polym. Chem.*, (2009), **47**, 4150-4164.

55. Q. Chen and B.-H. Han, *J. Polym. Sci. Part A: Polym. Chem.*, (2009), **47**, 2948-2957.
56. J.-F. Lutz, H. G. Börner and K. Weichenhan, *Macromol. Rapid Commun.*, (2005), **26**, 514-518.
57. A. Narumi, K. Fuchise, R. Kakuchi, A. Toda, T. Satoh, S. Kawaguchi, K. Sugiyama, A. Hirao and T. Kakuchi, *Macromol. Rapid Commun.*, (2008), **29**, 1126-1133.
58. Y.-Y. Tong, R. Wang, N. Xu, F.-S. Du and Z.-C. Li, *J. Polym. Sci. Part A: Polym. Chem.*, (2009), **47**, 4494-4504.
59. R. J. Thibault, K. Takizawa, P. Lowenheilm, B. Helms, J. L. Mynar, J. M. J. Fréchet and C. J. Hawker, *J. Am. Chem. Soc.*, (2006), **128**, 12084-12085.
60. S. Löber, P. Rodriguez-Loaiza and P. Gmeiner, *Org. Lett.*, (2003), **5**, 1753-1755.
61. D. R. Breed, R. Thibault, F. Xie, Q. Wang, C. J. Hawker, and D. J. Pine, *Langmuir*, (2009), **25**, 2857-2863.
62. B. Karagoz, Y. Y. Durmaz, B. N. Gacal, N. Bicak and Y. Yagci, *Designed Monomer and Polymers*, (2009), **12**, 511-522.
63. A. S. Goldmann, A. Walther, L. Nebhani, R. Joso, D. Ernst, K. Loos, C. Barner-Kowollik, L. Barner and A. H. E. Müller, *Macromolecules*, (2009), **42**, 3707-3714.
64. K. Welser, M. D. A. Perera, J. W. Aylott and W. C. Chan, *Chem. Commun*., (2009), 6601-6603.
65. M. Slater, M. Snauko, F. Svec and J. M. J. Fréchet, *Anal. Chem.*, (2006), **78**, 4969-4975.
66. R. Mark, Final Year MSci Thesis, University of Strathclyde, *Click Chemistry Functionalisation of Highly Porous Polymer Microspheres*, (2010).
67. B. Neises and W. Steglich, *Angew. Chem. Int. Ed. Engl.*, (1978), **17**, 522-524.
68. A. L. Castelhano, S. Horne, G. J. Taylor, R. Billedeau and A. Krantz, *Tetrahedron*, (1988), **44**, 5451-5466.
69. A. Davies, 9 Month PhD Report, University of Strathclyde, *Synthesis and Characterisation of Strong and Weak Ion-Exchange Materials*, (2009), Chpt. 3.5.
70. D. Bratkowska, N. Fontanals, F. Borrull, P. A. G. Cormack, D. C. Sherrington and R. M. Marcé, *J. Chromatogr. A*, (2010), **1217**, 1575-1582.
71. J. Geng, G. Mantovani, L. Tao, J. Nicolas, G. Chen, R. Wallis, D. A. Mitchell, B. R. G. Johnson, S. D. Evans and D. M. Haddleton, *J. Am. Chem. Soc.*, (2007), **129**, 15156-15163.
72. J. T. Lunquist IV and J. C. Pelletier, *Org. Lett.*, (2001), **3**, 781-783.

CHAPTER 5

GENERAL CONCLUSIONS AND FUTURE WORK

5.1. GENERAL CONCLUSIONS

In conclusion, several distinct methods for chemically modifying ultra-high specific surface area hypercrosslinked polymers have been demonstrated, through both post-polymerisation chemical modification reactions and copolymerisation of functional monomers.

Hypercrosslinked polymer microspheres were first modified with sulfonic acid residues through post-polymerisation sulfonation reactions to confer the microspheres with strong cation-exchange (SCX) functionality. It was demonstrated that both acetyl and lauroyl sulfate were able to sulfonate the hypercrosslinked materials, however the lauroyl sulfate reagent was shown to be much more effective than acetyl sulfate. The reason for this is unknown, however it is most likely that the more hydrophobic lauroyl sulfate is more compatible with the hydrophobic hypercrosslinked materials, and perhaps the DCE sulfonating solvent, and thus penetrates better the microspheres than acetyl sulfate, allowing for a higher degree of sulfonation. Polymeric microspheres suitable for use as SCX solid-phase extraction (SPE) sorbents were thus prepared by reaction of hypercrosslinked polymer microspheres with different levels of lauroyl sulfate. Using this method, polymers with ultra-high specific surface areas up to 1,370 m^2/g, and ion-exchange capacities of between 1.2 and 2.8 mmol/g were prepared.

Methods suitable for the preparation of a complementary strong anion-exchange (SAX) SPE sorbent, through introduction of quaternary ammonium groups, were also investigated. While it has been shown previously within our group that the residual chloromethyl groups present subsequent to hypercrosslinking can be reacted with primary and secondary amines, the tertiary amines required to provide SAX functionality did not show the same level of reactivity. Instead, the amination reaction had to be carried out prior to the hypercrosslinking reaction. This is perhaps a more effective method,

however, as it allows for a more controlled amination reaction, and thus materials with variable and controllable ion-exchange capacities could be accessed. Polymer microspheres suitable for use as SAX SPE sorbents were prepared using this method, which combined ion-exchange capacities of 0.2 and 0.4 mmol/g with ultra-high specific surface areas greater than 1,000 m^2/g.

While unmodified hypercrosslinked sorbents have, in the past, been shown to be comparable to commercially available hydrophobic SPE sorbents, addition of strong anion- and cation-exchange functionalities allowed for more selective extraction still. This was demonstrated in the extractions of acidic and basic pharmaceuticals from complex real water samples, using SAX and SCX sorbents, respectively. The ion-exchange functionalised hypercroslinked sorbents prepared were shown to compare favourably to commercially available mixed-mode ion-exchange SPE sorbents.

Azide-alkyne cycloaddition click chemistry was also exploited for the chemical modification of hypercrosslinked polymer microspheres. This was achieved in two ways, firstly through the preparation of azide- and alkyne-containing monomers, and incorporation of these monomers into precipitation polymerisations. An azide-containing monomer, vinylbenzyl azide (**22**) (VBAz), was synthesised by reaction of vinylbenzyl chloride (**7**) with sodium azide, while an alkyne-containing monomer, propargyl methacrylate (**27**), was prepared through reaction of methacryloyl chloride (**33**) and propargyl alcohol (**24**). Both of the synthesised monomers were successfully copolymerised with DVB (**2**) and VBC (**7**) under precipitation polymerisation conditions. These monomers were, however, not compatible with the conditions employed for the hypercrosslinking reaction, and thus the click functionalisation was required prior to hypercrosslinking. This method of functionalisation is thus only suitable for introduction of functional groups that can tolerate the hypercrosslinking conditions. Using this method, azide-functional microspheres were modified with propargyl alcohol (**24**) and Fmoc-glycine propargyl ester (**38**), and hypercrosslinked to give porous products with

specific surface areas in the region of 1,000 m^2/g. Alkyne-containing polymer microspheres were modified with the azide monomer, VBAz (**22**), and an azide protected phenylalanine, followed by hypercrosslinking to provide functionalised, porous polymers with specific surface areas well in excess of 1,000 m^2/g.

A second, more generic method of click functionalisation involving conversion of residual chlorine groups on hypercrosslinked polymers to azide, followed by a subsequent click modification was also demonstrated. Post-hypercrosslinking azidation was perhaps the more facile of the two methods and was thus used to functionalise hypercrosslinked microspheres with: a polar moiety through reaction with propargyl alcohol (**24**); an amino acid functionality through reaction with Fmoc-glycine propargyl ester (**38**); a weak anion-exchange functionality through reaction with propargyl amine (**35**); a weak cation-exchange functionality through reaction with 4-pentynoic acid (**36**). Thus it has been shown that the hypercrosslinked polymer microspheres can be functionalised in a facile manner with a variety of alkyne-containing functional groups in order to fulfil the needs of many applications.

A study of the efficiency of the hypercrosslinked reaction in the early stages of the reaction revealed that the majority of the reaction occurs within just 15 minutes. It is extremely pleasing and practically attractive that ultra-high specific surface area materials can be accessed in such a short time.

While the hypercrosslinking chemistry currently in use provides a fast and efficient reaction, the possibility to use click chemistry as an alternative means of hypercrosslinking was also investigated. A polymer with high azide loading was prepared in a precipitation copolymerisation of divinylbenzene and vinylbenzyl azide. Reaction of the azide-containing microspheres with a dialkyne species was investigated, however it was shown that this was an unsuccessful method for the generation of ultra-high specific surface area materials, since the specific surface areas observed were modest and nowhere

near those obtained using the already well-established Friedel-Crafts methodology. From the data obtained, it appears that, in many cases, only one alkyne of the dialkyne species is able to react with the azide polymer, however the second alkyne cannot react. This is perhaps due to the dialkyne not being able to adopt the appropriate conformation for the second reaction to occur, or more likely that the second alkyne cannot react due to all of the surrounding azides having already reacted with the first alkyne of a different molecule of dialkyne. However, the introduction of mesopores and modest specific surface areas (30 and 19 m^2/g) suggests that some of the dialkyne species have in fact been able to form bridges.

5.2. FUTURE WORK

New methods of functionalisation have been demonstrated, however many other methods for functionalisation exist and could thus be exploited with the hypercrosslinked materials. Investigation of other functionalisation routes would be a natural extension to the work presented herein.

The click chemistry functionalisation detailed in Chapter 4 could be further investigated as a means to introduce other functionalities for specific applications. The amino acids clicked on could also be further investigated, as the effect of the click reaction on the stereochemistry of the amino acids is not known. If these materials should find an application based on the amino acid presence, the enantiomeric purity may be of importance and thus an understanding of this aspect would be beneficial.

While the alternative click chemistry-derived hypercrosslinking method did not lead to ultra-high specific surface areas, further work in this area could potentially lead to the desired products. Other alternative methods for hypercrosslinking based on the functionalisation chemistries presented here could also be investigated. For example, a well known side-effect of some sulfonation reactions is the formation of sulfone bridges. While this destroys the ion-exchange capacity of the resultant materials, and was thus avoided in the preparation of SCX materials, it could be exploited as a metal-free hypercrosslinking reaction.

Additionally, polymer microspheres prepared with a high loading of the alkyne-containing monomer, propargyl methacrylate, could potentially be used to prepare hypercrosslinked microspheres using an alkyne coupling technique, such as the Glaser or Eglinton coupling reactions.

If both vinylbenzyl azide and propargyl methacrylate could be combined in the same microsphere, click chemistry coupling may also lead to materials with high levels of crosslinks. Such materials would be extremely interesting indeed.